Developing New Catalysts and Methods for Catalyst-transfer Polycondensations (CTP)

by

Zachary Jacob Bryan

A dissertation submitted in partial fulfillment of the requirements for the degree of Doctor of Philosophy (Chemistry) in the University of Michigan 2015

Doctoral Committee

Associate Professor Anne J. McNeil (Chair)
Associate Professor Kenichi Kuroda
Professor Adam J. Matzger
Professor Melanie S. Sanford

2015

Dedication

To my mother, father, brother, and wife for their unwavering support.

Acknowledgements

First and foremost I want to thank my advisor Prof. Anne J. McNeil for her guidance and assistance over the past five years. She is a wonderful scientist and an even better mentor, and I am very thankful and fortunate to have been able to develop under her supervision. She has provided the drive and encouragement necessary through the good and bad times, and has made me a much better scientist as a result. I would not be the person or scientist I am today without spending these years studying with her, and I am eternally grateful for that.

I also owe a great deal of thanks to my PhD committee. Prof. Kenichi Kurroda, Prof. Adam Matzger, and Prof. Melanie Sanford have been supportive and helpful every step of the way. They consistently challenged me to explore difficult ideas and made me strive for excellence. They also provided insightful advice and needed support. It was always reassuring to know I had such a knowledgeable and helpful group in my corner.

I want to thank the McNeil group members, past and present for their support and help over my time here. Danielle Zurcher has been with me every step of the way, and although we worked in different areas she was always someone who would listen. The current group members including Peter Goldberg, Mitchell Smith, Ariana Hall, Kendra Souther, and Dr. Gesine Veits have made me strive to be a better researcher. Your support and friendship helped keep me going. Previous group members including Dr. Kelsey King, Dr. Cheryl Moy, Dr. Ed Palermo, Yash Adhia, and Dr. Jonas Locke were excellent examples of scientists and lab mates that have encouraged me as well as helped numerous times over my years here. I want to thank the undergraduate students I worked with, Carolyn Zhao and Nadine Currie, for helping me learn about myself, and what is required to be a good mentor. I especially owe thanks to Dr.

Jing Chen and Dr. Se Ryeon Lee for mentoring me while I rotated in the lab. Your guidance helped me start strong and begin my long journey here.

I want to thank my friends within the chemistry department for their support and help throughout the years. Shawn Eady, Kayla Pyper, Amit Pithadia, Casey Dougherty, Laura Pfund, Brian Larsen, Tyler Carter, Cameron Moore, Tim Tseng, and Prof. Bart Bartlett.

I want to thank my friends outside of Ann Arbor, Daniel Mabel, Donny Weinbrenner, and Scott Cintron for helping keep me sane over the past five years. You have spent the better part of this time trying to convince me to do less work, and although I regularly ignored those requests, the distractions and comradery were priceless.

I want to thank my wife Rose Bryan for her love and support during this long adventure. She has stuck by my side through the good and bad, and has made me a better person through it all. You accepted the time I have had to spend away from you, whether it be in the lab or around the world, you have always been there for me. I do not know if I would have been able to make it through this without you, and I will never be able to thank you enough.

Finally, I need to thank my mother, father, and brother for their unconditional love and support. They have been by my side and in my corner my entire life. Whenever I get discouraged they are there to give me a boost. When something good happens they are there to congratulate me, even if they do not even begin to understand what I am talking about. I am the person I am today because of my family, and I eternally grateful for them.

Table of Contents

List of Figures

List of Tables

List of Schemes

List of Charts

List of Appendices

Abstract

Conjugated polymers remain an active area of research because they are electronically tunable and can be solution processed onto thin, flexible substrates. While π-conjugated polymers are traditionally synthesized via step-growth methodology, catalyst-transfer polycondensation (CTP) enables precise control over molecular weight and dispersity, as well as access to unique copolymer sequences (blocks and gradients). Unfortunately, limitations such as narrow monomer scope prevent widespread adoption of CTP as the preferred route to conjugated polymers. This thesis explains our efforts to address these limitations through investigation of the CTP mechanism, as well as development of new catalysts for the controlled synthesis of π-conjugated polymers.

Chapter 1 provides a general introduction and brief history of the controlled synthesis of π-conjugated polymers via catalyst-transfer polycondensation (CTP). We focus on the mechanistic underpinnings, as well as controversial hypotheses supporting information. The monomer scope is investigated, illustrating the current limitation of primarily electron-rich monomers. We also examine new materials that have been accessed via CTP.

Chapter 2 discusses the impact of an associative intermediate in Ni-catalyzed Kumada cross-couplings and CTP. While this intermediate had been implicated as a key feature of the CTP mechanism, no direct evidence had been provided. We observed preferential intramolecular oxidative addition even when a stoichiometric amount of competitive agent was present. At higher concentrations of competitive agent, we observed electron-rich bidentate phosphines showed higher amounts of intramolecular oxidative addition compared to electron-poor ligand analogues. Further study illustrated that these trends were also present in CTP polymerizations stylizing Ni catalysts. We

believe that intramolecular oxidative addition is the key step in CTP that determines between chain and step-growth polymerizations. As a result, new catalysts with electron-rich ligands are being targeted to facilitate preferential intramolecular oxidative addition.

Chapter 3 describes an N-heterocyclic carbene-ligated catalyst as a new route for CTP. Current Ni catalysts exhibited a limited monomer scope in CTP, so there was interest to expand into Pd catalysts as they have shown more substrate tolerance in small molecule cross-couplings. Using a Pd-NHC catalyst, we observed the controlled polymerization of both phenylene and thiophene monomers, while the polymerization of fluorene did not proceed through a living, chain-growth mechanism. This Pd-NHC was able to synthesize block copolymers of thiophene and phenylene, regardless of addition order, indicating more complicated block structures could be achieved. Some chain-termination was observed following these copolymerizations, but this could be minimized by adding the second block shortly after the first monomer is consumed. We suggest this catalyst scaffold be further investigated as an alternate path for developing new CTP conditions. Similar Pd-NHCs have recently used to synthesize polythiophenes via Suzuki and Stille controlled polymerizations.

Chapter 4 examines a new approach to try and address the limited monomer scope. New CTP conditions are mostly found serendipitously via polymerizations screens as failed results are usually ambiguous. To try and streamline this process, we develop a small molecule model system for screening new CTP conditions for the synthesis of poly(2,5-bis(hexyloxy)phenylene ethynylene) (PPE). We specifically targeted conditions that showed preferential multi-functionalization under sub-stoichiometric quantities. Hundreds of screens lead to several conditions that favored multi-functionalization, but unfortunately these conditions exhibited step-growth behavior when PPE monomer was used. Further investigation revealed the intermediates in the small molecule model system were significantly more reactive than the starting materials, leading to preferential multi-functionalization

without the presence of intramolecular oxidative addition. Comparison to Kumada CTP catalysts illustrated the need for small molecule screens to be tested over a range of starting material ratios. CTP catalysts displayed quantitative intramolecular oxidative addition independent to the starting material ratio, while the Sonogashira catalysts exhibited variance. This small molecule model system is currently being used to develop new conditions for electron-deficient monomers.

Chapter 5 describes our efforts at understanding the CTP mechanism and applying them towards new polymerization conditions. Future directions are outlined for each chapter, highlighting areas of needed research to address limited monomer scope of CTP. Additionally, relevant external papers that have been influenced by our work are also briefly discussed. We ultimately believe that mechanistic investigation of CTP is necessary to address the current limitations, namely limited monomer scope.

Chapter 1[1]

Introduction: Conjugated polymer synthesis via catalyst-transfer polycondensation (CTP): Mechanism, scope and applications

While most organic polymers are colorless insulators, a subset of polymers with a π-conjugated backbone can absorb/emit light as well as conduct charge. These polymers are utilized as the active layer in many optical and electronic devices.[1] Their commercial impact is expected to be significant, as it has been estimated that the conductive polymers market will reach 1.6 billion dollars in the US by 2017.[2] This growth can largely be traced back to the Nobel Prize-winning discovery by Shirakawa, MacDiarmid and Heeger that the simplest conjugated polymer, poly(acetylene), is conductive in the oxidized state.[3,4]

For decades the synthetic routes to soluble π-conjugated polymers were dominated by transition-metal catalyzed step-growth polymerizations and, as a result, little control could be exerted over the resulting polymer sequence. This landscape changed dramatically in 2004, when McCullough[5] and Yokozawa[6] independently identified a living, chain-growth method (now referred to as catalyst-transfer polycondensation (CTP)) for synthesizing poly(3-hexylthiophene) (Scheme 1.1). These initial reports sparked a flurry of activity in the field and more than 200 papers using CTP have been published since 2004.[7] The majority of these papers focused on: (i) gaining a mechanistic understanding of the chain-growth process, (ii) polymerizing other monomers, and (iii) synthesizing previously inaccessible materials, including gradient copolymers and surface-initiated polymers. This chapter will highlight the most significant advances in each of these areas, with a focus on the mechanistic studies, and discuss the current limitations.

---

[1] Adapted from Bryan, Z. J.; McNeil, A. J. "Conjugated Polymer Synthesis via Catalyst-transfer Polycondensation (CTP): Mechanism, Scope and Applications" *Macromolecules* **2013**, *46*, 8395-8405. Copyright 2013 American Chemical Society.

Scheme 1.1 CTP Discovery and Data

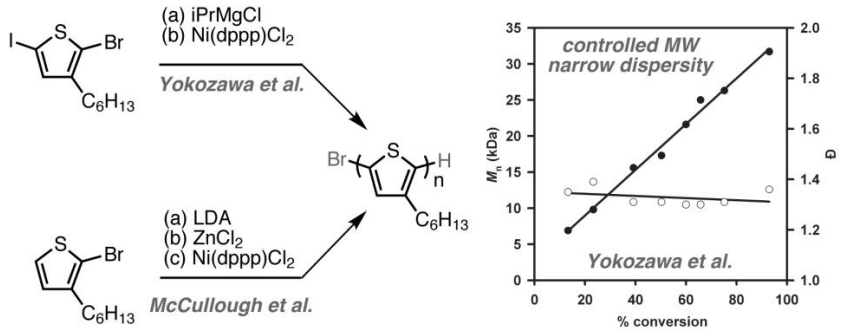

CTP Mechanism

Evidence for Chain-Growth. The first reports of poly(thiophene) synthesis using Ni catalysts and difunctional halo/Grignard monomers were by Yamamoto[8] and Lin[9] in 1980. A remarkable 24 years lapsed between these reports and the discovery that the mechanism is chain-growth.[5,6,10] This time lag can be attributed to the fact that the analogous small molecule reaction mechanism would predict a step-growth polymerization. Evidence of a living,[11] chain-growth polymerization provided by both McCullough[5] and Yokozawa[6] included: (i) linear correlations between the number-average molecular weight (M_n) and monomer conversion, (ii) the ability to control the M_n based on the monomer/catalyst ratio, and (iii) the creation of simple block copolymers via sequential monomer addition.

Chain Propagation via an Associative Complex. An early indication that the cross-coupling mechanism might be different for difunctional molecules was provided by Kumada and co-workers in 1976; they observed an unexpected double substitution reaction even with an excess of dichlorobenzene (Scheme 1.2).[12,13] This result suggested that after an initial cross-coupling, the Ni selectively reacts with the initial product a second time before consuming additional starting material. At the time, Kumada and co-workers simply stated that the second reaction is “mechanistically different” than the first, without proposing a specific pathway. In 2004, McCullough and co-workers also observed a preferential double substitution reaction with a dibromothiophene (Scheme 1.2).[5] Based on these observations, McCullough proposed that the

polymerization proceeds through a “nondiffusive associated pair”[14] between the Ni catalyst and the polymer, with a concomitant intramolecular oxidative addition.[5] Yokozawa suggested several potential mechanisms, including enhanced reactivity of the polymeric end group (relative to monomer) as well as polymer coordination to Ni via either a π-bond or the non-bonding electron pair on sulfur.[6] The majority of researchers in the field eventually gravitated toward a mechanism that proceeds through a Ni-polymer π-complex, which enables the active catalyst to stay associated with the growing polymer chain and facilitates chain propagation via an intramolecular oxidative addition (Scheme 1.3). The proposed mechanism seemed plausible because both arene- and alkene-based π-complexes with Ni have precedent in the literature[15] and several have been observed (or hypothesized) as intermediates in oxidative addition reactions.[16] Moreover, recent ^{13}C kinetic isotope effect measurements revealed that haloarene π-complexation to Ni(0) is the first irreversible step in small molecule cross-coupling reactions.[17]

Scheme 1.2 Preferential Double Substitution Reaction

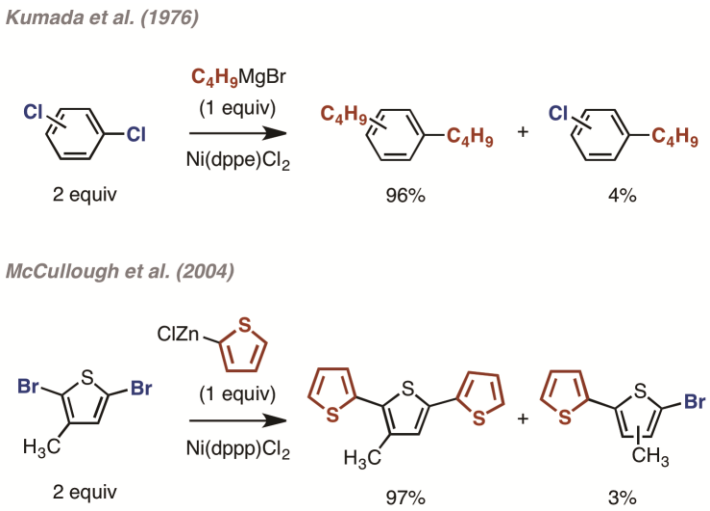

Support for Proposed Mechanism. McNeil and Lanni reported the first comprehensive mechanistic studies in 2009 and 2010.[18] Rate and spectroscopic studies were performed on the polymerizations of 4-bromo-2,5-bis(hexyloxy)phenylmagnesium chloride and 5-bromo-4-hexylthiophen-2-ylmagnesium chloride mediated by both $Ni(dppe)Cl_2$ and $Ni(dppp)Cl_2$. These

studies revealed that for both monomers the turnover-limiting step changes from transmetalation (with dppp (1,2-bis(diphenylphosphino)propane)) to reductive elimination (with dppe (1,2-bis(diphenylphosphino)ethane) as the ligand bite angle is altered. These studies also provided in-situ spectroscopic evidence for intermediates **II** and **III** in the proposed catalytic cycle (Scheme 1.3). The proposed Ni-polymer π-complex (**I**) was not observed because oxidative addition is not turnover-limiting with these monomer/catalyst combinations. Nevertheless, this work lent credence to the proposed mechanism and, importantly, eliminated other mechanistic possibilities including a Ni(I)/Ni(III) pathway championed by Kochi and Tsou.[19]

Scheme 1.3 Mechanism Proposed for Chain-Growth

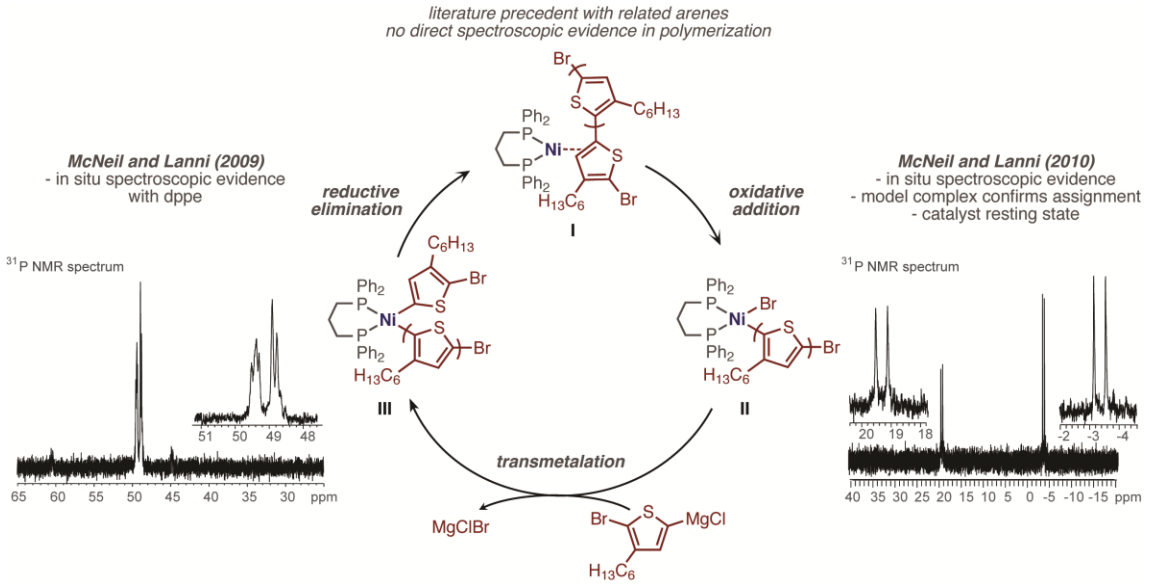

To date, there has not been any definitive evidence of a Ni-polymer π-complex forming during the polymerization.[20] However, several studies have shown that unactivated dihaloarene precursors, when present, are not significantly consumed during polymerization, consistent with an associative intermediate.[21] Compelling indirect evidence of an associative intermediate was provided by our group using competition experiments (Scheme 1.4).[22] Even though a high concentration of a more reactive competitive agent was utilized, the major products were from the intramolecular pathway. These small molecule

results were compared to the polymerizations under the same conditions, which revealed similar trends among the catalysts. These results will be discussed in greater detail in Chapter 2. Combined, these studies convincingly demonstrate that there is an associative intermediate with a subsequent intramolecular oxidative addition in the chain-growth polymerization. Whether this associative intermediate involves a η^2, η^4 or η^6 π-coordination to Ni(0), which undergoes oxidative addition via a two-electron pathway, or a caged radical pair that goes through a one-electron pathway, has not been distinguished at this time. Nevertheless, few definitive examples of the latter pathway exist,[19a] whereas Ni(0) π-complexes have precedent.[15,16]

Scheme 1.4 Indirect Evidence for Associative Intermediate

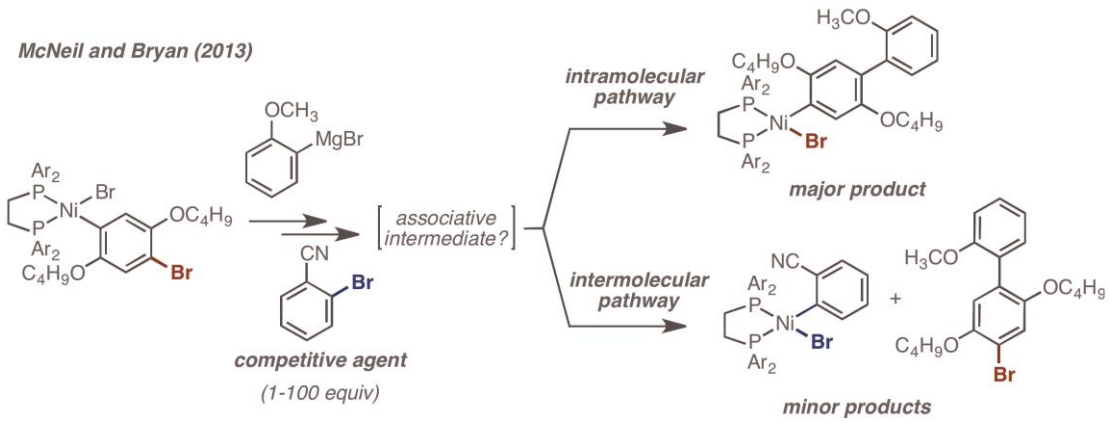

Limitation: Chain-Walking. Immediately following the initial reports, McCullough and co-workers made an unusual observation when end-capping their polymers: some Grignard reagents (e.g., CH_2=CHMgBr) led to mono-capped polymers while others (e.g., PhMgCl) led to di-capped polymers (Scheme 1.5).[23] They hypothesized that, following reduction elimination, the alkene- and alkyne-based end-groups formed irreversible π-complexes with Ni(0), thereby preventing further reaction. At the time, the di-capped polymer was presumed to form via an intermolecular reaction, though one could imagine the Ni(0) migrating to the other chain end in an intramolecular fashion via a series of π-complexes (i.e., chain-walking).

In 2010, Kiriy and co-workers provided compelling evidence of a chain-walking process during CTP: propagation from both ends of the polymer was observed when using a bromobenzene-functionalized Ni precatalyst (Scheme 1.5).[24] Because the Ni(0) walking along the polymer chain was not completely random, they concluded that the chemically distinct repeat units (e.g., thiophene versus phenyl) have different π-binding affinities for Ni(0).

The importance of chain-walking in copolymerizations cannot be overstated. Using the conventional L_nNiX_2 precatalysts allows propagation to occur at both chain ends. Thus, if sequence control is desired (e.g., in a diblock or gradient copolymer synthesis), Ni precatalysts with unfunctionalized reactive ligands must be utilized (vide infra). In retrospect, the chain-walking phenomenon explains the directional dependence observed in block copolymerizations when the monomers have different π-binding affinities;[25] that is, other competing pathways, such as chain-transfer and chain-termination can intervene before the desired intramolecular oxidative addition occurs at the chain end.

Scheme 1.5 Evidence for Ni(0) Chain-Walking

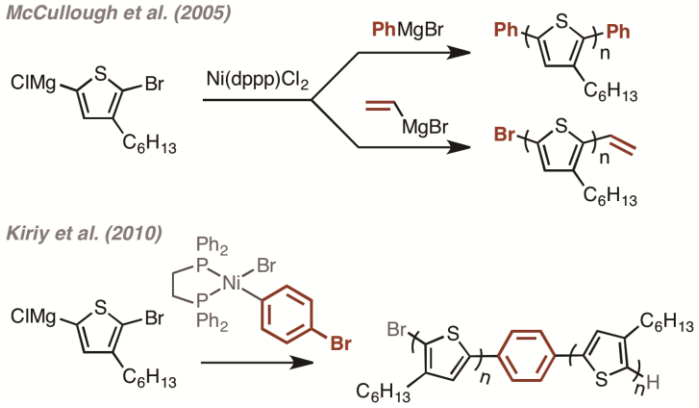

Limitation: Chain-Transfer and Chain-Termination. The presence of certain end-groups on the synthesized polymers (e.g., Br/Br and H/H starting from a L_nNiX_2 precatalyst) is indicative of competing reactions leading to chain-transfer and/or chain-termination. One such reaction involves the polymer being displaced from the Ni(0) by another molecule (e.g., solvent, monomer, oligomers, etc) in the π-complex. To date, this chain-transfer pathway has been considered relatively insignificant because numerous studies have shown that potentially

reactive species, such as 2,5-dibromo-3-hexylthiophene, do not get consumed during CTP.[21] An alternative reaction is disproportionation, wherein two Ni(II) catalysts swap ligands, generating L_nNiX_2 and $L_nNi(polymer)_2$ (Scheme 1.6). The latter complex undergoes reductive elimination to generate Ni(0) and a polymer with twice the expected molecular weight. In 2004, Yokozawa and co-workers suspected disproportionation occurred when neutral H_2O was used as the quenching reagent because the gel permeation chromatograms (GPC) were bimodal, and the M_n of the first eluting peak was approximately twice that of the second peak.[6b,26] Quenching with 5 M HCl resulted in unimodal chromatograms, suggesting that protonation was faster than this competing pathway. Quenching with strong acid is now standard within the field. Though experimental evidence of disproportionation has been circumstantial,[27] Locklin and co-workers recently provided computational support for this pathway using simplified model compounds.[28] Overall, chain-transfer or chain-termination reactions are indicative of non-living polymerizations, and if present, factors like the copolymer sequence can no longer be controlled.

Scheme 1.6 Disproportionation Pathway

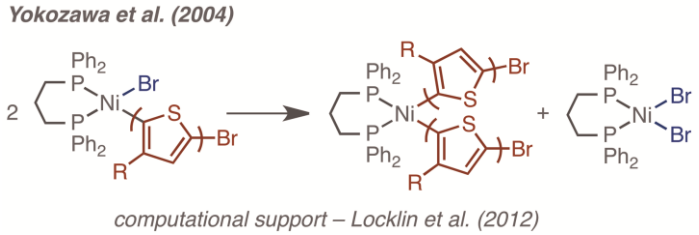

Limitation: Slow Initiation. The molecular weight dispersities (Đ) for most of these chain-growth polymerizations are significantly greater than the ideal 1.0. While chain-transfer and chain-termination are contributing factors, another source of broad Đ is the slow rate of precatalyst initiation relative to propagation. Slow initiation has been documented in several CTPs.[29] One notable example is that the "minor" thiophene regioisomer ((5-bromo-3-hexylthiophen-2-yl)magnesium chloride) exhibits negligible initiation rates with $Ni(dppe)Cl_2$ due to steric effects, which can be overcome using Ni(dppe)PhCl.[29c] In 2011, McNeil and co-workers first observed a product of initiation ($L_nNi(aryl)_2$ –

generated via reaction of monomer with L_nNiCl_2) persisting well into the polymerization, bringing slow initiation to center stage.[27] In 2012, the relative reaction rates were measured, revealing that initiation is approximately 20x slower than propagation for a conventional metal/ligand combination (Ni/dppe).[29b] In this case, selectively accelerating initiation was challenging because rate studies revealed that the turnover-limiting step for both initiation and propagation was reductive elimination (Scheme 1.7). Thus, modifying the ancillary ligand (e.g., the bidentate phosphine) will have a similar effect on both reaction rates. The solution involved modifying the reactive ligand (i.e., Ar in Scheme 1.7) to selectively accelerate the reductive elimination during initiation and leave the propagation rate unchanged.[29a] Because the same ancillary ligand was used, these studies provided a direct measure of the impact of initiation; the slowest initiators gave a Đ = 2.13 while the fastest initiator resulted in a Đ = 1.12 at the same conversion. Therefore, the impact of initiation on the polymer Đ should not be underestimated.

Scheme 1.7 Reactive Ligands Selectively Accelerate Initiation

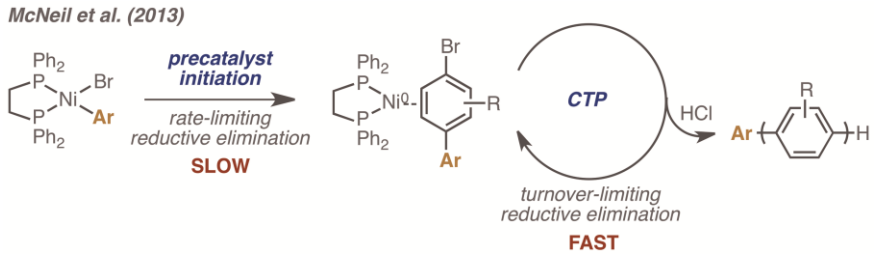

Catalyst Design: Ancillary Ligands. While a handful of monodentate phosphines,[30] carbenes[21a] and diimines[31] have been used in CTP, the vast majority of polymerizations use bidentate phosphines.[32] The steric and electronic properties of these phosphines can be tuned by modifying the substituents on phosphorus. McNeil and co-workers examined the impact of ligand steric properties and found that the chain-growth pathway was easily derailed when the ligand steric contribution was too little (e.g., with 1,2-bis(dimethylphosphino)ethane) or too much (e.g., with (1,2-bis(dicyclohexylphosphino)ethane), which was attributed to catalyst

decomposition and π-complex disruption, respectively.[27] In terms of ligand electronic properties, electron-rich ligands were expected to promote π-complex formation through donation of electron density from the metal into the arene LUMO.[33] Indeed, McNeil and co-workers have demonstrated that the electron-rich ligands consistently outperform the electron-poor analogues.[22,27,29b] Nevertheless, because most of these polymerizations proceed through a turnover-limiting reductive elimination, the increased electron density slows down the propagation rate and, as a consequence, quenching by adventitious moisture can be problematic.

Scheme 1.8 Electron-Rich Ancillary Ligands Promote Chain-Growth

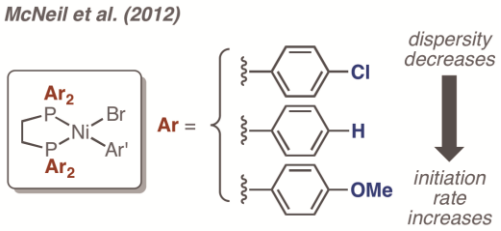

Catalyst Design: Reactive Ligands. Because the L_nNiCl_2 salts are largely insoluble in THF at the concentrations required for polymerization, many researchers began utilizing $L_nNi(Ar)X$ as soluble alternatives. These so-called reactive ligands have many additional advantages, such as providing specific end-capping groups on polymers,[34] ensuring unidirectional propagation for sequence control, [35] and enabling polymers to grow off of surfaces.[36] Reactive ligands can also be used to modify initiation rates.[29a]

Luscombe and co-workers were the first to introduce these functionalized precatalysts in 2009.[37] They postulated that including an *ortho* methyl substituent would stabilize the precatalyst species by forcing the arene into an orientation where the π* orbital overlaps with the d_{xy} orbital on Ni, which lowers the HOMO and decreases reactivity.[38] On the other hand, Kiriy and co-workers have had success with the unsubstituted $L_nNi(Ph)X$, particularly with sterically congested monomers.[29c] Ultimately, it is important that the substituent, if included, is not too large such that it hinders transmetalation during initiation.[39] Both Luscombe and Kiriy prepared these precatalysts in situ, and as a consequence, the reaction

mixtures often contained impurities, including uncoordinated Ph_3P or bpy, chelating ligand, and the bis-chelated Ni(II) complex. Though less convenient, isolating and purifying the precatalysts will ensure that no other catalytic species are present during both initiation and propagation. Overall, given the many advantages of using reactive ligands, we suspect that their frequency will only increase in the future.

Catalyst Design: Palladium versus Nickel. While Ni has remained a popular metal for CTP, the last five years have witnessed a substantial growth in reports of Pd-catalyzed chain-growth polymerizations. As highlighted in Chart 1.1, Pd precatalysts ligated with hindered carbenes[21a] and bulky, monodentate phosphines[21b,30a-g] have exhibited chain-growth behavior. Overall, the scope of these Pd-catalyzed polymerizations has been broader than Ni[40] and cross-propagation between two chemically different monomers has been demonstrated.[21a] Nevertheless, many of these polymerizations produced polymers with low molecular weights, broad dispersities, and a multitude of end-groups. A particular successful Pd-NHC catalyst is discussed in much greater detail in Chapter 3. Although the chain-growth mechanisms remain to be elucidated in most cases, Pd-based CTPs represent an emerging area for this field.

Chart 1.1 Selected Pd Precatalysts in CTP

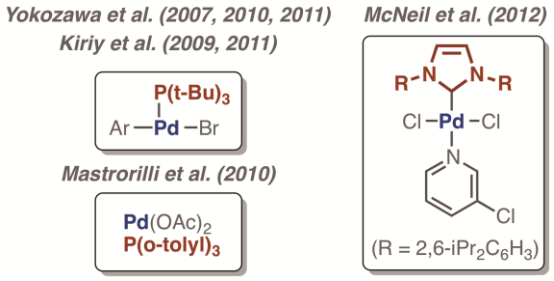

Additives. To date, several additives have been shown to improve the chain-growth polymerization behavior of certain monomers. For example, lithium chloride, which is known to accelerate Grignard metathesis reactions,[41] is frequently present during polymerizations. Although Yokozawa included LiCl in the initial polymerization reported in 2004,[6] it was not until 2006 that its impact on

the polymerization was noted.[42] Since then, LiCl has been known to both accelerate and decelerate the polymerization rate,[18,26,29d] increase the reactivity of sterically hindered monomers,[43] and improve the controlled,[44] chain-growth nature of the polymerization.[45] The mechanism(s) to explain these results have not been elucidated, but there are several possibilities: (1) LiCl forms mixed aggregates with the monomer and modifies its reactivity. (2) LiCl mediates a Br to Cl transformation on the Ni(II) catalyst, which facilitates transmetalation due to its smaller atomic size. Regardless of the mechanistic details, it is clear that LiCl is non-innocent, and as a consequence, its presence and concentration should be varied when optimizing polymerizations with different monomers and catalysts.

The ancillary and reactive ligand can also serve as a beneficial additive in CTP. For example, Yokozawa and co-workers found that an additional equiv of phosphine ligand (relative to Ni) led to narrower molecular weight distributions in synthesizing poly(*N*-hexylpyrrole), although the mechanistic role was not elucidated.[45a] In another example, Wang and co-workers found that Ni(dppp)$(acac)_2$ was superior to Ni(dppp)Cl_2 for polyfluorene synthesis.[32c] The improved polymerization behavior suggests a non-innocent role of the acac ligand during propagation since both acac ligands should be displaced from the catalyst during the initiation. Further studies are needed to determine whether the acac displaces the halogen after oxidative addition, stabilizes the π-complex, or serves some other mechanistic role.

Mechanism: Summary and Outlook. The past ten years have witnessed a tremendous growth in CTP-based mechanistic studies. Beyond providing a window into the polymerization mechanism, these studies have informed the design of new catalysts and reaction conditions. While some mechanistic details remain elusive, we are optimistic about the future. Moreover, as new monomers/catalysts/conditions are introduced, new mechanistic questions will undoubtedly arise, fueling more activity in this area.

CTP: Scope

Electron-Rich Monomers. To date, the vast majority of reported chain-growth polymerizations involve electron-rich monomers. Among this class of compounds, thiophene derivatives are the most abundant (Chart 1.2).[46] For example, carbon-, oxygen- and sulfur-based side-chains have been incorporated to modify the polymer's physical, optical and electronic properties. Thiophene analogues – selenophene,[47,48] tellurophene[32a] and pyrrole[49] – have also been successfully polymerized using CTP. Regioregular polymers can be prepared if (a) the monomer forms as a single regioisomer or (b) the two regioisomers are consumed at different rates due to steric interactions with the ancillary ligand on the catalyst. Although the mechanism for each of these derivatives has been assumed to be same as the one proposed for 3-hexylthiophene (see Scheme 1.3), the fact that each monomer/catalyst combination provides polymers varying Đ and end-group fidelity suggests that the impact of chain-walking, chain-transfer, chain-termination and initiation is different in each case. Until detailed mechanistic studies are performed on each system, this variability in polymerization results cannot be readily understood.

Chart 1.2 Selected Polymers Containing Thiophene or Related Compounds Synthesized via CTP

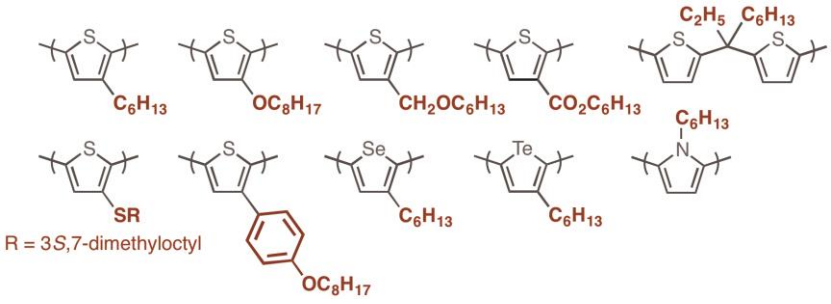

The first non-thiophene-based monomer to undergo CTP was dialkoxyphenylene, which was reported by Yokozawa and co-workers in 2006 (Chart 1.3).[42] Although commercial applications of poly(*p*-phenylene)s remain limited, this discovery was important because it suggested that the chain-growth method could be expanded to other monomers. Moreover, this result suggested

that CTP does not require sulfur coordination to Ni, as originally postulated by Yokozawa.[6] A closely related analogue, dialkylfluorene, was next discovered to undergo CTP.[21b,50] Poly(fluorene)s are used commercially as the blue emitter in light-emitting diodes. The initial reports revealed that the fluorene polymerizations were less controlled, with a variety of end-groups being observed, suggesting chain-transfer and chain-termination reactions were prevalent. A breakthrough was reported in 2012, when Wang and co-workers used (dppp)Ni(acac)$_2$ to synthesize poly(9,9-dioctylfluorene) with high molecular weight and narrow Đ.[32c] In 2012, Bielawski and co-workers utilized a monomer containing both phenylene and thiophene to synthesize an alternating copolymer.[25a]

Excitingly, the CTP method was recently expanded to prepare poly(fluorenylene vinylene)s (PFVs)[51] and poly(*p*-phenylene ethynylene)s (PPEs),[40a] respectively (Chart 1.3). Although the mechanisms remain to be elucidated, the chain-growth behavior is not surprising considering that both alkenes and alkynes are known to form π-complexes with Ni(0).[15] With further development in this area, we anticipate that these chain-growth methods could displace the traditional synthetic routes to PPVs and PPEs. Work in our lab focusing on the synthesis of PPE is highlighted in Chapter 4.

Chart 1.3 Selected Electron-Rich Polymers Synthesized via CTP

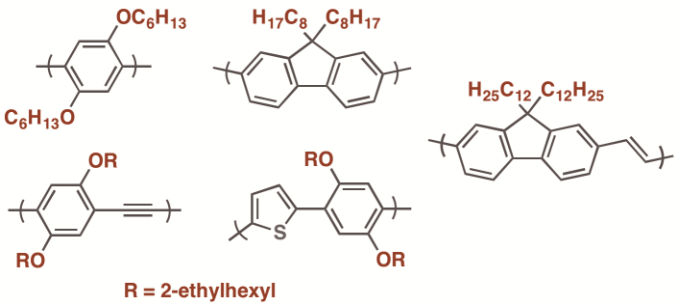

Electron-Deficient Monomers. To date, few chain-growth polymerizations of electron-deficient monomers have been reported (Chart 1.4).[52,31c] Because failed results often go unpublished, the rationale for this scarcity is unknown. From a mechanistic perspective, both the transmetalation and reductive elimination steps will be significantly slower with an electron-

deficient monomer, which can drastically impact the initiation rate. On the other hand, the π-binding between Ni (or Pd) and an electron-deficient monomer should be strong,[53] and oxidative addition will be accelerated, both of which would promote the chain-growth pathway and minimize the competing chain-transfer reactions. The inability to polymerize most electron-deficient monomers represents a significant limitation in the field as copolymerizing these monomers with their electron-rich counterparts provides access to low band gap donor-acceptor materials, with applications in organic solar cells.

In 2008, Rasmussen and co-workers reported polymerizing thienopyrazine monomers using the CTP method; however, the low molecular weight and relatively broad Đ of the isolated polymers suggests the polymerization is uncontrolled and possibly non-living.[52c] In 2011 and 2012, Kiriy and co-workers suggested that the Ni-catalyzed polymerization of a naphthalene diimide monomer was chain-growth, though the broad molecular weight distributions suggested several competing side-reactions.[16a,52b] The mechanism proposed involves an unusual reductive coupling step, stemming from the observed formation of a radical anion upon Zn-mediated activation of the monomer. It will be challenging to expand this method to other monomers without a more detailed understanding of the reaction mechanism. In 2011, Kiriy and co-workers also reported the successful polymerization of a benzothiazole monomer using Pd as the catalyst.[30d] The key to their success involved sandwiching an electron-rich and solubilizing fluorene ring between two benzothiazole units. Although high molecular weight polymers were not obtained, this approach of combining an electron-rich and electron-poor monomer can lead to low band gap materials.

The first and only electron-deficient monomer to be homopolymerized in a living, controlled chain-growth fashion is based on the pyridine scaffold, which was reported in 2012 by Yokozawa and co-workers.[32d,32e,52a] Using a clever experiment, the authors identified chain-growth conditions by looking for selective difunctionalization in an analogous small molecule reaction, similar to the Kumada[12] and McCullough[5] experiments (see Scheme 1.2). Typical of many polymerizations in this field, the resulting molecular weights, Đ, and end-groups

varied dramatically depending on catalyst, monomer activation method, presence of LiCl, and nature (and location) of the substituents. Although poly(pyridine)s have limited commercial impact, the method used to identify the chain-growth conditions has merit and should be utilized more in the future. A more general approach to discovering new chain-growth techniques is explored in much greater detail in Chapter 4.

Chart 1.4 Selected Electron-Deficient Polymers Synthesized via CTP

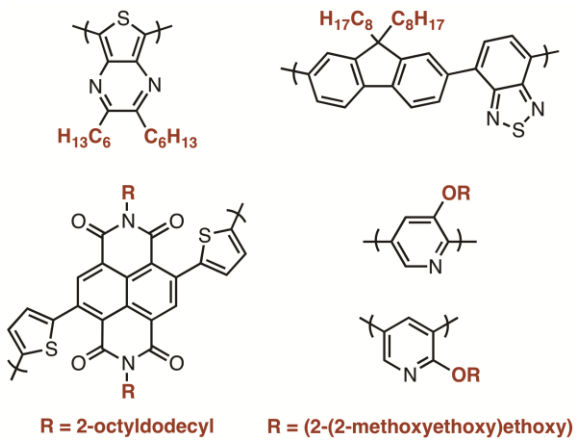

Scope: Summary and Outlook. The last decade has witnessed a tremendous growth in the variety of monomers that can undergo CTP. This achievement is made even more remarkable considering that the chain-growth mechanism(s) are still being elucidated. Many of these advances have been somewhat serendipitous as catalysts and conditions are screened for each monomer. Despite all this progress, the polymerization of electron-poor monomers remains a significant challenge. In addition, among the reported examples of CTP, there is a need for more controlled polymerizations that reproducibly give high molecular weight polymers with narrow dispersities and a single set of end-groups. We suspect that the number of failed experiments exceeds the successes, and because the failed results are often unpublished, it has been difficult to identify the mechanistic bottleneck. As such, we anticipate that a greater mechanistic understanding will lead to the discovery of new catalysts and conditions and, ultimately, the synthesis of new materials.

CTP: Applications

Block and Gradient Sequence Copolymers. Chain-growth methods that are both living and controlled can be used to synthesize copolymers with specific sequences, including blocks and gradients. Using CTP, copolymers containing conjugated/non-conjugated blocks[54] as well as conjugated/conjugated blocks[55] have been prepared (Chart 1.5). The all-conjugated block copolymers are synthesized via sequential monomer addition, wherein one monomer is added after the other monomer is completely consumed. Because chain-walking and chain-transfer reactions can be significant with specific catalyst/comonomers combinations, one needs to carefully select the monomer addition order for the best results. Most of these all-conjugated block copolymers are semicrystalline and self-assemble into lamellar morphologies. These solid-state structures are of interest because they facilitate charge separation and conduction in organic solar cells.

Several diblock copolymers containing both conjugated and non-conjugated segments have been prepared using CTP.[54] The non-conjugated block is usually initiated from the end-group of the conjugated block in a second step. This reactive end-group is installed in the first step via the reactive ligand in the initial precatalyst or as a quenching agent at the end of polymerization. Non-conjugated blocks are utilized to increase the copolymer solubility and influence the solid-state structure, however, these advantages can be offset by a decrease in conductivity due to the insulating properties of this block. In 2012, Bielawski and co-workers reported a streamlined approach that uses the same Ni catalyst for both blocks, however, this approach is limited to monomers that can be polymerized using Ni(II) or Pd(II) catalysts.[49a]

McNeil and Locke were the first to prepare all-conjugated gradient copolymers using CTP.[35b] To date, only thiophene/thiophene[35b,c] and thiophene/selenophene[35a] gradient sequence copolymers have been synthesized due to difficulties with cross-propagation among chemically distinct comonomers (Chart 1.5). In these examples, the comonomer reactivity ratios were close to 1, which means that the gradient sequence can only be generated via syringe pump

addition of one monomer into the catalyst/comonomer mixture. Compared to the analogous block and random copolymers with similar compositions, molecular weights, and Đ, the gradient copolymers have unique solid-state thermal properties and morphologies.[35] Moreover, the gradient copolymers have superior phase-compatibilizing properties when added to the homopolymer blend.[35c,d] An emerging theme from this research is that sequence matters and we anticipate that, as the diversity of comonomers increases, this subfield of conjugated copolymers will gain prominence.

Chart 1.5 Selected Block and Gradient Copolymers Synthesized via CTP

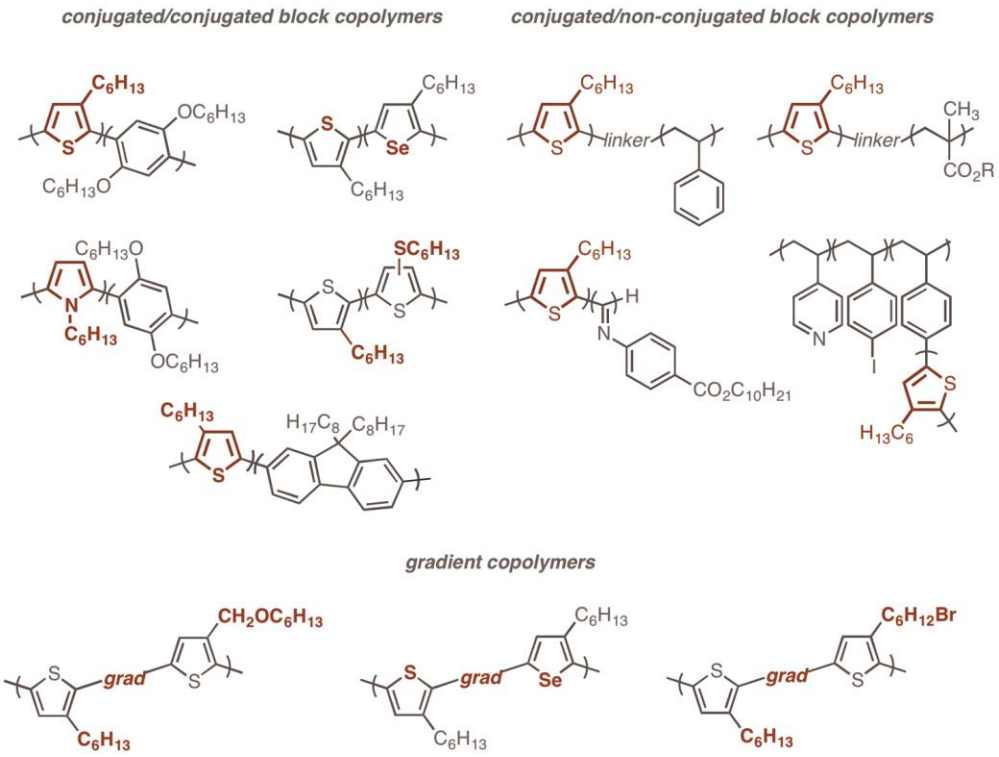

Surface-Initiated Polymerizations. In most device configurations, conjugated polymers are deposited as thin films onto metal or oxide surfaces. This interface can have a substantial impact on the overall device performance.[56] As a consequence, an alternative approach wherein the polymerizations are initiated from the metal or glass surface has recently gained attention. To date, several conjugated polymers have been synthesized using CTP from initiators that are covalently bonded to silica, indium tin oxide, gold, or polystyrene (Chart

1.6).[57] In each example, a surface-bound precatalyst is first prepared by reacting Ni(0) or Pd(0) with a surface-bound aryl-halide, from which the polymerization is initiated. Locklin and co-workers showed that, in practice, this approach is limited because high surface densities of catalyst lead to intermolecular disproportionation reactions.[36b] Although film thickness can be controlled, the surface coverage is uneven, limiting its practical application.

Branched Polymers. To date, only a handful of polymers with non-linear scaffolds have also been prepared via CTP. Kiriy[34e] and Luscombe[34a] independently reported star-shaped poly(thiophene) synthesis using a central core molecule that is functionalized with multiple Ni initiators (Chart 1.6). Kiriy and co-workers used Ni(bpy)-based initiators which led to broad Đ (1.98),[34e] while Luscombe and co-workers used Ni(dppp)-based initiators and obtained polymers with narrow Đ (1.15).[34a] These results are consistent with the fact that Ni(dppp)Cl_2 is a superior precatalyst for the linear poly(thiophene) synthesis.[36e] In related work, Bo and co-workers used AB_2 monomers containing non-conjugated linkers to generate a hyperbranched polymer using Pd.[58] This example is noteworthy because the degree of branching was 100%, indicating that catalyst transfer across the non-conjugated linker is highly efficient. Recently, Luscombe and co-workers reported an efficient route to hyperbranched polymers[36a] using direct arylation (rather than a preformed organometallic group).[40b]

Chart 1.6 Selected Grafted and Branched Polymers Synthesized via CTP

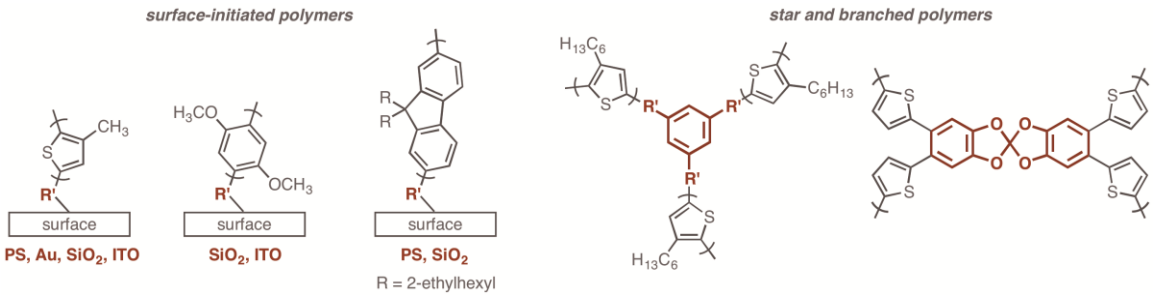

Applications: Summary and Outlook. While a number of novel polymer architectures have been accessed using CTP, the impact of these materials in real world applications (e.g., solar cells and light-emitting diodes) has been limited by the narrow scope of monomers used. Nevertheless, many of these

new materials have exhibited new and exciting properties, fueling the desire for continued development in this area. With improvements in catalyst design and monomer scope, we suspect that this research area will increase in the next decade.

Conclusions

Nearly a decade has passed since the discovery of CTP by McCullough[5] and Yokozawa.[6] As highlighted, a substantial number of researchers have contributed to unveil key aspects about the chain-growth mechanism, expand the monomer scope, and synthesize new materials. In the following chapters, specific contributions we have made will be explored in greater detail. First we will examine preferential intramolecular oxidative addition in CTP (Chapter 2). The methodology used to examine this associative complex led us to discover a new chain-growth Pd-NHC catalyst which is outlined in Chapter 3. Finally, the lessons from these previous studies guided us to design a more general approach to discovering novel chain-growth conditions, and the successes and failures of this methodology are discussed in Chapter 4. Nevertheless, each of these foci needs further development for this method to make a significant impact on the greater scientific community, analogous to the living, controlled radical polymerizations like ATRP, RAFT, and NMP. Future studies should focus on broadening the scope of monomers capable of undergoing CTP by exploring alternative metals, ligands, additives, and transmetalating agents. More generally, a greater mechanistic understanding of “failed” polymerizations should guide these efforts. CTP has already enabled access to exciting, new materials (e.g., surface-grown polymers and gradient copolymers), and it has the potential to completely transform conjugated polymers from a niche material to one that is widely used by chemists, biologists, and engineers.

References

(1) (a) Yeh, N.; Yeh, P. *Renew. Sust. Energ. Rev.* **2013**, *21*, 421–431. (b) Cataldo, S.; Pignataro, B. *Materials* **2013**, *6*, 1159–1190. (c) Li, G.; Zhu, R.; Yang, Y. *Nat. Photonics* **2012**, *6*, 153–161. (d) Boudreault, P.-L. T.; Najari, A.; Leclerc, M. *Chem. Mater*. **2011**, *23*, 456–469. (e) Facchetti, A. *Chem. Mater*. **2011**, *23*, 733–758

(2) Polymer Solutions Newsblog, Demand Grows for Conductive Polymers. http://www.polymersolutions.com/blog/demand-grows-for-conductive-polymers/ (accessed May 20, 2013).

(3) (a) Shirakawa, H.; Louis, E. J.; MacDiarmid, A. G.; Chiang, C. K.; Heeger, A. J. *J. Chem. Soc., Chem. Commun.,* **1977**, 578–580. (b) Chiang, C. K.; Fincher, C. R.; Park, Y. W.; Heeger, A. J.; Shirakawa, H.; Louis, E. J.; Gau S. C.; MacDiarmid, A. G. *Phys. Rev. Lett*. **1977**, *39*, 1098–1101. (c) Chiang, C. K.; Druy, M. A.; Gau, S. C.; Heeger, A. J.; Louis, E. J.; MacDiarmid, A. G.; Park, Y. W.; Shirakawa, H. *J. Am. Chem. Soc.* **1978**, *100*, 1013–1015.

(4) (a) Heeger, A. J. *Rev. Mod. Phys.* **2001**, *73*, 681–700. (b) MacDiarmid, A. G. *Rev. Mod. Phys.* **2001**, *73*, 701–712. (c) Shirakawa, H. *Rev. Mod. Phys.* **2001**, *73*, 713–718.

(5) Sheina, E. E.; Liu, J. S.; Iovu, M. C.; Laird, D. W.; McCullough, R. D. *Macromolecules* **2004**, *37*, 3526–3528.

(6) (a) Yokoyama, A.; Miyakoshi, R.; Yokozawa, T. *Macromolecules* **2004**, *37*, 1169–1171. (b) Miyakoshi, R.; Yokoyama, A.; Yokozawa, T. *Macromol. Rapid Commun*. **2004**, *25*, 1663–1666.

(7) For related reviews, see: (a) Yokozawa, T.; Nanashima, Y.; Ohta, Y. *ACS Macro. Lett.* **2012**, *1*, 862–866. (b) Marrocchi, A.; Lanari, D.; Facchetti, A.; Vaccaro, L. *Energy Environ. Sci.* **2012**, *5*, 8457–8474. (c) Stefan, M. C.; Bhatt, M. P.; Sista, P.; Magurudeniya, H. D. *Polym. Chem.* **2012**, *3*, 1693–1701. (d) Kiriy, A.; Senkovskyy, V.; Sommer, M. *Macro. Rapid Commun*. **2011**, *32*, 1503–1517. (e) Okamoto, K.; Luscombe, C. K. *Polym. Chem.* **2011**, *2*, 2424–2434. (f) Yokozawa, T.; Yokoyama, A. *Chem. Rev.* **2009**, *109*, 5595–5619. (g) Osaka, I.; McCullough, R. D. *Acc. Chem. Res.* **2008**, *41*, 1202–1214. (h) Miyakoshi, R.; Yokoyama, A.; Yokozawa, T. *J. Polym. Sci. Pol. Chem.* **2008**, *46*, 753–765. (i) Yokoyama, A.; Yokozawa, T. *Macromolecules* **2007**, *40*, 4093–4101. (j) Higashihara, T.; Ueda, M. *Macromol. Res.* **2013**, *21*, 257-271.

(8) Yamamoto, T.; Sanechika, K.; Yamamoto, A. *J. Polym. Sci., Polym. Lett. Ed.* **1980**, *18*, 9–12.

(9) Lin, J. W.-P.; Dudek, L. P. *J. Polym. Sci., Polym. Chem. Ed*. **1980**, *18*. 2869–2873.

(10) The IUPAC definition of a chain polymerization is “a chain reaction in which the growth of a polymer chain proceeds exclusively by reaction between monomer and reactive site(s) on the polymer chain with regeneration of the reactive site(s).” For reference, see: McNaught, A. D.; Wilkinson, A. *IUPAC. Compendium of Chemical Terminology [Online]*; 2nd Ed.; Blackwell Scientific Publications: Oxford, 1997. http://goldbook.iupac.org (accessed June 20, 2013).

(11) The IUPAC definition of a living polymerization is “a chain polymerization from which chain transfer and chain termination are absent.” For reference, see: McNaught, A. D.; Wilkinson, A. *IUPAC. Compendium of Chemical Terminology [Online]*; 2nd Ed.; Blackwell Scientific Publications: Oxford, 1997. http://goldbook.iupac.org (accessed June 20, 2013).

(12) Tamao, K.; Sumitani, K.; Kiso, Y.; Zembayashi, M.; Fujioka, A.; Kodama, S.; Nakajima, I.; Minato, A.; Kumada, M. *Bull. Chem. Soc. Jpn*. **1976**, *49*, 1958–1969.

(13) Preferential double substitution reactions have also been observed with Pd catalysts. For examples, see: (a) Larrosa, I.; Somoza, C.; Banquy, A.; Goldup, S. M. *Org. Lett*. **2011**, *13*, 146–149. (b) Guillén, E.; Hierrezuelo, J.; Martinez-Mallorquin, R.; Lopez-Romero, M.; Rico, R. *Tetrahedron* **2011**, *67*, 2555–2561.

(14) McCullough began using “π-complex” terminology in 2005. For reference, see: Iovu, M. C.; Sheina, E. E.; Gil, R. R.; McCullough, R. D. *Macromolecules* **2005**, *38*, 8649–8656.

(15) For recent examples, see: (a) Sylvester, K. T.; Wu, K.; Doyle, A. G. *J. Am. Chem. Soc.* **2012**, *134*, 16967–16970. (b) Ge, S.; Hartwig, J. F. *J. Am. Chem. Soc.* **2011**, *133*, 16330–16333. (c) Johnson, S. A.; Huff, C. W.; Mustafa, F.; Saliba, M. *J. Am. Chem. Soc.* **2008**, *130*, 17278–17280. (d) Garcia, J. J.; Brunkan, N. M.; Jones, W. D. *J. Am. Chem. Soc.* **2002**, *124*, 9547–9555. (e) Braun, T.; Cronin, L.; Higgitt, C. L.; McGrady, J. E.; Perutz, R. N.; Reinhold, M. *New J. Chem.* **2001**, *25*, 19–21. (f) Boese, R.; Stanger, A.; Stellberg, P.; Shazar, A. *Angew. Chem. Int. Ed.* **1993**, *32*, 1475–1477. (g) Benn, R.; Mynott, R.; Topalović, I.; Scott, F. *Organometallics*, **1989**, *8*, 2299–2305.

(16) For recent examples, see: (a) Senkovskyy, V.; Tkachov, R.; Komber, H.; John, A.; Sommer, J.-U.; Kiriy, A. *Macromolecules* **2012**, *45*, 7770−7777. (b) Hatnean, J. A.; Johnson, S. A. *Organometallics* **2012**, *31*, 1361–1373. (c) Li, T.; García, J. J.; Brennessel, W. W.; Jones, W. D. *Organometallics* **2010**, *29*, 2430–2445. (d) Zenkina, O. V.; Karton, A.; Freeman, D.; Shimon, L. J. W.; J. M. L. Martin, L. J. W.; van der Boom, M. E. *Inorg. Chem.*, **2008**, *47*, 5114–5121.

(17) (a) Yoshikai, N.; Matsuda, H.; Nakamura, E. *J. Am. Chem. Soc.* **2009**, *131*, 9590–9599. (b) Yoshikai, N.; Matsuda, H.; Nakamura, E. *J. Am. Chem. Soc*. **2008**, *130*, 15258–15259.

(18) (a) Lanni, E. L.; McNeil, A. J. *Macromolecules* **2010**, *43*, 8039–8044. (b) Lanni, E. L.; McNeil, A. J. *J. Am. Chem. Soc.* **2009**, *131*, 16573–16579.

(19) (a) Tsou, T. T.; Kochi, J. K. *J. Am. Chem. Soc.* **1979**, *101*, 6319–6332. (b) Tsou, T. T.; Kochi, J. K. *J. Am. Chem. Soc.* **1979**, *101*, 7547–7560.

(20) (a) In a somewhat unconventional system, Kiriy and co-workers reported formation of a Ni(0) π-complex with an unfunctionalized naphthalene diimide; however, the spectra acquired during polymerization were not a complete match. See reference 16a. (b) See also: Komber, H.; Senkovskyy, V.; Tkachov, R.; Johnson, K.; Kiriy, A.; Huck, W. T. S.; Sommer, M. *Macromolecules* **2011**, *44*, 9164–9172.

(21) For examples, see: (a) Bryan, Z. J.; Smith, M. L.; McNeil, A. J. *Macromol. Rapid Comm.* **2012**, *33*, 842–847. (b) Yokoyama, A.; Suzuki, H.; Kubota, Y.; Ohuchi, K.; Higashimura, H.; Yokozawa, T. *J. Am. Chem. Soc.* **2007**, *129*, 7236–7237. (c) Beryozkina, T.; Senkovskyy, V.; Kaul, E.; Kiriy, A. *Macromolecules* **2008**, *41*, 7817–7823. (d) See also, reference 22.

(22) Bryan, Z. J.; McNeil, A. J. *Chem. Sci.* **2013**, *4*, 1620–1624.

(23) (a) Jeffries-EL, M.; Sauvé, G.; McCullough, R. D. *Macromolecules* **2005**, *38*, 10346–10352. (b) Jeffries-EL, M.; Sauvé, G.; McCullough, R. D. *Adv. Mater*. **2004**, *16*, 1017–1019.

(24) Tkachov, R.; Senkovskyy, V.; Komber, H.; Sommer, J.-U.; Kiriy, A. *J. Am. Chem. Soc*. **2010**, *132*, 7803–7810.

(25) (a) Ono, R. J.; Kang, S. S.; Bielawski, C. W. *Macromolecules* **2012**, *45*, 2321–2326. (b) Wu, S. P.; Bu, L. J.; Huang, L.; Yu, X. H.; Han, Y. C.; Geng, Y. H.; Wang, F. S. *Polymer* **2009**, *50*, 6245–6251. (c) Miyakoshi, R.; Yokoyama, A.; Yokozawa, T. *Chem. Lett*. **2008**, *37*, 1022–1023.

(26) Neutral methanol as a quenching reagent has also been shown to give disproportionation. For reference, see: Lohwasser, R. H.; Thelakkat, M. *Macromolecules* **2011**, *44*, 3388–3397.

(27) The sudden formation of $LnNiBr_2$ and $LnNiCl_2$ at the end of a polymerization is consistent with a disproportionation mechanism. For a recent example, see: Lanni, E. L.; Locke, J. R.; Gleave, C. M.; McNeil, A. J. *Macromolecules* **2011**, *44*, 5136–5145.

(28) Bilbrey, J. A.; Sontag, S. K.; Huddleston, N. E.; Allen, W. D.; Locklin, J. *ACS Macro Lett.* **2012**, *1*, 995–1000.

(29) For examples, see: (a) Lee, S. R.; Bloom, J. W. G.; Wheeler, S. E.; McNeil, A. J. *Dalton Trans.* **2013**, *42*, 4218–4222. (b) Lee, S. R.; Bryan, Z. J.; Wagner, A. M.; McNeil, A. J. *Chem. Sci*. **2012**, *3*, 1562–1566. (c) Tkachov, R.; Senkovskyy,

V.; Komber, H.; Kiriy, A. *Macromolecules* **2011**, *44*, 2006–2015. (d) Lamps, J.-P.; Catala, J.-M. *Macromolecules* **2011**, *44*, 7962–7968. (e) Wu, S. P.; Huang, L.; Tian, H. K.; Geng, Y. H.; Wang, F. S. *Macromolecules* **2011**, *44*, 7558–7567.

(30) For examples, see: (a) Zhang, H. H.; Xing, C. H.; Hu, Q. S. *J. Am. Chem. Soc.* **2012**, *134*, 13156–13159. (b) Huddleston, N. E.; Sontag, S. K.; Bilbrey, J. A.; Sheppard, G. R.; Locklin, J. *Macromol. Rapid Comm.* **2012**, *33*, 2115–2120. (c) Yokozawa, T.; Suzuki, R.; Nojima, M.; Ohta, Y.; Yokoyama, A. *Macromol. Rapid Comm.* **2011**, *32*, 801–806. (d) Elmalem, E.; Kiriy, A.; Huck, W. T. S. *Macromolecules* **2011**, *44*, 9057–9061. (e) Verswyvel, M.; Verstappen, P.; De Cremer, L.; Verbiest, T.; Koeckelberghs, G. *J. Polym. Sci. Pol. Chem.* **2011**, *49*, 5339–5349. (f) Yokozawa, T.; Kohno, H.; Ohta, Y.; Yokoyama, A. *Macromolecules* **2010**, *43*, 7095–7100. (g) Beryozkina, T.; Boyko, K.; Khanduyeva, N.; Senkovskyy, V.; Horecha, M.; Oertel, U.; Simon, F.; Stamm, M.; Kiriy, A. *Angew. Chem. Int. Ed.* **2009**, *48*, 2695–2698. (h) Doubina, N.; Ho, A.; Jen, A. K.-Y.; Luscombe, C. K. *Macromolecules* **2009**, *42*, 7670–7677. (i) Sontag, S. K.; Marshall, N.; Locklin, J. *Chem. Commun.* **2009**, 3354–3356. (j) Senkovskyy, V.; Khanduyeva, N.; Komber, H.; Oertel, U.; Stamm, M.; Kuckling, D.; Kiriy, A. *J. Am. Chem. Soc.* **2007**, *129*, 6626–6632. (k) See also, references 21b, 21c and 22b. (l) Zhang, Z.; Hu, P.; Li, X.; Zhan, H.; Cheng, Y. *J. Polym. Sci. Pol. Chem.* **2015**, DOI: 10.1002/pola.27577.

(31) (a) Magurudeniya, H. D.; Sista, P.; Westbrook, J. K.; Ourso, T. E.; Nguyen, K.; Maher, M. C.; Alemseghed, M. G.; Biewer, M. C.; Stefan, M. C. *Macromol. Rapid Commun*. **2011**, *32*, 1748–1752. (b) Bridges, C. R.; McCormick, T. M.; Gibson, G. L., Hollinger, J.; Seferos, D. S. *J. Am. Chem. Soc.* **2013**, *135*, 13212-13219. (c) Bridges, C. R.; Yan, H.; Pollit, A. A.; Seferos, D. S. *ACS Macro Lett.* **2014**, *3*, 671-674.

(32) For recent examples, see: (a) Jahnke, A. A.; Djukic, B.; McCormick, T. M.; Buchaca Domingo, E.; Hellmann, C.; Lee, Y.; Seferos, D. S. *J. Am. Chem. Soc.* **2013**, *135*, 951–954. (b) Kohn, P.; Huettner, S.; Komber, H.; Senkovskyy, V.; Tkachov, R.; Kiriy, A.; Friend, R. H.; Steiner, U.; Huck, W. T.; Sommer, J. U.; Sommer, M. *J. Am. Chem. Soc.* **2012**, *134*, 4790–4805. (c) Sui, A.; Shi, X.; Wu, S.; Tian, H.; Geng, Y.; Wang, F. *Macromolecules* **2012**, *45*, 5436−5443. (d) Nanashima, Y.; Shibata, R.; Miyakoshi, R.; Yokoyama, A.; Yokozawa, T. *J. Polym. Sci. Pol. Chem.* **2012**, *50*, 3628–3640. (e) Nanashima, Y.; Yokoyama, A.; Yokozawa, T. *Macromolecules* **2012**, *45*, 2609–2613. (f) See also, references 16a, 22, 25a, 29a, 29b.

(33) (a) Tolman, C. A.; Seidel, W. C.; Gosser, L. W. *Organometallics* **1983**, *2*, 1391–1396. (b) Tolman, C. A. *J. Am. Chem. Soc*. **1974**, *96*, 2780–2789.

(34) (a) Yuan, M. J.; Okamoto, K.; Bronstein, H. A.; Luscombe, C. K. *ACS Macro. Lett.* **2012**, *1*, 392–395. (b) Elmalem, E.; Biedermann, F.; Johnson, K.; Friend, R. H.; Huck, W. T. S. *J. Am. Chem. Soc.* **2012**, *134*, 17769–17777. (c) Smeets, A.; Willot, P.; De Winter, J.; Gerbaux, P.; Verbiest, T.; Koeckelberghs, G.

Macromolecules **2011**, *44*, 6017–6025. (d) Doubina, N.; Paniagua, S. A.; Soldatova, A. V.; Jen, A. K.-Y.; Marder, S. R.; Luscombe, C. K. *Macromolecules* **2011**, *44*, 512–520. (e) Senkovskyy, V.; Beryozkina, T.; Bocharova, V.; Tkachov, R.; Komber, H.; Lederer, A.; Stamm, M.; Severin, N.; Rabe, J. P.; Kiriy, A. *Macromol. Symp.* **2010**, *291-292*, 17–25. (f) Smeets, A.; Van den Bergh, K.; De Winter, J.; Gerbaux, P.; Verbiest, T.; Koeckelberghs, G. *Macromolecules* **2009**, *42*, 7638–7641. (g) See also, reference 30h.

(35) (a) Palermo, E. F.; McNeil, A. J. *Macromolecules* **2012**, *45*, 5948–5955. (b) Locke, J. R.; McNeil, A. J. *Macromolecules* **2010**, *43*, 8709–8710. (c) Palermo, E. F.; van der Laan, H. L.; McNeil, A. J. *Polym. Chem*. **2013**, *4*, 4606-4611. (d) Palermo, E. F.; Darling, S. B.; McNeil, A. J. *J. Mater. Chem C.* **2014**, *2*, 3401-3406.

(36) (a) Senkovskyy, V.; Senkovska, I.; Kiriy, A. *ACS Macro. Lett.* **2012**, *1*, 494–498. (b) Sontag, S. K.; Sheppard, G. R.; Usselman, N. M.; Marshall, N.; Locklin, J. *Langmuir* **2011**, *27*, 12033–12041. (c) Marshall, N.; Sontag, S. K.; Locklin, J. *Chem. Commun.* **2011**, *47*, 5681–5689. (d) Tkachov, R.; Senkovskyy, V.; Horecha, M.; Oertel, U.; Stamm, M.; Kiriy, A. *Chem. Commun.* **2010**, *46*, 1425–1427. (e) Senkovskyy, V.; Tkachov, R.; Beryozkina, T.; Komber, H.; Oertel, U.; Horecha, M.; Bocharova, V.; Stamm, M.; Gevorgyan, S. A.; Krebs, F. C.; Kiriy, A. *J. Am. Chem. Soc.* **2009**, *131*, 16445–16453. (f) Khanduyeva, N.; Senkovskyy, V.; Beryozkina, T.; Bocharova, V.; Simon, F.; Nitschke, M.; Stamm, M.; Grotzschel, R.; Kiriy, A. *Macromolecules* **2008**, *41*, 7383–7389. (g) See also, references 30b, 30g, 30i, 30j.

(37) (a) Bronstein, H. A.; Luscombe, C. K. *J. Am. Chem. Soc*. **2009**, *131*, 12894–12895. (b) Boyd, S. D.; Jen, A. K.-Y.; Luscombe, C. K. *Macromolecules* **2009**, *42*, 9387–9389. (c) See also, reference 30h.

(38) Hidai, M.; Kashiwag, T.; Ikeuchi, T.; Uchida, Y. *J. Organomet. Chem*. **1971**, *30*, 279–282.

(39) Senkovskyy, V.; Sommer, M.; Tkachov, R.; Komber, H.; Huck, W. T. S. Kiriy, A. *Macromolecules* **2010**, *43*, 10157–10161.

(40) For examples, see: (a) Kang, S.; Ono, R. J.; Bielawski, C. W. *J. Am. Chem. Soc.* **2013**, *135*, 4984–4987. (b) Okamoto, K.; Housekeeper, J.; Michael, F. E.; Luscombe, C. K. *Poly. Chem.* **2013**, *4*, 3499–3506. (c) Wang, Q.; Takita, R.; Kikuzaki, Y.; Ozawa, F. *J. Am. Chem. Soc*. **2010**, *132*, 11420–11421. (d) See also, references 21a, 30a, 30c, 30d, and 30f.

(41) (a) Kopp, F.; Wunderlich, S.; Knochel, P. *Chem. Commun*. **2007**, 2075–2077. (b) Liu, C.-Y.; Ren, H.; Knochel, P. *Org. Lett*. **2006**, 8, 617–619. (c) Liu, C.-Y.; Knochel, P. *Org. Lett*. **2005**, 7, 2543–2546. (d) Ren, H.; Krasovskiy, A.; Knochel, P. *Chem. Commun*. **2005**, 543–545. (e) Kopp, F.; Krasovskiy, A.; Knochel, P. *Chem. Commun*. **2004**, 2288–2289. (f) Ren, H.; Krasovskiy, A.;

Knochel, P. Org. Lett. **2004**, 6, 4215–4217. (g) Krasovskiy, A.; Knochel, P. *Angew. Chem. Int. Ed*. **2004**, 43, 3333–3336.

(42) Miyakoshi, R.; Shimono, K.; Yokoyama, A.; Yokozawa, T. *J. Am. Chem. Soc.* **2006**, *128*, 16012–16013.

(43) (a) Stefan, M. C.; Javier, A. E.; Osaka, I.; McCullough, R. D. *Macromolecules* **2009**, *42*, 30–32. (b) See also, references 26, 29d, and 29e.

(44) A controlled polymerization is “a synthetic method to prepare polymers which are well-defined with respect to topology, terminal functionality, and composition and arrangement of comonomers, have molecular weights predetermined by the ratio of concentrations of reacted monomer to introduced initiator, as well as unimodal and narrow molecular weight distribution.” For reference, see: McNaught, A. D.; Wilkinson, A. *IUPAC. Compendium of Chemical Terminology [Online]*; 2nd Ed.; Blackwell Scientific Publications: Oxford, 1997. http://goldbook.iupac.org (accessed June 20, 2013).

(45) (a) Yokoyama, A.; Kato, A.; Miyakoshi, R.; Yokozawa, T. *Macromolecules* **2008**, *41*, 7271–7273. (b) See also, references 26, 28, 29e, and 43a.

(46) For representative examples, see: (a) Verswyvel, M.; Koeckelberghs, G. *Polym. Chem.* **2012**, *3*, 3203–3216. (b) Hollinger, J.; Jahnke, A. A.; Coombs, N.; Seferos, D. S. *J. Am. Chem. Soc.* **2010**, *132*, 8546–8547. (c) Van den Bergh, K.; Cosemans, I.; Verbiest, T.; Koeckelberghs, G. *Macromolecules* **2010**, *43*, 3794–3800. (d) Wang, Q.; Takita, R.; Kikuzaki, Y.; Ozawa, F. *J. Am. Chem. Soc.* **2010**, *132*, 11420–11421. (e) Doubina, N.; Stoddard, M.; Bronstein, H. A.; Jen, A. K. Y.; Luscombe, C. K. *Macromol. Chem. Phys.* **2009**, *210*, 1966–1972. (f) Vandeleene, S.; Van den Bergh, K.; Verbiest, T.; Koeckelberghs, G. *Macromolecules* **2008**, *41*, 5123–5131. (g) Koeckelberghs, G.; Cornelis, D.; Persoons, A.; Verbiest, T. *Macromol. Rapid Commun.* **2006**, *27*, 1132–1136. (h) Koeckelberghs, G.; Vangheluwe, M.; Van Doorsselaere, K.; Robijns, E.; Persoons, A.; Verbiest, T. *Macromol. Rapid Commun.* **2006**, *27*, 1920–1925. (i) Adachi, I.; Miyakoshi, R.; Yokoyama, A.; Yokozawa, T. *Macromolecules* **2006**, *39*, 7793–7795. (j) Koeckelberghs, G.; Vangheluwe, M.; Samyn, C.; Persoons, A.; Verbiest, T. *Macromolecules* **2005**, *38*, 5554–5559. (k) See also, references 21c, 23, 25, 29e, 30c, 30h, 32b, 37a, 34a, and 34f.

(47) (a) Li, L. S.; Hollinger, J.; Jahnke, A. A.; Petrov, S.; Seferos, D. S. *Chem. Sci.* **2011**, *2*, 2306–2310. (b) Hollinger, J.; Jahnke, A. A.; Coombs, N.; Seferos, D. S. *J. Am. Chem. Soc.* **2010**, *132*, 8546–8547. (c) See also, reference 35a.

(48) A statistical copolymer with thiophene was also prepared. For reference, see: Hollinger, J.; Sun, J.; Gao, D.; Karl, D.; Seferos, D. S. *Macromol. Rapid Commun.* **2013**, *34*, 437–441.

(49) (a) Wu, Z. Q.; Radcliffe, J. D.; Ono, R. J.; Chen, Z.; Li, Z. C.; Bielawski, C. W. *Polym. Chem.* **2012**, *3*, 874–881. (b) See also, references 27, 43a, and 45a.

(50) Huang, L.; Wu, S. P.; Qu, Y.; Geng, Y. H.; Wang, F. S. *Macromolecules* **2008**, *41*, 8944–8947.

(51) Grisorio, R.; Suranna, G. P.; Mastrorilli, P. *Chem. Eur. J.* **2010**, *16*, 8054–8061.

(52) (a) Nanashima, Y.; Yokoyama, A.; Yokozawa, T. *J. Polym. Sci. Pol. Chem.* **2012**, *50*, 1054–1061. (b) Senkovskyy, V.; Tkachov, R.; Komber, H.; Sommer, M.; Heuken, M.; Voit, B.; Huck, W. T. S.; Kataev, V.; Petr, A.; Kiriy, A. *J. Am. Chem. Soc.* **2011**, *133*, 19966–19970. (c) Duck, B. C.; Dastoor, P. C.; Rasmussen, M. C. *Macromolecules* **2008**, *41*, 4576–4578. (d) See also, references 16a, 30d, 32d, and 32e.

(53) (a) Ateşin, T. A,; Li, T.; Lachaize, S.; García, J. J.; Jones, W. D. *Organometallics* **2008**, *27*, 3811–3817. (b) See also, reference 33b.

(54) (a) Kaul, E.; Senkovskyy, V.; Tkachov, R.; Bocharova, V.; Komber, H.; Stamm, M.; Kiriy, A. *Macromolecules* **2010**, *43*, 77–81. (b) Khanduyeva, N.; Senkovskyy, V.; Beryozkina, T.; Horecha, M.; Stamm, M.; Uhrich, C.; Riede, M.; Leo, K.; Kiriy, A. *J. Am. Chem. Soc.* **2009**, *131*, 153–161. (c) Craley, C. R.; Zhang, R.; Kowalewski, T.; McCullough, R. D.; Stefan, M. C. *Macromol. Rapid Comm.* **2009**, *30*, 11–16. (d) Iovu, M. C.; Zhang, R.; Cooper, J. R.; Smilgies, D. M.; Javier, A. E.; Sheina, E. E.; Kowalewski, T.; McCullough, R. D. *Macromol. Rapid Comm.* **2007**, *28*, 1816–1824. (e) Iovu, M. C.; Jeffries-El, M.; Zhang, R.; Kowalewski, T.; Mccullough, R. D. *J. Macromol. Sci. A* **2006**, *43*, 1991–2000. (f) Iovu, M. C.; Jeffries-El, M.; Sheina, E. E.; Cooper, J. R.; McCullough, R. D. *Polymer* **2005**, *46*, 8582–8586. (g) See also, reference 49a.

(55) (a) Javier, A. E.; Varshney, S. R.; McCullough, R. D. *Macromolecules* **2010**, *43*, 3233–3237. (b) Wu, S.; Sun, Y.; Huang, L.; Wang, J.; Zhou, Y.; Geng, Y.; Wang, F. *Macromolecules* **2010**, *43*, 4438–4440. (c) Van den Bergh, K.; Huybrechts, J.; Verbiest, T.; Koeckelberghs, G. *Chem. Eur. J.* **2008**, *14*, 9122–9125. (d) Yokozawa, T.; Adachi, I.; Miyakoshi, R.; Yokoyama, A. *High Perform. Polym.* **2007**, *19*, 684–699. (e) See also, references 21a, 25a, 25c, 27, 30f, 32c, 34c, 45a, 46a 46b, 46c, and 47a.

(56) (a) Steim, R.; Kogler, F. R.; Brabec, C. J. *J. Mater. Chem*., **2010**, *20*, 2499–2512. (b) Steim, R.; Choulis, S. A.; Schilinsky, P.; Brabec, C. J. *Appl. Phys. Lett*. **2008**, *92*, 0933303.

(57) (a) Marshall, N.; Sontag, S. K.; Locklin, J. *Macromolecules* **2010**, *43*, 2137–2144. (b) Khanduyeva, N.; Senkovskyy, V.; Beryozkina, T.; Bocharova, V.; Simon, F.; Nitschke, M.; Stamm, M.; Grotzschel, R.; Kiriy, A. *Macromolecules* **2008**, *41*, 7383–7389. (c) See also, references 30b, 30g, 30i, 30j, 36a, 36b, 36c, 36d, 36e and 40a.

(58) (a) Huang, W.; Su, L.; Bo, Z. *J. Am. Chem. Soc*. **2009**, *131*, 10348–10349. (b) See also: Segawa, Y.; Higashihara, T.; Ueda, M. *Polym. Chem*. **2013**, *4*, 1208–1215.

Chapter 2[1]

Evidence for a preferential intramolecular oxidative addition in Ni-catalyzed cross-coupling reactions and their impact on chain-growth polymerizations

Organic π-conjugated polymers are being investigated as the active components in many optoelectronic devices due to their ability to absorb/emit light and conduct charge.[1] These properties can be tuned for specific applications based on the polymer structure (e.g., monomer identity, regioregularity, and copolymer sequence). A significant advance in the field of π-conjugated polymers occurred in 2004, when Yokozawa[2] and McCullough[3] independently reported the first chain-growth method for synthesizing poly(3-hexylthiophene). This method has enabled many new materials to be prepared,[4] including all-conjugated block[5] and gradient copolymers,[6] as well as surface-grafted[7] and end-functionalized polymers.[8] Synthesizing these polymers has been challenging, however, as it requires extensive screening of catalysts and reaction conditions for each new application. Moreover, for many monomers of interest, conditions for chain-growth homo- and copolymerization have not been found.

A more detailed understanding of what factors promote chain-growth polymerization over competing reaction pathways is needed to increase the utility of this method. To accomplish this goal, the chain-growth mechanism must be elucidated. The conventional M(0)/M(II) mechanism for small molecule cross-coupling reactions does not account for the chain-growth behavior observed in the polymerizations. An alternative mechanism was therefore proposed[2,3]

[1] Reproduced with permission from Bryan, Z. J.; McNeil, A. J. "Evidence for a Preferential Intramolecular Oxidative Addition in Ni-catalyzed cross-coupling Reactions and their Impact on Chain-growth Polymerizations" *Chem. Sci.* **2013**, *4*, 1620-1624. Copyright 2013 Royal Society of Chemistry.

wherein an associative complex forms between the Ni catalyst and the polymer chain after reductive elimination, facilitating an intramolecular oxidative addition. In principle, this associative complex could be an η^2, η^4 or η^6 Ni(0) π-complex which undergoes oxidative addition via a two-electron pathway, or a caged radical pair which undergoes oxidative addition through a one-electron pathway. Few definitive examples of the latter pathway exist,[9] while many Ni(0) arene π-complexes have been characterized[10] and implicated in oxidative addition reactions.[11] As a consequence, we[12] and others have invoked a π-complex intermediate in the chain-growth polymerizations (Scheme 2.1). We further hypothesized that the formation and reactivity of the π-complex determines whether the chain-growth or undesired reaction pathways occur. Based on this hypothesis, we investigated the impact of electron-rich ligands in the polymerizations,[13] which should both promote the formation of an associative Ni(0) π-complex[14] and accelerate the intramolecular oxidative addition.[15] Although this approach has led to an improved catalyst,[13] it remains unclear whether these results were due to stabilizing the proposed π-complex or some other factor. Further studies on the formation of this intermediate, as well as the factors controlling its reactivity were warranted.

In related small molecule cross-coupling reactions, indirect evidence supporting an preferential intramolecular oxidative addition has been reported.[16,17,18] For example, several groups have reported selective difunctionalization reactions of dihaloarenes when sub-stoichiometric quantities of the cross-coupling partner are used,[17] which is consistent with preferential oxidation addition into the initial product via an associative intermediate. In a different example, van der Boom et al. generated a Ni(0)-olefin π-complex in situ and observed selective oxidative addition into the less reactive, intramolecular Ar-Br bond versus a more reactive, intermolecular Ar-I bond.[18] We were inspired by the latter example and designed a series of competition experiments to distinguish whether the proposed Ni(0) π-complex is an intermediate in Ni-catalyzed small molecule cross-coupling reactions and chain-growth polymerizations.[19]

As described herein, these experiments have provided compelling evidence of an associative intermediate, with a subsequent intramolecular oxidative addition. We further revealed that bidentate, electron-rich ligands promote the formation and reactivity of this intermediate. Most significantly, we have demonstrated that the results from the small molecule studies correlate with chain-growth behavior in polymerizations, suggesting that the associative complex is the key intermediate between the desired and undesired reaction pathways. Overall, these studies indicate that the utility and scope of these chain-growth polymerizations can be improved by considering the formation and reactivity of the Ni(0) π-complex intermediate.

Scheme 2.1 Proposed Chain-Growth Mechanism

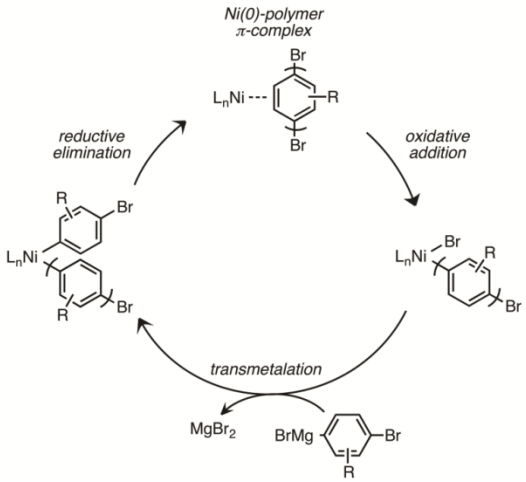

Results and Discussion

To determine whether a Ni(0) π-complex forms after reductive elimination, we designed a competition experiment wherein the proposed intramolecular oxidative addition must outcompete an intermolecular oxidative addition involving a more reactive coupling partner. As highlighted in Scheme 2.2, the hypothesized[2,3] Ni(0) π-complex (**I_{intra}**) is generated in situ via transmetalation of complex **1** using Grignard **2**, followed by reductive elimination. Based on the observed chain-growth behavior in the polymerizations, this π-complex is expected to undergo preferential intramolecular oxidative addition to generate **P_{intra}**. The presence of a competitive agent (i.e., aryl bromide **3**) provides an

alternative pathway. The more reactive[20] and better π-binding[21] **3** can intercept $\mathbf{I_{intra}}$,[22] undergo intermolecular oxidation addition and generate $\mathbf{P_{inter}}$.[23] If the proposed π-complex does not form at all, then the resulting "free" Ni(0) should be selectively trapped by **3** to produce $\mathbf{P_{inter}}$. To verify that **3** is more reactive towards Ni(0), we measured the relative intermolecular oxidative addition rates of **3** and **4** to $Ni(PPh_3)_2(cod)$ (equation 1).[24] A >99:1 preference for oxidative addition into **3** was observed, consistent with its anticipated higher reactivity.[25] Due to this large difference in reactivity between **3** and **4** in the intermolecular competition, we can assume that any $\mathbf{P_{intra}}$ formed during the reaction stems from the proposed π-complex. The analysis proved more complicated than depicted in Scheme 2.2, as both $\mathbf{P_{intra}}$ and $\mathbf{P_{inter}}$ can undergo transmetalation by **2** and reductive elimination to generate additional organic and organometallic products (Appendix 1). For the sake of simplicity in the discussion, we will refer to the collection of products stemming from each pathway as $\mathbf{P_{intra}}$ and $\mathbf{P_{inter}}$.

Chart 2.1 Selected Ligand Scope

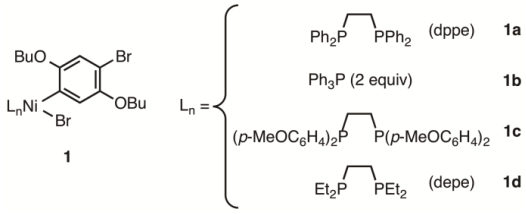

Scheme 2.2 Competition Experiment

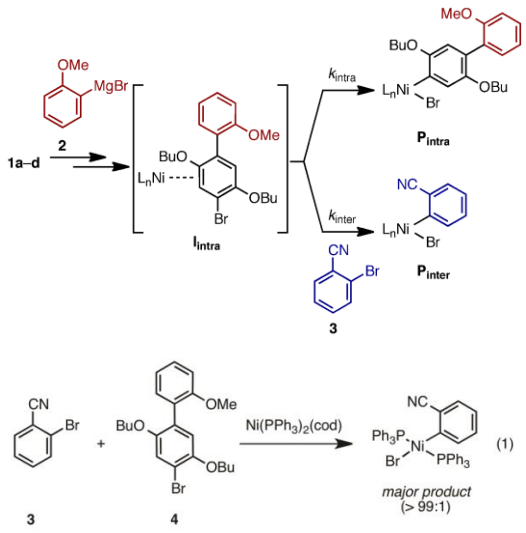

Competition experiments were first performed using complex **1a** because related Ni complexes containing the ligand, 1,2-bis(diphenylphosphino)ethane (dppe), mediate chain-growth polymerizations of several different monomers.[26] With near stoichiometric quantities of **1a**, **2** and **3**, we observed a 95:5 ratio of $\mathbf{P_{intra}}$:$\mathbf{P_{inter}}$ (Table 2.1). The observed large preference for $\mathbf{P_{intra}}$ is remarkable considering that $\mathbf{P_{inter}}$ is the favored product if the π-complex did not form. Combined, these results provide compelling evidence of an associative intermediate and intramolecular oxidative addition.[27] Because ligand steric and electronic properties have a dramatic influence on chain-growth polymerizations, we compared several different ligands under identical conditions to determine their impact on the π-complex. Complex **1b**, containing monodentate ligand PPh_3, was selected for comparison because it does not mediate controlled, chain-growth polymerizations.[28] Consistent with this observation, at near stoichiometric quantities of **1b**, **2** and **3**, a 65:35 ratio of $\mathbf{P_{intra}}$:$\mathbf{P_{inter}}$ was observed. This result indicates that the π-complex is either weakly associated or that rate of dissociation is similar to the rate of intermolecular oxidative addition. Because bidentate, electron-rich ligands have been reported to yield improved chain-growth polymerizations relative to dppe,[13] complexes **1c** and **1d** were also examined. Both **1c** and **1d** gave higher ratios of $\mathbf{P_{intra}}$:$\mathbf{P_{inter}}$ than **1a** and **1b** at the near stoichiometric conditions (Table 2.1), suggesting that the chain-growth behavior and π-complex formation/reactivity are related. Overall, the observed dominance of the intramolecular oxidative addition in all four cases provides strong evidence of an intermediate π-complex in these Ni-catalyzed cross-coupling reactions.

Table 2.1 Results of the competition experiments.[a]

	P_{intra}:P_{inter}			
equiv of **3**[b]	**1a**	**1b**	**1c**	**1d**
1	95:5	65:35	97:3	98:2
2	91:9	55:45	94:6	96:4
10	69:31	28:72	78:22	87:13
50	40:60	13:87	49:51	71:29
100	32:68	11:89	40:60	64:36

a.The reactions were run in THF at rt for 2 h ([Ni] = 0.02 M; [**2**] = 0.016 M). The reported ratios reflect the averages of three runs, with standard deviations ranging from 0.06-2%. *b*. Relative to **2**.

$$\mathbf{I_{intra}} \xrightarrow{k_{intra}} \mathbf{P_{intra}} \quad (2)$$

$$\mathbf{I_{intra}} + \mathbf{3} \xrightarrow{k_{inter}} \mathbf{P_{inter}} \quad (3)$$

$$\frac{d[\mathbf{P_{intra}}]}{dt} = k_{intra}[\mathbf{I_{intra}}] \quad (4)$$

$$\frac{d[\mathbf{P_{inter}}]}{dt} = k_{inter}[\mathbf{I_{intra}}][\mathbf{3}] \quad (5)$$

$$\frac{[\mathbf{P_{intra}}]}{[\mathbf{P_{inter}}]} = \frac{k_{intra}}{k_{inter}[\mathbf{3}]} \quad (6)$$

Further insight into the formation and reactivity of these Ni(0) π-complexes can be elucidated based on how the product ratios change as a function of [**3**]. As evident in Table 2.1, the products stemming from the intramolecular reaction ($\mathbf{P_{intra}}$) decrease with increasing concentrations of **3** for all four complexes. Nevertheless, the magnitude of the change in these ratios is different for each ligand. Comparing the bidentate ligands, the preference for the intramolecular pathway has the following order: **1a** < **1c** < **1d**. This result parallels their electron-donating abilities, which were measured for the analogous monodentate ligands (PPh_3 < $P(C_6H_4$-*p*-$OMe)_3$ < PEt_3).[29] As noted above, the electron-rich ligands are expected to promote the formation of the π-complex,[14] consistent with the Dewar-Chatt-Duncanson model of metal-π coordination,[30] and also increase the rate of oxidative addition.[15] Both factors would result in larger quantities of the intramolecular oxidative addition product ($\mathbf{P_{intra}}$), as observed herein. A plot of the

product ratio ([$\mathbf{P_{intra}}$]/[$\mathbf{P_{inter}}$]) versus 1/[**3**] reveals the inherent preference for the intramolecular pathway for each ligand (equations 2–6).[31] The slope provides the relative rate constants (k_{intra}/k_{inter}), which we can use to compare the ligands. As evident in Figure 2.1, among the bidentate ligands the most electron-rich ligand (depe) exhibits the largest slope while the least electron-rich ligand (dppe) provides the smallest slope. In addition, PPh_3, which exhibits the most uncontrolled polymerization, exhibits the smallest overall slope. These results are again consistent with the expectation that electron-donating ligands promote the formation and reactivity of the associative complex. Overall, these slopes provide a convenient and quantitative comparison between these and future ligands using this methodology.

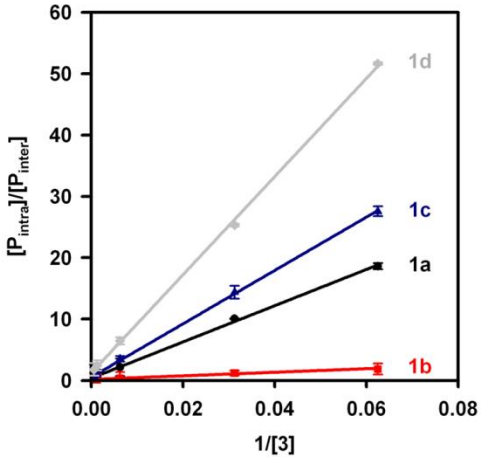

Figure 2.1 Plot of the product ratio ([$\mathbf{P_{intra}}$]/[$\mathbf{P_{inter}}$]) versus 1/[**3**] for complexes **1a** (●), **1b** (■), **1c** (▲), and **1d** (◆). The lines represent nonlinear least-squares fits to the equation [$\mathbf{P_{intra}}$]/[$\mathbf{P_{inter}}$] = $k_{intra}/(k_{inter}$[**3**]) + b where k_{intra}/k_{inter} = 295 (**1a**), 29 (**1b**), 435 (**1c**), and 800 (**1d**).

To determine the relevance of the Ni(0) π-complex on the chain-growth nature of the polymerizations, (4-bromo-2,5-bis(hexyloxy)phenyl)magnesium bromide was polymerized with catalysts **1a**-**d** (Appendix 1). The molecular weight dispersity (Đ), which reflects the breadth of the distribution, is predicted to be 1.0 in a perfectly controlled chain-growth polymerization.[32] Many factors, including the frequency of chain-transfer/termination events (i.e., intermolecular reactions) as well as the relative rates of initiation and propagation, contribute to broaden this distribution. As a result, the Đ from the standard polymerizations cannot be

compared directly to the small molecule studies. Because the intermolecular reactions are favored at high concentrations of competitive agent, the polymerizations were run with 50 and 100 equiv of **3** (Table 2.2). As anticipated, the Đ broadened substantially (**1a** (1.38 → 2.35), **1c** (1.29 → 2.28), and **1d** (1.44 → 2.15)) with increasing concentrations of the competitive agent, consistent with an increase in the number of undesired intermolecular reactions. In contrast, catalyst **1b** gave polymer samples that were broad regardless of whether competitive agent was present, suggesting an uncontrolled or step-growth process. Significantly, at high concentrations of **3**, the Đ follow the same trend as observed in the small molecule studies (**1d** (2.15) < **1c** (2.28) < **1a** (2.35)), consistent with the anticipated impact of electron-donating ligands on the formation and reactivity of the π-complex. The absence of a trend at lower concentrations of **3** is likely due to the dominance of other factors on the Đ, such as a slow initiation relative to propagation.[13,33] Note that the number-average molecular weights also decreased with increasing concentrations of **3** (Appendix 1), consistent with the initiation of new polymer chains via the intermolecular pathway. Overall, these results provide compelling evidence that the Ni(0) π-complex is an important intermediate in the chain-growth polymerizations.

Table 2.2 Results of the polymerizations.[a]

	Đ			
equiv of **3**[b]	**1a**	**1b**	**1c**	**1d**
0	1.38	2.42	1.29	1.44
50	2.30	2.50	1.89	1.98
100	2.35	2.42	2.28	2.15

a. The reactions were run in THF at rt for 24 h ([Ni] = 0.0015 M; [**2**] = 0.036 M). The reported *Đ* reflect the averages of two runs, with standard deviations ranging from ± 0.01–0.03. *b*. Relative to **1**.

Conclusions

In summary, both small molecule cross-coupling reactions as well as chain-growth polymerizations were found to proceed via an associative

intermediate. By varying the ligand electronic properties, we observed that electron-rich, bidentate ligands lead to a higher preference for this intramolecular pathway. Further studies revealed that the fate of this intermediate correlates with the chain-growth behavior of the polymerizations. As a consequence, this type of competition experiment should prove valuable for expanding the scope and utility of these polymerizations, particularly in identifying catalysts for currently challenging monomers (e.g., electron-deficient monomers). These studies also suggest that electron-rich, bidentate ligands can be used to achieve selective polyfunctionalizations of small molecules in related cross-coupling reactions.

References

(1) For recent reviews, see: (a) Li, G.; Zhu, R.; Yang, Y. *Nature Photon.* **2012**, *6*, 153–161. (b) Boudreault, P.-L. T.; Najari, A.; Leclerc, M. *Chem. Mater.* **2011**, *23*, 456–469. (c) Facchetti, A. *Chem. Mater.* **2011**, *23*, 733–758.

(2) (a) Yokoyama, A.; Miyakoshi, R.; Yokozawa, T. *Macromolecules*, **2004**, *37*, 1169–1171. (b) Miyakoshi, R.; Yokoyama, A.; Yokozawa, T. *Macromol. Rapid Commun.* **2004**, *25*, 1663–1666.

(3) Sheina, E. E.; Liu, J. S.; Iovu, M. C.; Laird, D. W.; McCullough, R. D. *Macromolecules*, **2004**, *37*, 3526–3528.

(4) For recent reviews, see: (a) Yokozawa, T.; Nanashima, Y.; Ohta, Y. *ACS Macro Lett.* **2012**, *1*, 862–866. (b) McNeil, A. J.; Lanni, E. L. New Conjugated Polymers and Synthetic Methods. In *Synthesis of Polymers*; Schlüter, D. A.; Hawker, C. J.; Sakamoto, J. Eds; Wiley-VCH: Germany, 2012; Vol. 1, pp 475−486.

(5) For recent examples, see: (a) Bhatt, M. P.; Huynh, M. K.; Sista, P.; Nguyen, H. Q.; Stefan, M. C. *J. Polym. Sci. Part A: Polym. Chem.* **2012**, *50*, 3086–3094. (b) Sui, A. G.; Shi, X. C.; Wu, S. P.; Tian, H. K.; Geng, Y. H.; Wang, F. S. *Macromolecules*, **2012**, *45*, 5436–5443. (c) Song, I. Y.; Kim, J.; Im, M. J.; Moon, B. J.; Park, T. *Macromolecules*, **2012**, *45*, 5058−5068. (d) Hollinger, J.; DiCarmine, P. M.; Karl, D.; Seferos, D. S. *Macromolecules*, **2012**, *45*, 3772−3778.

(6) (a) Palermo, E. F.; McNeil, A. J. *Macromolecules*, **2012**, *45*, 5948–5955. (b) Locke, J. R.; McNeil, A. J. *Macromolecules*, **2010**, *43*, 8709–8710.
(7) For a recent review, see: Marshall, N.; Sontag, S. K.; Locklin, J. *Chem. Commun*. **2011**, ***47***, 5681–5689.

(8) For recent examples, see: (a) Kochemba, W. M.; Kilbey, S. M.; Pickel, D. L. *J. Polym. Sci. Part A: Polym. Chem.* **2012**, *50*, 2762–2769. (b) Stefan, M. C.; Bhatt, M. P.; Sista, P.; Magurudeniya, H. D. *Polym. Chem*. **2012**, *3*, 1693–1701. (c) Yuan, M.; Okamoto, K.; Bronstein, H. A.; Luscombe, C. K. *ACS Macro Lett*. **2012**, *1*, 392–395.

(9) Tsou, T. T.; Kochi, J. K. *J. Am. Chem. Soc*. **1979**, *101*, 6319–6332.

(10) For recent examples of Ni(0) arene π-complexes, see: (a) Johnson, S. A.; Huff, C. W.; Mustafa, F.; Saliba, M. *J. Am. Chem. Soc.* **2008**, *130*, 17278–17280. (b) Garcia, J. J.; Brunkan, N. M.; Jones, W. D. *J. Am. Chem. Soc.* **2002**, *124*, 9547-9555; (c) Braun, T.; Cronin, L.; Higgitt, C. L.; McGrady, J. E.; Perutz, R. N.; Reinhold, M. *New J. Chem.* **2001**, *25*, 19-21.

(11) Ni(0)-arene π-complexes have previously been implicated as intermediates in oxidative addition reactions. For a recent example, see: Li, T.; García, J. J.; Brennessel, W. W.; Jones, W. D. *Organometallics*, **2010**, *29*, 2430–2445.

(12) (a) Lanni, E. L.; McNeil, A. J. *Macromolecules*, **2010**, *43*, 8039–8044. (b) Lanni, E. L.; McNeil, A. J. *J. Am. Chem. Soc.* **2009**, *131*, 16573–16579.

(13) (a) Lee, S. R.; Bryan, Z. J.; Wagner, A. M.; McNeil, A. J. *Chem. Sci.* **2012**, *3*, 1562–1566. (b) Lanni, E. L.; Locke, J. R.; Gleave, C. M.; McNeil, A. J. *Macromolecules*, **2011**, *44*, 5136–5145.

(14)Tolman, C. A.; Seidel, W. C.; Gosser, L. W. *Organometallics*, **1983**, *2*, 1391–1396.

(15) Electron-donating bidentate phosphines have been shown to accelerate Pd-catalyzed oxidative additions. For leading references, see: Slagt, V. F.; de Vries, A. H. M.; de Vries, J. G.; Kellogg, R. M. *Org. Process Res. Dev*. **2010**, *14*, 30–47. This result has theoretical support: Fazaeli, R.; Ariafard, A.; Jamshidi, S.; Tabatabaie, E. S.; Pishro, K. A. *J. Organomet. Chem*. **2007**, *692*, 3984–3993.

(16) (a) Yoshikai, N.; Matsuda, H.; Nakamura, E. *J. Am. Chem. Soc*. **2009**, *131*, 9590–9599. (b) Yoshikai, N.; Matsuda, H.; Nakamura, E. *J. Am. Chem. Soc.* **2008**, *130*, 15258–15259.

(17) For recent examples, see: (a) Nanashima, Y.; Yokoyama, A.; Yokozawa, T. *Macromolecules*, **2012**, *45*, 2609–2613. (b) Larrosa, I.; Somoza, C.; Banquy, A.; Goldup, S. M. *Org. Lett.* **2011**, *13*, 146–149. (c) Guillén, E.; Hierrezuelo, J.; Martinez-Mallorquin, R.; Lopez-Romero, M.; Rico, R. *Tetrahedron*, **2011**, *67*, 2555–2561.

(18) Zenkina, O. V.; Karton, A.; Freeman, D.; Shimon, L. J. W.; Martin, J. M. L.; van der Boom, M. E. *Inorg. Chem.* **2008**, *47*, 5114–5121.

(19) Spectroscopic evidence suggestive of a Ni(0) π-complex has been reported, although the results are inconclusive. For reference, see: Senkovskyy, V.; Tkachov, R.; Komber, H.; John, A.; Sommer, J.-U.; Kiriy, A. *Macromolecules*, **2012**, *45*, 7770–7777.

(20) For recent examples, see: (a) Puri, M.; Gatard, S.; Smith, D. A.; Ozerov, O. V. *Organometallics*, **2011**, *30*, 2472–2482. (b) Dong, Z.-B., Manolikakes, G.; Shi, L.; Knochel, P.; Mayr, H. *Chem. Eur. J.* **2010**, *16*, 248–253.

(21) (a) Ateşin, T. A.; Li, T.; Lachaize, S.; García, J. J.; Jones, W. D. *Organometallics*, **2008**, *27*, 3811–3817. (b) Tolman, C. A. *J. Am. Chem. Soc.* **1974**, *96*, 2780–2789.

(22) One possible mechanism is via formation of a nitrile-bound π-complex with **3**. For related π-complexes, see: (a) Ge, S.; Hartwig, J. F. *J. Am. Chem. Soc*. **2011**, *133*, 16330–16333. (b) Li, T.; García, J. J.; Brennessel, W. W.; Jones, W. D. *Organometallics*, **2010**, *29*, 2430–2445.

(23) Note that no reaction occurs when **2** and **3** are stirred together in the absence of catalyst (Appendix 1).

(24) Bidentate ligands were not used because their complexation to $Ni(cod)_2$ leads to an inseparable mixture of products (e.g., Ni(cod)(dppe), $Ni(cod)_2$, and $Ni(dppe)_2$).

(25) Using $Ni(PMe_3)_2(cod)$ revealed a similar product ratio (Appendix 1).

(26) For recent examples, see: (a) Senkovskyy, V.; Tkachov, R.; Komber, H.; Sommer, M.; Heuken, M.; Voit, B.; Huck, W. T. S.; Kataev, V.; Petr, A.; Kiriy, A. *J. Am. Chem. Soc.* **2011**, *133*, 19966–19970. (b) Senkovskyy, V.; Sommer, M.; Tkachov, R.; Komber, H.; Huck, W. T. S.; Kiriy, A. *Macromolecules*, **2010**, *43*, 10157–10161.

(27) Several studies have shown that unactivated dihaloarenes are not consumed during chain-growth polymerizations. For leading references, see: Kiriy, A.; Senkovskyy, V.; Sommer, M. *Macromolecular Rapid Commun*. **2011**, *32*, 1503–1517. See also, ref 4a.

(28) (a) Woody, K. B.; Leever, B. J.; Durstock, M. F.; Collard, D. M. *Macromolecules*, 2011, **44**, 4690–4698. (b) Doubina, N.; Ho, A.; Jen, A. K.-J.; Luscombe, C. K. *Macromolecules*, **2009**, *42*, 7670–7677. (c) Beryozkina, T.; Senkovskyy, V.; Kaul, E.; Kiriy, A. *Macromolecules*, **2008**, *41*, 7817–7823. (d) Senkovskyy, V.; Khanduyeva, N.; Komber, H.; Oertel, U.; Stamm, M.; Kuckling, D.; Kiriy, A. *J. Am. Chem. Soc.* **2007**, *129*, 6626–6632.

(29) (a) Haar, C. M.; Nolan, S. P.; Marshall, W. J.; Moloy, K. G.; Prock, A.; Giering, W. P. *Organometallics*, **1999**, *18*, 474–479. (b) Li, C.; Nolan, S. P. *Organometallics*, **1995**, *14*, 1327–1332. (c) Dias, P. B.; Minas de Piedade, M. E.; JSimões, . A. M. *Coord. Chem. Rev.* **1994**, *135/136*, 737–807. (d) Tolman, C. A. *J. Am. Chem. Soc*. **1970**, *92*, 2953–2956.

(30) (a) Dewar, J. S. *Bull. Soc. Chim. Fr.* **1951**, *18*, C71–79. (b) Chatt, J.; Duncanson, L. A. *J. Chem. Soc.* **1953**, 2939–2947.

(31) Similar ratios of $\mathbf{P_{intra}/P_{inter}}$ were obtained with excess **4,** suggesting that dissociation of $\mathbf{I_{intra}}$ does not involve an equilibrium.

(32) This statement refers to chain-growth polymerizations that reach high conversions.

(33) Lee, S. R.; Bloom, J. W. G.; Wheeler, S. E.; McNeil, A. J. *Dalton Trans*. **2013**, *42*, 4218-4222.

Chapter 3[1,2]

Chain-growth polymerization of aryl Grignards initiated by a stabilized NHC-Pd precatalyst

The recent discovery of chain-growth methods for synthesizing π-conjugated polymers[1] has generated significant interest because copolymers with specific sequences and potentially advantageous properties can now be targeted.[2] For example, all-conjugated block[3] and gradient[4] copolymers as well as surface-grafted[5] and end-functionalized[6] polymers have been prepared. These chain-growth methods largely consist of cross-coupling reactions between difunctionalized arenes (e.g., Br/MgX) using Ni catalysts ligated by chelating phosphines.[7] One current limitation is the narrow scope of monomers that are capable of undergoing chain-growth homo- and copolymerizations. As a consequence, there is an ongoing search for a more universal catalyst.

One approach is to modify the steric and electronic properties of the ligand. In 2011, we reported on a series of bis(dialkylphosphino)ethane-based ligands and demonstrated that unhindered ligands led to facile catalyst decomposition while hindered ligands interfered with the chain-growth pathway.[8] More recently, we examined the influence of ligand electronic properties and found that electron-rich ligands promoted the chain-growth pathway.[9] We hypothesized that this electronic effect was due, in part, to stabilization of the key intermediate (complex **I** in Scheme 2). Combined, these results suggest that electron-donating ligands with moderate steric properties are ideal for chain-growth polymerizations. Because N-heterocyclic carbenes (NHCs) are stronger

[1]Reproduced with permission from Bryan, Z. J.; Smith, M. L.; McNeil, A. J. "Chain-growth Polymerization of Aryl Grignards Initiated by a Stabilized NHC-Pd Precatalyst" *Macromol. Rapid Commun.* **2012**, *33*, 842-847. Copyright 2012 WILEY-VCH Verlag GmbH & Co.

[2]Z. J. B gratefully acknowledges the contributions of the co-author. M. L. S. assisted in running several reactions and provided valuable feedback during the manuscript preparation.

σ-donors than phosphines,[10,11] and their steric properties are easily modified, we anticipated that they would be ideal ligands for the chain-growth polymerizations.[12]

An alternative approach for developing new catalysts is to change the nature of the metal species. Pd catalysts have recently emerged as an alternative to Ni in the chain-growth polymerizations.[13,14,15] For example, using (t-Bu_3P)Pd(Ph)Br
as the catalyst, both Suzuki-Miyaura[13] and Suzuki-Heck[14] conditions have led to chain-growth polymerizations. Excitingly, the scope of monomers is broad and even includes n-type monomers, which have been rare in the Ni-catalyzed processes.[16] Nevertheless, these methods need further improvement. For example, in most cases the MALDI-TOF MS analysis of the resulting polymers revealed a significant amount of polymers with Ph/Br end-groups. These end-groups indicate that either the catalyst fails to undergo an intramolecular oxidative addition into the growing polymer chain or the propagating species is unstable, leading to premature reductive elimination of polymer-Br.

We selected NHC-ligated Pd precatalyst **1**[17,18] based on a recent report by Larrosa, Goldup, and co-workers, who observed an unexpected difunctionalization of 1,4-dibromobenzene when one equivalent of PhMgCl was used.[19] A diffusion-controlled oxidative addition was invoked to rationalize this selectivity.[20] This mechanism is similar to that proposed for the Ni-catalyzed chain-growth polymerizations (see Scheme 2),[21,22] suggesting that this Pd precatalyst might also mediate chain-growth polymerization of aryl monomers. In addition, Organ and co-workers demonstrated that this precatalyst could facilitate cross-coupling reactions between two hindered arenes,[17c] suggesting that precatalyst **1** will readily polymerize the *ortho*-functionalized monomers typically used to make soluble π-conjugated polymers. Finally, these pyridine-stabilized Pd precatalysts have additional advantages in that they are air- and moisture-stable as well as commercially available.

We report herein the homo- and copolymerizations of (4-bromo-2,5-bis(hexyloxy)phenyl)magnesium chloride (**2**), (5-bromo-4-hexylthiophen-2-

yl)magnesium chloride (**3**), and (7-bromo-9,9-dioctyl-fluoren-2-yl)magnesium chloride (**4**) mediated by Pd precatalyst **1** (Scheme 1). A chain-growth homopolymerization was observed for both monomers **2** and **3**, with linear increases in the number-average molecular weight (M_n) with conversion as well as constant, narrow molecular weight distributions (Đ). Block copolymerizations gave the expected chain extension when the second monomer was added soon after complete consumption of the first monomer. In contrast, polymerization of monomer **4** was neither living nor perfectly chain-growth. Overall, these studies indicate that further modifications to the catalyst scaffold, either by selecting an alternative NHC ligand or by varying the steric and electronic properties of the stabilizing ligand (i.e., 3-chloropyridine),[23] are needed to further improve the chain-growth polymerizations.

Scheme 3.1 Syntheses of π-Conjugated Polymers Mediated by a Pd-NHC Precatalyst

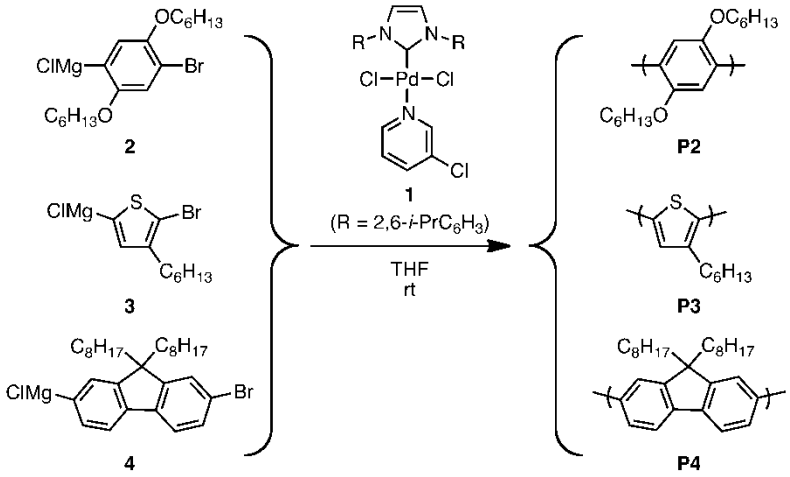

Experimental Section

Monomer Preparation

Monomers **2**, **3**, and **4** were generated in situ via Grignard metathesis of the dibromo precursors using *i*-PrMgCl (see Supporting Information, SI).[24, 25]

General Procedure for Homopolymerizations

A 25 mL Schlenk flask was equipped with a stir bar, precatalyst **1** (10.2 mg, 0.0150 mmol, 1 equiv), and THF (7.5 mL) in a glovebox under an N_2 atmosphere. The flask was then equipped with a septum (secured with copper wire), removed

from the glovebox, and put under an N_2 atmosphere. Monomer **2** (2.25 mL, 1.01 mmol) was then added via syringe and stirred for 90 min at rt. The reaction was then quenched with aq. HCl (5 M, 10 mL) and extracted with CH_2Cl_2 (3 x 10 mL). The combined organic extracts were dried over $MgSO_4$, filtered, and the solvent was removed in vacuo. The resulting white solid was then washed with MeOH and dried under vacuum. (209 mg, 75% yield) M_n = 28.2 kDa, Đ = 1.19.

General Procedure for Block Copolymerizations

A 25 mL Schlenk flask was equipped with a stir bar, precatalyst **1** (10.2 mg, 0.0150 mmol, 1 equiv), and THF (5.0 mL) in a glovebox under an N_2 atmosphere. The flask was then equipped with a septum (secured with copper wire), removed from the glovebox, and put under an N_2 atmosphere. Monomer **2** (1.8 mL, 0.50 mmol) was then added via syringe and stirred for 180 min at rt. After 180 min, an aliquot (0.5 mL) was withdrawn via syringe and immediately quenched with aq. HCl (12 M, 1 mL). The mixture was extracted with $CHCl_3$ (3 x 1 mL) with mild heating and the combined aliquots were dried over $MgSO_4$, filtered, and analyzed by GPC (M_n = 9.2 kDa, Đ = 1.24). Monomer **3** (3.2 mL, 0.90 mmol) was then added via syringe and stirred for 60 min at rt. After 60 min, the reaction was quenched with aq. HCl (5 M, 10 mL) and extracted with $CHCl_3$ (3 x 10 mL). The combined organic extracts were dried over $MgSO_4$, filtered, and the solvent was removed in vacuo. The resulting purple solid was then dissolved in a minimum amount of $CHCl_3$ and precipitated into MeOH. The precipitate was collected and dried under vacuum (223 mg, 78% yield). M_n = 17.8 kDa, Đ = 1.32.

Results and Discussion

Homopolymerizations

The homopolymerizations of **2** and **3** mediated by precatalyst **1** showed linear increases in the number-average molecular weight (M_n) with conversion and narrow molecular weight distributions (Đ) (Figure 3.1 A/B). Both results are consistent with a chain-growth mechanism. Further support was provided by examining the relationship between the [monomer]/[catalyst] ratio and the M_n (Figure 3.1 C/D). The observed linear relationship suggests that each Pd precatalyst initiates a single-polymer chain.

Low molecular weight polymers were subjected to MALDI-TOF MS analysis after quenching, which revealed predominantly polymers with H/Br end-groups. These end-groups reveal that the catalyst is located at the polymer chain end, as evidenced by its replacement with a proton during the acidic quench. To support the living nature of these polymerizations, a second aliquot of the same monomer was added immediately after consumption of the first aliquot. The observed increases in M_n with only minor broadening of the dispersities indicates that most polymer chains remain living under these conditions (Appendix 2).

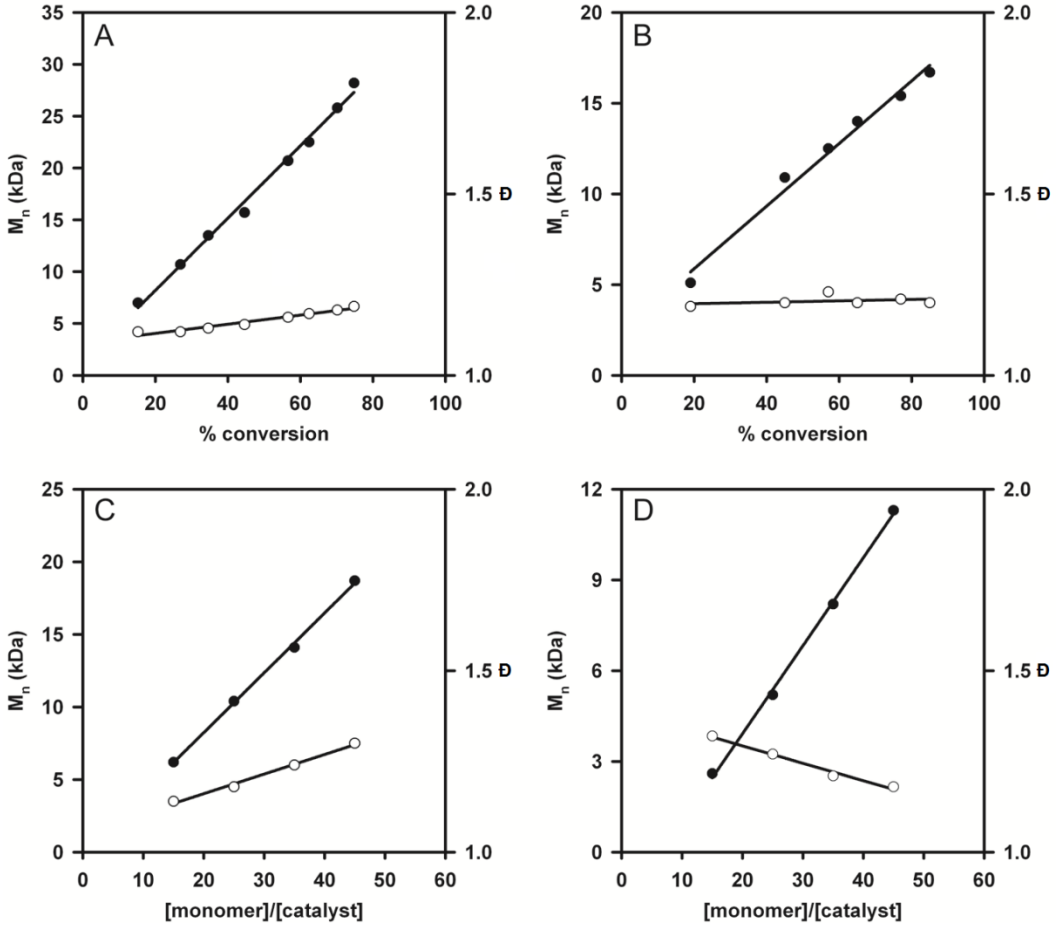

Figure 3.1 Plots of M_n (●) and Đ (○) versus conversion for the polymerization of monomers (A) **2** and (B) **3** using precatalyst **1** ([**1**] = 1.5 mM; [**2**] = 77 mM; [**3**] = 98 mM; 25 °C; THF). Plots of M_n (●) and Đ (○) versus [monomer]/[catalyst] ratio for polymerization of monomers (C) **2** and (D) **3** using precatalyst **1** (25 °C, THF).

The regioregularity of the poly(3-hexylthiophene) will depend on the relative reactivities of the regioisomers of monomer **3** (~80:20 mixture, major

isomer is shown in Scheme 1). By monitoring their relative conversions, we observed that the major regioisomer is predominantly consumed within the first 50% conversion (Appendix 2). As the concentration of the major regioisomer decreased, the minor regioisomer was consumed. As a consequence, the poly(3-hexylthiophene) regioregularity was low (80%). The increased reactivity of the major regioisomer has been attributed to the lack of a substituent *ortho* to the reactive carbon, which leads to a faster transmetalation onto the catalyst compared to the minor regioisomer.[26] Though not explored herein, if the I/Br functionalized precursor is used to regioselectively generate **3**, a highly regioregular poly(3-hexylthiophene) is expected using this method.[27,28]

In contrast to both monomers **2** and **3**, the polymerization of fluorene monomer **4** with precatalyst **1** is pseudo-chain-growth but not living. For example, MALDI-TOF MS analysis at low monomer conversions indicated a variety of different end-groups, suggesting that chain-transfer and chain-termination were occurring, even at early conversions (Appendix 2). It is interesting to note that the largest peak corresponded to polymers with iPr/H end-groups. These end-groups could arise via competitive transmetalation of iPrMgCl (leftover from the Grignard metathesis)[29] or oxidative addition of the iPrBr (formed via Grignard metathesis) into "free" $L_nPd(0)$.[17a] ^1H NMR analysis of a sample before and after polymerization (referenced to an internal standard) revealed complete consumption of iPrMgCl and no consumption of the iPrBr, consistent with the transmetalation hypothesis.

Adding a second aliquot of monomer **4** immediately following consumption of the first aliquot did not result in a significant amount of chain extension. Instead, a broadening of the molecular weight distribution was observed and new chains were initiated (Appendix 2). These results suggest that either the Pd catalyst is not efficiently transferred to the chain end during the polymerization of **4**[15] or there may be a stability issue with the catalyst at the chain end. In both cases, "free" $L_nPd(0)$ is generated and can initiate new chains. Between 5-30% of the dibromo precursor (leftover from an incomplete Grignard metathesis) is consumed during polymerization, consistent with "free" Pd(0) forming during

polymerization (Appendix 2). As discussed below, some time-dependent catalyst stability issues are observed with both monomers **2** and **3** after complete consumption of monomer. Thus, the observed uncontrolled polymerization of monomer **4** may be due to a similar decomposition pathway.

Block Copolymerizations

Previous studies with both Pd and Ni catalysts have shown that copolymerizations can be challenging even when homopolymerizations were successful.[30] For example, the order of monomer addition can influence the results of these block copolymerizations. In contrast to these previous studies, we observed the expected increases in the polymer molecular weights regardless of the order of monomer addition in the copolymerizations of monomers **2** and **3** with Pd precatalyst **1** (Figure 3.2 A/B). These results were obtained when the second monomer was added within 3 h after addition of the first monomer. If longer periods between monomer additions were used, some chain termination was observed. This result is most consistent with a catalyst stability issue at the end of the polymerization, once the monomer concentration is depleted.

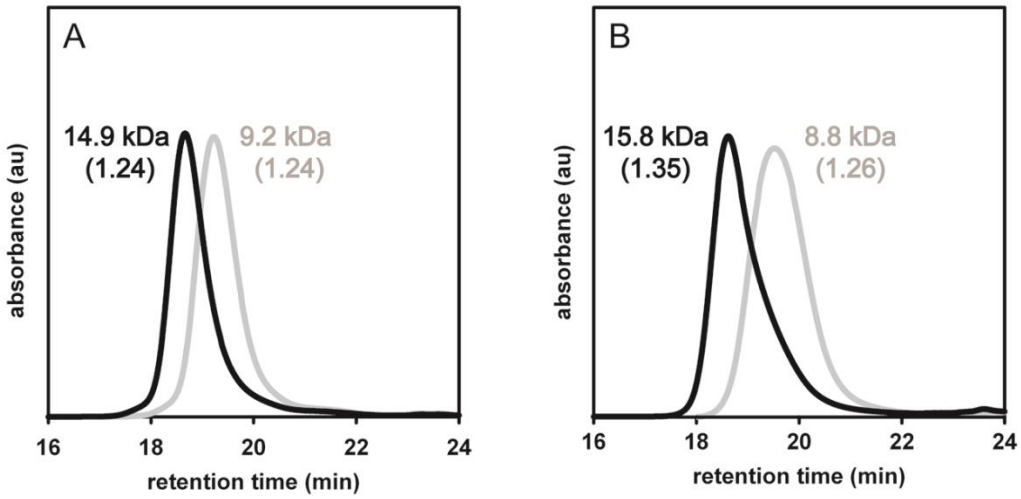

Figure 3.2 Gel permeation chromatograms (GPC) for block copolymerizations using Pd precatalyst **1** to generate (A) **P2**-*block*-**P3** and (B) **P3**-*block*-**P2**. The grey line represents the GPC curve immediately before second monomer addition. The black line represents the GPC curves after copolymerization is complete.

It is important to note that there is no evidence of catalyst decomposition during the polymerization. For example, at low conversions, the MALDI-TOF MS analysis revealed predominantly H/Br end-groups, whereas Br/Br end-groups would have resulted if catalyst stability was an issue (Appendix 2). In addition, a control experiment, wherein only 50% of the dibromo precursor was activated with *i*-PrMgCl, revealed no significant consumption of the dibromo starting material, even up to 80% conversion of the Grignard monomer (Appendix 2). This result suggests that "free" Pd(0) is not formed during the polymerization. The fact that the decomposition does not occur during polymerization suggests that a different catalyst resting state is present under those conditions. We[8,9,22] and others[15,21] have been probing the mechanistic details with Ni catalysts chelated by phosphine ligands, and these studies have revealed structures similar to both complexes **II** and **III** as catalyst resting states during polymerization, depending on the ligand structure.[8,9,22] At the end of these Ni-catalyzed polymerizations, structures similar to complex **II** are observed, regardless of the ligand structure. Roy and Hartwig previously reported that reductive eliminations of Ar-Br can occur from LPd(Ar)Br complexes when sufficiently hindered ligands are used.[31] Thus, one mechanism for decomposition is the reductive elimination of polymer-Br from this complex. Mechanistic studies of the Pd-catalyzed polymerizations described herein are needed to address these catalyst stability issues.

Scheme 3.2 Proposed Mechanism for the Observed Chain-Growth Behavior

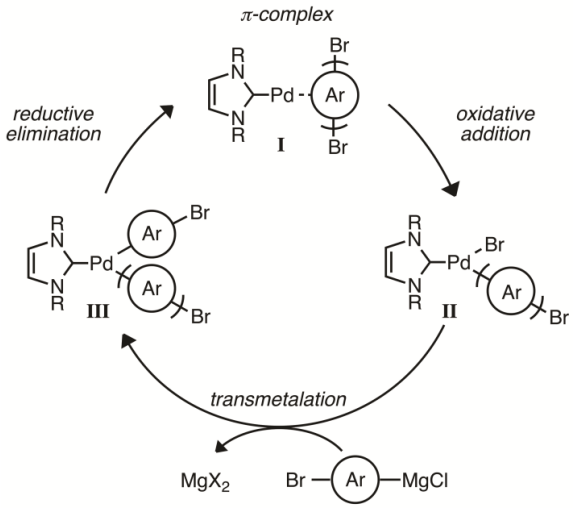

Conclusions

NHC-ligated Pd precatalyst **1** mediates chain-growth homo- and copolymerizations of both phenylene- and thiophene-based monomers. On the other hand, polymerization of a fluorene-based monomer was problematic, with evidence of both chain-termination and re-initiation pathways occurring. In addition, the catalyst appears to be moderately unstable once monomer consumption is complete. Although not explored herein, the "throw-away" ligand (3-chloropyridine) may play a non-innocent role in the mechanism.[32] In addition, less sterically encumbered NHCs might represent a promising alternative to IPr.[31] Mechanistic studies are needed to elucidate the precise role of ligand steric and electronic properties, as well as monomer structure, on the chain-growth and competing reaction pathways. Studies aimed at addressing these issues, as well as examining the substrate scope (e.g., electron-poor monomers) for precatalyst **1** and related NHC-Pd catalysts are currently underway.

References

(1) (a) Sheina, E. E.; Liu, J.; Iovu, M. C.; Laird, D. W.; McCullough, R. D. *Macromolecules* **2004**, *37*, 3526–3528. (b) Yokoyama, A.; Miyakoshi, R.; Yokozawa, T. *Macromolecules* **2004**, *37*, 1169–1171. (c) Miyakoshi, R.; Yokoyama, A.; Yokozawa, T. *Macromol. Rapid Commun*. **2004**, *25*, 1663–1666.

(2) For recent reviews, see: (a) Kiriy, A.; Senkovskyy, V.; Sommer, M. *Macromol. Rapid Commun.* **2011**, *32*, 1503–1517. (b) Okamoto, K.; Luscombe, C. K. *Polym. Chem.* **2011**, *2*, 2424–2434.

(3) For recent examples of block copolymers prepared via this method, see: (a) Verswyvel, M.; Monnaie, F.; Koeckelberghs, G. *Macromolecules* **2011**, *44*, 9489–9498. (b) Kim, J.; Siva, A.; Song, I. Y.; Park, T. *Polymer* **2011**, *52*, 3704–3709. (c) Higashihara, T.; Ohshimizu, K.; Ryo, Y.; Sakurai, T.; Takahashi, A.; Nojima, S.; Ree, M.; Ueda, M. *Polymer* **2011**, *52*, 3687–3695. (d) Ohshimizu, K.; Takahashi, A.; Higashihara, T.; Ueda, M. *J. Polym. Sci., Part A: Polym. Chem.* **2011**, *49*, 2709–2714. (e) Hollinger, J.; Jahnke, A. A.; Coombs, N.; Seferos, D. S. *J. Am. Chem. Soc.* **2010**, *132*, 8546–8547. (f) Van den Bergh, K.; Cosemans, I.; Verbiest, T.; Koeckelberghs, G. *Macromolecules* **2010**, *43*, 3794–3800. (g) Javier, A. E.; Varshney, S. R.; McCullough, R. D. *Macromolecules* **2010**, *43*, 3233–3237. (h) Miyanishi, S.; Zhang, Y.; Tajima, K.; Hashimoto, K. *Chem. Commun*. **2010**, *46*, 6723–6725.
(4) Locke, J. R.; McNeil, A. J. *Macromolecules* **2010**, *43*, 8709–8710.

(5) For a recent review, see: Marshall, N.; Sontag, S. K.; Locklin, J. *Chem. Commun*. **2011**, *47*, 5681–5689.

(6) For recent examples, see: (a) Doubina, N.; Paniagua, S. A.; Soldatova, A. V.; Jen, A. K. Y.; Marder, S. R.; Luscombe, C. K. *Macromolecules* **2011**, *44*, 512–520. (b) Smeets, A.; Willot, P.; De Winter, J.; Gerbaux, P.; Verbiest, T.; Koeckelberghs, G. *Macromolecules* **2011**, *44*, 6017–6025.

(7) For a recent example of an non-phosphine based Ni-catalyst, see: Magurudeniya, H. D.; Sista, P.; Westbrook, J. K.; Ourso, T. E.; Nguyen, K.; Maher, M. C.; Alemseghed, M. G.; Biewer, M. C.; Stefan, M. C. *Macromol. Rapid Commun*. **2011**, *32*, 1748–1752.

(8) Lanni, E. L.; Locke, J. R.; Gleave, C. M.; McNeil, A. J. *Macromolecules* **2011**, *44*, 5136–5145.

(9) Lee, S. R.; Bryan, Z. J.; Wagner, A. M.; McNeil, A. J. *Chem. Sci.* **2012**, *3*, 1562-1566.

(10) (a) Chianese, A. R.; Li, X.; Janzen, M. C.; Faller, J. W.; Crabtree, R. H. *Organometallics* **2003**, *22*, 1663–1667. (b) Herrmann, W. A.; Schütz, J.; Frey, G. D.; Herdtweck, E. *Organometallics* **2006**, *25*, 2437–2448.

(11) For recent reviews, see: (a) G. C. Fortman, S. P. Nolan, *Chem. Soc. Rev.* **2011**, *40*, 5151–5169. (b) S. Díez-González, N. Marion, S. P. Nolan, *Chem. Rev.* **2009**, *109*, 3612–3676. (c) E. A. B. Kantchev, C. J. O'Brien, M. G. Organ, *Angew. Chem. Int. Ed.* **2007**, *46*, 2768–2813.

(12) Tamba, S.; Shono, K.; Sugie, A.; Mori, A. *J. Am. Chem. Soc.* **2011**, *133*, 9700–9703.

(13) (a) Yokozawa, T.; Suzuki, R.; Nojima, M.; Ohta, Y.; Yokoyama, A. *Macromol. Rapid Commun*. **2011**, *32*, 801–806. (b) Elmalem, E.; Kiriy, A.; Huck, W. T. S. *Macromolecules* **2011**, *44*, 9057–9061. (c) Yokozawa, T.; Kohno, H.; Ohta, Y.; Yokoyama, A. *Macromolecules* **2010**, *43*, 7095–7100. (d) Huang, W.; Su, L.; Bo, Z. *J. Am. Chem. Soc.* **2009**, *131*, 10348–10349. (e) Beryozkina, T.; Boyko, K.; Khanduyeva, N.; Senkovskyy, V.; Horecha, M.; Oertel, U.; Simon, F.; Stamm, M.; Kiriy, A. *Angew. Chem. Int. Ed.* **2009**, *48*, 2695–2698. (f) Yokoyama, A.; Suzuki, H.; Kubota, Y.; Ohuchi, K.; Higashimura, H.; Yokozawa, T. *J. Am. Chem. Soc.* **2007**, *129*, 7236–7237.

(14) Grisorio, R.; Suranna, G. P.; Mastrorilli, P. *Chem. Eur. J.* **2010**, *16*, 8054–8061.
(15) Verswyvel, M.; Verstappen, P.; De Cremer, L.; Verbiest, T.; Koeckelberghs, G. *J. Polym. Sci., Part A: Polym. Chem.* **2011**, *49*, 5339–5349.

(16) Senkovskyy, V.; Tkachov, R.; Komber, H.; Sommer, M.; Heuken, M.; Voit, B.; Huck, W. T. S.; Kataev, V.; Petr, A.; Kiriy, A. *J. Am. Chem. Soc*. **2011**, *133*, 19966–19970.

(17) (a) O'Brien, C. J.; Kantchev, E. A. B.; Valente, C.; Hadei, N.; Chass, G. A.; Lough, A.; Hopkinson, A. C.; Organ, M. G. *Chem. Eur. J.* **2006**, *12*, 4743–4748. (b) Organ, M. G.; Avola, S.; Dubovyk, I.; Hadei, N.; Kantchev, E. A. B.; O'Brien, C. J.; Valente, C. *Chem. Eur. J.* **2006**, *12*, 4749–4755. (c) Organ, M. G.; Abdel-Hadi, M.; Avola, S.; Hadei, N.; Nasielski, J.; O'Brien, C. J.; Valente, C. *Chem. Eur. J.* **2007**, *13*, 150–157.

(18) For recent reviews, see: (a) Valente, C.; Çalimsiz, S.; Hoi, K. H.; Mallik, D.; Sayah, M.; Organ, M. G. *Angew. Chem. Int. Ed.* **2012**, *51*, 2-21. (b) Organ, M. G.; Chass, G. A.; Fang, D.-C.; Hopkinson, A. C.; Valente, C. *Synthesis* **2008**, *17*, 2776–2797.

(19) Larrosa, I.; Somoza, C.; Banquy, A.; Goldup, S. M. *Org. Lett*. **2011**, *13*, 146–149.

(20) Unusually selective difunctionalizations have previously been observed with other Pd catalysts. Similar mechanisms have been proposed. For examples, see: (a) Weber, S. K.; Galbrecht, F.; Scherf, U. *Org. Lett.* **2006**, *8*, 4039–4041. (b) Sinclair, D. J.; Sherburn, M. S. *J. Org. Chem.* **2005**, *70*, 3730–3733. (c) Dong, C.-G.; Hu, Q.-S. *J. Am. Chem. Soc.* **2005**, *127*, 10006–10007.

(21) (a) Tkachov, R.; Senkovskyy, V.; Komber, H.; Kiriy, A. *Macromolecules* **2011**, *44*, 2006-2015. (b) Tkachov, R.; Senkovskyy, V.; Komber, H.; Sommer, J.-U.; Kiriy, A. *J. Am. Chem. Soc*. **2010**, *132*, 7803–7810. (c) Beryozkina, T.; Senkovskyy, V.; Kaul, E. A. Kiriy, *Macromolecules* **2008**, *41*, 7817–7823. (d) Miyakoshi, R.; Yokoyama, A.; Yokozawa, T. *J. Am. Chem. Soc*. **2005**, *127*, 17542–17547. (e) Iovu, M. C.; Sheina, E. E.; Gil, R. R.; McCullough, R. D. *Macromolecules* **2005**, *38*, 8649–8656.

(22) (a) Lanni, E. L.; McNeil, A. J. *Macromolecules* **2010**, *43*, 8039–8044. (b) Lanni, E. L.; McNeil, A. J. *J. Am. Chem. Soc.* **2009**, *131*, 16573–16579. (c) See also, ref 8.

(23) Nasielski, J.; Hadei, N.; Achonduh, G.; Kantchev, E. A. B.; O'Brien, C. J.; Lough, A.; Organ, M. G. *Chem. Eur. J.* **2010**, *16*, 10844–10853.

(24) (a) Shi, L.; Chu, Y.; Knochel, P.; Mayr, H. *Org. Lett.* **2009**, *11*, 3502–3505. (b) Shi, L.; Chu, Y.; Knochel, P.; Mayr, H. *J. Org. Chem.* **2009**, *74*, 2760–2764.

(25) Excess i-PrMgCl (or t-BuMgCl) can be detrimental. For example, see: Lohwasser, R. H.; Thelakkat, M. *Macromolecules* **2011**, *44*, 3388-3397.
(26) (a) Lamps, J.-P.; Catala, J.-M. *Macromolecules* **2011**, *44*, 7962–7968. (b) See also, ref 21a.

(27) For example, see ref 1b.

(28) Note that the radical-based mechanisms have been proposed with *i*-PrI is generated in situ. For reference, see: (a) Kienle, M.; Knochel, P. *Org. Lett.* **2010**, *12*, 2702–2705. (b) Manolikakes, G.; Knochel, P. *Angew. Chem. Int. Ed.* **2009**, *48*, 205–209.

(29) Stefan, M. C.; Javier, A. E.; Osaka, I.; McCullough, R. D. *Macromolecules* **2009**, *42*, 30–32.

(30) (a) Wu, S.; Bu, L.; Huang, L.; Yu, X.; Han, Y.; Geng, Y.; Wang, F. *Polymer* **2009**, *50*, 6245–6251. (b) Miyakoshi, R.; Yokoyama, A.; Yokozawa, T. *Chem. Lett.* **2008**, *37*, 1022–1023. (c) Yokoyama, A.; Kato, A.; Miyakoshi, R.; Yokozawa, T. *Macromolecules* **2008**, *41*, 7271–7273. (e) See also, ref 3f.

(31)Roy, A. H.; Hartwig, J. F. *J. Am. Chem. Soc*. **2003**, *125*, 13944–13945. See also: Roy, A. H.; Hartwig, J. F. *Organometallics* **2004**, *23*, 1533–1541.

(32) (a) Chen, M.-T.; Vicic, D. A.; Turner, M. L.; Navarro, O. *Organometallics* **2011**, *30*, 5052–5056. (b) See also, ref 23.

Chapter 4[1]

Using small molecules to identify new catalysts for catalyst-transfer polycondensation (CTP)

Conjugated polymers continue to garner considerable attention in research due to their applications in optoelectronic devices. These polymers are attractive because they are electronically tunable and can be solution processed onto thin, flexible substrates.[1] Traditionally, conjugated polymers are synthesized using step-growth methodology which does not offer control over molecular weight or dispersity, and unique sequences such as block and gradient copolymers cannot be prepared.[2]

In 2004, Yokozawa[3] and McCullough[4] independently discovered a chain-growth method for synthesizing conjugated polymers. Now referred to as catalyst-transfer polycondensation (CTP), this process involves a unique associative complex formed after reductive elimination which facilitates intramolecular oxidative addition into the growing polymer chain.[5] It has become apparent that universal conditions cannot be developed for the desired monomers, and the overall monomer scope of CTP remains limited. Most new conditions for CTP are discovered somewhat serendipitously or through polymerization screens. A failed polymerization generally provides little more than yes/no dichotomy of results. For this reason small molecules have been targeted to simulate polymerization reactivity.

There have been several examples of small molecule models leading to new conditions for conjugated polymer synthesis. These small molecule models

[1]Z. J. B gratefully acknowledges the contributions of Carolyn Zhao for assisting with monomer synthesis and polymerization screens.

test for preferential multi-functionalization under substoichiometric conditions. Kumada and co-workers observed conditions that produced nearly quantitative di-functionalization using nickel catalysts and alkyl Grignards[6] (Scheme 4.1). These conditions were similar to the methods used decades later by Yokozawa to polymerize poly(2,5-bis(hexyloxy)phenylene) via CTP[7]. McCullough and coworkers also observed selective di-functionalization with thiophene Grignards which ultimately led to the chain-growth synthesis of poly(3-hexylthiophene)[4] (Scheme 4.1). Small molecules have also been used by Yokozawa and coworkers to develop chain-growth conditions for the synthesis of poly(2-alkoxypyridine-3,5-diyl).[8] Most recently, our group was inspired by conditions Goldup and coworkers[9] generated for small molecules and applied them towards the first chain-growth polymerization utilizing a Pd-NHC catalyst and Grignards.[10] However, this methodology has not been successfully applied towards expanding the monomer scope outside of traditional Grignards. Additionally, literature reports exhibiting preferential multi-functionalization remain sparse, so a targeted approach is desired.

Scheme 4.1 Small Molecule Studies Inspiring CTP Conditions

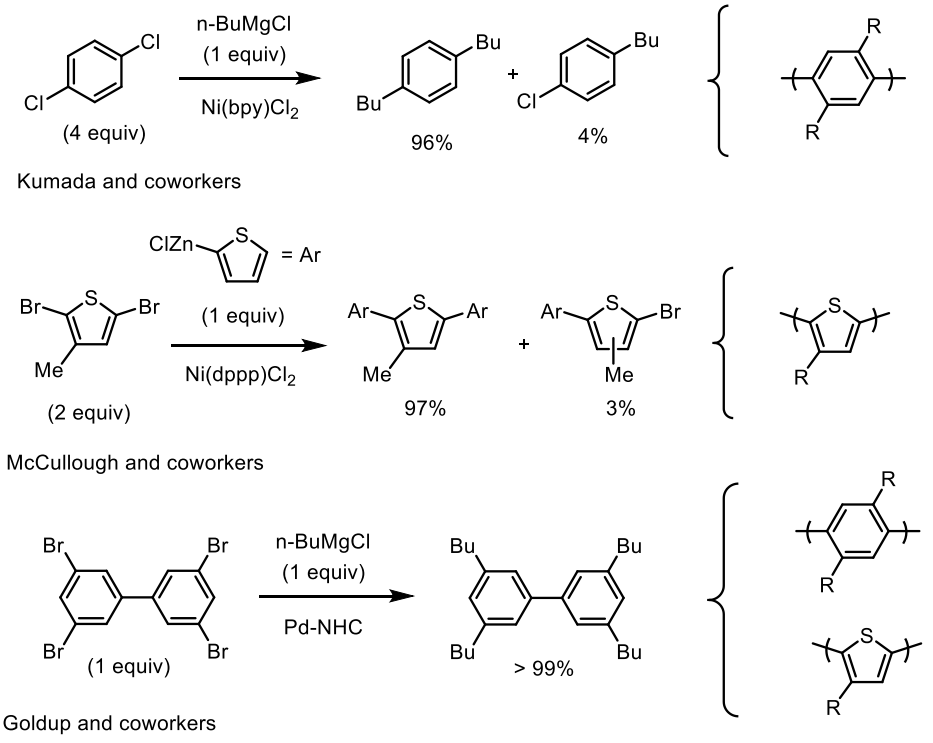

We envisioned a small molecule model system with an adaptable design allowing it to be tailored for any monomer (Scheme 4.2). We began by targeting poly(2,5-bis(hexyloxy)phenylene ethynylene) (PPE) because it has found applications in light emitting diodes (LEDs),[11] molecular wires,[12] and sensors.[13] Additionally, there has only been one report of PPE synthesized using CTP from Bielawski and coworkers, and this study generated stoichiometric amounts of tin as a byproduct, therefore limiting its commercial application.[14]

Scheme 4.2 Small Molecule Model System for Developing New CTP Conditions

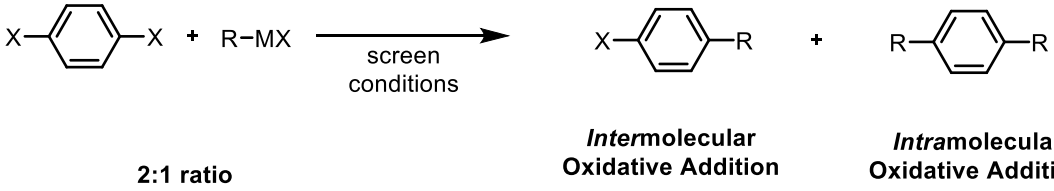

Herein, we report an extensive case study utilizing small molecules as a guide for developing chain-growth conditions for the Sonogashira polymerization of poly(2,5-bis(hexyloxy)phenylene ethynylene). A small molecule model system was developed to accurately emulate the electronic and steric contributions of the desired monomer. Hundreds of small molecule experiments were quickly examined, with the goal of determining ideal conditions for selective di-functionalization, as this intramolecular oxidative addition suggests an associative intermediate which is indicative of a controlled chain-growth process. The small molecule model system afforded product ratios and conversions which directly influenced the subsequent rounds of screening. While selective di-functionalization was ultimately achieved, these conditions were found to exhibit step-growth polymerization characteristics when examined, which is indicative of intermolecular oxidative addition. A further investigation revealed that relative reactivity differences between intermediates and starting materials influenced the product ratios. As long as these reactivity differences are examined during the small molecule screens, we believe screenings like this can still be effective at targeting new CTP conditions.

Results and Discussion

To begin, we used 1,4-diethoxy-2,5-dibromobenzene as multi-functional substituent as it contains similar electronic and steric properties as the monomer 1-bromo-2,5-bis(hexyloxy)-4-ethynylbenzene (**1**). We then selected 4-tolylacetylene (**2**) as the reactive partner as it was commercially available and would be easy to monitor via gas chromatography (GC). We used twice the amount of multi-functional arene to acetylene so there would be a 4:1 ratio of ArBr reactive sites for the acetylene to cross-couple with, and would always leave excess ArBr sites (Scheme 4.3). This set-up also provided a simple way to access the reactivity via GC. Conversion of the starting materials and formation of the products would be rapidly assessed on a small scale, allowing for rapid iteration and efficient screening.

Scheme 4.3 Small Molecule Model System Used to Determine CTP Conditions for the Synthesis of PPE

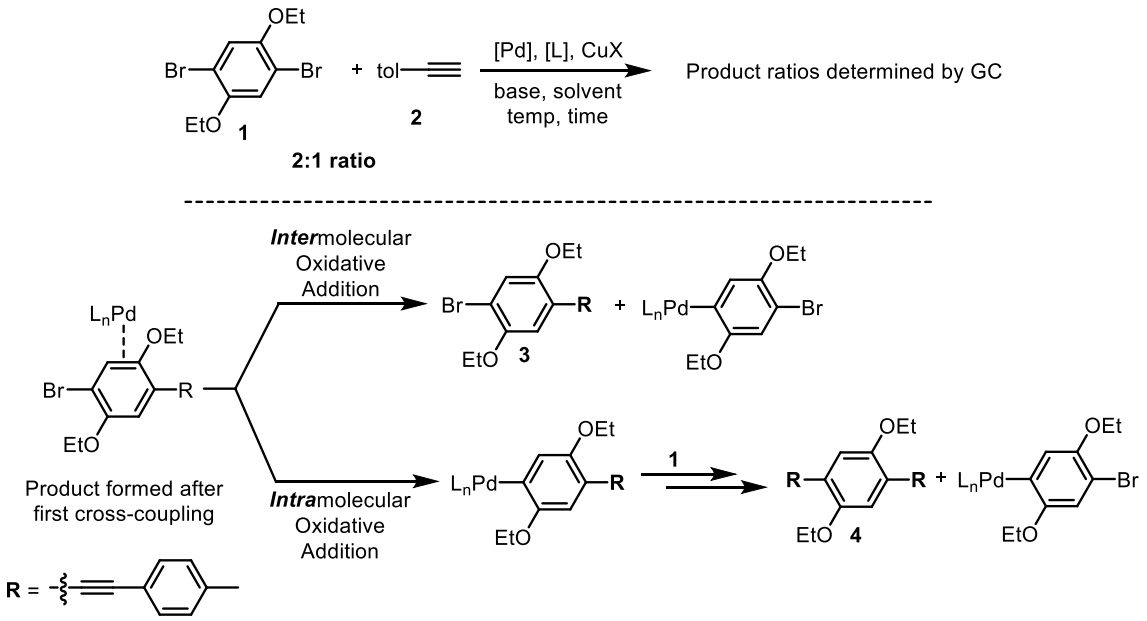

Hundreds of small molecule screens were carried out examining the role of catalyst, co-catalyst (copper), ligand, co-catalyst ligand, base, solvent, and temperature (Appendix 3). Ultimately, these experiments found that selective di-functionalization could be achieved utilizing Buchwald Pd pre-catalysts, with

ligated copper, in toluene, at room temperature, with increasingly higher amounts of triethylamine. More specifically, Generations 1–3 Buchwald precatalysts ligated with SPhos or XPhos showed the most consistent preference for multi-functionalization. Additionally, the tridentate ligand *N,N,N'N',N''*-pentamethyldiethylenetriamine (PMDTA) was observed to increase multi-functionalization, likely through solubilizing the CuI co-catalyst (Scheme 4.4). The observed product ratios generally were around 33:67 in terms of species **3**:**4**, however several conditions produced ratios as high as 5:95, suggesting intramolecular oxidative addition. The most promising results were then examined utilizing the targeted monomer, as we expected to observe chain-growth behavior. However, we observed that the average molecular weight (M_n) only increased at high conversion in an exponential fashion along with steady increase in molecular weight distribution (Đ), which is indicative of classical step-growth behavior (Figure 4.1). In contrast, CTP is characterized by a linear increase in M_n and decreasing Đ with conversion.[15] There was clearly a discord between the small molecule screens and the polymerizations that needed to be determined.

Scheme 4.4 Small Molecule Conditions with the Highest Preference for Multi-functionalization

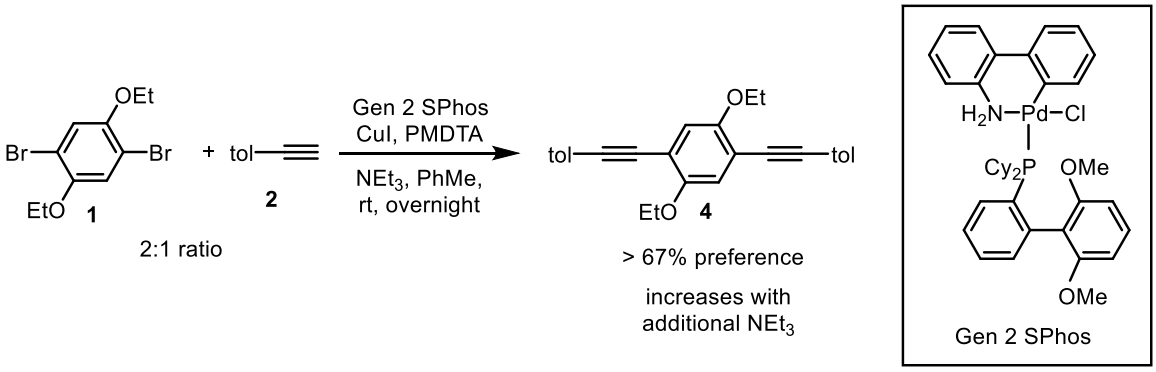

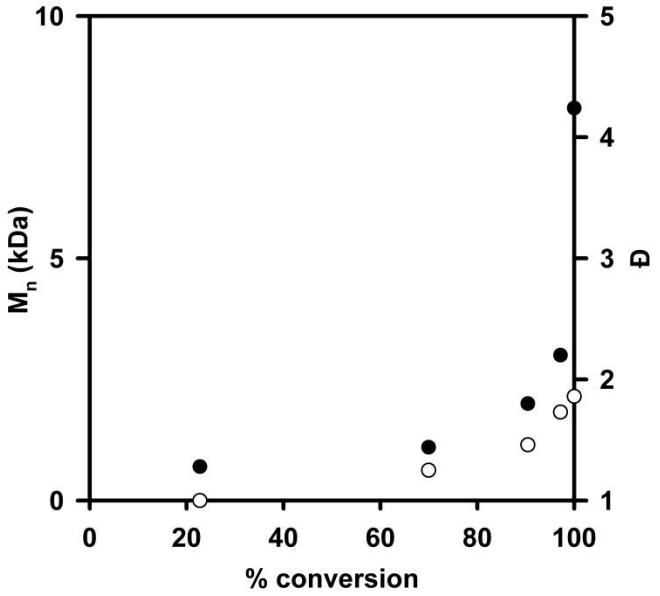

Figure 4.1 Plot of M_n (•) and Đ (o) versus conversion utilizing the most favorable small molecule conditions (Appendix 3).

We started by running a reaction profile using a single set of small molecule conditions. Periodic aliquots were taken to examine how the products form over time (Table 4.1). We observed the selective formation of mono-functional **3** is favored initially, and only at high conversion of acetylene **2** did mono-functional **3** undergo the second turnover to favor di-functionalized product **4**. This initial buildup of product mono-functional intermediate **3** suggested that these product ratios were governed predominantly by reactivity differences as opposed to an associative intermediate. To examine these reactivity differences, a competition experiment was designed where the catalyst was given equal opportunity to react with either the di-functional $ArBr_2$ **5** or the product formed after a single turnover (**3**) (Scheme 4.5). Despite equal amounts of both reactants only the mono-functionalized product (**3**) was consumed (Appendix 3). This reactivity indicates that the second turnover in the small molecule screen is at least twenty times more reactive under the tested conditions.

Table 4.1 Results of the reaction profile using the best conditions[a]

time (min)	conversion of acetylene (**2**)	% mono-substituted (**3**)	% di-substituted (**4**)
0	0	0	0
30	33	91	9
60	55	65	35
90	89	34	66
120	100	24	76
150	100	18	82
180	100	13	87

a.The reactions were run in 0.67 μM Gen 2 SPhos, 3.2 μM CuI, 3.2 μM PMDTA, 50 μM ArX_2, 25 μM **1**, 50% by volume NEt_3, rt, 3 h.

Scheme 4.5 Competition Experiment to Examine Reactivity Differences

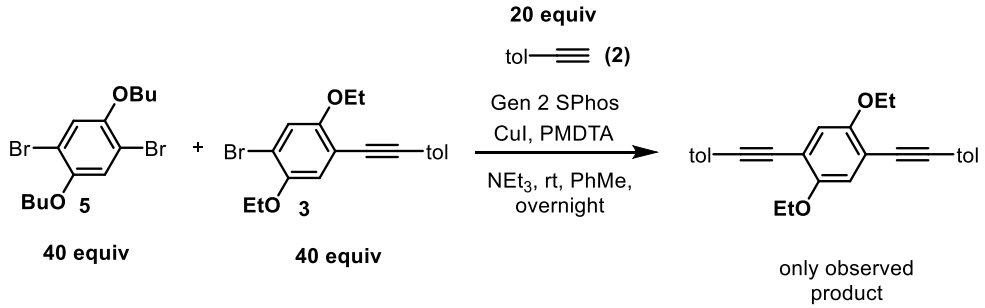

To more generally examine these competition experiments, we decided to compare the Sonogashira conditions that showed the highest preference for di-functionalization to commercial catalysts[16,17] in an analogous Kumada competition experiment. The Sonogashira small molecule screens were set up identical as outlined in Scheme 4.1. We used aryl Grignard **6** to model the reaction with Kumada chain-growth catalysts (Scheme 4.6). We began by running several small molecule screens with varying amounts of **2** and **6** (5-40 equiv) respective to **5** (80 or 2000 equiv). The Kumada chain-growth catalysts showed essentially quantitative amounts of intramolecular oxidative addition regardless of ratio between reactants (Table 4.2). This independence from the

starting material indicates that the observed products are purely determined by the presence of an associative intermediate and behave regardless of concentration. However, the Sonogashira conditions showed a great deal of variance, suggesting the products are determined by concentration and reactivity as opposed to an associative intermediate (Table 4.3). It is important to note that if the reactivity difference between intermediates and starting materials is high enough, it could show quantitative multi-functionalization despite not preceding through an associative complex even when exposed to a range of starting materials. Regardless, we strongly recommend varying the relative amount of the starting materials to ensure that the observed product ratios are independent of concentration. By examining a wide range of starting material ratios (1:50, 1:1, 50:1), false positives can quickly be eliminated as the observed products should be unaffected by these changes.

Scheme 4.6 Kumada Small Molecule Model System

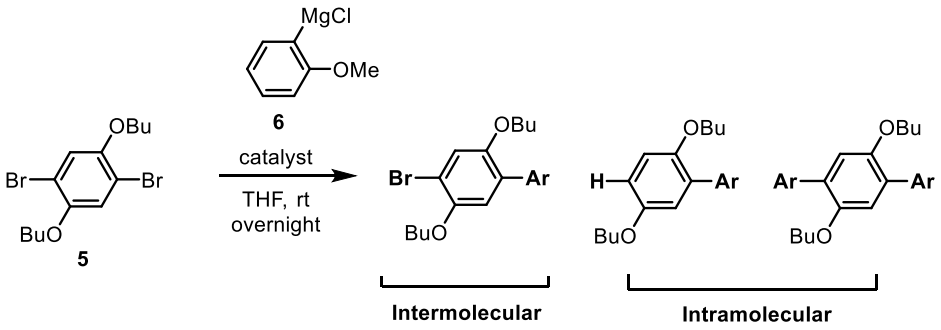

Table 4.2 Results of the small molecule screen with Kumada catalysts[a]

	$Ni(dppe)Cl_2$		Pd-NHC	
Ratio of **6:5**	Inter	Intra	Inter	Intra
1:2	1	99	0	100
1:4	1	99	0	100
1:8	2	98	0	100
1:16	2	98	0	100
1:50	1	99	0	100

a.The reactions were run in 0.83 μM Ni or Pd, 3 mL THF, rt, overnight.

Table 4.3 Results of the small molecule screen with Gen 2 SPhos[a]

Ratio of **2:5**	Mono-functionalized	Di-functionalized
1:2	13	87
1:4	26	74
1:8	58	42
1:16	68	32
1:50	46	54

a. The reactions were run in 0.83 μM Pd Gen 2 SPhos, 4.2 μM CuI, 4.2 μM PMDTA, 1 mL NEt_3, 2 mL PhMe, rt, overnight.

Conclusions

In summary, small molecule cross-coupling reactions were carried out to determine new chain-growth conditions for Sonogashira polymerizations. Several promising conditions were found that favored preferential di-functionalization. However when these parameters were examined under polymerization conditions, they resulted in a step-growth polymerization as opposed to CTP. Compared to traditional Kumada chain-growth catalysts[16,17], this work illustrated the importance of screening these catalysts at a number of different reactant ratios. However, the reactivity difference between intermediates could still result in misleading data causing false positives. Regardless, we recommend varying the ratio of starting materials for any small molecule systems used to determine new CTP conditions. It is notable that the small molecule model system did provide much faster iteration as each screen afforded product ratios, allowing us to target selective di-coupling. We are currently utilizing this small molecule model system outlined in this chapter to compare known CTP catalysts while screening new target monomers for CTP conditions.

References

(1) (a) Yeh, N.; Yeh, P. *Renew. Sust. Energ. Rev.* **2013**, *21*, 421–431. (b) Cataldo, S.; Pignataro, B. *Materials* **2013**, *6*, 1159–1190. (c) Li, G.; Zhu, R.; Yang, Y. *Nat. Photonics* **2012**, *6*, 153–161. (d) Boudreault, P.-L. T.; Najari, A.; Leclerc, M. *Chem. Mater*. **2011**, *23*, 456–469. (e) Facchetti, A. *Chem. Mater*. **2011**, *23*, 733–758

(2) For recent examples, see: (a) Bhatt, M. P.; Huynh, M. K.; Sista, P.; Nguyen, H. Q.; Stefan, M. C. *J. Polym. Sci. Part A: Polym. Chem.* **2012**, *50*, 3086–3094. (b) Sui, A. G.; Shi, X. C.; Wu, S. P.; Tian, H. K.; Geng, Y. H.; Wang, F. S. *Macromolecules*, **2012**, *45*, 5436–5443. (c) Song, I. Y.; Kim, J.; Im, M. J.; Moon, B. J.; Park, T. *Macromolecules*, **2012**, *45*, 5058−5068. (d) Hollinger, J.; DiCarmine, P. M.; Karl, D.; Seferos, D. S. *Macromolecules*, **2012**, *45*, 3772−3778. (e) Palermo, E. F.; McNeil, A. J. *Macromolecules*, **2012**, *45*, 5948–5955. (f) Locke, J. R.; McNeil, A. J. *Macromolecules*, **2010**, *43*, 8709–8710.

(3) (a) Yokoyama, A.; Miyakoshi, R.; Yokozawa, T. *Macromolecules*, **2004**, *37*, 1169–1171. (b) Miyakoshi, R.; Yokoyama, A.; Yokozawa, T. *Macromol. Rapid Commun.* **2004**, *25*, 1663–1666.

(4) Sheina, E. E.; Liu, J. S.; Iovu, M. C.; Laird, D. W.; McCullough, R. D. *Macromolecules*, **2004**, *37*, 3526–3528.

(5) Bryan, Z. J.; McNeil, A. J. *Chem. Sci.* **2013**, *4*, 1620-1624.

(6) Tamao, K.; Sumitani, K.; Kiso, Y.; Zembayashi, M.; Fujioka, A.; Kodama, S.; Nakajima, I.; Minato, A.; Kumada, M. *Bull. Chem. Soc. Jpn*. **1976**, *49*, 1958–1969.

(7) Miyakoshi, R.; Shimono, K.; Yokoyama, A.; Yokozawa, T. *J. Am. Chem. Soc.* **2006**, *128*, 16012–16013.

(8) (a) Nanashima, Y.; Shibata, R.; Miyakoshi, R.; Yokoyama, A.; Yokozawa, T. *J. Polym. Sci. Pol. Chem.* **2012**, *50*, 3628–3640. (b) Nanashima, Y.; Yokoyama, A.; Yokozawa, T. *Macromolecules* **2012**, *45*, 2609–2613.

(9) Larrosa, I.; Somoza, C.; Banquy, A.; Goldup, S. M. *Org. Lett*. **2011**, *13*, 146–149.

(10) Bryan, Z. J.; Smith, M. L.; McNeil, A. J. *Macromol. Rapid Comm.* **2012**, *33*, 842–847.

(11) (a) Grimsdale, A. C.; Leok Chan, K.; Martin, R. E.; Jokisz, P. G.; Holmes, A. B. *Chem. Rev*. **2009**, *109*, 897-1091. (b) Pschirer, N. G.; Miteva, T.; Evans, U.;

Roberts, R. S.; Marshall, A. R.; Neher, D.; Myrick, M. L.; Bunz, U. H. F. *Chem. Mater.* **2001**, *13*, 2691-2696.

(12) Allara, D. L.; Arnold, J. J.; Bumm, L. A.; Burgin, T. P.; Cygan, M. T.; Dunbar, T. D.; Jones, L., II; Tour, J. M.; Weiss, P. S. *Science* **1996**, *271*, 1705-1707.

(13) (a) Thomas, S. W.; Joly, G. D.; Swager, T. M. *Chem. Rev*. **2007**, *107*, 1339-1386. (b) Yang, J.-S.; Swager, T. M. *J. Am. Chem. Soc.* **1998**, *120*, 11864-11873.

(14) Kang, S.; Ono, R. J.; Bielawski, C. W. *J. Am. Chem. Soc.* **2013**, *135*, 4984-4987.

(15) The IUPAC definition of a living polymerization is “a chain polymerization from which chain transfer and chain termination are absent.” For reference, see: McNaught, A. D.; Wilkinson, A. *IUPAC. Compendium of Chemical Terminology [Online]*; 2nd Ed.; Blackwell Scientific Publications: Oxford, 1997. http://goldbook.iupac.org (accessed April 12, 2015).

(16) Examples of CTP with Ni(dppe)Cl_2: (a) Lanni, E. L.; McNeil, A. J. *Macromolecules* **2010**, *43*, 8039–8044. (b) Lanni, E. L.; McNeil, A. J. *J. Am. Chem. Soc.* **2009**, *131*, 16573–16579. (c) Tkachov, R.; Senkovskyy, V.; Komber, H.; Kiriy, A. *Macromolecules* **2011**, *44*, 2006–2015. (d) Lanni, E. L.; Locke, J. R.; Gleave, C. M.; McNeil, A. J. *Macromolecules* **2011**, *44*, 5136–5145.

(17) Examples of CTP with Pd-PEPPSI-IPr: (a) Qiu, Y.; Mohin, J.; Tsai, C.-H.; Tristram-Nagle, S.; Gil, R. R.; Kowalewski, T.; Noonan, K. J. T. *Macromol. Rapid Comm.* **2015**, DOI: 10.1002/marc.20150030. (b) Shi, X.; Wang, Y.; Li, Y.; Geng, Y.; Wang, F. *Chem. Comm.* **2015**, *51*, 2138-2140. (c) Sui, A.; Shi, X.; Tian, H.; Geng, Y.; Wang, F. *Polym. Chem.* **2014**, *5*, 7072-7080. (d) See also reference 10.

Chapter 5

Conclusions and Future Directions

The commercial and academic interest in π-conjugated polymers has continued to rise since Heeger, MacDiarmid, and Shirawaka demonstrated that poly(acetylene) conducts charge in the oxidized state.[1] The role that catalyst-transfer polycondensation (CTP) will ultimately play has yet to be determined. On the one hand CTP enables precise manipulation of molecular weight, dispersity,[2] and copolymer sequence (blocks[3] and gradients[4]). As discussed in the introduction, a number of important contributions to CTP have been made by a variety of different research groups from around the world since 2004.[5] New catalysts have been discovered, new conditions have been developed for interesting monomers, and in depth mechanistic investigations have been conducted.[6] However, the limitations, namely narrow monomer scope, prevent more widespread application as the most efficient polymers cannot be accessed via CTP. We strongly believe determining the mechanistic underpinnings of CTP will lead the way to expanding the monomer scope, and ultimately lead to more widespread commercial applications utilizing π-conjugated polymers.

In the second chapter we discussed a small molecule model system that examined preferential intramolecular oxidative addition in CTP. Prior to this work, an associative intermediate had been implicated in the CTP mechanism,[7] but no definitive evidence had been presented. We demonstrated that Ni catalysts that undergo controlled CTP exhibit a strong preference for intramolecular oxidative addition. These catalysts also exhibited preferential oxidative addition when 2-bromobenzonitrile was added in extreme excesses (100 equiv) as a competitive pathway. It was demonstrated that electron-rich ligands showed higher rates of intramolecular oxidative addition compared to electron-poor analogues. We believe the increased electron density stabilized the associative intermediate,

preventing dissociation. Additionally, we showed that these small molecule results directly correlated with the polymerizations. Ultimately this study highlighted the importance of intramolecular oxidative addition as a key step that determines between a step-growth and chain-growth mechanism, and we also showed that electron-rich ligands could favorably increase this pathway.[8]

Since this investigation of intramolecular oxidative addition in CTP, several notable studies by other groups have expanded upon this result. The most notable investigation was done by Locklin and coworkers when the used density functional theory computations and kinetic isotope effects to provide additional support for this intramolecular oxidative addition.[9] Specifically, they invoked an η^2-bound π-complex which was in accordance with the findings in our study. Additional studies have been done by Koeckelberghs,[10] Kiry,[11] Yokozawa,[12] and others have begun developing new conditions for CTP by targeting preferential oxidative addition.

Future work in the area of preferential oxidative addition should focus on utilizing this small molecule model system to probe other aspects of CTP. The most pressing attribute is investigating the ligand steric influence on the associative intermediate (Chart 5.1). We know that electron-rich catalysts are advantageous,[8] and previous work in the group has shown that moderate steric contributions are preferred,[13] but at the time we could only speculate that this was caused by disruption of the associative intermediate. However, with the small molecule model system presented, the ligand steric component can directly be investigated. Ligand cone and bite angle studies would illustrate the role these steric parameters play on a catalysts ability to undergo intramolecular oxidative addition. Additionally, a small molecule model system would be ideal for probing the reactive ligand of the catalyst. Substantial work in our lab has focused on modifying the reactive ligand of catalysts to improve initiation rates.[2] By modifying this reactive ligand on the catalyst in a small molecule model system, we could examine which monomers are able to effectively cross propagate and undergo intramolecular oxidative addition.

Chart 5.1 Selected Ligands Containing Various Steric Parameters

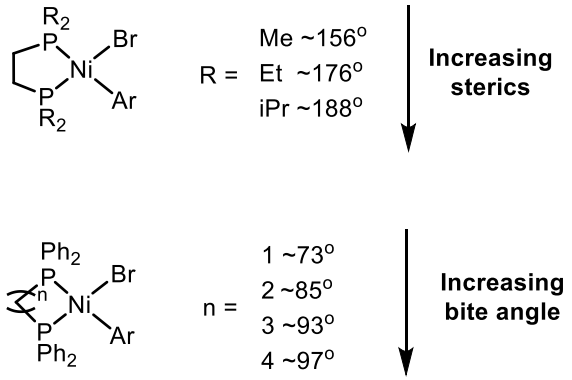

In the third chapter we discussed the first Pd-catalyzed CTP of phenylene and thiophene utilizing Grignards.[14] We targeted this Pd-NHC catalyst due to preferential multi-functionalization demonstrated by Goldup and coworkers in small molecule reactions.[15] We hypothesized that this preferential intramolecular oxidative addition could be due to an associate complex similar to CTP catalysts. Gratifyingly, we found this catalyst was able to perform homo- and block copolymerizations with thiophene and phenylene like current nickel catalysts. However, unlike current nickel catalysts which can only form blocks if thiophene is added after the initial phenylene block, this Pd-NHC catalyst could form block copolymers regardless of monomer order of addition. A catalyst that can add monomers in both directions is desirable because it allows the creation of more interesting sequences, such as multi-block copolymers. There were some stability concerns if the catalyst was left for several hours after reaching a high conversion, but this limitation is easily avoided by either adding a new monomer or quenching the reaction. We also examined this catalyst in the polymerization of fluorene, but polyfluorene was formed through an uncontrolled chain-growth mechanism.[14]

Since the application of this Pd-NHC catalyst towards CTP, several notable studies have been done to synthesize new polymers. Recently, Noonan and coworkers have used this Pd-NHC catalyst to polymerize thiophene under Stille conditions.[16] Wang and coworkers also replaced the 3-chloropyridine “throw away” ligand to acetylacetonate (acac) in the polymerization of thiophene and

fluorene.[17] This ligand substitution also allowed them to warm the reaction and change the solvent allowing for the highest recorded molecular weight of P3HT at 416 kDa, with a moderate Đ (1.72).

Future work in the area of Pd-NHC CTP should focus on elucidating the reaction mechanism. We expect the key mechanistic steps of oxidative addition, transmetalation, and reductive elimination will be similar to current nickel catalysts, however the rate-determining step and the role of the 3-chloropyridine could shed vital information for improving this catalyst. For instance, the rate determining step could explain why there are stability issues at low concentrations of monomer. The role of the "throw away" ligand could enable a more stabilizing ligand to be targeted to address this concern. Furthermore, modifications to the NHC ligand and "throw-away" ligand should be examined as previous studies have shown that electronic and steric contributions can play a big role in small molecule substrate scope (Chart 5.2). Based on small molecule experiments done by Organ and coworkers, we believe that Pd-NHC catalysts with higher steric values could accommodate additional monomers.[18] Studies within our lab suggest that increasing the electron-density of the ligand will improve the chain-growth behavior of CTP catalysts. However, trends should be determined as no mechanistic work has been done on the Pd-NHC catalyst. Additionally, electron-poor monomers should also be tested with this catalyst. Polymerization of fluorene was shown to follow an uncontrolled chain-growth mechanism, however we also observed active iPrMgCl remained following the Grignard metathesis. This active iPrMgCl capped growing chain-ends leading to premature chain-termination consistent with an uncontrolled mechanism. An alternative activation of the fluorene Grignard monomer presented by Wang and coworkers did not show any unreacted iPrMgCl,[19] therefore circumventing this side reaction.

Chart 5.2 Selected Modifications to the Pd-NHC Scaffold

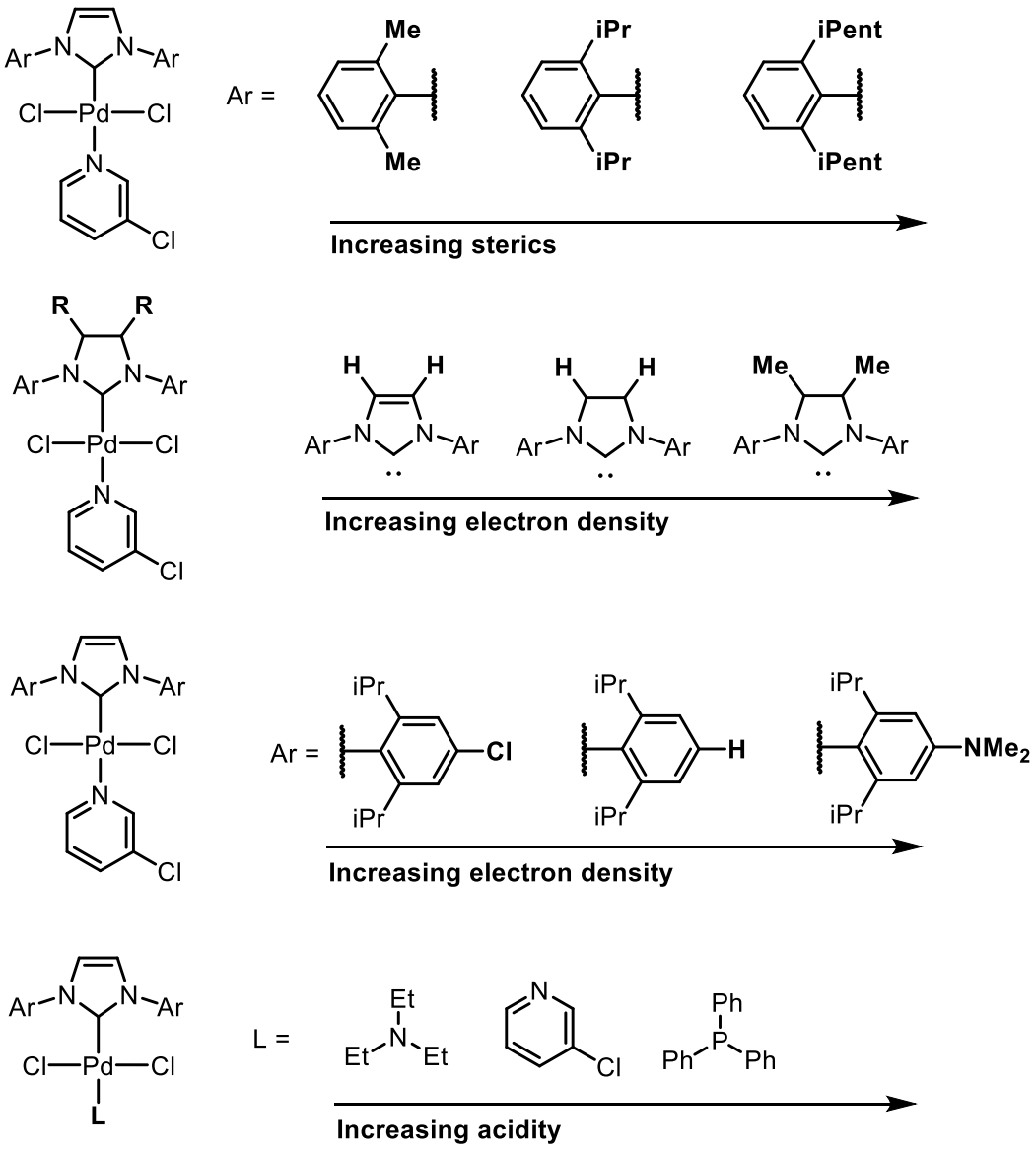

Finally, in Chapter 4 we discussed developing a small molecule model system as a means for investigating and optimizing new conditions for CTP. We initially targeted the Sonogashira synthesis of poly(2,5-bis(hexyloxy)phenylene ethynylene) as it was significantly different than other CTP methodology while Sonogashira cross-couplings are well established in the small molecule literature. Currently, the only CTP conditions for the synthesis of PPE were presented by Bielawski and coworkers, and this produced a stoichiometric amount of tin.[20] We were able to quickly and efficiently screen hundreds of conditions, looking for

preferential intramolecular oxidative addition and found several promising conditions. Unfortunately, it was discovered that these conditions lead to traditional step-growth polymerization behavior. This surprising result was further studied, which revealed that selective multi-functionalization could be achieved through relative reactivity differences between the starting materials and intermediates. By varying the ratio of starting materials, as well as comparing the Sonogashira conditions to known CTP catalysts under Kumada conditions, we observed that CTP catalysts exhibit nearly quantitative intramolecular oxidative addition regardless of the starting material ratios. However, the Sonogashira conditions exhibited variance as the starting material ratio changed, illustrating that it was governed by reactivity as opposed to an associative complex. These results illustrate that small molecule model systems need to control for these reactivity differences, which can lead to false positives.

Although the small molecule screen that we developed has not produced any new CTP conditions to this point, it is still reasonable to assume it could be used to examine new monomers. The most pressing need in the field is for electron-deficient monomers, and a small molecule screen would be ideal for testing new conditions as it utilizes simple small molecules which are typically easier to synthesize than the monomer, and most importantly it enables targeted iteration as the results give product ratios instead of an ambiguous failed polymerization. As these small molecule reactions give ratios, they can be directly compared to each other which will enables trends to be elucidated among the catalysts used.

Overall, the conjugated polymer field has advanced a great deal in a short period of time. Many new polymers[21] and copolymers[3,4] have been synthesized, and new applications have been discovered as groups have attached them to various surfaces.[22] However, we still need to focus on generating new CTP conditions for electron-deficient monomers as they are required to generate the most efficient optoelectronic devices currently being made with polymers.[23] We believe that the shortcomings, namely limited monomer scope, can be

accomplished through mechanistic investigation and small molecule probes. The work highlighted in this thesis has provided avenues for improvement in several areas. Intramolecular oxidative addition has been shown to be the key step in CTP, and electron-rich ligands favor this selectivity. CTP conditions for a Pd-NHC catalyst were found that are able to outperform current nickel catalysts in the copolymerization of thiophene and phenylene. A small molecule model system to quickly screen and iterate on cross-coupling conditions which can be used to test for intramolecular oxidative addition has also been presented. We also have shown that varying the starting material ratios is important to differentiate between intramolecular oxidative addition and relative reactivity differences. The key to making progress on these shortcomings are fundamental mechanistic understandings of the system in question. Insight on the underpinnings of CTP will inform design and allow for iteration. We must also apply this towards electron deficient-monomers. CTP will enable these n-type materials to be synthesized with unique copolymer structures (gradient and block) as well as grown from surfaces. With more research and continued vigor in the field, CTP could become the preferred route for the synthesis of π-conjugated polymers being used in LEDs, photovoltaics, transistors, and sensors.

References

(1) (a) Shirakawa, H.; Louis, E. J.; MacDiarmid, A. G.; Chiang, C. K.; Heeger, A. J. *J. Chem. Soc., Chem. Commun.,* **1977**, 578–580. (b) Chiang, C. K.; Fincher, C. R.; Park, Y. W.; Heeger, A. J.; Shirakawa, H.; Louis, E. J.; Gau S. C.; MacDiarmid, A. G. *Phys. Rev. Lett*. **1977**, *39*, 1098–1101. (c) Chiang, C. K.; Druy, M. A.; Gau, S. C.; Heeger, A. J.; Louis, E. J.; MacDiarmid, A. G.; Park, Y. W.; Shirakawa, H. *J. Am. Chem. Soc.* **1978**, *100*, 1013–1015. (d) Heeger, A. J. *Rev. Mod. Phys.* **2001**, *73*, 681–700. (e) MacDiarmid, A. G. *Rev. Mod. Phys.* **2001**, *73*, 701–712. (f) Shirakawa, H. *Rev. Mod. Phys.* **2001**, *73*, 713–718.

(2) (a) Lee, S. R.; Bloom, J. W. G.; Wheeler, S. E.; McNeil, A. J. *Dalton Trans.* **2013**, *42*, 4218–4222. (b) Lee, S. R.; Bryan, Z. J.; Wagner, A. M.; McNeil, A. J. *Chem. Sci*. **2012**, *3*, 1562–1566.

(3) (a) Javier, A. E.; Varshney, S. R.; McCullough, R. D. *Macromolecules* **2010**, *43*, 3233–3237. (b) Wu, S.; Sun, Y.; Huang, L.; Wang, J.; Zhou, Y.; Geng, Y.; Wang, F. *Macromolecules* **2010**, *43*, 4438–4440. (c) Van den Bergh, K.; Huybrechts, J.; Verbiest, T.; Koeckelberghs, G. *Chem. Eur. J.* **2008**, *14*, 9122–9125. (d) Yokozawa, T.; Adachi, I.; Miyakoshi, R.; Yokoyama, A. *High Perform. Polym.* **2007**, *19*, 684–699.

(4) (a) Palermo, E. F.; McNeil, A. J. *Macromolecules* **2012**, *45*, 5948–5955. (b) Locke, J. R.; McNeil, A. J. *Macromolecules* **2010**, *43*, 8709–8710. (c) Palermo, E. F.; van der Laan, H. L.; McNeil, A. J. *Polym. Chem*. **2013**, *4*, 4606-4611. (d) Palermo, E. F.; Darling, S. B.; McNeil, A. J. *J. Mater. Chem C.* **2014**, *2*, 3401-3406.

(5) For related reviews, see: (a) Yokozawa, T.; Nanashima, Y.; Ohta, Y. *ACS Macro. Lett.* **2012**, *1*, 862–866. (b) Marrocchi, A.; Lanari, D.; Facchetti, A.; Vaccaro, L. *Energy Environ. Sci.* **2012**, *5*, 8457–8474. (c) Stefan, M. C.; Bhatt, M. P.; Sista, P.; Magurudeniya, H. D. *Polym. Chem.* **2012**, *3*, 1693–1701. (d) Kiriy, A.; Senkovskyy, V.; Sommer, M. *Macro. Rapid Commun*. **2011**, *32*, 1503–1517. (e) Okamoto, K.; Luscombe, C. K. *Polym. Chem.* **2011**, *2*, 2424–2434. (f) Yokozawa, T.; Yokoyama, A. *Chem. Rev.* **2009**, *109*, 5595–5619. (g) Osaka, I.; McCullough, R. D. *Acc. Chem. Res.* **2008**, *41*, 1202–1214. (h) Miyakoshi, R.; Yokoyama, A.; Yokozawa, T. *J. Polym. Sci. Pol. Chem.* **2008**, *46*, 753–765. (i) Yokoyama, A.; Yokozawa, T. *Macromolecules* **2007**, *40*, 4093–4101. (j) Higashihara, T.; Ueda, M. *Macromol. Res.* **2013**, *21*, 257-271.

(6) (a) Lanni, E. L.; McNeil, A. J. *Macromolecules* **2010**, *43*, 8039–8044. (b) Lanni, E. L.; McNeil, A. J. *J. Am. Chem. Soc.* **2009**, *131*, 16573–16579. (c) See references 2 and 7.

(7) McCullough began using “π-complex” terminology in 2005. For reference, see: Iovu, M. C.; Sheina, E. E.; Gil, R. R.; McCullough, R. D. *Macromolecules* **2005**, *38*, 8649–8656.

(8) Bryan, Z. J.; McNeil, A. J. *Chem. Sci.* **2013**, *4*, 1620-1624.

(9) Bilbrey, J. A.; Sontag, S. K.; Huddleston, N. E.; Allen, W. D.; Locklin, J. *ACS Macro Lett.* **2012**, *1*, 995–1000.

(10) Willot, P.; Koeckelberghs, G. *Macromolecules*, **2014**, *47*, 8548-8555.

(11) (a) Senkovskyy, V.; Senkovska, I.; Kiriy, A. *ACS Macro. Lett.* **2012**, *1*, 494–498. (b) Kohn, P.; Huettner, S.; Komber, H.; Senkovskyy, V.; Tkachov, R.; Kiriy, A.; Friend, R. H.; Steiner, U.; Huck, W. T.; Sommer, J. U.; Sommer, M. *J. Am. Chem. Soc.* **2012**, *134*, 4790–4805. (c) Senkovskyy, V.; Tkachov, R.; Komber, H.; John, A.; Sommer, J.-U.; Kiriy, A. *Macromolecules* **2012**, *45*, 7770−7777.

(12) (a) Nanashima, Y.; Yokoyama, A.; Yokozawa, T. *J. Polym. Sci. Pol. Chem.* **2012**, *50*, 1054–1061. (b) Nanashima, Y.; Shibata, R.; Miyakoshi, R.; Yokoyama, A.; Yokozawa, T. *J. Polym. Sci. Pol. Chem.* **2012**, *50*, 3628–3640. (c) Nanashima, Y.; Yokoyama, A.; Yokozawa, T. *Macromolecules* **2012**, *45*, 2609–2613.

(13) Lanni, E. L.; Locke, J. R.; Gleave, C. M.; McNeil, A. J. *Macromolecules* **2011**, *44*, 5136–5145.

(14) Bryan, Z. J.; Smith, M. L.; McNeil, A. J. *Macromol. Rapid Comm.* **2012**, *33*, 842–847.

(15) Larrosa, I.; Somoza, C.; Banquy, A.; Goldup, S. M. *Org. Lett*. **2011**, *13*, 146–149.

(16) Qiu, Y.; Mohin, J.; Tsai, C.-H.; Tristram-Nagle, S.; Gil, R. R.; Kowalewski, T.; Noonan, K. J. T. *Macromol. Rapid Comm.* **2015**, DOI: 10.1002/marc.20150030.

(17) (a) Shi, X.; Wang, Y.; Li, Y.; Geng, Y.; Wang, F. *Chem. Comm.* **2015**, *51*, 2138-2140. (b) Sui, A.; Shi, X.; Tian, H.; Geng, Y.; Wang, F. *Polym. Chem.* **2014**, *5*, 7072-7080.

(18) (a) Nasielski, J.; Hadei, N.; Achonduh, G.; Kantchev, E. A. B.; O’Brien, C. J.; Lough, A.; Organ, M. G. *Chem. Eur. J.* **2010**, *16*, 10844–10853. (b) Tamba, S.; Shono, K.; Sugie, A.; Mori, A. *J. Am. Chem. Soc.* **2011**, *133*, 9700–9703. (c) Roy, A. H.; Hartwig, J. F. *J. Am. Chem. Soc*. **2003**, *125*, 13944–13945. (d) Roy, A. H.; Hartwig, J. F. *Organometallics* **2004**, *23*, 1533–1541.

(19) Sui, A.; Shi, X.; Wu, S.; Tian, S.; Geng, Y.; Wang, F. *Macromolecules*, **2012**, *45*, 5436-5443.

(20) Kang, S.; Ono, R. J.; Bielawski, C. W. *J. Am. Chem. Soc.* **2013**, *135*, 4984-4987.

(21) For representative examples, see: (a) Verswyvel, M.; Koeckelberghs, G. *Polym. Chem.* **2012**, *3*, 3203–3216. (b) Hollinger, J.; Jahnke, A. A.; Coombs, N.; Seferos, D. S. *J. Am. Chem. Soc.* **2010**, *132*, 8546–8547. (c) Van den Bergh, K.; Cosemans, I.; Verbiest, T.; Koeckelberghs, G. *Macromolecules* **2010**, *43*, 3794–3800. (d) Wang, Q.; Takita, R.; Kikuzaki, Y.; Ozawa, F. *J. Am. Chem. Soc.* **2010**, *132*, 11420–11421. (e) Doubina, N.; Stoddard, M.; Bronstein, H. A.; Jen, A. K. Y.; Luscombe, C. K. *Macromol. Chem. Phys.* **2009**, *210*, 1966–1972. (f) Li, L. S.; Hollinger, J.; Jahnke, A. A.; Petrov, S.; Seferos, D. S. *Chem. Sci.* **2011**, *2*, 2306–2310. (g) Hollinger, J.; Jahnke, A. A.; Coombs, N.; Seferos, D. S. *J. Am. Chem. Soc.* **2010**, *132*, 8546–8547. (h) Wu, Z. Q.; Radcliffe, J. D.; Ono, R. J.; Chen, Z.; Li, Z. C.; Bielawski, C. W. *Polym. Chem.* **2012**, *3*, 874–881. (i) Grisorio, R.; Suranna, G. P.; Mastrorilli, P. *Chem. Eur. J.* **2010**, *16*, 8054–8061. (j) Nanashima, Y.; Yokoyama, A.; Yokozawa, T. *J. Polym. Sci. Pol. Chem.* **2012**, *50*, 1054–1061. (k) Senkovskyy, V.; Tkachov, R.; Komber, H.; Sommer, M.; Heuken, M.; Voit, B.; Huck, W. T. S.; Kataev, V.; Petr, A.; Kiriy, A. *J. Am. Chem. Soc.* **2011**, *133*, 19966–19970. (l) Duck, B. C.; Dastoor, P. C.; Rasmussen, M. C. *Macromolecules* **2008**, *41*, 4576–4578.

(22) (a) Senkovskyy, V.; Senkovska, I.; Kiriy, A. *ACS Macro. Lett.* **2012**, *1*, 494–498. (b) Sontag, S. K.; Sheppard, G. R.; Usselman, N. M.; Marshall, N.; Locklin, J. *Langmuir* **2011**, *27*, 12033–12041. (c) Marshall, N.; Sontag, S. K.; Locklin, J. *Chem. Commun.* **2011**, *47*, 5681–5689. (d) Tkachov, R.; Senkovskyy, V.; Horecha, M.; Oertel, U.; Stamm, M.; Kiriy, A. *Chem. Commun.* **2010**, *46*, 1425–1427. (e) Senkovskyy, V.; Tkachov, R.; Beryozkina, T.; Komber, H.; Oertel, U.; Horecha, M.; Bocharova, V.; Stamm, M.; Gevorgyan, S. A.; Krebs, F. C.; Kiriy, A. *J. Am. Chem. Soc.* **2009**, *131*, 16445–16453. (f) Khanduyeva, N.; Senkovskyy, V.; Beryozkina, T.; Bocharova, V.; Simon, F.; Nitschke, M.; Stamm, M.; Grotzschel, R.; Kiriy, A. *Macromolecules* **2008**, *41*, 7383–7389.

(23) (a) Zhao, X.; Zhan, X. *Chem. Soc. Rev.* **2011**, *40*, 3728–3743. (b) Beaujuge, P. M.; Fréchet, J. M. J. *J. Am. Chem. Soc.* **2011**, *133*, 20009-20029. (c) Zhan, X. W.; Zhu, D. B. *Polym. Chem*. **2010**, *1*, 409-419. (d) Zhan, X.; Tan, Z.; Domercq, B.; An, Z.; Zhang, X.; Barlow, S.; Li, Y.; Zhu, D.; Kippelen B.; Marder, S. R. *J. Am. Chem. Soc*. **2007**, *129*, 7246–7247. (e) Li, H.; Kim, F. S.; Jenekhe, S. A. *J. Am. Chem. Soc.* **2013**, *135*, 14920-14923.

Appendix 1

Supporting Information for Chapter 2:
Evidence for a preferential intramolecular oxidative addition in Ni-catalyzed cross-coupling reactions and their impact on chain-growth polymerizations

Contents **Page**

I. Materials

Flash chromatography was performed on SiliCycle silica gel (40-63 μm) and thin layer chromatography was performed on Merck TLC plates pre-coated with silica gel 60 F254. *i*-PrMgCl (2 M in THF), **2** (1 M in THF), and *i*-PrMgBr (2.7 M in 2-MeTHF) were purchased in 100 mL quantities from Aldrich. $Ni(cod)_2$, depe, and dppe were purchased from Strem. All other reagent grade materials and solvents were purchased from Aldrich, Acros, EMD, or Fisher and used without further purification unless otherwise noted. THF was dried and deoxygenated using an Innovative Technology (IT) solvent purification system composed of activated alumina, copper catalyst, and molecular sieves. *N*-Bromosuccinimide was recrystallized from hot water and dried over P_2O_5. All glassware was oven-dried at 120 °C for at least 1 h before use. Compounds **S11**[1] and **S12**[1] were prepared according to modified literature procedures.

II. General Experimental

NMR Spectroscopy: Unless otherwise noted, ^{1}H, ^{13}C, and ^{31}P NMR spectra for all compounds were acquired at rt in $CDCl_3$ or CD_2Cl_2 on a Varian vnmrs 500 operating at 500, 126, and 202 MHz or a Varian MR 400 operating at 400, 100 and 162 MHz, respectively. For ^{1}H, and ^{13}C NMR spectra in deuterated solvents, the chemical shift data are reported in units of δ (ppm) relative to tetramethylsilane (TMS) and referenced with residual solvent. For ^{31}P NMR spectra in deuterated solvents, the chemical shift data are reported in units of δ (ppm) relative to H_3PO_4 and referenced with residual solvent. For ^{1}H and ^{31}P NMR spectra in non-deuterated THF, the chemical shift data are reported in units of δ (ppm) and referenced with the THF peak at 3.58 ppm in the ^{1}H NMR spectrum, which is then applied to all nuclei. Multiplicities are reported as follows: singlet (s), doublet (d), doublet of doublets (dd), triplet (t), quartet (q), multiplet (m), and broad resonance (br).

Gel-Permeation Chromatography: Polymer molecular weights were determined by comparison with polystyrene standards (Varian, EasiCal PS-2 MW 580-377,400) on a Waters 1515 HPLC instrument equipped with Waters Styragel® (7.8 x 300 mm) THF HR 0.5, THF HR 1, and THF HR 4 type columns in sequence and analyzed with Waters 2487 dual absorbance detector (254 nm). Samples were dissolved in THF (with mild heating) and passed through a 0.2 µm PTFE filter prior to analysis.

Titrations of the Grignard Reagents: An accurately weighed sample of salicylaldehyde phenylhydrazone (typically between 290-310 mg) was dissolved in 5.00 mL of THF. A 0.50 mL aliquot of this solution was stirred at rt while ArMgBr was added dropwise using a 500 µL syringe. The initial solution is yellow and turns bright orange at the end-point.[2]

Gas Chromatography: Gas chromatography was carried out using a Shimadzu GC 2010 containing a Shimadzu SHRX5 (crossbound 5% diphenyl – 95% dimethyl polysiloxane; 15 m 0.25 mm ID, 0.25 µm df) column.

III. Synthetic Procedures

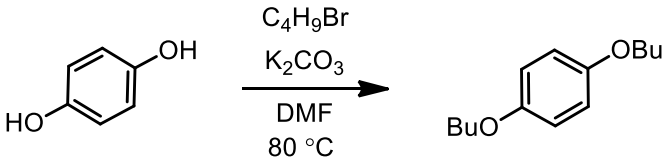

S1

S1.[1] A 500 mL round-bottom flask was equipped with a stir bar. Sequentially, hydroquinone (20. g, 0.20 mol, 1.0 equiv), anhydrous DMF (120 mL), and 1-bromobutane (49 mL, 0.45 mol, 2.5 equiv) were added to the flask. The flask was put under N_2 atmosphere and stirred vigorously while heated to 80 °C. Once at 80 °C, potassium carbonate (63 g, 0.45 mmol, 2.5 equiv) was slowly added and subsequently put under N_2 atmosphere again for 5 d. After cooling to rt, the reaction mixture was poured into water (400 mL). The reaction mixture was extracted with hexanes (3 x 200 mL). The organic layers were combined and washed with water (2 x 200 mL) and brine (1 x 200 mL), dried over $MgSO_4$, filtered, and concentrated in vacuo. The resulting oil was passed though silica gel with neat DCM as the eluent. Recrystallization from hot methanol produced 35 g of **S1** as a white crystalline solid (86% yield). HRMS (EI): Calcd. For $C_{14}H_{22}O_2$, 222.1620 [M+]; found, 222.1626.

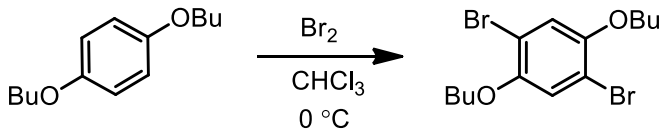

S1 **S2**

S2.[1] A 500 mL round-bottom flask was equipped with a stir bar. Sequentially, **S1** (17 g, 0.078 mol, 1.0 equiv), and $CHCl_3$ (90 mL) were added to the flask. The reaction flask was cooled to 0 °C in an ice/water bath and fitted with an addition funnel. Bromine (10 mL, 0.19 mol, 2.5 equiv) was added dropwise under N_2 and the pressure was vented through a solution of aq saturated Na_2SO_3 and $NaHCO_3$ (50:50). After 3 h, the reaction was quenched with an aq saturated solution of Na_2CO_3 (100 mL) and stirred vigorously until colorless. The aqueous mixture was extracted with DCM (3 x 100 mL). The organic layers were combined and washed with water (2 x 200 mL) and brine (1 x 200 mL), dried over $MgSO_4$, filtered, and concentrated in vacuo. The residue was recrystallized from DCM/methanol to produce 23 g of **S2** as a white solid (79% yield). HRMS (EI): Calcd. For $C_{14}H_{20}Br_2O_2$, 377.9830 [M+]; found, 377.9824.

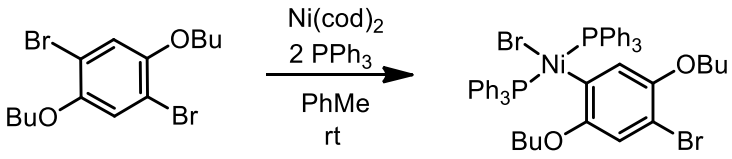

S2 **1b**

1b.[3] In the glovebox, an oven-dried 25 mL flask was equipped with a stir bar and charged with $Ni(cod)_2$ (0.25 g, 0.91 mmol, 1.0 equiv), PPh_3 (0.48 g, 1.8 mmol, 2.0 equiv), and toluene (10 mL). After 30 min of stirring, **S2** (0.68 g, 1.8 mmol, 2.0 equiv) was dissolved in a minimal amount of toluene and added dropwise to the flask and allowed to stir for 1 h at rt. Once the reaction was complete as observed by ^{31}P NMR spectroscopy, the product was precipitated with hexanes (25 mL) and removed from the glovebox. The air-stable solid was collected by filtration and washed with MeOH to produce 0.58 g of yellow-orange solid (66% yield). Elemental Analysis: Calcd for $C_{50}H_{50}Br_2NiO_2P_2$, C, 62.34, H, 5.23, Br 16.59; Found C, 62.26, H, 5.08, Br, 16.42. ^{31}P NMR (202 MHz, $CDCl_3$) δ 21.50.

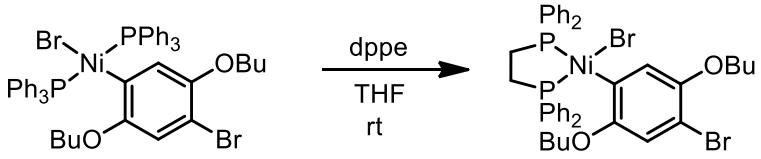

1b **1a**

1a.[3] In the glovebox a 20 mL vial was equipped with a stir bar and charged with **1b** (0.25 g, 0.26 mmol, 1.0 equiv), dppe (0.10 g, 0.26 mmol, 1.0 equiv), and THF (5 mL). The reaction was left to stir for 1 h at rt. The solution was partially concentrated (50%) and hexanes (15 mL) was added. The resulting orange solid was then recrystallized from THF/hexanes and filtered to produce 0.16 g of **1a** (73% yield). Elemental Analysis: Calcd for $C_{40}H_{44}Br_2NiO_2P_2$, C, 57.38, H, 5.30, Br 19.09; Found C, 57.33, H, 5.39, Br, 18.98. ^{31}P NMR (202 MHz, CD_2Cl_2) δ 57.69 (d, J = 29.2 Hz), 41.15 (d, J = 29.2 Hz).

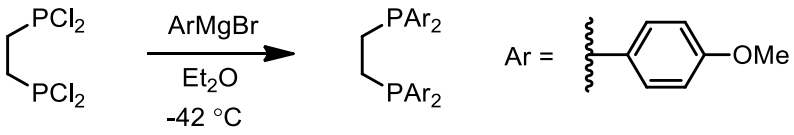

S3

S3.[4] In the glovebox an oven-dried 50 mL Schlenk flask was equipped with a stir bar and charged with 1,2-bis(dichlorophosphino)ethane (0.39 mL, 2.6 mmol, 1.0 equiv) and anhydrous Et_2O (15 mL). The flask was removed, placed under an N_2 atmosphere on a Schlenk line, and then cooled to -42 °C in a $MeCN/CO_2$ bath. Once cooled, *p*-methoxyphenylmagnesium bromide, 0.5 M solution in THF (31 mL, 15 mmol, 6.0 equiv) was added dropwise over the course of an hour. The reaction was stirred for an additional 1 h at -42 °C and warmed to rt over 1.5 h. Additional *p*-methoxyphenylmagnesium bromide, 0.5 M solution in THF (10 mL, 5.1 mmol, 2.0 equiv) was then added dropwise and the reaction was warmed to 45 °C for 4 h. Upon completion as determined by ^{31}P NMR spectroscopy, the reaction was cooled to rt and quenched with saturated aq NH_4Cl (50 mL). The mixture was extracted with Et_2O (3 x 25 mL) and the organic layers were combined, dried over $MgSO_4$, filtered and concentrated in vacuo. Recrystallization in methanol/THF produced 0.42 g of white crystalline solid (32% yield). ^{31}P NMR (202 MHz, $CDCl_3$) δ 16.50.

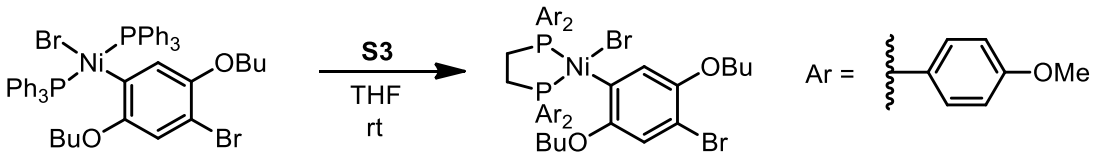

1b **1c**

1c.[5] In the glovebox a 20 mL vial was equipped with a stir bar and charged with **1b** (0.25 g, 0.26 mmol, 1.0 equiv), **S3** (0.14 g, 0.26 mmol, 1.0 equiv), and THF (5 mL). The reaction was left to stir for 1 h at rt. The solution was concentrated and precipitated with hexanes (18 mL). The orange solid was then recrystallized from THF/hexanes, filtered, and triturated with hexanes to produce 0.15 g of **1c** (61% yield). Elemental Analysis: Calcd for $C_{44}H_{52}Br_2NiO_6P_2$, C, 55.20, H, 5.47, Br 16.69; Found C, 55.30, H, 5.50, Br, 16.41. ^{31}P NMR (202 MHz, CD_2Cl_2) δ 55.77 (d, *J* = 32.8 Hz), 39.75 (d, *J* = 32.8 Hz).

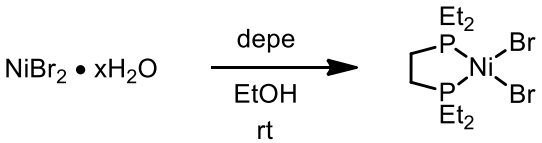

S4

S4.[4] A 25 mL Schlenk flask was placed under N_2 and equipped with a stir bar. Sequentially, $NiBr_2 \bullet xH_2O$ (0.20 g, 0.69 mmol, 1.0 equiv) and ethanol (13 mL) were added to the flask and the solution was sparged with N_2 for 15 min. Then, 1,2-bis(diethylphosphino)ethane (depe) (0.14 g, 0.69 mmol, 1.0 equiv) was taken from the glovebox in a syringe and injected directly into the flask. The reaction was stirred for 25 min and a dark red solid formed. The reaction was left overnight uncapped to crystallize, filtered, and washed with cold EtOH to produce 0.16 g of **S4** (55% yield). HRMS (EI): Calcd. For $NiC_{10}H_{24}Br_2$, 421.9073 [M+]; found, 421.9066. ^{31}P NMR (202 MHz, $CDCl_3$) δ 82.58.

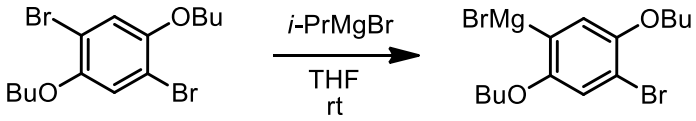

S2 **S5**

S5.[1] All actions were performed in a glovebox under N_2 atmosphere. A 20 mL vial was equipped with a stir bar. Sequentially, **S2** (0.90 g, 2.3 mmol, 1.0 equiv), THF (2.5 mL), and *i*-PrMgBr (0.79 mL, 2.1 mmol, 0.9 equiv) were added to the flask. The reaction was stirred at rt overnight. Concentration was determined by titration immediately before use as described in the general experimental (page S2).

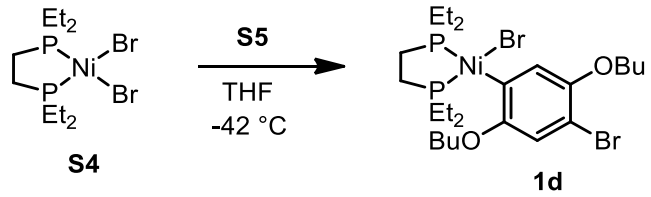

1d. In the glovebox an oven-dried 50 mL Schlenk flask was equipped with a stir bar. Sequentially, **S4** (0.15 g, 0.37 mmol, 1.0 equiv) and THF (12 mL) were added and the flask was equipped with a septum secured with copper wire. Freshly prepared **S5** (0.84 mL, 0.44 M, 0.37 mmol, 1.0 equiv) was placed in an oven-dried Schlenk tube, diluted with THF (12 mL), and sealed. Both flasks were removed from the glovebox and placed under N_2 atmosphere. The Schlenk flask containing **S4** was then cooled to -42 °C in a MeCN/CO_2 bath. Next, the solution of **S5** was cannula transferred to the Schlenk flask containing **S4** dropwise over the course of 5 min and stirred for 1 h. Upon completion as determined by ^{31}P NMR spectroscopy, the reaction was warmed to rt and quenched with saturated aq NaBr (25 mL). The mixture was extracted with hexanes (3 x 25 mL) and the organic layers were combined, dried over $MgSO_4$, filtered, concentrated in vacuo, and taken back into the glovebox. Recrystallization in THF/hexanes produced 0.12 g of yellow-orange crystalline solid (50% yield). Elemental Analysis: Calcd for $C_{24}H_{44}Br_2NiO_2P_2$, C, 44.69, H, 6.88, Br 24.77; Found C, 44.58, H, 6.85, Br, 24.97. ^{31}P NMR (202 MHz, CD_2Cl_2) δ 65.48 (d, *J* = 33.6 Hz), 58.80 (d, *J* = 33.6 Hz).

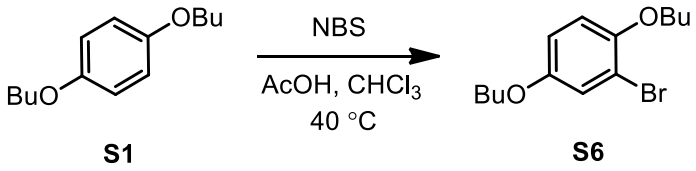

S6.[1] A 150 mL round-bottom flask was equipped with a stir bar. Sequentially, **S1** (5.0 g, 23 mmol, 1.0 equiv), $CHCl_3$ (85 mL), N-bromosuccinimide (NBS) (4.0 g, 23 mmol, 1.0 equiv), and acetic acid (43 mL) were added. The mixture was stirred at 40 °C for 24 h. Upon completion, the reaction solution was quenched with H_2O (50 mL). The aqueous layer was then extracted with $CHCl_3$ (2 x 50 mL), and the combined organic layers were washed with 20% w/v aq NaOH (1 x 50 mL), water (3 x 125 mL), dried over $MgSO_4$, filtered, and concentrated in vacuo. Distillation (158 °C , 0.2 torr) produced 2.7 g of **S6** as a light yellow oil (40% yield). HRMS (EI): Calcd. For $C_{14}H_{21}Br$, 300.0725 [M+]; found, 300.0730.

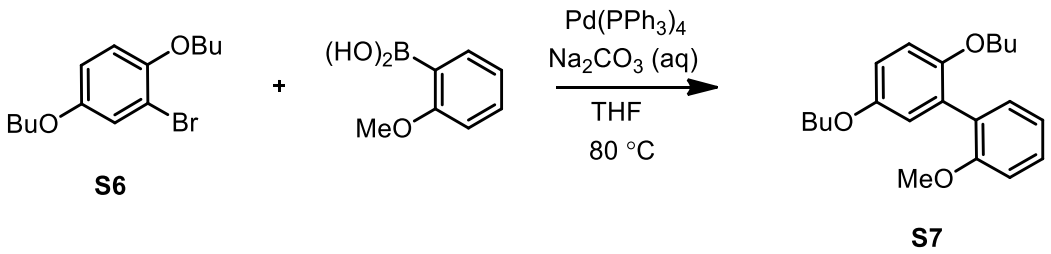

S6 **S7**

S7. A 250 mL Schlenk flask was equipped with a stir bar and placed under N_2 atmosphere. Sequentially, **S6** (1.4 g, 4.6 mmol, 1.0 equiv), 2-methoxyphenylboronic acid (0.6 g, 4.2 mmol, 0.9 equiv), THF (85 mL), tetrakis(triphenylphosphine)palladium(0) (0.3 g, 0.2 mmol, 0.05 equiv), and aq Na_2CO_3 (2 M, 80 mL) were added with stirring. This Schlenk flask was then equipped with a reflux condenser, heated to 80 °C for 36 h. Upon completion, the reaction was cooled to rt and extracted with DCM (3 x 50 mL). The combined organic layers were washed with water (2 x 75 mL) and brine (1 x 75 mL), dried over $MgSO_4$, filtered, and concentrated in vacuo. Column chromatography (85% hexanes, 15% DCM) gave 0.6 g of the product as a clear oil (42% yield). HRMS (EI): Calcd. For $C_{21}H_{28}O_3$, 329.2111 [M+]; found, 329.2105.

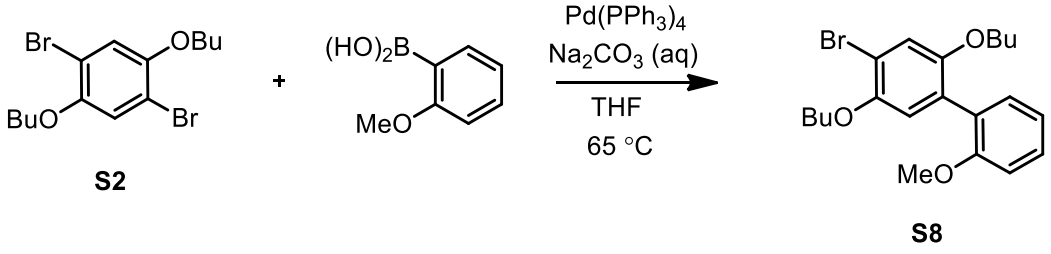

S2 **S8**

S8. A 50 mL Schlenk flask was equipped with a stir bar and placed under N_2 atmosphere. Sequentially, **S2** (0.50 g, 1.3 mmol, 1.0 equiv), 2-methoxyphenylboronic acid (0.15 g, 0.99 mmol, 0.75 equiv), THF (15 mL), tetrakis(triphenylphosphine)palladium(0) (0.08 g, 0.07 mmol, 0.05 equiv), and aq Na_2CO_3 (2 M, 10 mL) were added with stirring. This Schlenk flask was then equipped with a reflux condenser, heated to 65 °C for 18 h. Upon completion, the reaction was cooled, and extracted with DCM (3 x 25 mL). The combined organic layers were washed with water (2 x 50 mL) and brine (1 x 50 mL), dried over $MgSO_4$, filtered, and concentrated in vacuo. Column chromatography (85% hexanes, 15% DCM) gave 0.09 g of the product as a clear oil (22% yield). HRMS (EI): Calcd. For $C_{21}H_{27}BrO_3$, 407.1216 [M+]; found, 407.1215.

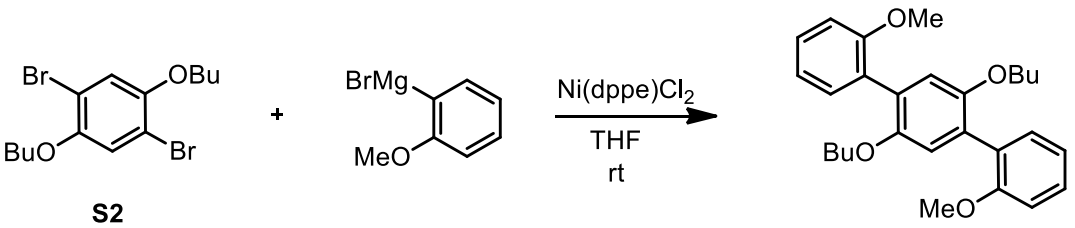

S2 **S9**

S9. In the glovebox, a 20 mL vial was equipped with a stir bar. Sequentially, **S2** (1.0 g, 2.6 mmol, 1.0 equiv), 2-methoxyphenylmagnesium bromide (1 M, 6.6 mmol, 2.5 equiv), THF (15 mL), and Ni(dppe)Cl_2 (0.07 g, 0.1 mmol, 0.05 equiv) were added with stirring. This mixture was then stirred at rt for 2 h. Upon completion, the vial was removed from the glovebox and quenched with hydrochloric acid (12.1 M, 5 mL) and subsequently diluted with water (25 mL). The reaction was then extracted with DCM (3 x 25 mL). The combined organic layers were washed with aq saturated $NaHCO_3$ (1 x 50 mL), water (2 x 50 mL) and brine (1 x 50 mL), dried over $MgSO_4$, filtered, and concentrated in vacuo. Column chromatography (85% hexanes, 15% DCM) gave 0.11 g of the product as a clear oil (10% yield). HRMS (EI): Calcd. For $C_{28}H_{34}O_4$, 407.1216 [M+]; found, 407.1215.

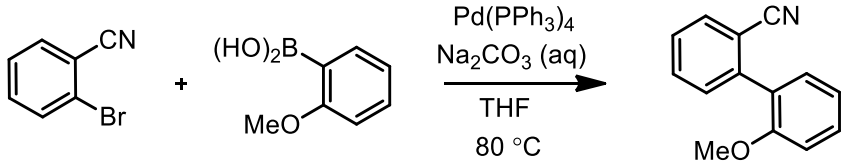

S10

S10. A 50 mL Schlenk flask was equipped with a stir bar and placed under N_2 atmosphere. Sequentially, 2-bromobenzonitrile (0.50 g, 2.8 mmol, 1.0 equiv), 2-methoxyphenylboronic acid (0.42 g, 2.8 mmol, 1.0 equiv), THF (15 mL), tetrakis(triphenylphosphine)palladium(0) (0.16 g, 0.14 mmol, 0.050 equiv), and aq Na_2CO_3 (2 M, 10 mL) were added with stirring. This Schlenk flask was then equipped with a reflux condenser and heated to 80 °C for 36 h. Upon completion, the reaction was cooled and extracted with DCM (3 x 25 mL). The combined organic layers were washed with water (2 x 50 mL) and brine (1 x 50 mL), dried over $MgSO_4$, filtered, and concentrated in vacuo. Column chromatography (85% hexanes, 15% DCM) gave 0.32 g of the colorless oil as a product (55% yield). HRMS (EI): Calcd. For $C_{14}H_{11}NO$, 210.0913 [M+]; found, 210.0907.

IV. NMR Spectra

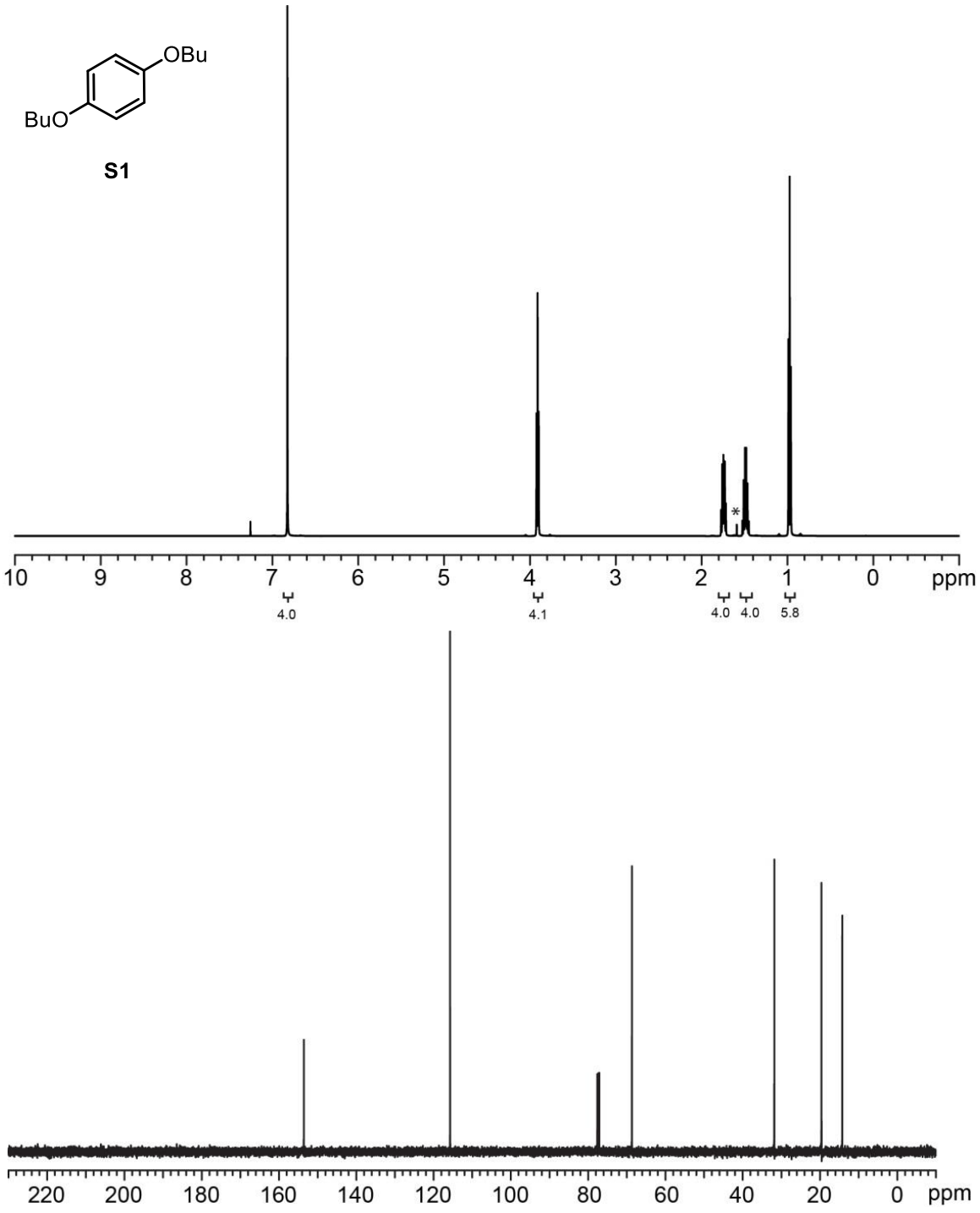

Figure S1.1 ^{1}H and ^{13}C NMR spectra for **S1**. ^{1}H NMR (500 MHz, $CDCl_3$) δ 6.83 (s, 4H), 3.92 (t, *J* = 7.0 Hz, 4H), 1.75 (m, 4H), 1.49 (m, 4H), 0.98 (t, *J* = 7.3 Hz, 6H). * indicates residual H_2O. ^{13}C NMR (126 MHz, $CDCl_3$) δ 153.19, 115.36, 68.30, 31.45, 19.24, 13.84.

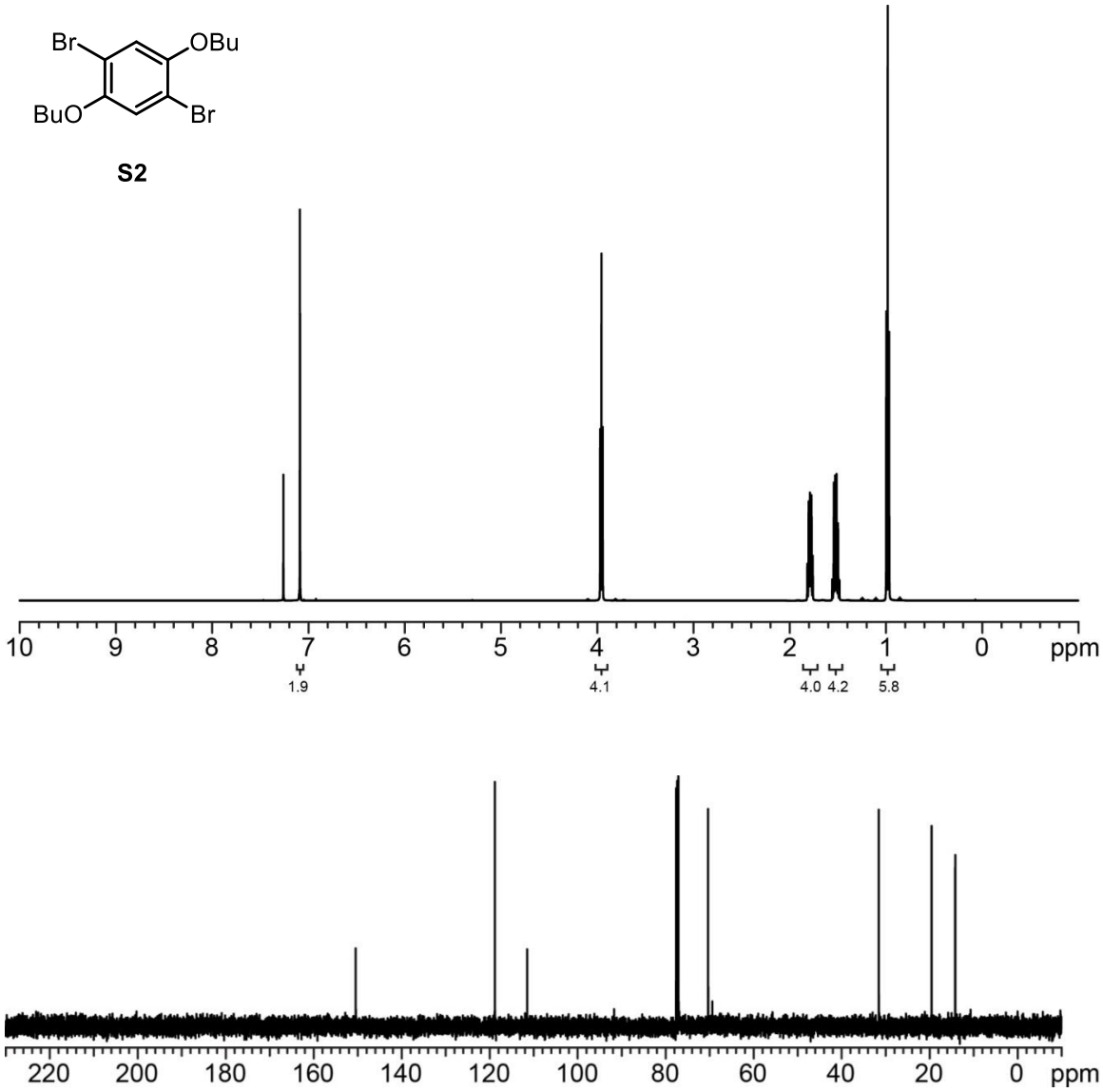

Figure S1.2 ^{1}H and ^{13}C NMR spectra for **S2**. ^{1}H NMR (500 MHz, $CDCl_3$) δ 7.09 (s, 2H), 3.96 (t, *J* = 6.7 Hz, 4H), 1.79 (m, 4H), 1.53 (m, 4H), 0.98 (t, *J* = 7.2 Hz, 6H). ^{13}C NMR (126 MHz, $CDCl_3$) δ 150.08, 118.46, 111.13, 69.99, 31.19, 19.19, 13.81.

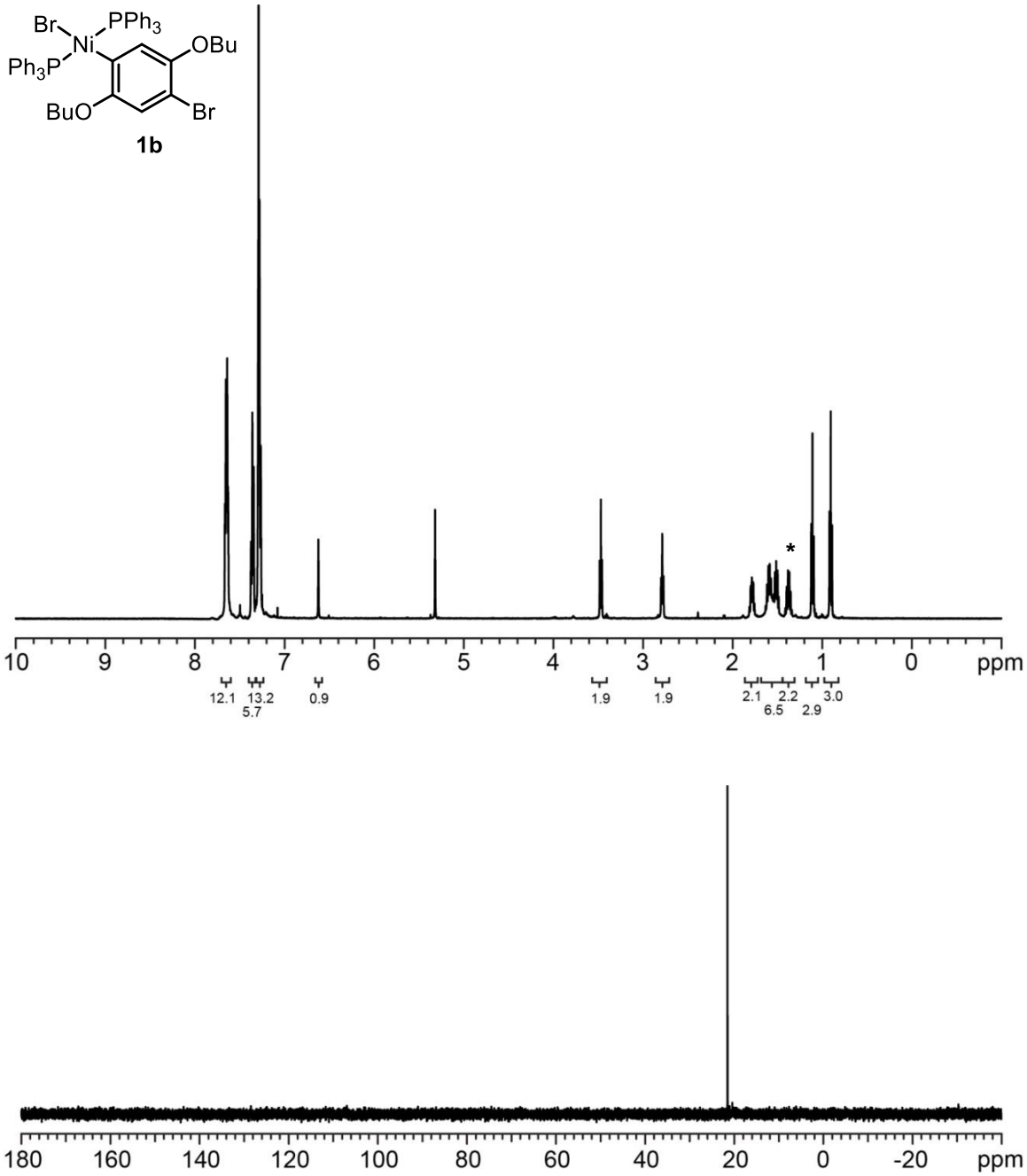

Figure S1.3 ^{1}H and ^{31}P NMR spectra for **1b**. ^{1}H NMR (500 MHz, CD_2Cl_2) δ 7.66-7.63 (br, 12H), 7.37-7.34 (br m, 6H), 7.29-7.27 (br m, 13H), 6.62 (s, 1H), 3.47 (t, *J* = 6.6 Hz, 2H), 2.79 (t, *J* = 6.6 Hz, 2H), 1.79 (m, 2H), 1.61-1.45 (br m, 4H), 1.37 (m, 2H), 1.11 (t, *J* = 7.4 Hz, 3H), 0.91 (t, *J* = 7.4 Hz, 3H). * indicates residual H_2O. ^{31}P NMR (202 MHz, CD_2Cl_2) δ 21.50.

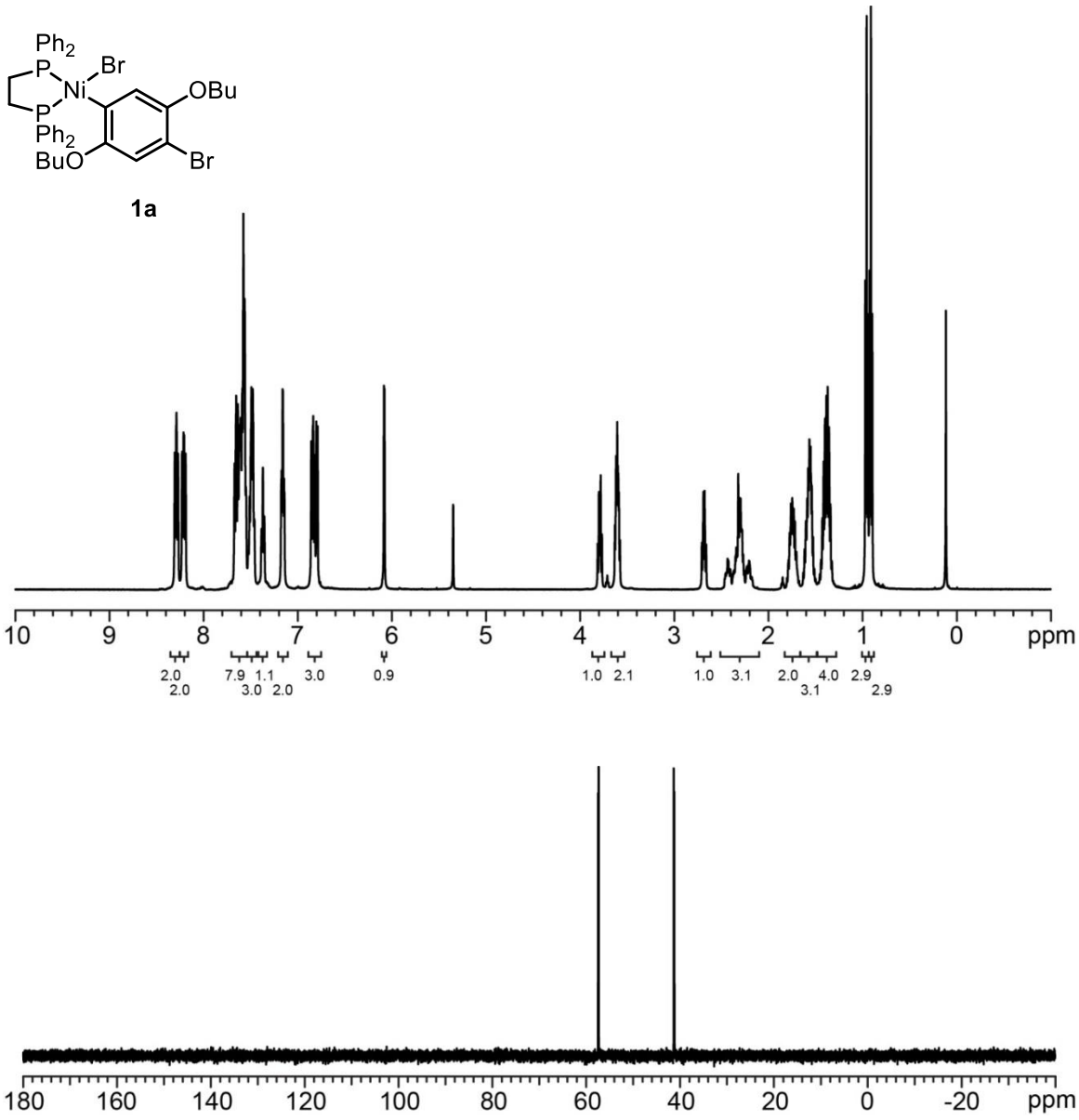

Figure S1.4 ^{1}H and ^{31}P NMR spectra for **1a**. ^{1}H NMR (500 MHz, CD_2Cl_2) δ 8.29 (t, *J* = 8.7 Hz, 2H), 8.21 (t, *J* = 9.2 Hz, 2H), 7.67-7.56 (m, 8H), 7.52-7.45 (m, 3H), 7.37 (t, *J* = 7.2 Hz, 1H), 7.16 (t, *J* = 7.4 Hz, 2H), 6.86-6.79 (m, 3H), 6.08 (s, 1H), 3.79 (q, *J* = 6.6 Hz, 1H), 3.64-3.57 (m, 2H), 2.68 (q, *J* = 5.9 Hz, 1H), 2.48-2.18 (m, 3H), 1.75 (m, 2H), 1.57 (m, 3H), 1.39 (m, 4H), 0.96 (t, *J* = 7.5 Hz, 3H), 0.91 (t, *J* = 7.5 Hz, 3H) . ^{31}P NMR (202 MHz, CD_2Cl_2) δ 57.69 (d, *J* = 29.2 Hz), 42.15 (d, *J* = 29.2 Hz).

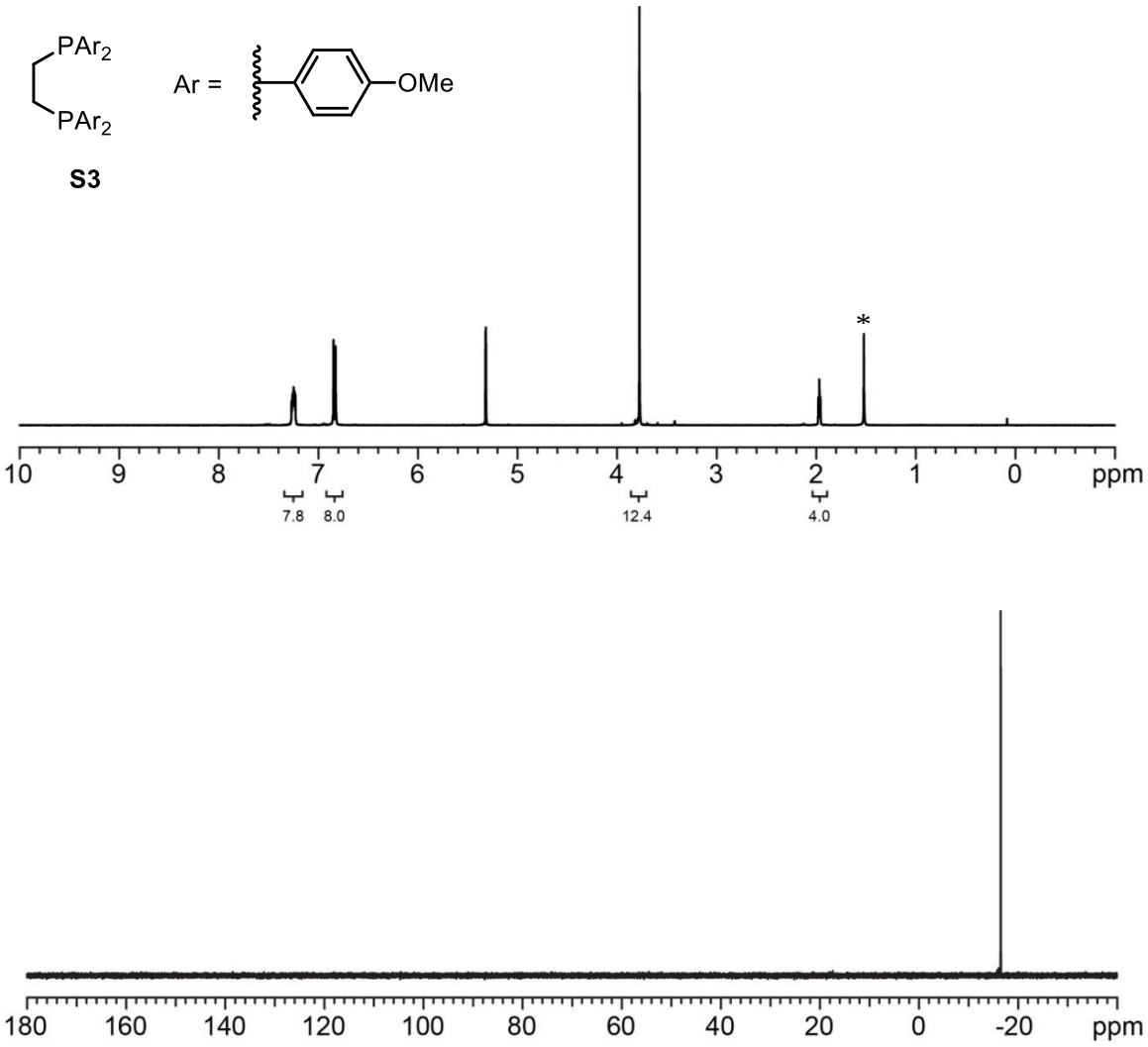

Figure S1.5 ^{1}H and ^{31}P NMR spectra for **S3**. ^{1}H NMR (400 MHz, CD_2Cl_2) δ 7.26-7.24 (m, 8H), 6.84 (d, *J* = 8.6 Hz, 8H), 3.78 (s, 12H), 1.97 (t, *J* = 4.7, 4H). * indicates residual H_2O. ^{31}P NMR (162 MHz, CD_2Cl_2) δ -16.50.

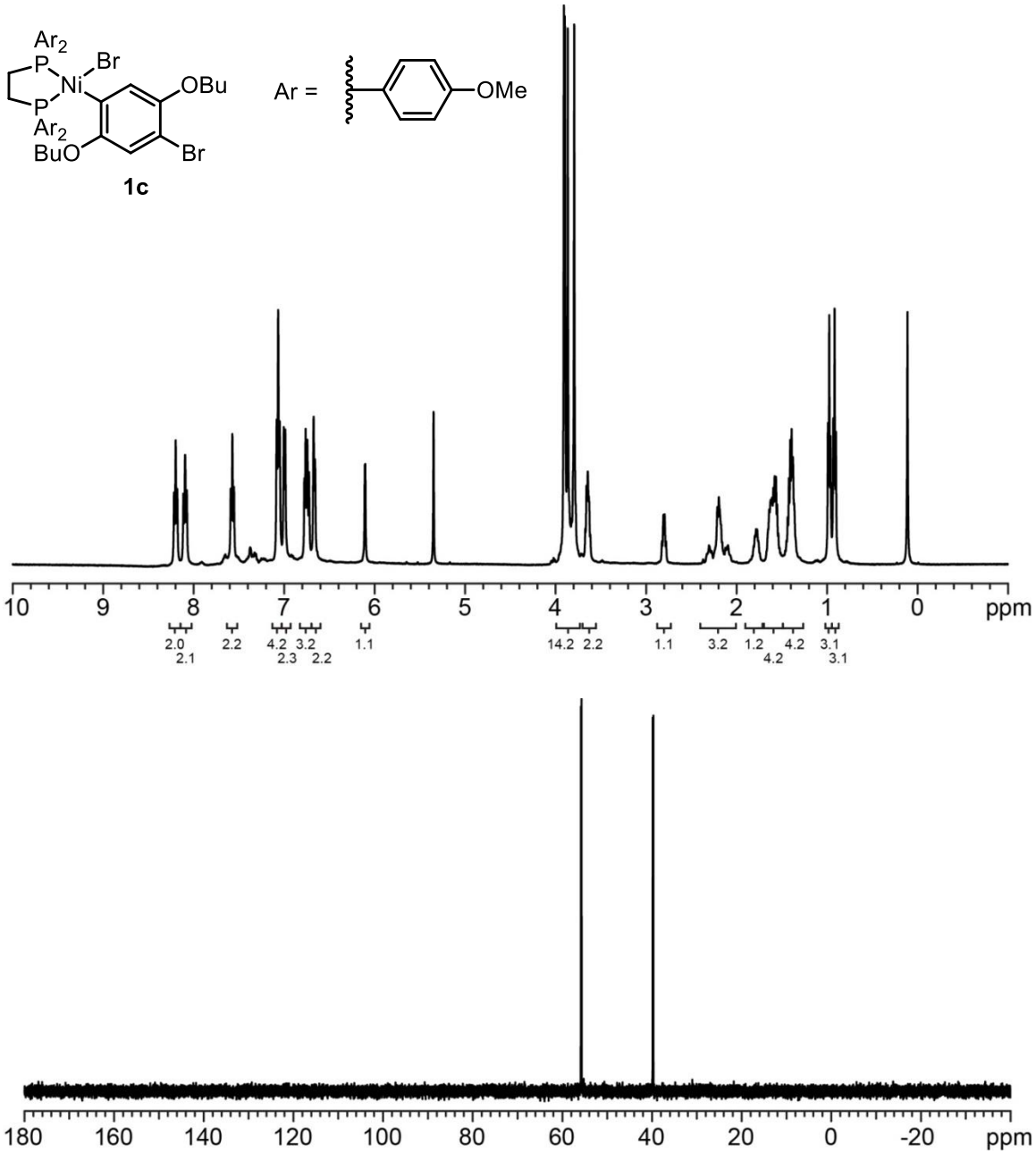

Figure S1.6 ^{1}H and ^{31}P NMR spectra for **1c**. ^{1}H NMR (500 MHz, CD_2Cl_2) δ 8.20 (t, *J* = 9.2 Hz, 2H), 8.10 (t, *J* = 9.7 Hz, 2H), 7.57 (t, *J* = 9.0 Hz, 2H), 7.07 (t, *J* = 8.5 Hz, 4H), 6.99 (d, *J* = 7.8 Hz, 2H), 6.77-6.71 (m, 3H), 6.66 (d, *J* = 7.8 Hz, 2H), 6.10 (s, 1H), 3.91-3.79 (m, 14H), 3.66-3.63 (m, 2H), 2.80 (q, *J* = 6.6 Hz, 1H), 2.38-2.05 (m, 2H), 1.83-1.72 (m, 1H), 1.64-1.55 (m, 4H), 1.40 (m, 4H), 0.98 (t, *J* = 7.4 Hz, 3H), 0.92 (t, *J* = 7.4 Hz, 3H) . ^{31}P NMR (202 MHz, CD_2Cl_2) δ 55.77 (d, *J* = 32.8 Hz), 39.75 (d, *J* = 32.8 Hz).

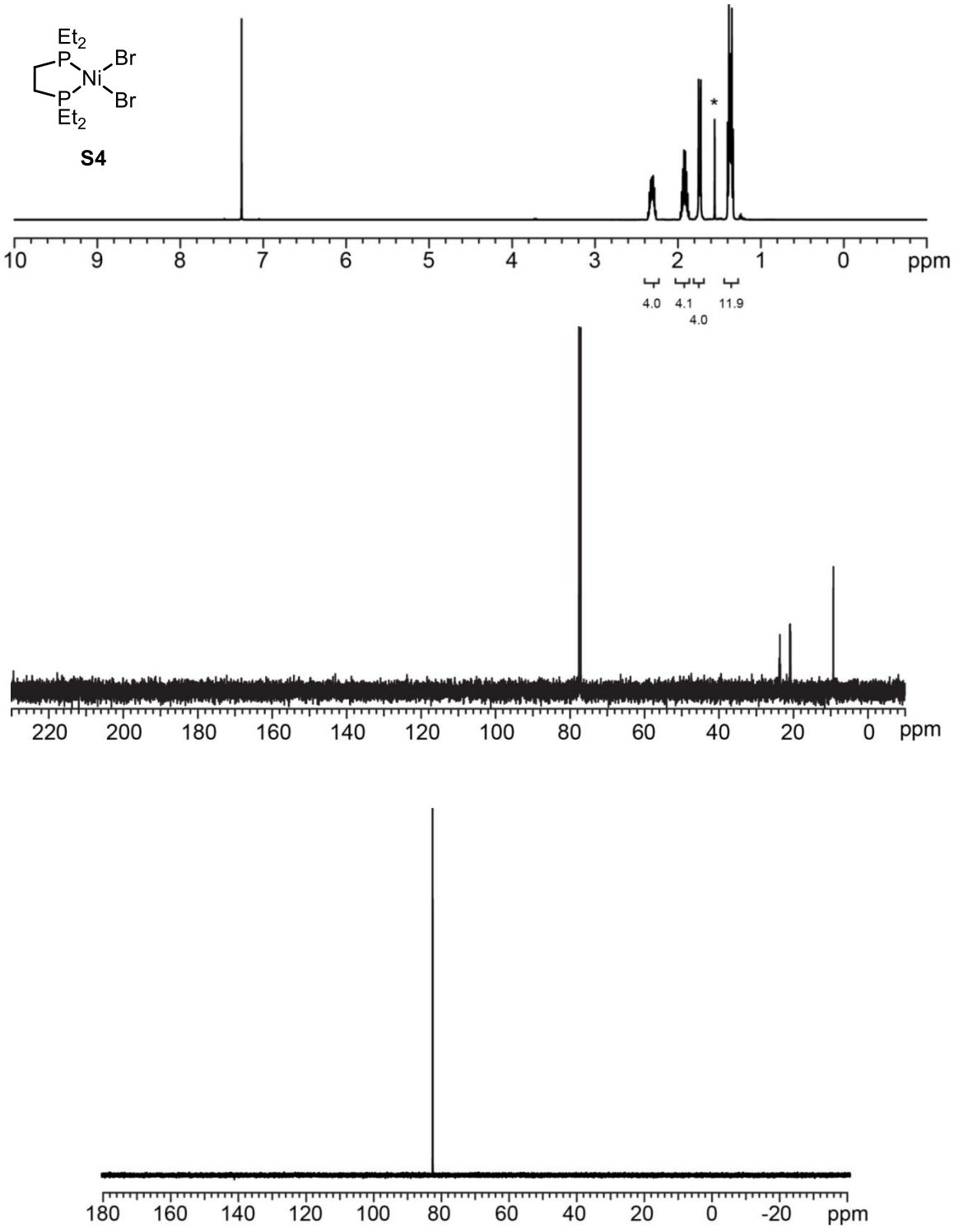

Figure S1.7 ^{1}H, ^{13}C, and ^{31}P NMR spectra for **S4**. ^{1}H NMR (500 MHz, $CDCl_3$) δ 2.26 (m, 4H), 1.90 (m, 4H), 1.71 (br, 4H), 1.39-1.30 (m, 12H). * indicates residual H_2O. ^{13}C NMR (126 MHz, $CDCl_3$) δ 23.32 (m), 20.53 (t, J = 15.5 Hz), 8.93. ^{31}P NMR (202 MHz, $CDCl_3$) δ 82.58.

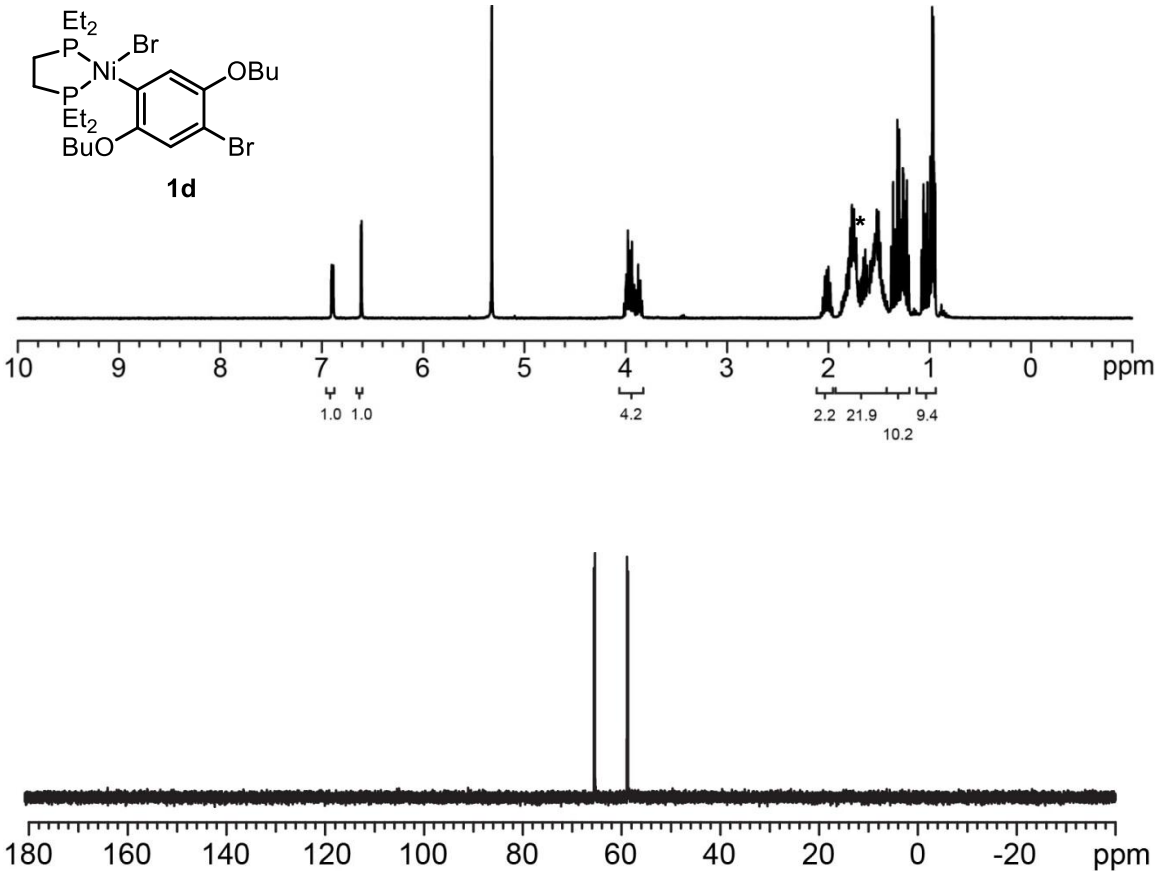

Figure S1.8 ^{1}H and ^{31}P NMR spectra for **1d**. ^{1}H NMR (400 MHz, CD_2Cl_2) δ 6.96 (d, *J* = 6.6 Hz, 1H), 6.61 (d, *J* = 3.1 Hz, 1H), 4.02-3.84 (m, 4H), 2.01 (m, 2H), 1.89-1.42 (m, 16H), 1.38-1.21 (m, 10H), 1.08-0.94 (m, 10H). * indicates residual H_2O. ^{31}P NMR (162 MHz, CD_2Cl_2) δ 64.48 (d, *J* = 33.6 Hz), 58.80 (d, *J* = 33.6 Hz).

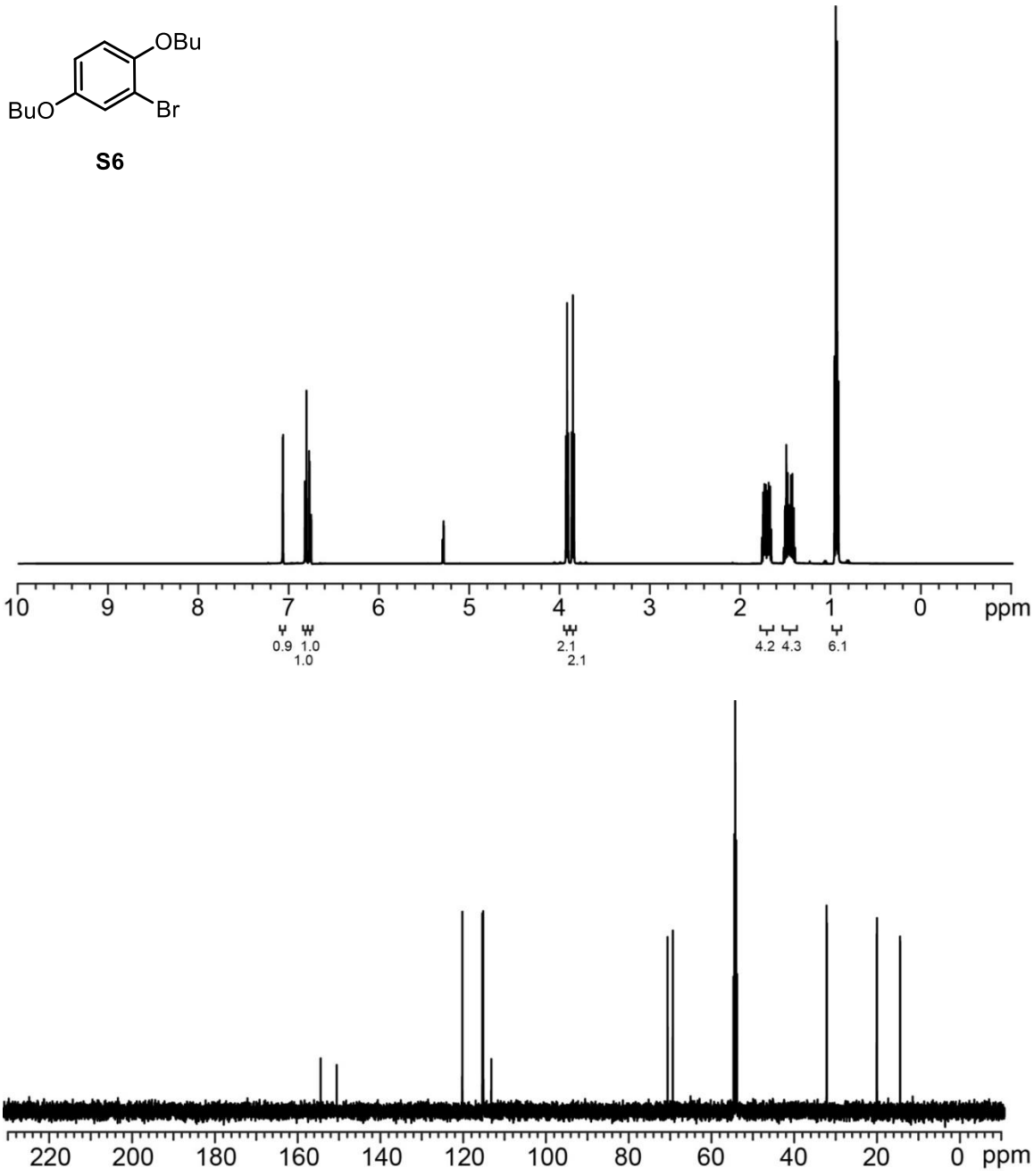

Figure S1.9 ^{1}H and ^{13}C NMR spectra for **S6**. ^{1}H NMR (500 MHz, CD_2Cl_2) δ 7.07 (d, *J* = 2.9 Hz, 1H), 6.84 (d, *J* = 9.0 Hz, 1H), 6.80 (dd, *J* = 9.0, 2.9 Hz, 1H), 3.95 (t, *J* = 6.6 Hz, 2H), 3.89 (t, *J* = 6.6 Hz, 2H), 1.80-1.69 (m, 4H), 1.55-1.42 (m, 4H), 0.97 (t, *J* = 7.8 Hz, 6H). ^{13}C NMR (126 MHz, CD_2Cl_2) δ 153.59, 149.72, 119.38, 114.53, 114.31, 112.38, 69.76, 68.52, 31.35, 31.29, 19.23, 19.16, 13.60, 13.58.

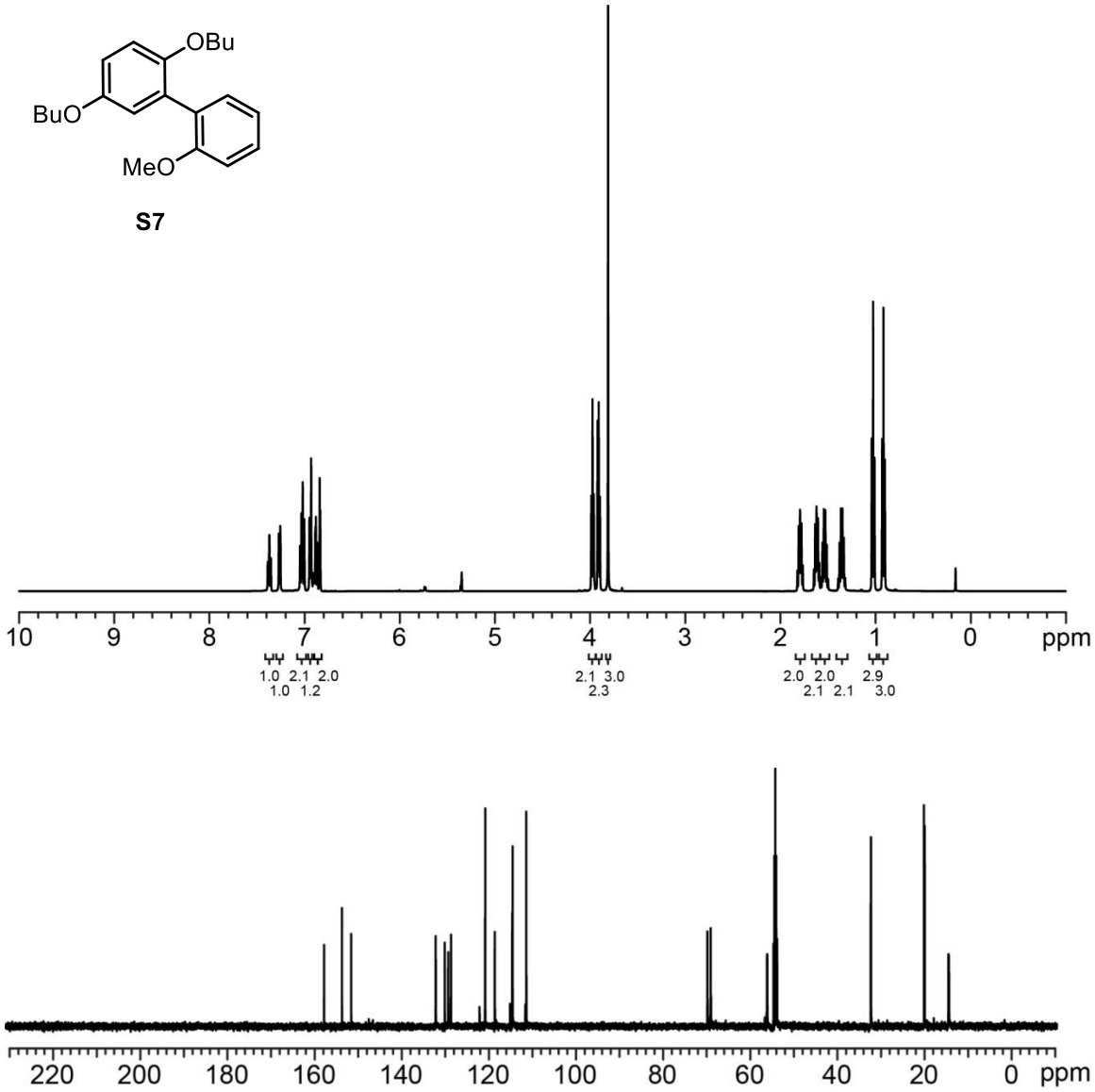

Figure S1.10 ^{1}H and ^{13}C NMR spectra for **S7**. ^{1}H NMR (500 MHz, CD_2Cl_2) δ 7.38 (t, *J* = 7.3 Hz, 1H), 7.23 (d, *J* = 7.5 Hz, 1H), 7.02-6.97 (m, 2H), 6.92-6.90 (m, 1H), 6.86-6.80 (m, 2H), 3.95 (t, *J* = 6.5 Hz, 2H), 3.88 (t, *J* = 6.0 Hz, 2H), 3.72 (s, 3H), 1.77 (m, 2H), 1.59 (m, 2H), 1.50 (m, 2H), 1.33 (m, 2H), 1.00 (t, *J* = 7.5 Hz, 3H), 0.89 (t, *J* = 7.5 Hz, 3H). ^{13}C NMR (126 MHz, CD_2Cl_2) δ 156.96, 152.87, 150.75, 131.35, 129.27, 128.48, 127.84, 120.99, 117.78, 113.79, 113.69, 110.54, 68.97, 68.22, 55.32, 31.48, 31.43, 19.25, 19.08, 13.65, 13.52.

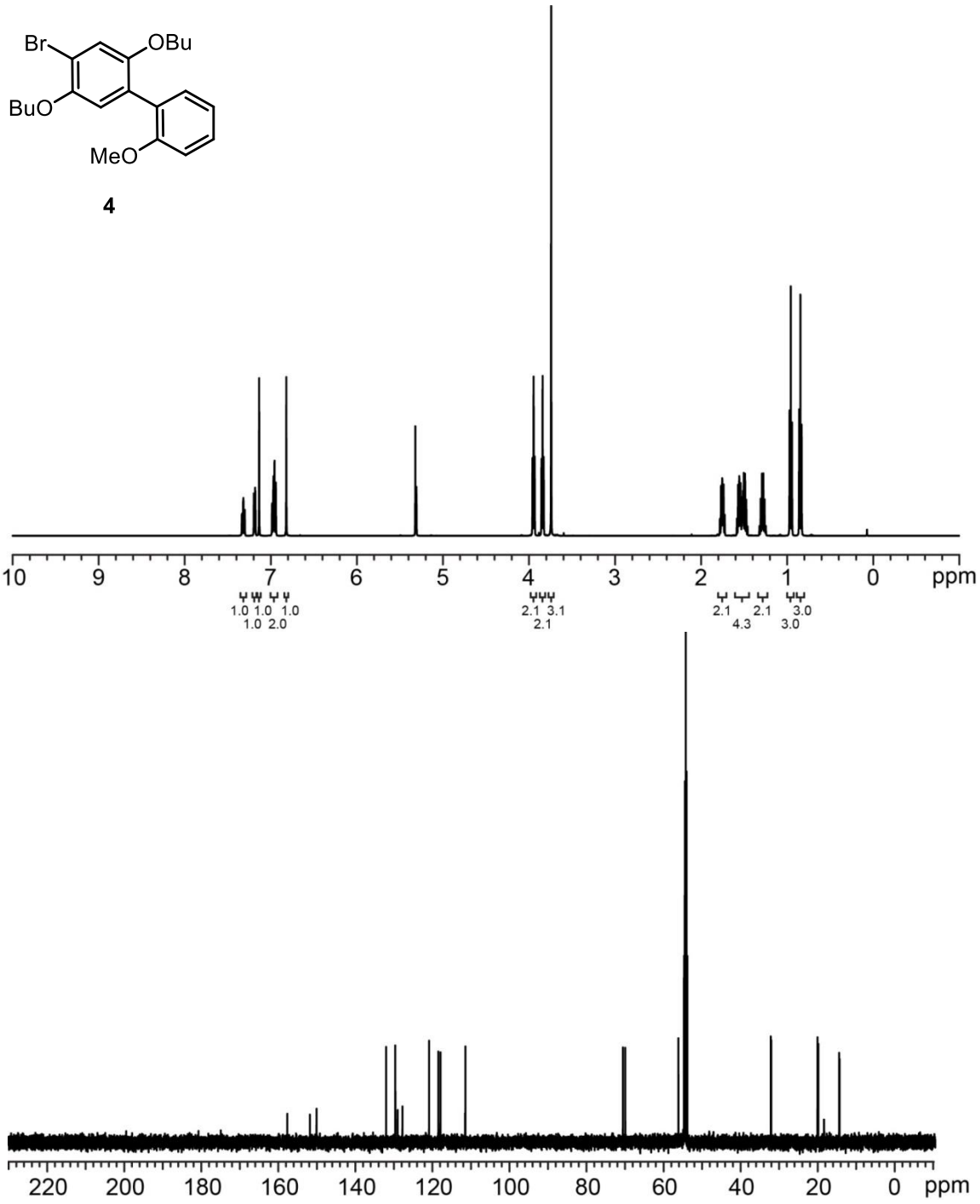

Figure S1.11 ^{1}H and ^{13}C NMR spectra for **4**. ^{1}H NMR (500 MHz, CD_2Cl_2) δ 7.33 (t, *J* = 7.7 Hz, 1H), 7.20 (d, *J* = 7.7 Hz, 1H), 7.15 (s, 1H), 6.98 (m, 2H), 6.83 (s, 1H), 3.96 (t, *J* = 6.4 Hz, 2H), 3.84 (t, *J* = 6.5 Hz, 2H), 3.75 (s, 3H), 1.77 (m, 2H), 1.59-1.49 (m, 4H), 1.29 (m, 2H), 0.97 (t, *J* = 7.4 Hz, 3H), 0.86 (t, *J* = 7.5 Hz, 3H). ^{13}C NMR (126 MHz, CD_2Cl_2) δ 156.81, 150.94, 149.22, 131.17, 128.77, 128.17, 126.94, 120.00, 117.62, 117.04, 110.65, 110.59, 69.70, 69.09, 55.29, 31.30, 31.20, 19.19, 18.98, 13.58, 13.44.

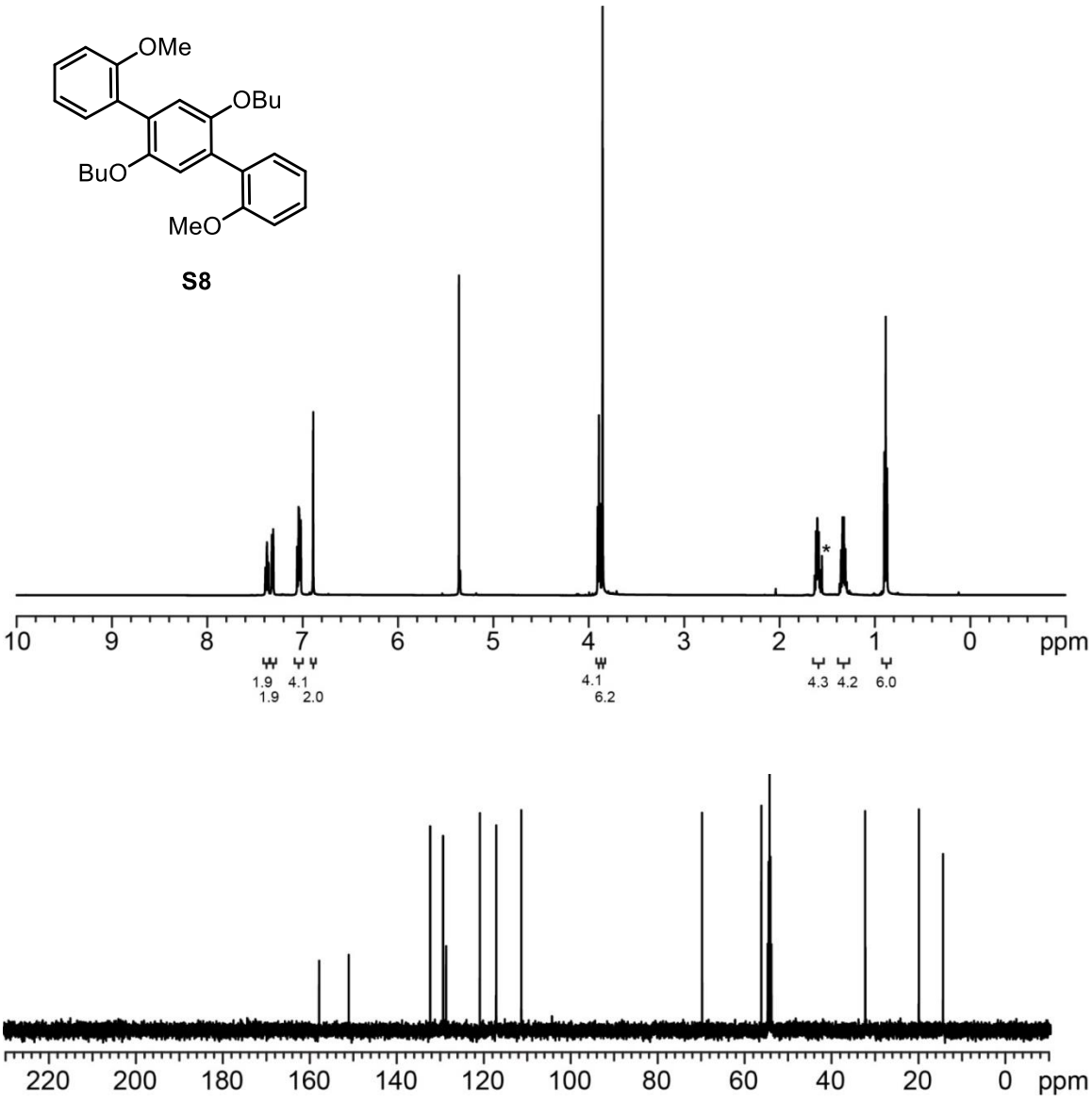

Figure S1.12 ^{1}H and ^{13}C NMR spectra for **S8**. ^{1}H NMR (500 MHz, CD_2Cl_2) δ 7.34 (t, *J* = 8.0 Hz, 2H), 7.28 (d, *J* = 7.3 Hz, 2H), 7.03-6.99 (m, 4H), 6.86 (s, 2H), 3.86 (t, *J* = 6.7 Hz, 4H), 3.83 (s, 6H), 1.57 (m, 4H), 1.30 (m, 4H), 0.86 (t, *J* = 7.5 Hz, 6H). * indicates residual H_2O. ^{13}C NMR (126 MHz, CD_2Cl_2) δ 157.41, 150.60, 131.86, 128.89, 128.20, 128.18, 120.43, 116.69, 110.91, 69.33, 55.69, 31.80, 19.46, 13.91.

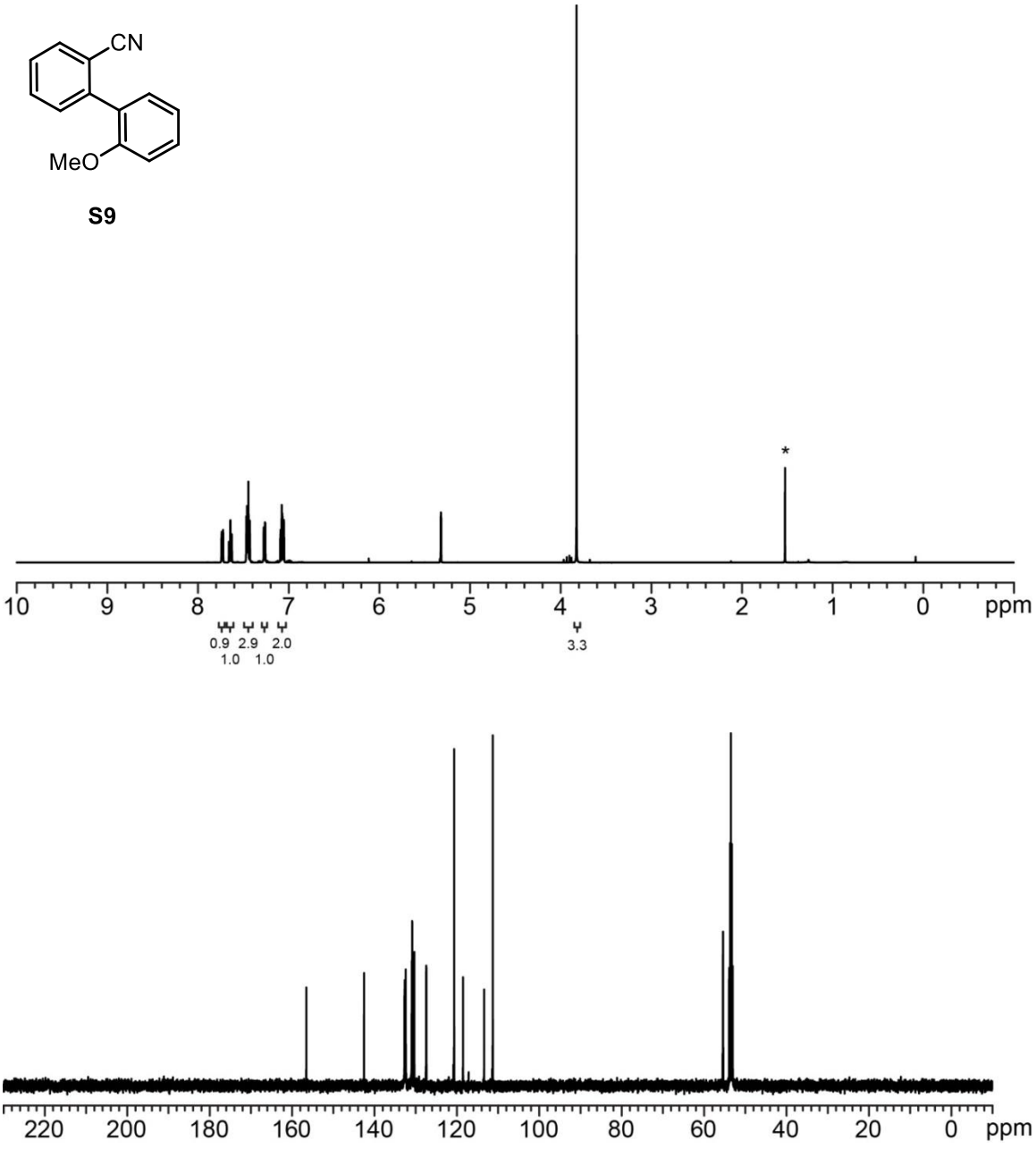

Figure S1.13 ^{1}H and ^{13}C NMR spectra for **S9**. ^{1}H NMR (500 MHz, CD_2Cl_2) δ 7.73 (d, *J* = 7.7 Hz, 1H), 7.64 (t, *J* = 7.7 Hz, 1H), 7.47-7.43 (m, 3H), 7.27 (d, *J* = 7.4 Hz, 1H), 7.09-7.05 (m, 2H), 3.82 (s, 3H). * indicates residual H_2O. ^{13}C NMR (126 MHz, CD_2Cl_2) δ 156.86, 142.85, 133.03, 132.98, 132.73, 131.24, 130.66, 127.77, 127.71, 120.98, 118.83, 113.69, 111.61, 55.74.

V. Oxidative Addition Comparison

To determine the reactive preference for Ni(0) towards aryl bromides **3** and **4**, $Ni(cod)(PR_3)_2$ was utilized as a model with PPh_3 and PMe_3.

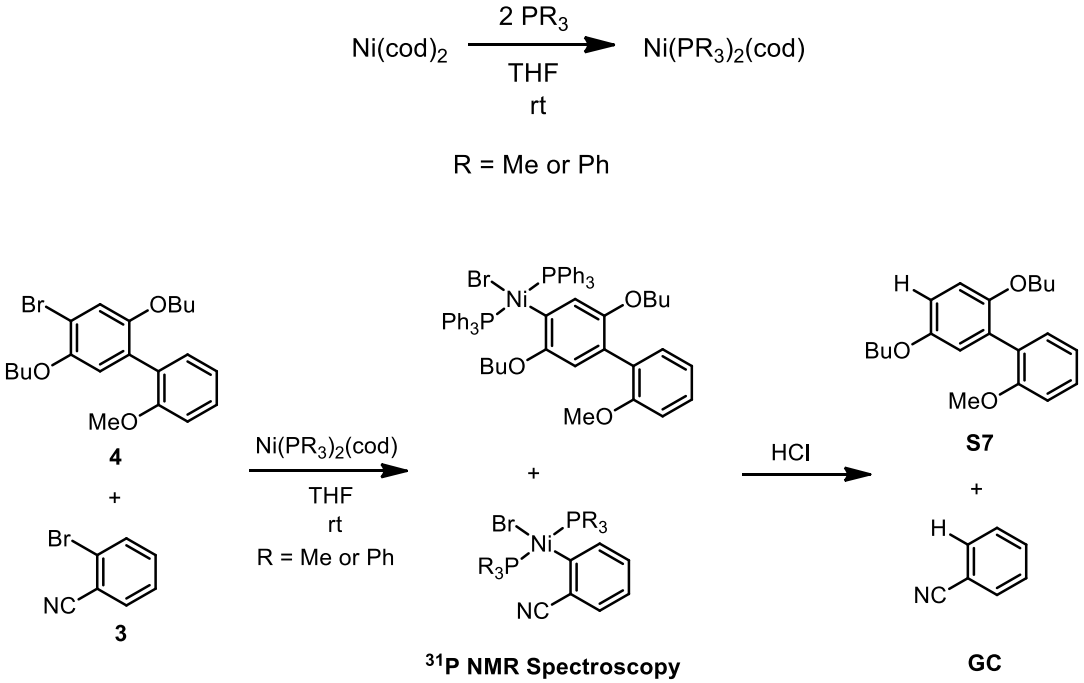

Representative Procedure for Oxidative Addition Comparisons:

In the glovebox, a 20 mL vial was equipped with a stir bar. Sequentially, $Ni(cod)_2$ (25 mg, 0.091 mmol, 1 equiv), PPh_3 (48 mg, 0.18 mmol, 2 equiv), and THF (3 mL) were added. This mixture was then stirred at rt for 1 h. Then, **3** (37 mg, 0.091 mmol, 1 equiv) and **4** (17 mg, 0.091 mmol, 1 equiv) were dissolved in THF (1 mL). This solution was subsequently taken up in a syringe and quickly added to the vial containing $Ni(cod)(PPh_3)_2$. This solution was left stirring for 1 h at rt. An aliquot was then removed and placed in a J. Young NMR tube for ^{31}P NMR Spectroscopic analysis. The remaining solution was removed from the glovebox and quenched with hydrochloric acid (12.1 M, 3 mL) and subsequently diluted with water (8 mL). The reaction was then extracted with DCM (3 x 3 mL). The combined organic layers were dried over $MgSO_4$, filtered through a 0.2 μm PTFE filter, and subjected to GC analysis.

^{31}P NMR Spectrum of the comparison of PPh_3

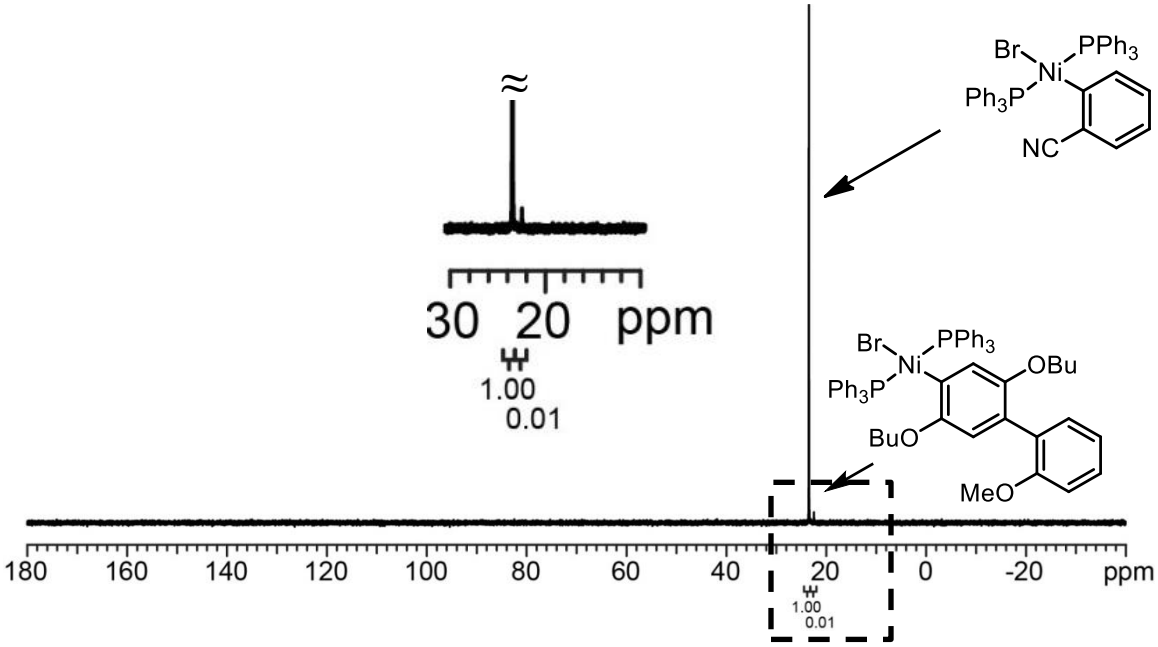

Figure S1.14 ^{31}P NMR Spectrum for the oxidative addition comparison using PPh_3

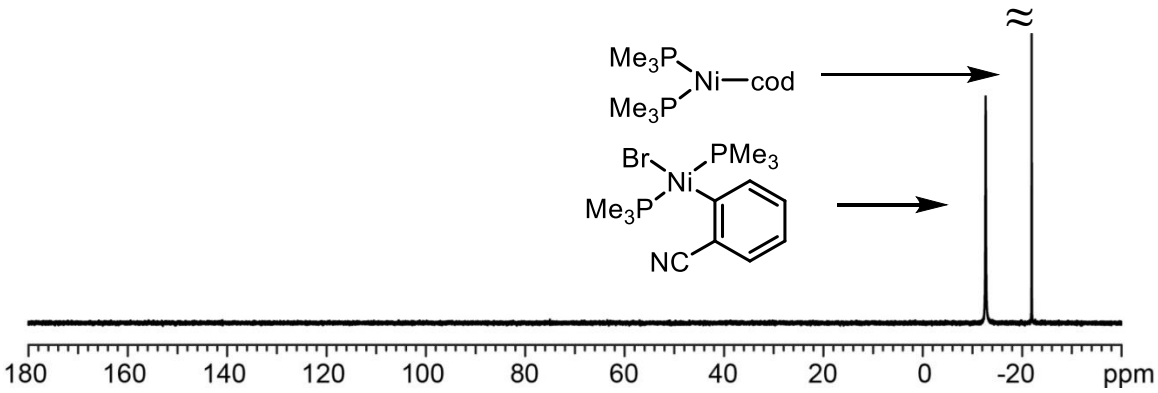

Figure S1.15 ^{31}P NMR Spectrum for the oxidative addition comparison using PMe_3

Table S1.1 Data for oxidative addition comparisons in **Figure S1.14** and **Figure S1.15**.

Ligand	Conversion of **3*** (%)	% Conversion of **4*** (%)	Ratio of **3**:**4** - GC	Ratio of **3**:**4** - NMR
PPh_3	98.3	0.9	99.1:0.9	99:1
PMe_3	36.4	0.2	99.2:0.8	>99.9:0.1

* Based on relative areas as determined by GC

VI. Calibration Curves

Representative Procedure for Preparing Calibration Curves:
A stock solution was made by weighing ~25 mg of each compound into a 5 mL volumetric flask which was then filled with CH_2Cl_2. A separate stock solution of internal standard (nonadecane) was also made by placing ~25 mg into a 5 mL volumetric flask and filling with CH_2Cl_2. These stock solutions were then used to make 5 samples with known dilutions within the expected range of concentrations of the experiment (0.02 M – 0.001 M for compounds **S6**, **S7**, **4**, **S8**, **S9**, and PhCN, 0.2 M – 0.002 M for compound **3**). Each of these samples were analyzed by GC and the areas plotted against the known concentrations, producing a calibration curve. The process was performed twice per compound and the ratios were averaged. Error bars are included in figures.

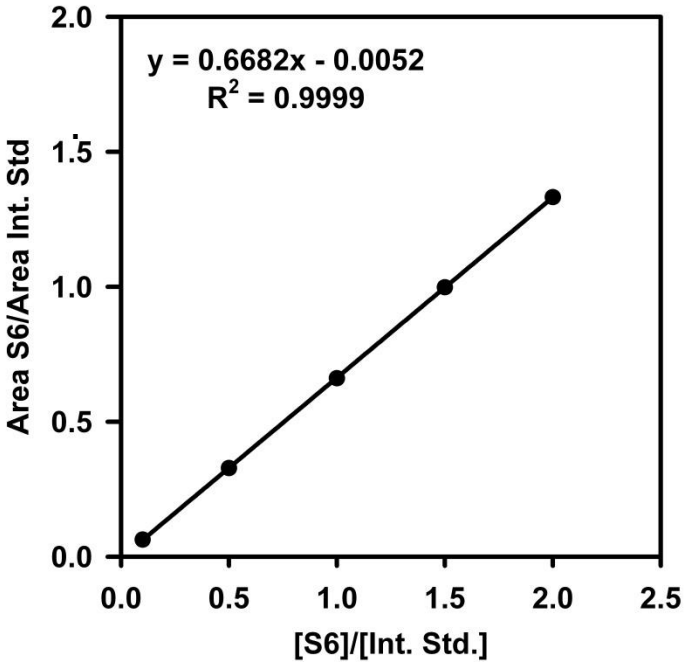

Figure S1.16 Calibration curve for **S6**.

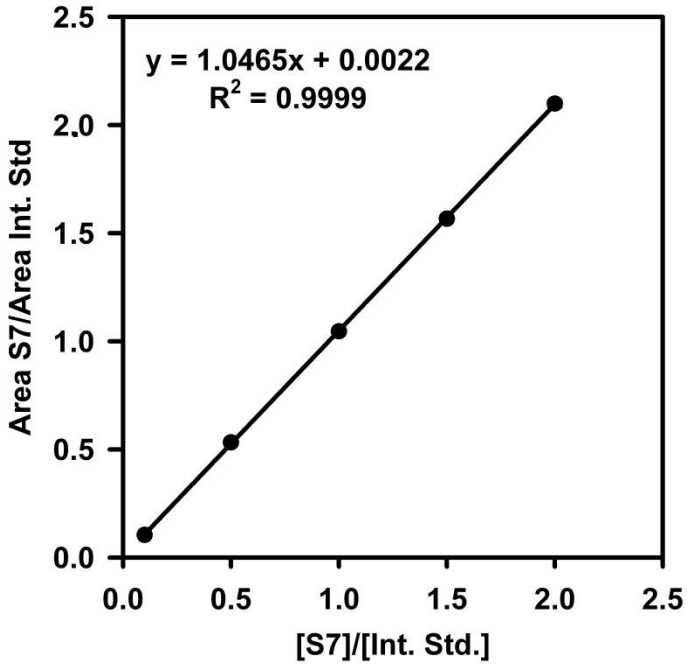

Figure S1.17 Calibration curve for **S7**.

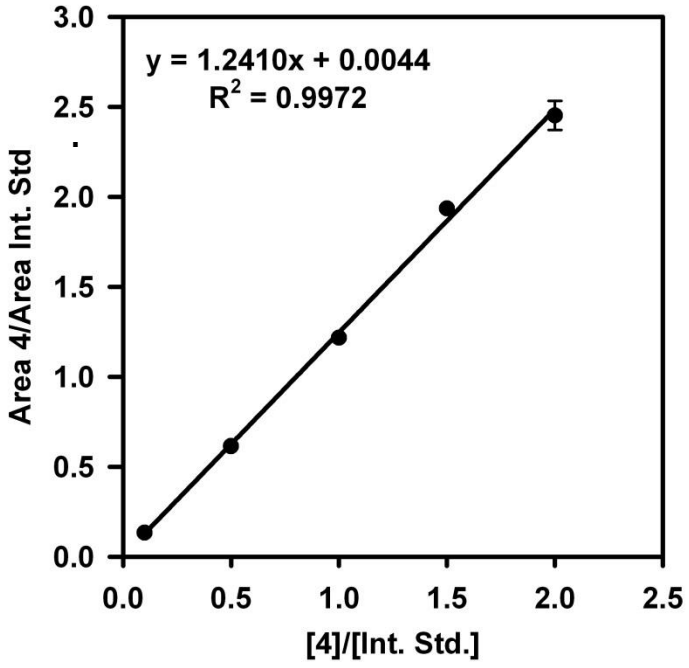

Figure S1.18 Calibration curve for **4**.

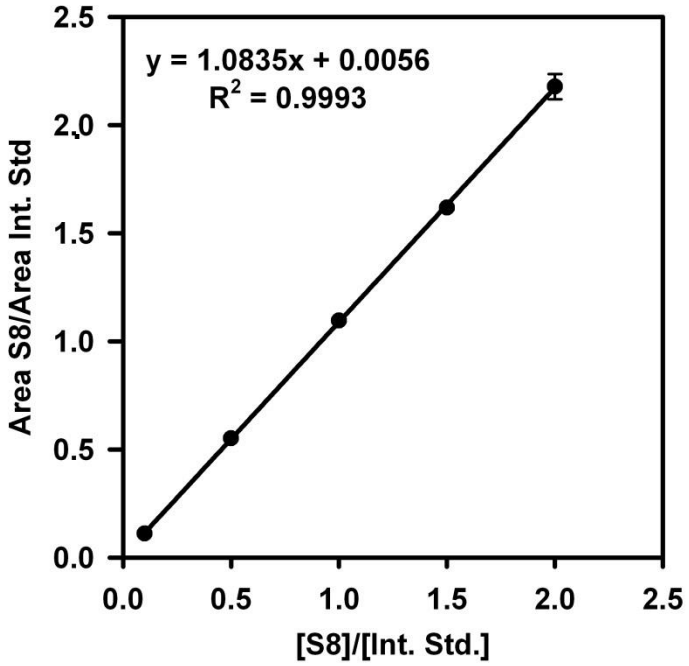

Figure S1.19 Calibration curve for **S8**.

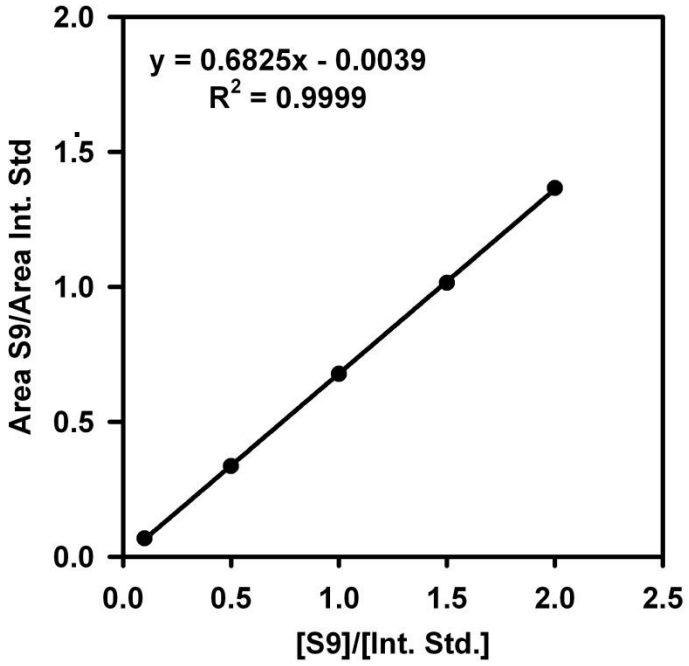

Figure S1.20 Calibration curve for **S9**.

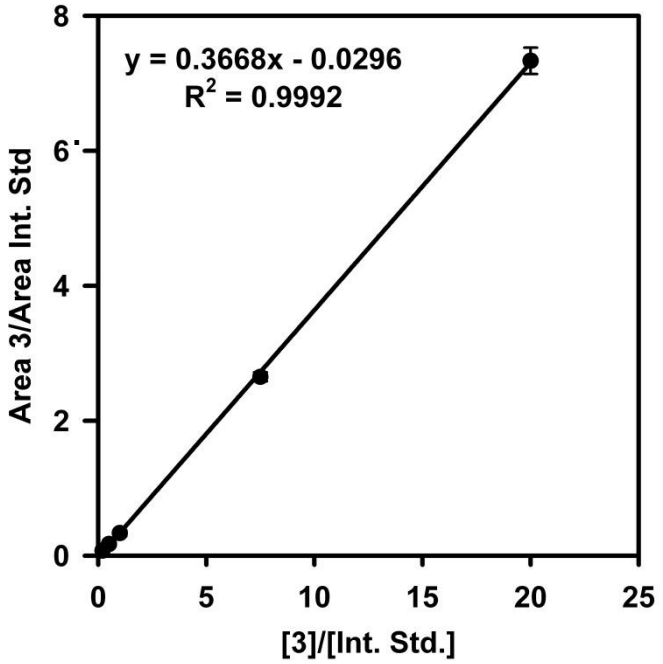

Figure S1.21 Calibration curve for **3**.

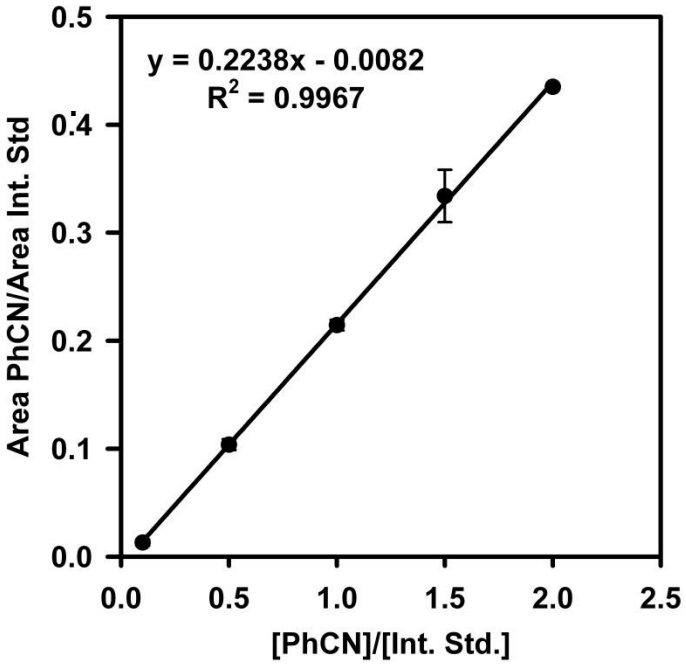

Figure S1.22 Calibration curve for **PhCN**.

VII. Competition Experiments

Representative Procedure for Performing Competition Experiments:

Prior to starting, separate stock solutions of catalysts **1a-d**, internal standard (nonadecane), and **3** were made. In the glovebox, a 4 mL vial was equipped with a stir bar. Sequentially, **1a** (12.9 mg, 0.020 mmol, 1.0 equiv), **3** (2.9 mg, 0.016 mmol, 0.8 equiv), and nonadecane (internal standard) (2.7 mg, 0.010 mmol, 0.5 equiv) were added with stirring resulting in a total volume of 1 mL (THF). With a microsyringe, **2** (0.16 µL, 0.016 mmol, 0.8 equiv) was added and stirred for 2 h at rt. Upon completion, the vial was removed from the glovebox and quenched with hydrochloric acid (12.1 M, 1 mL) and subsequently diluted with water (1 mL). The reaction was then extracted with DCM (3 x 2 mL). The combined organic layers were dried over $MgSO_4$, filtered through a 0.2 µm PTFE filter, and subjected to GC analysis.

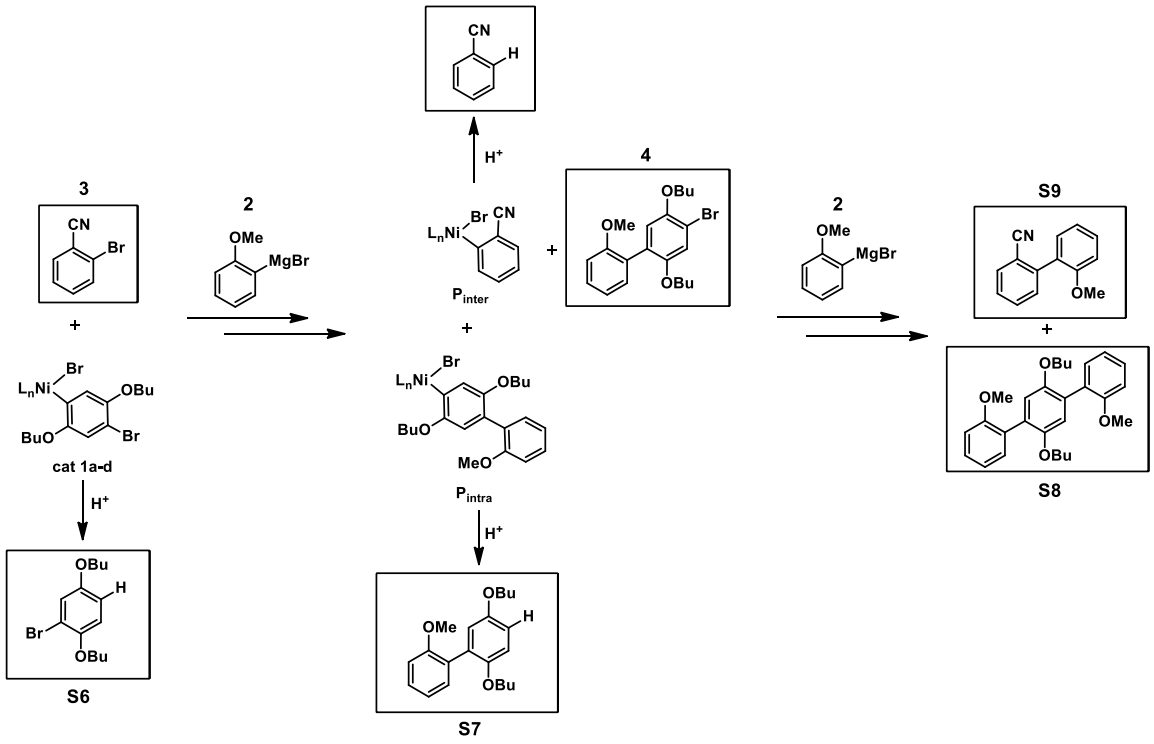

Description of Competition Experiments:

Shown above is a diagram of the reactions that occur during the competition experiments. Along the bottom is the pathway that is consistent with intramolecular oxidative addition. The products along the top are those that correspond to intermolecular oxidative addition. The compounds with boxes around them are those that can be quantified by GC following the hydrolysis of the nickel containing compounds with conc. HCl. As shown above, both P_{inter} and P_{intra} can undergo an additional cycle of transmetallation and reductive elimination producing **S8**, **S9**, and Ni(0). This "free" Ni(0) will react with **3** to

generate additional P_{inter}. Therefore, P_{intra} was quantified by **S7** and **S8**, whereas P_{inter} was determined from **4**.

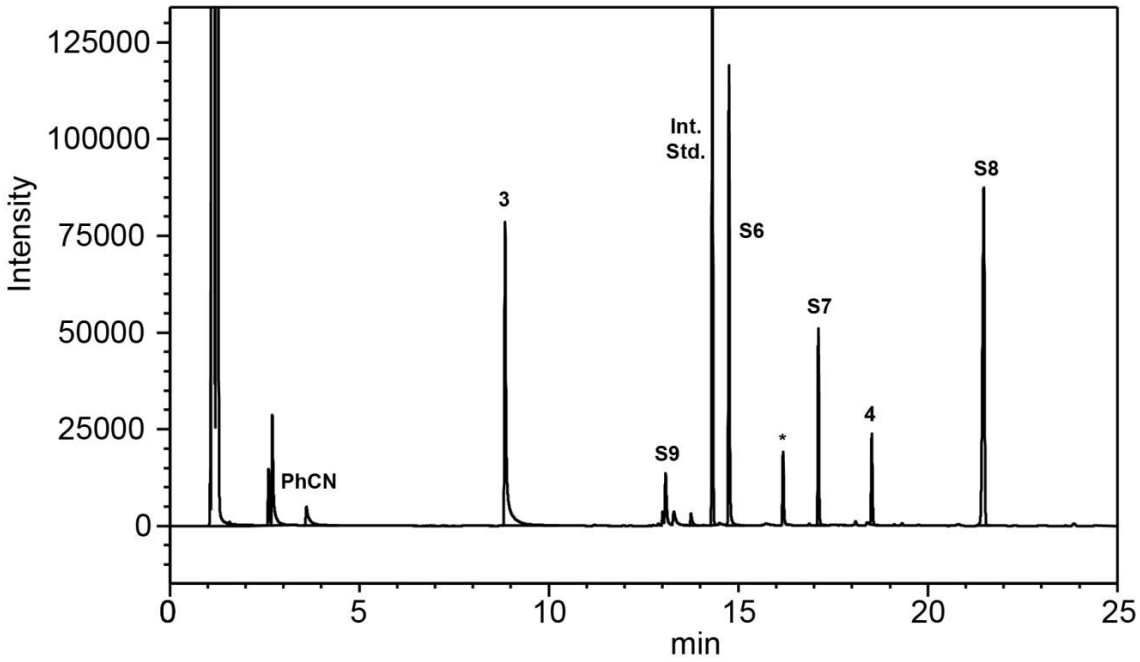

Figure S1.23 Representative GC of competition experiment using catalyst **1a** and 2 equiv of **3**. * indicates peaks from the corresponding ligand.

Table S1.2 Summary of competition experiments for catalyst **1a**, with 1 equiv of **3**.

	P_{intra}	P_{inter}	Mass Balance (%)
Run 1	95.14	4.86	116
Run 2	95.14	4.86	130
Run 3	94.27	5.73	99
Average	94.9 ± 0.5	5.1 ± 0.5	115 ± 16

Table S1.3 Summary of competition experiments for catalyst **1a**, with 2 equiv of **3**.

	P_{intra}	P_{inter}	Mass Balance (%)
Run 1	90.75	9.25	109
Run 2	90.68	9.32	103
Run 3	90.63	9.37	104
Average	90.69 ± 0.06	9.31 ± 0.06	105 ± 3

Table S1.4 Summary of competition experiments for catalyst **1a**, with 10 equiv of **3**.

	P_{intra}	P_{inter}	Mass Balance (%)
Run 1	68.08	31.92	114
Run 2	68.21	31.79	116
Run 3	70.59	29.41	98
Average	69 ± 1	31 ± 1	109 ± 10

Table S1.5 Summary of competition experiments for catalyst **1a**, with 50 equiv of **3**.

	P_{intra}	P_{inter}	Mass Balance (%)
Run 1	39.31	60.69	106
Run 2	39.49	60.51	112
Run 3	41.22	58.78	103
Average	40 ± 1	60 ± 1	107 ± 5

Table S1.6 Summary of competition experiments for catalyst **1a**, with 100 equiv of **3**.

	P_{intra}	P_{inter}	Mass Balance (%)
Run 1	32.05	67.95	103
Run 2	31.53	68.47	106
Run 3	32.05	67.95	98
Average	31.9 ± 0.3	68.1 ± 0.3	102 ± 4

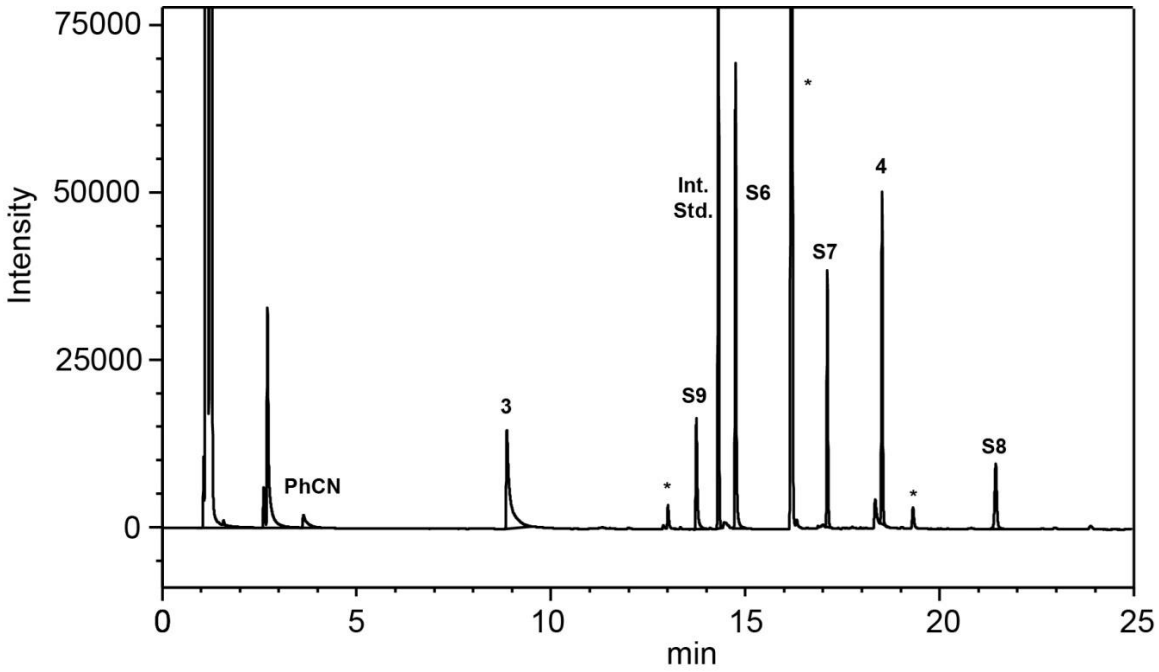

Figure S1.24 Representative GC of competition experiment using catalyst **1b** and 2 equiv of **3**. * indicates peaks from the corresponding ligand.

Table S1.7 Summary of competition experiments for catalyst **1b**, with 1 equiv of **3**.

	P_{intra}	P_{inter}	Mass Balance (%)
Run 1	65.38	34.62	105
Run 2	64.56	35.44	99
Run 3	66.26	33.74	97
Average	65.4 ± 0.9	34.6 ± 0.9	100 ± 4

Table S1.8 Summary of competition experiments for catalyst **1b**, with 2 equiv of **3**.

	P_{intra}	P_{inter}	Mass Balance (%)
Run 1	55.05	44.95	96
Run 2	55.23	44.77	103
Run 3	55.82	44.18	97
Average	55.4 ± 0.4	44.6 ± 0.4	99 ± 4

Table S1.9 Summary of competition experiments for catalyst **1b**, with 10 equiv of **3**.

	P_{intra}	P_{inter}	Mass Balance (%)
Run 1	26.80	73.20	102
Run 2	27.20	72.81	99
Run 3	28.66	71.34	95
Average	28 ± 1	72 ± 1	99 ± 4

Table S1.10 Summary of competition experiments for catalyst **1b**, with 50 equiv of **3**.

	P_{intra}	P_{inter}	Mass Balance (%)
Run 1	13.27	86.74	96
Run 2	13.31	86.69	97
Run 3	11.86	88.14	95
Average	12.8 ± 0.8	87.2 ± 0.8	96 ± 1

Table S1.11 Summary of competition experiments for catalyst **1b**, with 100 equiv of **3**.

	P_{intra}	P_{inter}	Mass Balance (%)
Run 1	11.27	88.73	92
Run 2	11.10	88.90	96
Run 3	9.27	90.73	94
Average	11 ± 1	89 ± 1	94 ± 2

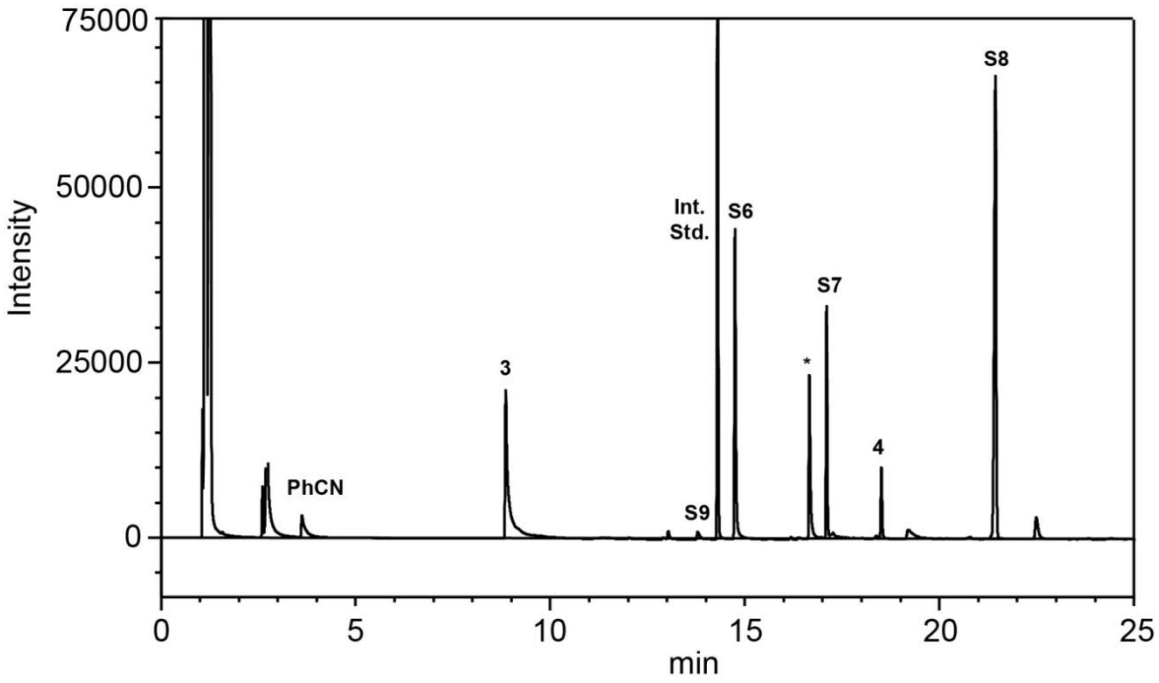

Figure S1.25 Representative GC of competition experiment using catalyst **1c** and 2 equiv of **3.** * indicates peaks from the corresponding ligand.

Table S1.12 Summary of competition experiments for catalyst **1c**, with 1 equiv of **3**.

	P_{intra}	P_{inter}	Mass Balance (%)
Run 1	96.46	3.54	115
Run 2	97.25	2.75	110
Run 3	95.65	4.35	112
Average	96.5 ± 0.8	3.6 ± 0.8	112 ± 3

Table S1.13 Summary of competition experiments for catalyst **1c**, with 2 equiv of **3**.

	P_{intra}	P_{inter}	Mass Balance (%)
Run 1	93.91	6.09	111
Run 2	94.34	5.66	103
Run 3	92.35	7.65	106
Average	94 ± 1	6 ± 1	107 ± 4

Table S1.14 Summary of competition experiments for catalyst **1c**, with 10 equiv of **3**.

	P_{intra}	P_{inter}	Mass Balance (%)
Run 1	77.39	22.61	111
Run 2	77.62	22.38	115
Run 3	78.25	21.75	105
Average	77.8 ± 0.5	22.2 ± 0.5	110 ± 5

Table S1.15 Summary of competition experiments for catalyst **1c**, with 50 equiv of **3**.

	P_{intra}	P_{inter}	Mass Balance (%)
Run 1	48.46	51.54	104
Run 2	50.04	49.96	101
Run 3	45.37	54.63	98
Average	48 ± 2	52 ± 0.2	101 ± 3

Table S1.16 Summary of competition experiments for catalyst **1c**, with 100 equiv of **3**.

	P_{intra}	P_{inter}	Mass Balance (%)
Run 1	39.86	60.14	94
Run 2	41.08	58.92	95
Run 3	37.20	62.80	94
Average	39 ± 2	61 ± 2	94.3 ± 0.6

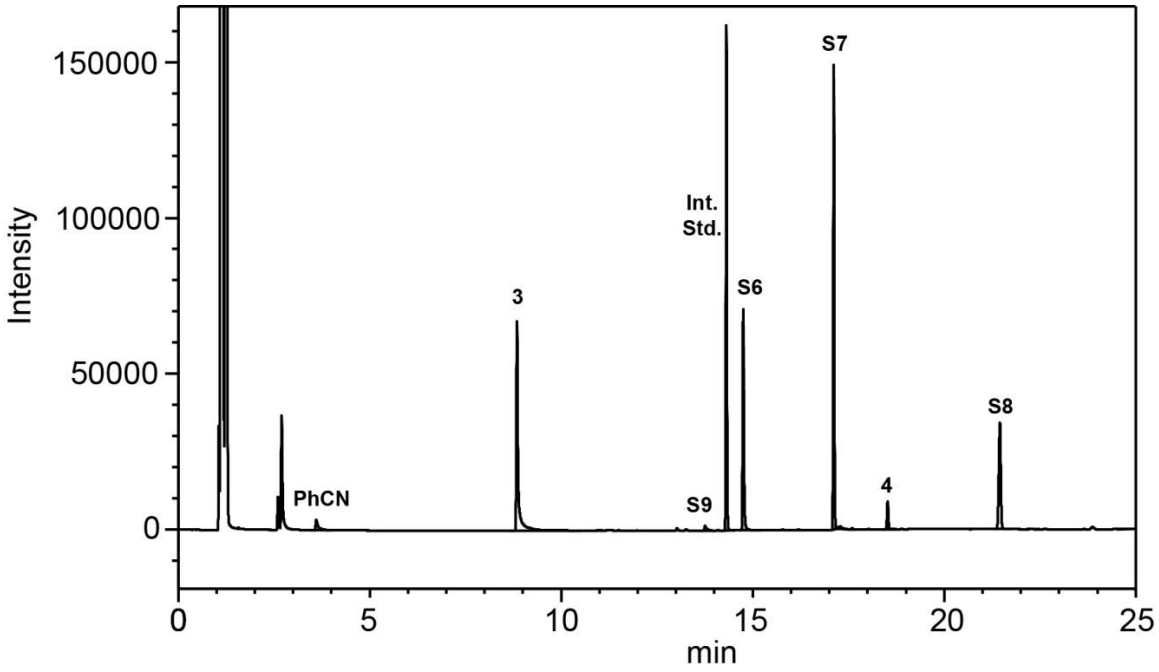

Figure S1.26 Representative GC of competition experiment using catalyst **1d** and 2 equiv of **3.**

Table S1.17 Summary of competition experiments for catalyst **1d**, with 1 equiv of **3**.

	P_{intra}	P_{inter}	Mass Balance (%)
Run 1	98.08	1.92	102
Run 2	98.37	1.63	105
Run 3	97.99	2.01	110
Average	98.1 ± 0.2	1.9 ± 0.2	106 ± 4

Table S1.18 Summary of competition experiments for catalyst **1d**, with 2 equiv of **3**.

	P_{intra}	P_{inter}	Mass Balance (%)
Run 1	95.90	4.10	112
Run 2	96.29	3.71	103
Run 3	96.35	3.65	105
Average	96.2 ± 0.2	3.8 ± 0.2	106 ± 5

Table S1.19 Summary of competition experiments for catalyst **1d**, with 10 equiv of **3**.

	P_{intra}	P_{inter}	Mass Balance (%)
Run 1	86.43	13.57	105
Run 2	86.12	13.88	109
Run 3	87.25	12.75	97
Average	86.6 ± 0.6	13.4 ± 0.6	104 ± 6

Table S1.20 Summary of competition experiments for catalyst **1d**, with 50 equiv of **3**.

	P_{intra}	P_{inter}	Mass Balance (%)
Run 1	70.11	29.89	105
Run 2	70.52	29.48	102
Run 3	71.69	28.31	108
Average	70.8 ± 0.8	29.2 ± 0.8	105 ± 3

Table S1.21 Summary of competition experiments for catalyst **1d**, with 100 equiv of **3**.

	P_{intra}	P_{inter}	Mass Balance (%)
Run 1	62.93	37.07	94
Run 2	64.43	35.57	97
Run 3	64.89	35.11	96
Average	64 ± 1	34 ± 1	96 ± 2

VIII. Relative Rate Constants for Intra- versus Intermolecular Pathways

$$\mathbf{I}_{intra} \xrightarrow{k_{intra}} \mathbf{P}_{intra} \quad (2)$$

$$\mathbf{I}_{intra} + \mathbf{3} \xrightarrow{k_{inter}} \mathbf{P}_{inter} \quad (3)$$

$$\frac{d[\mathbf{P}_{intra}]}{dt} = k_{intra}[\mathbf{I}_{intra}] \quad (4)$$

$$\frac{d[\mathbf{P}_{inter}]}{dt} = k_{inter}[\mathbf{I}_{intra}][\mathbf{3}] \quad (5)$$

$$\frac{[\mathbf{P}_{intra}]}{[\mathbf{P}_{inter}]} = \frac{k_{intra}}{k_{inter}[\mathbf{3}]} \quad (6)$$

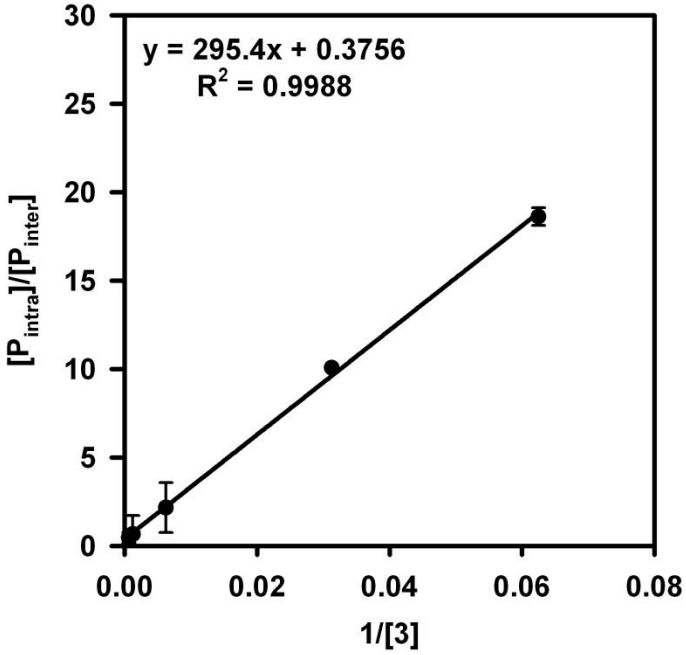

Figure S1.27 Plot of the relative rate constants for intra- versus intermolecular pathways versus concentration of **3** for **1a**.

Table S1.22 Data for the plot in **Figure S1.27**.

3 (equiv)	$[P_{intra}]$	$[P_{inter}]$	$[P_{intra}]/[P_{inter}]$	1/[**3**]
1	94.9	5.1	18.6	0.0625
2	90.7	9.3	10.1	0.03125
10	69.0	31.0	2.16	0.00625
50	40.0	61.0	0.66	0.00125
100	31.9	68.1	0.47	0.000625

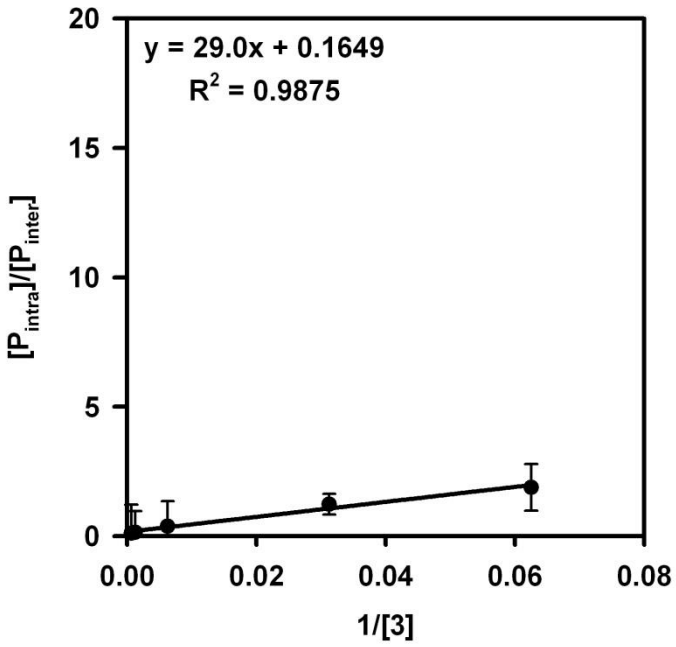

Figure S1.28 Plot of the relative rate constants for intra- versus intermolecular pathways versus concentration of **3** for **1b**.

Table S1.23 Data for the plot in **Figure S1.28**.

3 (equiv)	$[P_{intra}]$	$[P_{inter}]$	$[P_{intra}]/[P_{inter}]$	1/[**3**]
1	65.4	34.6	1.89	0.0625
2	55.4	44.6	1.24	0.03125
10	27.6	72.4	0.38	0.00625
50	12.8	87.2	0.15	0.00125
100	10.6	89.4	0.12	0.000625

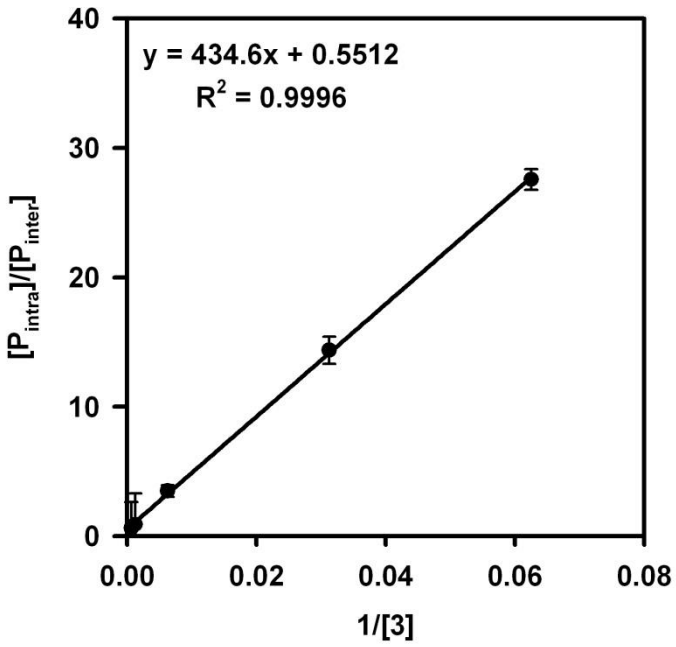

Figure S1.29 Plot of the relative rate constants for intra- versus intermolecular pathways versus concentration of **3** for **1c**.

Table S1.24 Data for the plot in **Figure S1.29**.

3 (equiv)	[P_{intra}]	[P_{inter}]	[P_{intra}]/[P_{inter}]	1/[**3**]
1	96.5	3.5	27.6	0.0625
2	93.5	6.5	14.4	0.03125
10	77.8	22.2	3.50	0.00625
50	48.0	52.0	0.92	0.00125
100	39.4	60.6	0.65	0.000625

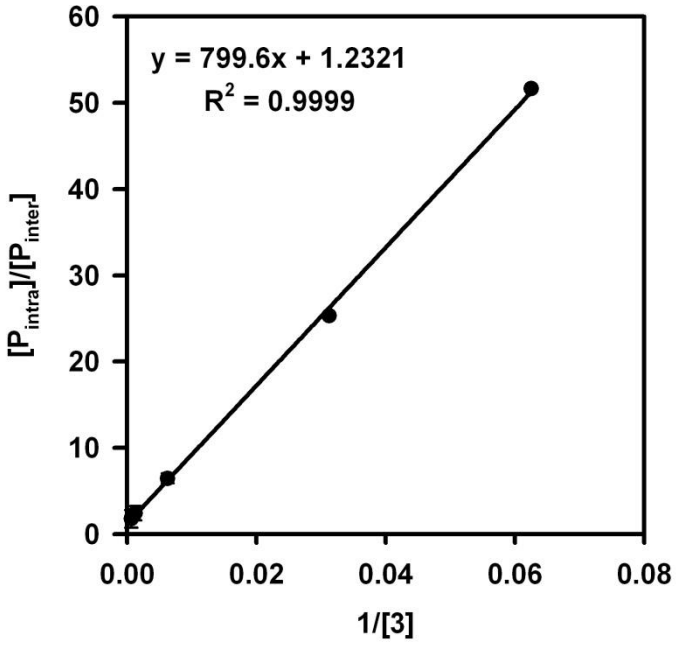

Figure S1.30 Plot of the relative rate constants for intra- versus intermolecular pathways versus concentration of **3** for **1d**.

Table S1.25 Data for the plot in **Figure S1.30**.

3 (equiv)	$[P_{intra}]$	$[P_{inter}]$	$[P_{intra}]/[P_{inter}]$	1/[**3**]
1	98.1	1.9	51.6	0.0625
2	96.2	3.8	25.3	0.03125
10	86.6	13.4	6.46	0.00625
50	70.8	29.2	2.42	0.00125
100	64.1	35.9	1.79	0.000625

IX. Evidence for Irreversible Dissociation

To determine whether the dissociation of I_{intra} is irreversible (see Scheme 1.1), a competition experiment was performed as described previously (page S30) for catalysts **1a** and **1d** with an additional 100 equiv **4** added.

Scheme S1.1 Determination of Irreversible Dissociation

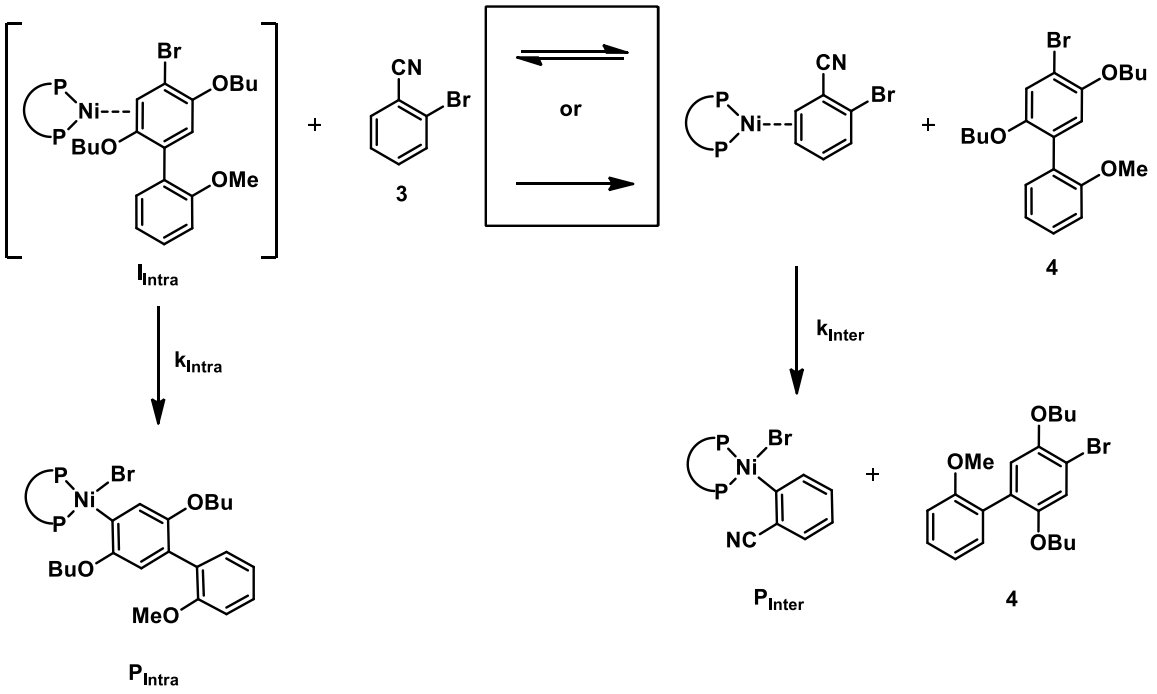

Table S1.26 Summary of competition experiments for catalyst **1a**, with 100 equiv of **3** and variable equiv of **4**.

	4 (equiv)	P_{intra}	P_{inter}	Mass Balance (%)
Run 1	0	32.05	67.95	103
Run 2	0	31.53	68.47	106
Run 3	0	32.05	67.95	98
Average of 1-3	0	31.9 ± 0.3	68.1 ± 0.3	102 ± 4
Run 4	100	29.71	70.29	124
Run 5	100	27.85	72.15	116
Average of 4 and 5	100	29 ± 1	71 ± 1	120 ± 6

Table S1.27 Summary of competition experiments for catalyst **1d**, with 100 equiv of **3** and variable equiv of **4**.

	4 (equiv)	P_{intra}	P_{inter}	Mass Balance (%)
Run 1	0	62.93	37.07	94
Run 2	0	64.43	35.57	97
Run 3	0	64.89	35.11	96
Average of 1-3	0	64 ± 1	36 ± 1	96 ± 2
Run 4	100	63.09	36.91	110
Run 5	100	64.63	35.37	116
Average of 4 and 5	100	64 ± 1	36 ± 1	113 ± 4

X. Summary of Polymerization Results

Representative Procedure for Preparing Monomer for Polymerizations:

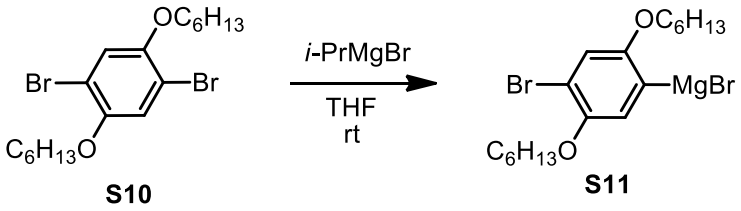

S10 **S11**

S11. In the glovebox, **S10** (2.00 g, 4.32 mmol, 1.0 equiv) was dissolved in THF (4 mL) in a 20 mL vial equipped with a stir bar. Then, *i*-PrMgBr (1.44 mL, 3.89 mmol, 0.9 equiv) was added via syringe, the vial was capped, and the reaction was stirred overnight at rt.

Representative Procedure for Polymerizations:

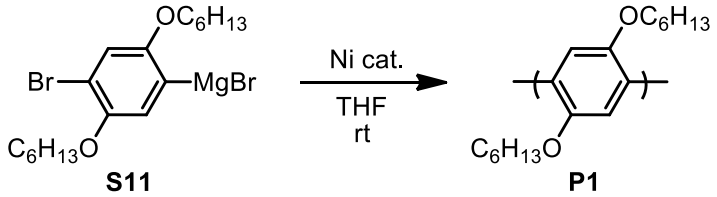

S11 **P1**

S12. All actions were performed in a glovebox under N_2 atmosphere. A 20 mL vial was equipped with a stir bar. Sequentially, catalyst **1a** (6.3 mg, 0.0075 mmol, 1.0 equiv), THF (3.60 mL), and **S11** (1.40 mL, 0.359 M, 0.5025 mmol, 67 equiv), with docosane added (as an internal standard), were added to the vial with stirring. After 24 h, the reaction was removed from the glovebox, and poured into aq. HCl (12.1 M, 5 mL). This mixture was then extracted with CH_2Cl_2 (3 x 5 mL). The combined organic layers were dried over $MgSO_4$ and filtered. To monitor conversion, GC samples were prepared by taking aliquots (~0.25 mL) of this organic phase and diluting with CH_2Cl_2 (~0.75 mL). Conversion was determined relative to the initial concentration, using the internal standard as a reference. To measure molecular weight and molecular weight distribution, the remaining organic phase was concentrated in vacuo, redissolved in THF (~1.5 mL) with mild heating and passed through a 0.2 μm PTFE filter for GPC analysis.

Representative Procedure for Competitive Polymerizations:

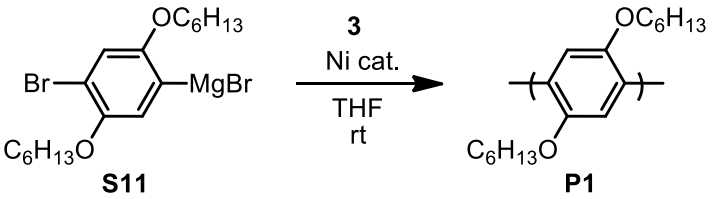

S11 **P1**

S13. All actions were performed in a glovebox under N_2 atmosphere. A 20 mL vial was equipped with a stir bar. Sequentially, catalyst **1a** (6.3 mg, 0.0075 mmol, 1.0 equiv), THF (3.60 mL), **3** (137.5 mg, 0.75 mmol, 100 equiv), and **S11** (1.40 mL, 0.359 M, 0.5025 mmol, 67 equiv), with docosane added (as an internal standard), were added to the vial with stirring. After 24 h, the reaction was removed from the glovebox, and poured into aq. HCl (12.1 M, 5 mL). This mixture was then extracted with CH_2Cl_2 (3 x 5 mL). The combined organic layers were dried over $MgSO_4$ and filtered. To monitor conversion, GC samples were prepared by taking aliquots (~0.25 mL) of this organic phase and diluting with CH_2Cl_2 (~0.75 mL). Conversion was determined relative to the initial concentration, using the internal standard as a reference. To measure molecular weight and molecular weight distribution, the remaining organic phase was concentrated in vacuo, redissolved in THF (~1.5 mL) with mild heating and passed through a 0.2 μm PTFE filter for GPC analysis.

Table S1.28 Summary of results with 0 equiv **3** added.

Catalyst	Experiment	% Conversion **S11**	% Conversion **S10**	M_n (kDa)	Đ
	Run 1	89	0	31.2	1.36
1a	Run 2	93	0	27.1	1.39
	Average	91	0	29 ± 3	1.38 ± 0.02
	Run 1	59	51	2.1	2.40
1b	Run 2	72	66	2	2.44
	Average	66	59	2.05 ± 0.07	2.42 ± 0.03
	Run 1	88	0	37.8	1.27
1c	Run 2	93	0	28.5	1.31
	Average	91	0	33 ± 6	1.29 ± 0.03
	Run 1	89	0	30.5	1.43
1d	Run 2	93	0	26.7	1.45
	Average	91	0	29 ± 3	1.44 ± 0.01

Table S1.29 Summary of results with 50 equiv **3** added.

Catalyst	Experiment	% Conversion **S11**	% Conversion **S10**	% Conversion **3**	M_n (kDa)	Đ
1a	Run 1	93	0	24	25.5	2.30
	Run 2	93	0	24	24.4	2.29
	Average	93	0	24	25.0 ± 0.8	2.30 ± 0.01
1b	Run 1	66	59	64	1.1	2.61
	Run 2	67	61	69	1	2.33
	Average	67	60	67	1.05 ± 0.07	2.50 ± 0.2
1c	Run 1	93	0	12	28.3	1.87
	Run 2	94	0	19	29.4	1.90
	Average	94	0	16	28.9 ± 0.8	1.89 ± 0.02
1d	Run 1	92	0	27	22.8	1.97
	Run 2	93	0	10	23.9	1.99
	Average	93	0	19	23.4 ± 0.8	1.98 ± 0.01

Table S1.30 Summary of results with 100 equiv **3** added.

Catalyst	Experiment	% Conversion **S11**	% Conversion **S10**	% Conversion **3**	M_n (kDa)	Đ
1a	Run 1	92	0	10	17.4	2.33
	Run 2	92	0	6	16.3	2.36
	Average	92	0	8	16.9 ± 0.8	2.35 ± 0.02
1b	Run 1	69	61	68	1.0	2.47
	Run 2	71	63	65	1.1	2.36
	Average	70	62	67	1.05 ± 0.07	2.42 ± 0.08
1c	Run 1	93	0	17	21.5	2.29
	Run 2	93	0	19	29.4	2.26
	Average	93	0	18	25 ± 6	2.28 ± 0.02
1d	Run 1	93	0	8	19.1	2.17
	Run 2	93	0	6	19.7	2.12
	Average	93	0	7	19.4 ± 0.4	2.15 ± 0.04

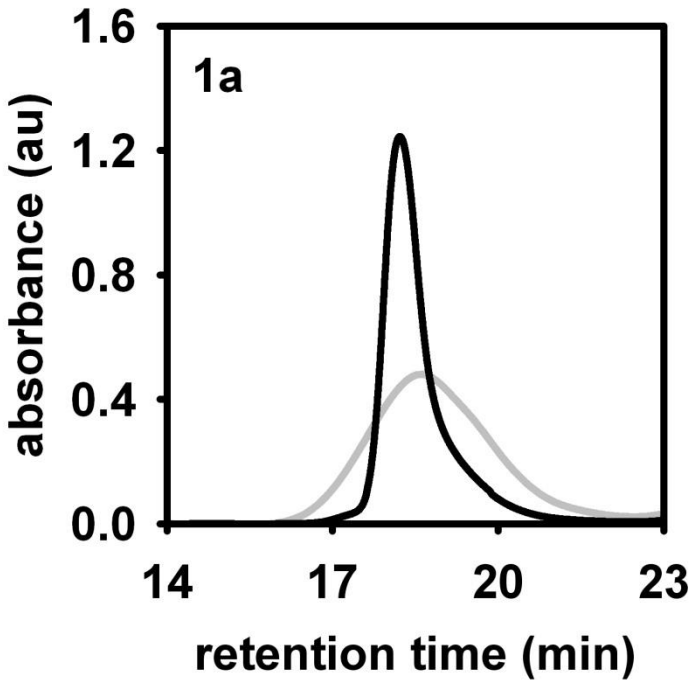

Figure S1.31 Representative GPC traces of polymer formed by catalyst **1a** with 0 equiv (black) and 100 equiv (grey) **3**.

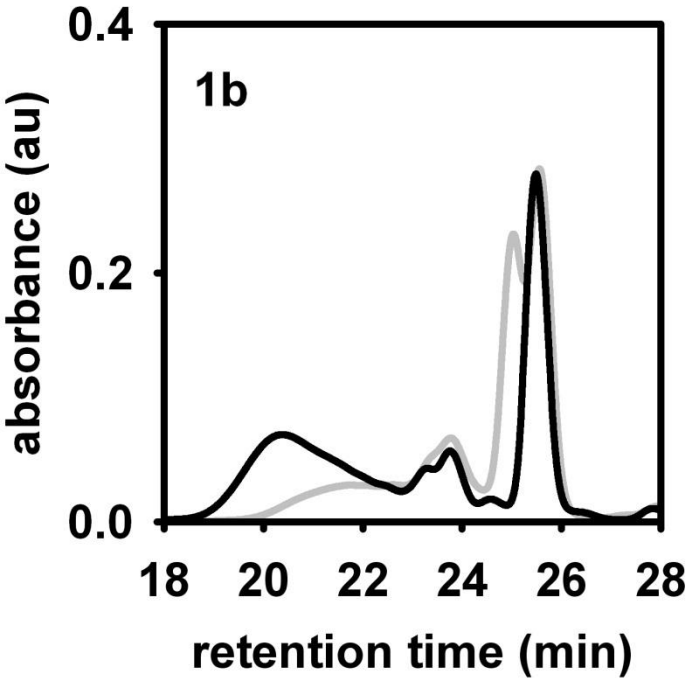

Figure S1.32 Representative GPC traces of polymer formed by catalyst **1b** with 0 equiv (black) and 100 equiv (grey) **3**.

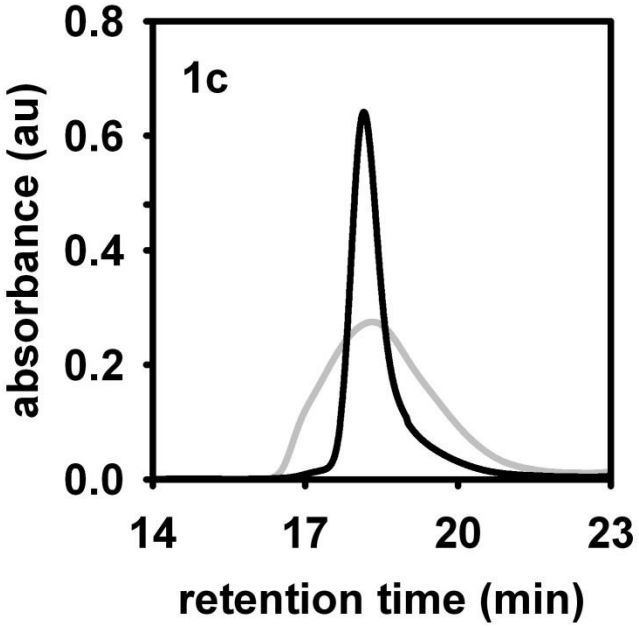

Figure S1.33 Representative GPC traces of polymer formed by catalyst **1c** with 0 equiv (black) and 100 equiv (grey) **3**.

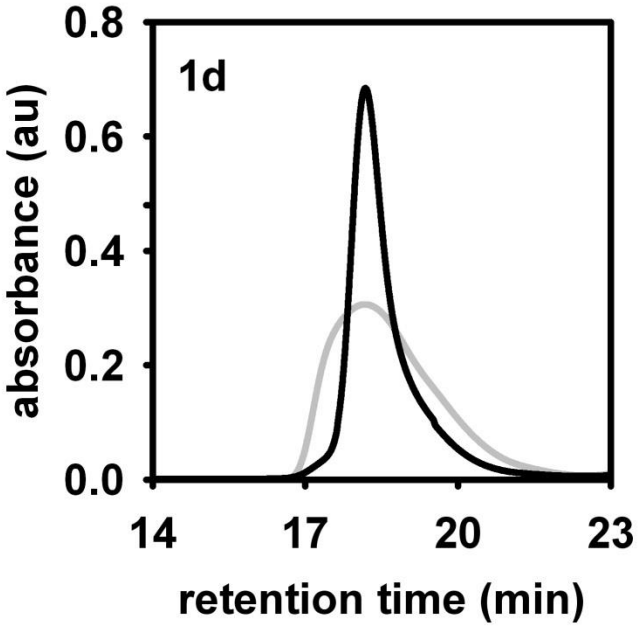

Figure S1.34 Representative GPC traces of polymer formed by catalyst **1d** with 0 equiv (black) and 100 equiv (grey) **3**.

XI. Crystal Structure of S4.

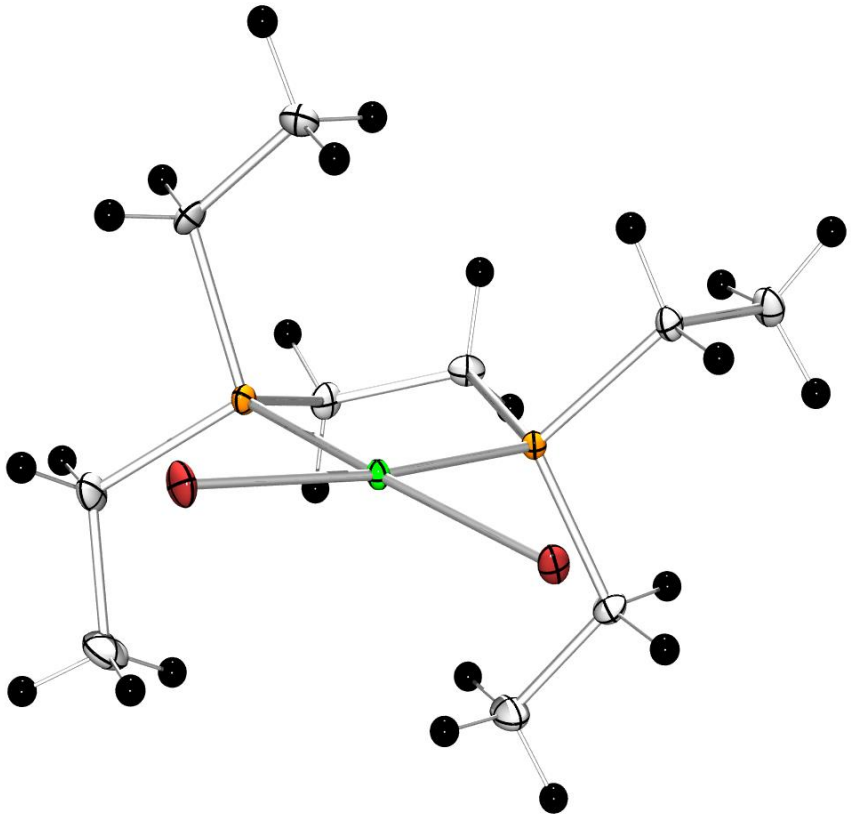

Figure S1.35 Crystal structure of **S4**. The Ni-P bond lengths are 2.14, 2.15 Å, the Ni-Br bond lengths are 2.34, 2.35 Å. The P-Ni-P bond angle is 87.53°. The Br-Ni-Br bond angle is 96.10°.

XII. Schlenk Equilibrium between 2 and 3

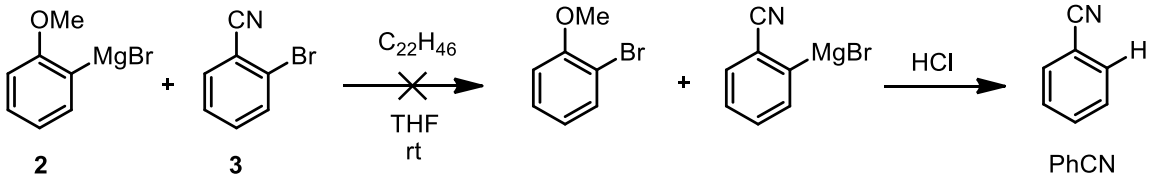

*Representative Procedure for investigating the Schlenk equilibrium of **2** and **3**:*
All actions were performed in a glovebox under N_2 atmosphere. A 20 mL vial was equipped with a stir bar. Sequentially, **3** (18 mg, 0.10 mmol, 1.0 equiv) and THF (3.0 mL), with docosane added (as an internal standard), were added to the vial with stirring. Once dissolved, **2** (0.10 mL, 0.10 mmol, 1.0 equiv) was added and the vial was capped. After 2 h, the reaction was removed from the glovebox, and poured into aq. HCl (12.1 M, 3 mL). This mixture was then extracted with CH_2Cl_2 (3 x 2 mL). The combined organic layers were dried over $MgSO_4$ and filtered. Conversion was determined relative to the initial concentration, using the internal standard as a reference.

Sample	Production of PhCN (%)
Run 1	0.0
Run 2	0.0
Run 3	0.0
Run 4	0.0

XIII. References

(1) Lanni, E. L.; McNeil, A. J. *J. Am. Chem. Soc.* **2009**, *131*, 16573-16579.
(2) Love, B. D.; Jones, E. G. *J. Org. Chem.* **1999**, *64*, 3755-3756.
(3) Lanni, E. L.; McNeil, A. J. *Macromolecules* **2010**, *43*, 8039-8044.
(4) Lee, S. R.; Bryan, Z. J.; Wagner, A. M.; McNeil, A. J. *Chem. Sci.* **2012**, *3*, 1562-1566.
(5) Lanni, E. L.; Locke; J. R.; Gleave, C. M.; McNeil, A. J. *Macromolecules* **2011**, *44*, 5136-5145.

Appendix 2

Supporting Information for Chapter 3:
Chain-growth polymerization of aryl Grignards initiated by a stabilized NHC-Pd precatalyst

Contents **Page**

I. Materials

Flash chromatography was performed on SiliCycle silica gel (40-63 μm) and thin layer chromatography was performed on Merck TLC plates pre-coated with silica gel 60 F254. *i*-PrMgCl (2 M in THF) was purchased in 100 mL quantities from Aldrich. [1,3-Bis(2,6-Diisopropylphenyl)imidazol-2-ylidene](3-chloropyridyl) palladium(II) dichloride was purchased from Aldrich. All other reagent grade materials and solvents were purchased from Aldrich, Acros, EMD, or Fisher and used without further purification unless otherwise noted. THF was dried and deoxygenated using an Innovative Technology (IT) solvent purification system composed of activated alumina, copper catalyst, and molecular sieves. All glassware was oven dried at 120 °C for at least 1 h before use. Compounds **S1**[1] and **S2**[2] were prepared according to literature procedures.

II. General Experimental

NMR Spectroscopy: ^{1}H NMR spectra for all compounds were acquired at rt in $CDCl_3$ on a Varian vnmrs 500 operating at 500 MHz. For ^{1}H NMR spectra in deuterated solvents, the chemical shift data are reported in units of δ (ppm) relative to tetramethylsilane (TMS) and referenced with residual solvent. Multiplicities are reported as follows: singlet (s), multiplet (m), pentet (p), and broad resonance (br).

MALDI-TOF MS: MALDI-TOF mass spectra were recorded using Waters Tofspec-2E in reflectron mode at a unit mass resolution of 4000. The matrix, α-cyano-4-hydroxy-cinnamic acid (CHCA), was prepared at a concentration of 10 mg/mL in a solution of 50/50 (v/v) CH_3CN/EtOH. The instrument was mass calibrated with a mixture of peptides in the CHCA matrix. The polymer sample was dissolved in CH_2Cl_2 to obtain a ~1 mg/mL solution. A 3 µL aliquot of the polymer solution was mixed with 3 µL of the matrix solution. 1 µL of this mixture was placed on the target plate and then air-dried.

Gel-Permeation Chromatography: Polymer molecular weights were determined by comparison with polystyrene standards (Varian, EasiCal PS-2 MW 580-377,400) on a Waters 1515 HPLC instrument equipped with Waters Styragel® (7.8 x 300 mm) THF HR 0.5, THF HR 1, and THF HR 4 type columns in sequence and analyzed with Waters 2487 dual absorbance detector (254 nm). Samples were dissolved in THF (with mild heating) and passed through a 0.2 µm PTFE filter prior to analysis.

Titrations of the Grignard Reagents: An accurately weighed sample of salicylaldehyde phenylhydrazone (typically between 290-310 mg) was dissolved in 5.00 mL of THF. A 0.50 mL aliquot of this solution was stirred at rt while ArMgCl was added dropwise using a 500 µL syringe. The initial solution is yellow and turns bright orange at the end-point.[3]

Gas Chromatography: Gas chromatography was carried out using a Shimadzu GC 2010 containing a Shimadzu SHRX5 (crossbound 5% diphenyl – 95% dimethyl polysiloxane; 15 m 0.25 mm ID, 0.25 µm df) column.

IR Spectroscopy: Samples were recorded using a Mettler Toledo ReactIR iC10 fitted with a Mercury Cadmium Telluride (MCT) detector, and AgX probe (9.5 mm x 1.5 mm) with a SiComp tip. The spectra were processed using icIR 4.0 software and raw absorbances were exported into Microsoft Excel or Sigma Plot 10 for analysis.

III. Synthetic Procedures

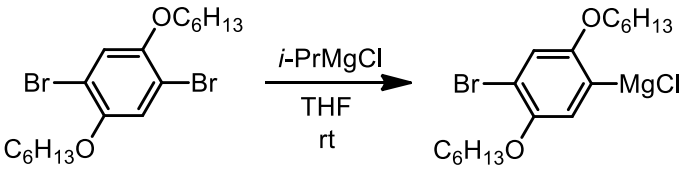

S1 **2**

2. In the glovebox, **S1** (1.025 g, 2.350 mmol, 1.0 equiv) was dissolved in THF (2.5 mL) in a 20 mL vial equipped with a stir bar. Then, *i*-PrMgCl (1.07 mL, 2.12 mmol, 0.9 equiv) was added via syringe, the vial was capped, and the reaction was stirred overnight at rt.

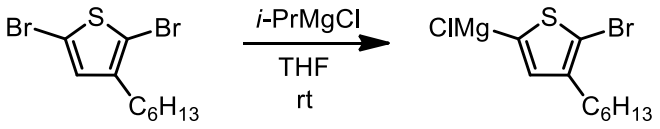

S2 **3**

3. In the glovebox, **S2** (0.424 g, 1.30 mmol, 1.0 equiv) was dissolved in THF (3.5 mL) in a 20 mL vial equipped with a stir bar. Then, *i*-PrMgCl (0.59 mL, 1.2 mmol, 0.9 equiv) was added via syringe, the vial was capped, and the reaction was stirred for 30 min at rt.

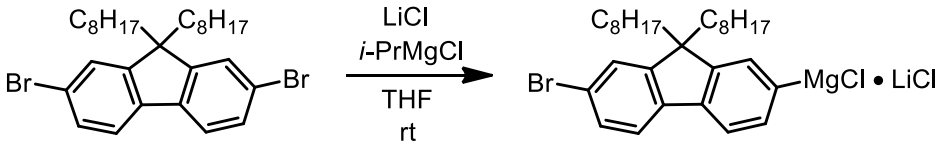

S3 **4**

4. In the glovebox, 9,9-dioctyl-2,7-dibromofluorene (2.742 g, 5.000 mmol, 1.0 equiv) and lithium chloride (0.463 g, 5.00 mmol, 1.0 equiv) was dissolved in THF (5.0 mL) in a 20 mL vial equipped with a stir bar. Then, *i*-PrMgCl (2.25 mL, 4.50 mmol, 0.9 equiv) was added via syringe, the vial was capped, and the reaction was stirred overnight at rt.

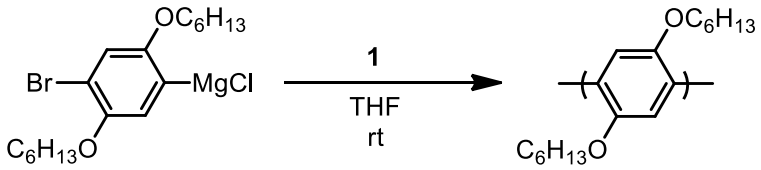

2 **P2**

P2. A 25 mL Schlenk flask was equipped with a stir bar, precatalyst **1** (10.2 mg, 0.0150 mmol, 1 equiv), and THF (7.75 mL) in a glovebox under an N_2 atmosphere. The flask was then equipped with a septum (secured with copper wire), removed from the glovebox, and put under an N_2 atmosphere. Monomer **2** (2.25 mL, 0.466 M, 1.01 mmol, 67 equiv) was then added via syringe and stirred for 90 min at rt. The reaction was quenched with aq. HCl (5 M, 10 mL), extracted with CH_2Cl_2 (3 x 10 mL), dried over $MgSO_4$, filtered, and the solvent was removed in vacuo. The resulting white solid was then washed with MeOH, and dried under vacuum (209 mg, 75% yield) M_n = 28.2 kDa, Đ = 1.19.

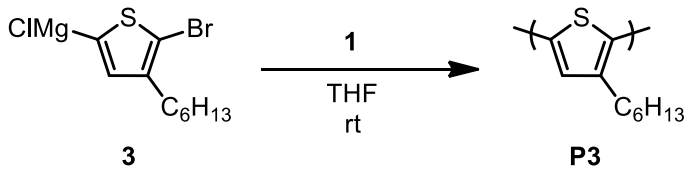

3 **P3**

P3. A 25 mL Schlenk flask was equipped with a stir bar, precatalyst **1** (10.2 mg, 0.0150 mmol, 1 equiv), and THF (8.07 mL) in a glovebox under an N_2 atmosphere. The flask was then equipped with a septum (secured with copper wire), removed from the glovebox, and put under an N_2 atmosphere. Monomer **3** (1.93 mL, 0.466 M, 0.900 mmol, 60 equiv) was then added via syringe and stirred for 90 min at rt. The reaction was quenched with aq. HCl (5 M, 10 mL), extracted with $CHCl_3$ (3 x 10 mL), dried over $MgSO_4$, filtered, and the solvent was removed in vacuo. The resulting purple solid was then dissolved in a minimum amount of $CHCl_3$ and precipitated into MeOH. The precipitate was collected and dried under vacuum (130 mg, 87% yield) M_n = 18.1 kDa, Đ = 1.19.

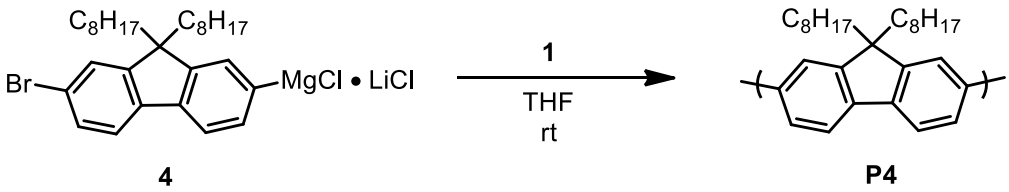

4 **P4**

P4. A 25 mL Schlenk flask was equipped with a stir bar, precatalyst **1** (10.2 mg, 0.0150 mmol, 1 equiv), and THF (6.33 mL) in a glovebox under an N_2 atmosphere. The flask was then equipped with a septum (secured with copper wire), removed from the glovebox, and put under an N_2 atmosphere. Monomer **4** (3.67 mL, 0.286 M, 1.01 mmol, 67 equiv) was then added via syringe and stirred for 60 min at rt. The reaction was quenched with aq. HCl (5 M, 10 mL), extracted with $CHCl_3$ (3 x 10 mL), dried over $MgSO_4$, filtered, and the solvent was removed in vacuo. The resulting yellow solid was then washed with acetone, and dried under vacuum. (246 mg, 63% yield) M_n = 7.2 kDa, Đ = 1.73.

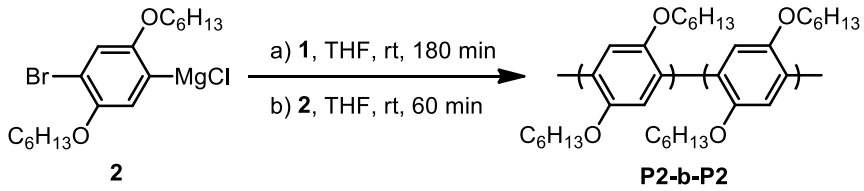

2 **P2-b-P2**

P2-b-P2. A 25 mL Schlenk flask was equipped with a stir bar, precatalyst **1** (10.2 mg, 0.0150 mmol, 1 equiv), and THF (4.6 mL) in a glovebox under an N_2 atmosphere. The flask was then equipped with a septum (secured with copper wire), removed from the glovebox, and put under an N_2 atmosphere. Monomer **2** (2.70 mL, 0.210 M, 0.567 mmol, 38 equiv) was then added via syringe and stirred for 180 min at rt. After 180 min, an aliquot was withdrawn via syringe and immediately quenched with aq. HCl (12 M, 1 mL). Monomer **2** (2.70 mL, 0.210 M, 0.567 mmol, 38 equiv) was then added via syringe and stirred for 60 min at rt. After 60 min, an aliquot was withdrawn via syringe and immediately quenched with aq. HCl (12 M, 1 mL). Each aliquot was then extracted with CH_2Cl_2 (3 x 1 mL) with mild heating, dried over $MgSO_4$, filtered, and concentrated in vacuo. The resulting solid was then dissolved in THF (~1.5 mL) with mild heating and passed through a 0.2 µm PTFE filter for GPC analysis. Block 1: M_n = 13.8 kDa, Đ = 1.13, Block 2: M_n = 21.8 kDa, Đ = 1.18.

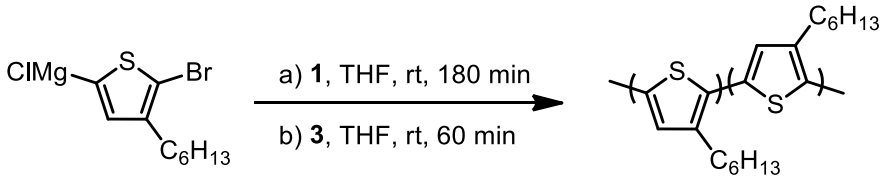

3 **P3-b-P3**

P3-b-P3. A 25 mL Schlenk flask was equipped with a stir bar, precatalyst **1** (10.2 mg, 0.0150 mmol, 1 equiv), and THF (7.8 mL) in a glovebox under an N_2 atmosphere. The flask was then equipped with a septum (secured with copper wire), removed from the glovebox, and put under an N_2 atmosphere. Monomer **3** (1.06 mL, 0.525 M, 0.557 mmol, 37 equiv) was then added via syringe and stirred for 180 min at rt. After 180 min, an aliquot was withdrawn via syringe and immediately quenched with aq. HCl (12 M, 1 mL). Monomer **3** (1.06 mL, 0.525 M, 0.557 mmol, 37 equiv) was then added via syringe and stirred for 60 min at rt. After 60 min, an aliquot was withdrawn via syringe and immediately quenched with aq. HCl (12 M, 1 mL). Each aliquot was then extracted with $CHCl_3$ (3 x 1 mL) with mild heating, dried over $MgSO_4$, filtered, and concentrated in vacuo. The resulting solid was then dissolved in THF (~1.5 mL) with mild heating and passed through a 0.2 μm PTFE filter for GPC analysis. Block 1: M_n = 11.2 kDa, Đ = 1.22, Block 2: M_n = 17.8 kDa, Đ = 1.35.

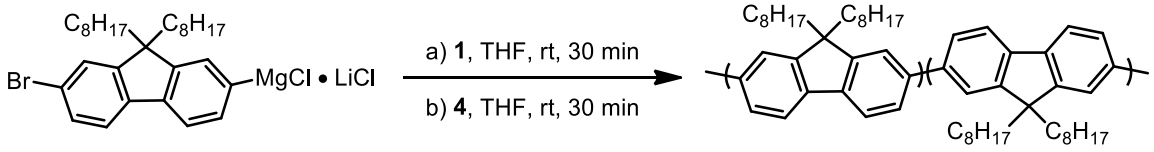

4 **P4-b-P4**

P4-b-P4. A 25 mL Schlenk flask was equipped with a stir bar, precatalyst **1** (10.2 mg, 0.0150 mmol, 1 equiv), and THF (6.48 mL) in a glovebox under an N_2 atmosphere. The flask was then equipped with a septum (secured with copper wire), removed from the glovebox, and put under an N_2 atmosphere. Monomer **3** (1.76 mL, 0.286 M, 0.503 mmol, 35 equiv) was then added via syringe and stirred for 30 min at rt. After 30 min, an aliquot was withdrawn via syringe and immediately quenched with aq. HCl (12 M, 1 mL). Monomer **3** (1.76 mL, 0.286 M, 0.503 mmol, 35 equiv) was then added via syringe and stirred for 30 min at rt. After 30 min, an aliquot was withdrawn via syringe and immediately quenched with aq. HCl (12 M, 1 mL). Each aliquot was then extracted with $CHCl_3$ (3 x 1 mL) with mild heating, dried over $MgSO_4$, filtered and concentrated in vacuo. The resulting solid was then dissolved in THF (~1.5 mL) with mild heating and passed through a 0.2 μm PTFE filter for GPC analysis. Block 1: M_n = 7.0 kDa, Đ = 1.97, Block 2: M_n = 7.3 kDa, Đ = 2.04.

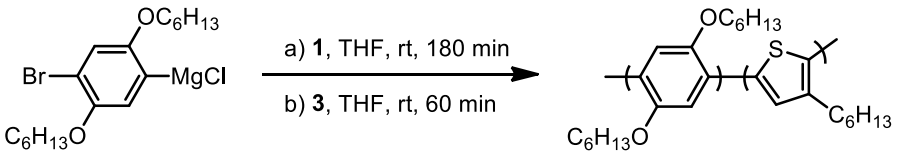

2 **P2-b-P3**

P2-b-P3. A 25 mL Schlenk flask was equipped with a stir bar, precatalyst **1** (10.2 mg, 0.0150 mmol, 1 equiv), and THF (7.11 mL) in a glovebox under an N_2 atmosphere. The flask was then equipped with a septum (secured with copper wire), removed from the glovebox, and put under an N_2 atmosphere. Monomer **2** (0.96 mL, 0.52 M, 0.50 mmol, 33 equiv) was then added via syringe and stirred for 180 min at rt. After 180 min, an aliquot was withdrawn via syringe and immediately quenched with aq. HCl (12 M, 1 mL). Monomer **3** (1.93 mL, 0.466 M, 0.900 mmol, 60 equiv) was then added via syringe and stirred for 60 min at rt. After 60 min, an aliquot was withdrawn via syringe and immediately quenched with aq. HCl (12 M, 1 mL). The aliquots were extracted with $CHCl_3$ (3 x 1 mL) with mild heating and the combined aliquots were dried over $MgSO_4$. The organic phase was then concentrated in vacuo, redissolved in THF (~1.5 mL) with mild heating and passed through a 0.2 µm PTFE filter for GPC analysis (Block 1: M_n = 9.2 kDa, Đ = 1.24, Block 2: M_n = 17.8 kDa, Đ = 1.32). The reaction was quenched with aq. HCl (5 M, 10 mL), extracted with $CHCl_3$ (3 x 10 mL), dried over $MgSO_4$, filtered, and the solvent was removed in vacuo. The resulting purple solid was then dissolved in a minimum amount of $CHCl_3$ and precipitated into MeOH. The precipitate was collected and dried under vacuum (223 mg, 78% yield).

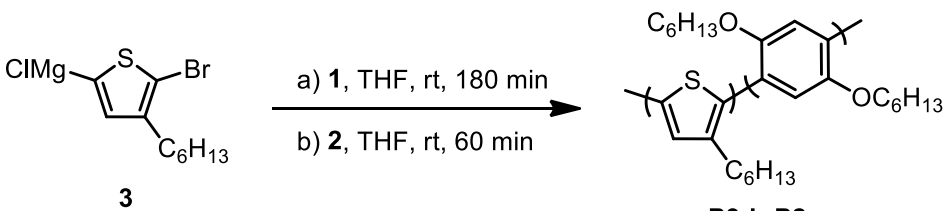

3 **P3-b-P2**

P3-b-P2. A 25 mL Schlenk flask was equipped with a stir bar, precatalyst **1** (10.2 mg, 0.0150 mmol, 1 equiv), and THF (7.11 mL) in a glovebox under an N_2 atmosphere. The flask was then equipped with a septum (secured with copper wire), removed from the glovebox, and put under an N_2 atmosphere. Monomer **3** (1.93 mL, 0.466 M, 0.900 mmol, 60 equiv) was then added via syringe and stirred for 180 min at rt. After 180 min, an aliquot was withdrawn via syringe and immediately quenched with aq. HCl (12 M, 1 mL). Monomer **2** (0.96 mL, 0.52 M, 0.50 mmol, 33 equiv) was then added via syringe and stirred for 60 min at rt. After 60 min, an aliquot was withdrawn via syringe and immediately quenched with aq. HCl (12 M, 1 mL). The aliquots were extracted with $CHCl_3$ (3 x 1 mL) with mild heating and the combined aliquots were dried over $MgSO_4$. The organic phase was then concentrated in vacuo, redissolved in THF (~1.5 mL) with mild heating and passed through a 0.2 µm PTFE filter for GPC analysis (Block 1: M_n = 8.8 kDa, Đ = 1.26, Block 2: M_n = 15.8 kDa, Đ = 1.35). The reaction was quenched with aq. HCl (5 M, 10 mL), extracted with $CHCl_3$ (3 x 10 mL), dried over $MgSO_4$, filtered, and the solvent was removed in vacuo. The resulting purple solid was then dissolved in a minimum amount of $CHCl_3$ and precipitated into MeOH. The precipitate was collected and dried under vacuum (238 mg, 83% yield).

IV. ^{1}H NMR Spectra

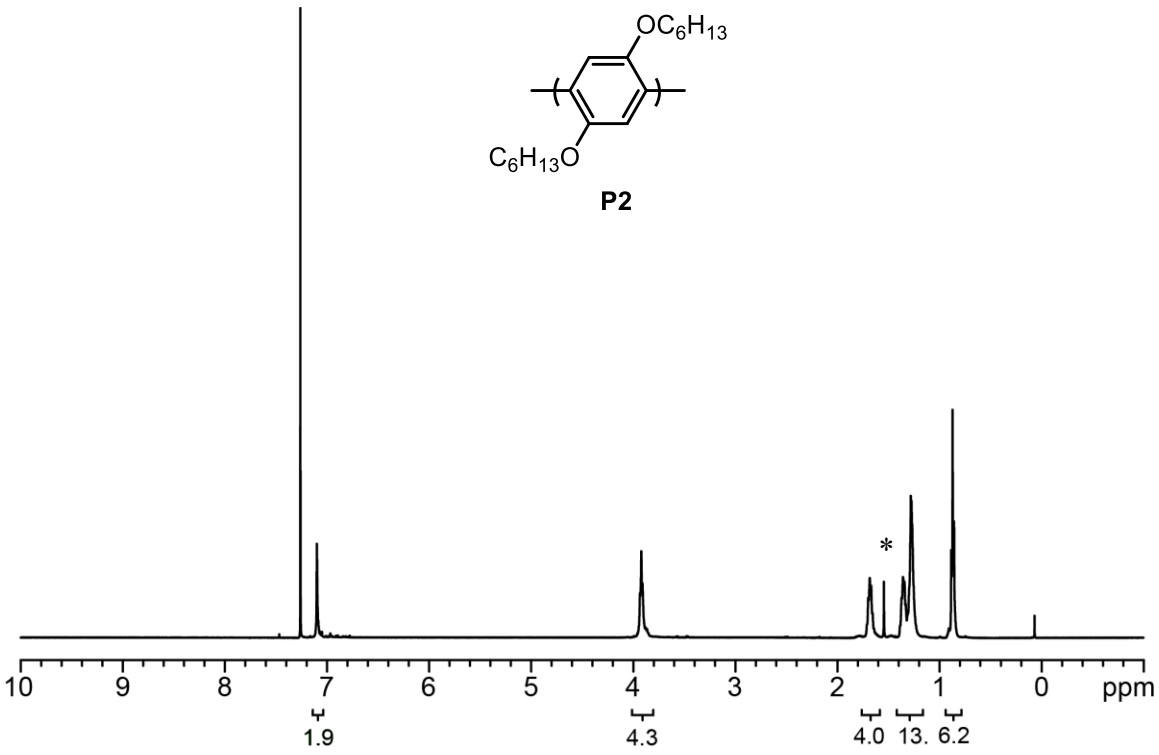

Figure S2.1 ^{1}H NMR spectrum for **P2**.
^{1}H NMR (500 MHz, $CDCl_3$) δ 7.10 (br s, 2H), 3.92 (br m, 4H), 1.68 (br m, 4H) 1.40-1.21 (br m, 12H), 0.87 (br m, 6H). * indicates residual H_2O

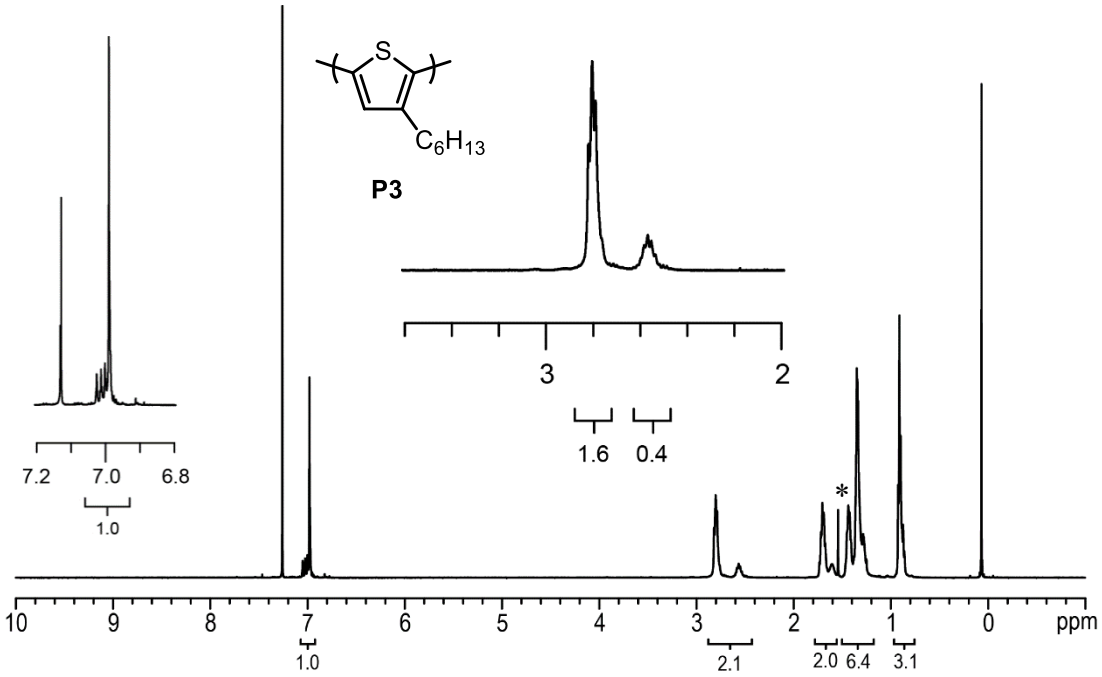

Figure S2.2 ^{1}H NMR spectrum for **P3**.
^{1}H NMR (500 MHz, $CDCl_3$) δ 6.98 (s, 1H), 2.83-2.50 (br m, 2H), 1.74-1.57 (m, 2H) 1.47-1.24 (br m, 6H), 0.91 (br m, 3H). * indicates residual H_2O

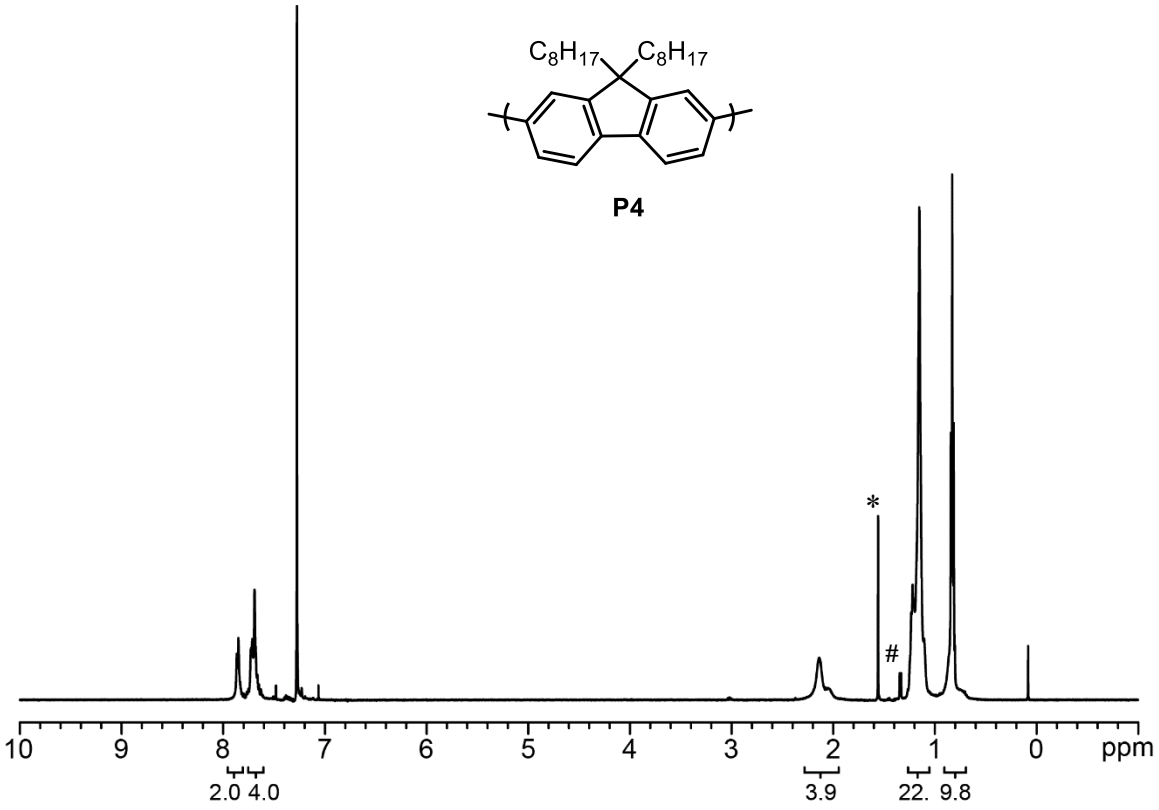

Figure S2.3 ^{1}H NMR spectrum for **P4**.
^{1}H NMR (500 MHz, $CDCl_3$) δ 7.85 (br m, 2H), 7.69 (br m, 4H), 2.22-1.89 (br m, 4H), 1.27-1.06 (br m, 20H), 0.90-0.71 (br m, 10H). * indicates residual H_2O, # indicates iPr end groups

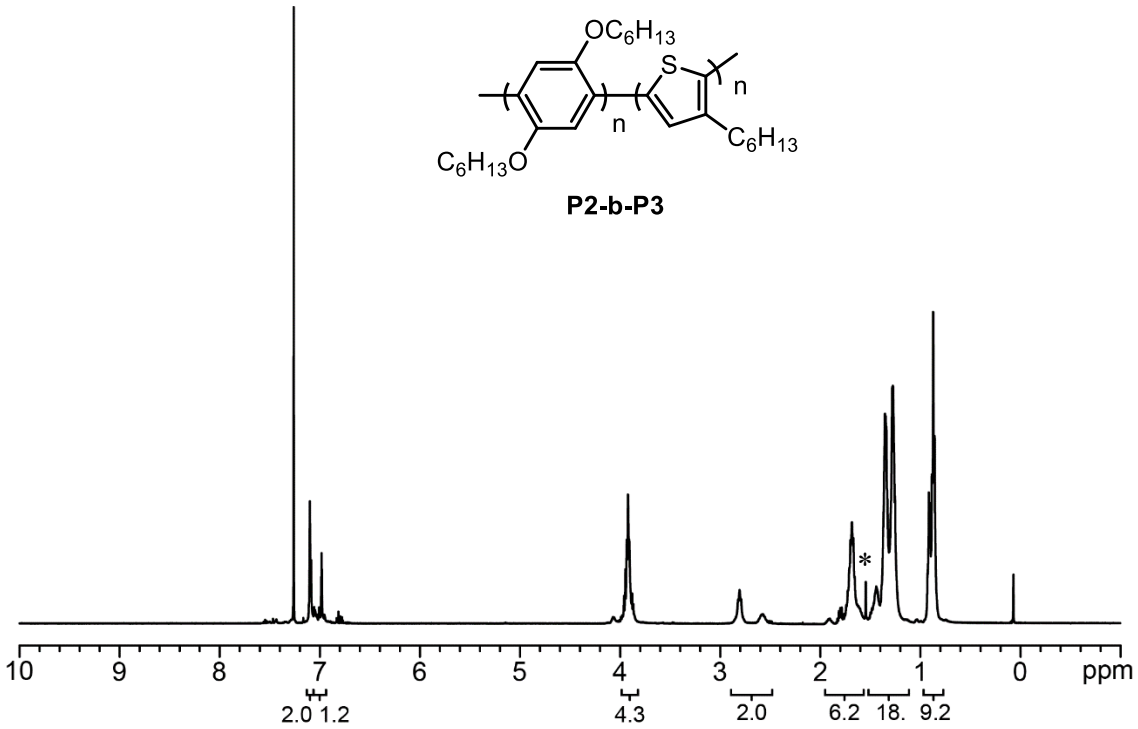

Figure S2.4 ^{1}H NMR spectrum for **P2-b-P3**.
^{1}H NMR (500 MHz, $CDCl_3$) δ 7.10 (br s, 2H), 6.98 (s, 1H), 4.09-3.84 (br m, 4H), 2.83-2.50 (br m, 2H), 1.74-1.57 (br m, 6H) 1.47-1.24 (br m, 18H), 0.94-0.84 (br m, 9H). * indicates residual H_2O

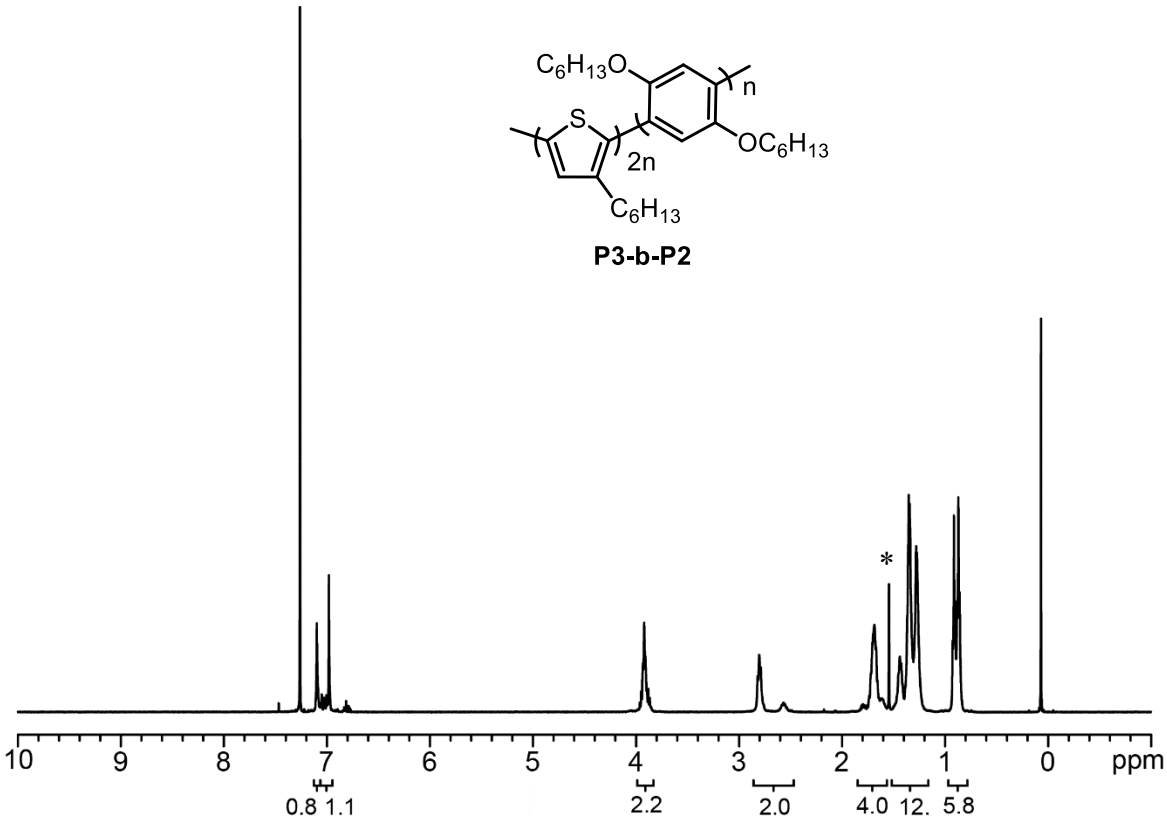

Figure S2.5 ^{1}H NMR spectrum for **P3-b-P2**
^{1}H NMR (500 MHz, $CDCl_3$) δ 7.10 (br s, 1H), 6.98 (m, 1H), 4.09-3.84 (br m, 2H), 2.83-2.50 (br m, 2H), 1.74-1.57 (br m, 4H) 1.47-1.24 (br m, 12H), 0.94-0.84 (br m, 6H). * indicates residual H_2O

V. M_n and Đ versus Conversion

Representative Procedure for M_n and Đ versus Conversion Studies utilizing GC analysis:

A 25 mL Schlenk flask was equipped with a stir bar, precatalyst **1** (10.2 mg, 0.0150 mmol, 1 equiv), and THF (7.75 mL) in a glovebox under an N_2 atmosphere. The flask was then equipped with a septum (secured with copper wire), removed from the glovebox, and put under an N_2 atmosphere. Monomer **2** (2.25 mL, 0.466 M, 1.01 mmol, 67 equiv), with docosane added (as an internal standard), was then added via syringe and stirred for 90 min at rt. Aliquots (~0.5 mL) were withdrawn via syringe and immediately quenched with aq. HCl (12 M, 1 mL). Each aliquot was then extracted with CH_2Cl_2 (3 x 1 mL) with mild heating and the combined aliquots were dried over $MgSO_4$. To monitor conversion, GC samples were prepared by taking aliquots (~0.25 mL) of this organic phase and diluting with CH_2Cl_2 (~0.75 mL). Conversion was determined relative to the initial concentration, using the internal standard as a reference. To measure molecular weight and molecular weight distribution, the remaining organic phase was concentrated in vacuo, redissolved in THF (~1.5 mL) with mild heating and passed through a 0.2 μm PTFE filter for GPC analysis.

Note: nonadecane was used as internal standard with monomer **3**, docosane was used as internal standard with monomer **4**.

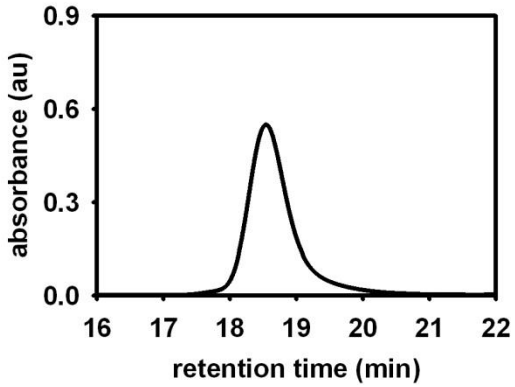

Figure S2.6 Representative GPC trace of **P2** at 60% conversion with precatalyst **1** (M_n: 22.5 kDa, Đ: 1.17).

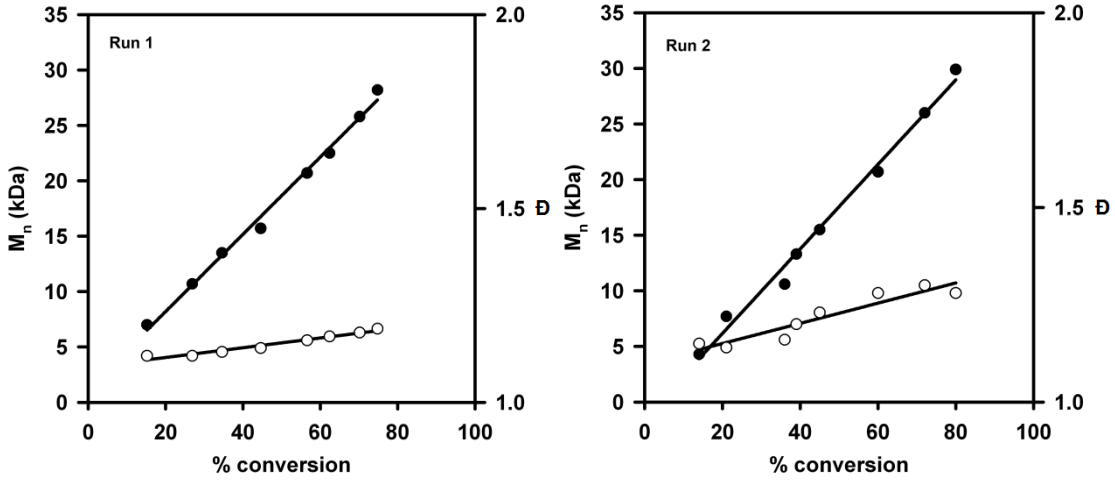

Figure S2.7 Plots of M_n (●) and Đ (○) versus conversion for the polymerization of monomer **2** using precatalyst **1**. ([**1**] = 1.5 mM, [**2**] = 77 mM (run 1), 91 mM (run 2), 25 °C, THF).

Table S2.1 Data for the plot in **Figure S2.7**, run 1.

% Conversion	M_n (kDa)	Đ
15	7.0	1.12
27	10.7	1.12
35	13.5	1.13
45	15.7	1.14
57	20.7	1.16
62	22.5	1.17
70	25.8	1.18
75	28.2	1.19

Table S2.2 Data for the plot in **Figure S2.7**, run 2.

% Conversion	M_n (kDa)	Đ
14	4.3	1.15
21	7.7	1.14
36	10.6	1.16
39	13.3	1.20
45	15.5	1.23
60	20.7	1.28
72	26.0	1.30
80	29.9	1.28

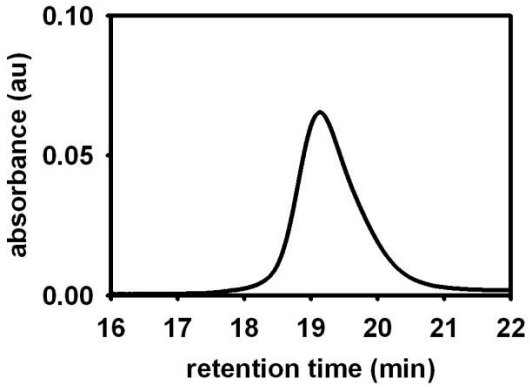

Figure S2.8 Representative GPC trace of **P3** at 60% conversion with precatalyst **1** (M_n: 11.5 kDa, Đ: 1.20).

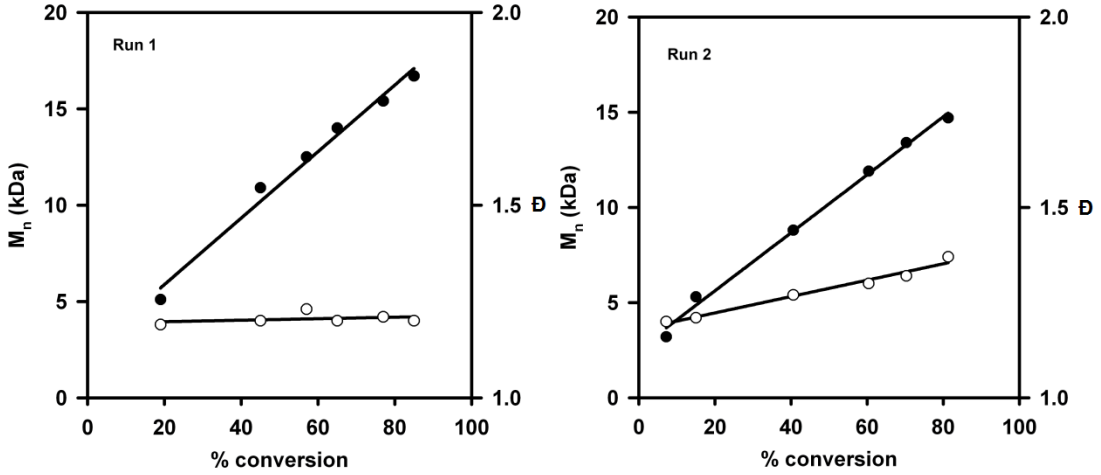

Figure S2.9 Plots of M_n (●) and Đ (○) versus conversion for the polymerization of monomer **3** using precatalyst **1**. ([**1**] = 1.5 mM, [**3**] = 98 mM (run 1), 88 mM (run 2), 25 °C, THF).

Table S2.3 Data for the plot in **Figure S2.9**, run 1.

% Conversion	M_n (kDa)	Đ
19	5.1	1.19
45	10.9	1.20
57	12.5	1.23
65	14.0	1.20
77	15.4	1.21
85	16.7	1.20

Table S2.4 Data for the plot in **Figure S2.9**, run 2.

% Conversion	M_n (kDa)	Đ
7	3.2	1.20
15	5.3	1.21
41	8.8	1.27
60	11.9	1.30
70	13.4	1.32
81	14.7	1.37

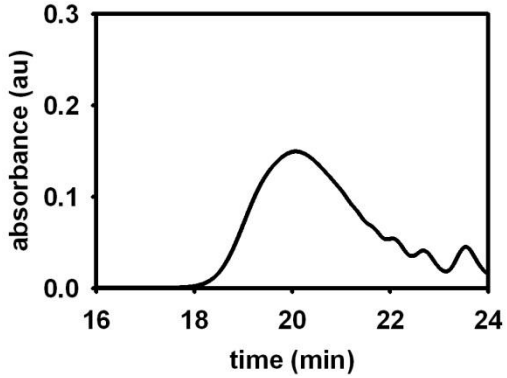

Figure S2.10 Representative GPC trace of **P4** at 60% conversion with precatalyst **1** (M_n: 4.3 kDa, Đ: 1.53).

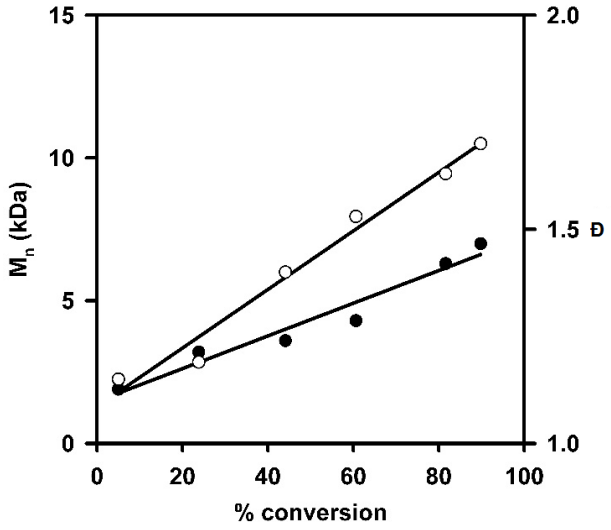

Figure S2.11 Plot of M_n (●) and Đ (○) versus conversion for the polymerization of monomer **4** using precatalyst **1**. ([**1**] = 1.5 mM, [**2**] = 101 mM, 25 °C, THF).

Table S2.5 Data for the plot in **Figure S2.11**.

% Conversion	M_n (kDa)	Đ
5	1.9	1.15
24	3.2	1.19
44	3.6	1.40
61	4.3	1.53
82	6.3	1.63
90	7.0	1.70

VI. M_n and Đ versus [monomer]/[catalyst]

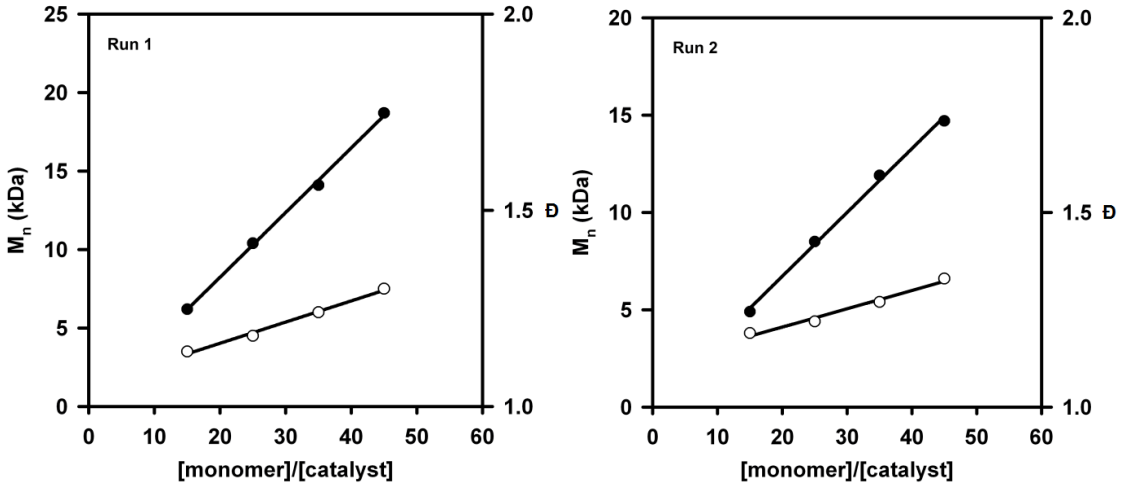

Figure S2.12 Plots of M_n (●) and Đ (○) versus [monomer]/[catalyst] for the polymerization of monomer **2** using precatalyst **1**. ([**1**] = 1.5 mM, [**2**] = 23 mM, 38 mM, 53 mM, 68 mM, 25 °C, THF).

Table S2.6 Data for the plot in **Figure S2.12**, run 1.

[monomer]/[catalyst]	M_n (kDa)	Đ
15	6.2	1.14
25	10.4	1.18
35	14.1	1.24
45	18.7	1.30

Table S2.7 Data for the plot in **Figure S2.12**, run 2.

[monomer]/[catalyst]	M_n (kDa)	Đ
15	4.9	1.19
25	8.5	1.22
35	11.9	1.27
45	14.7	1.33

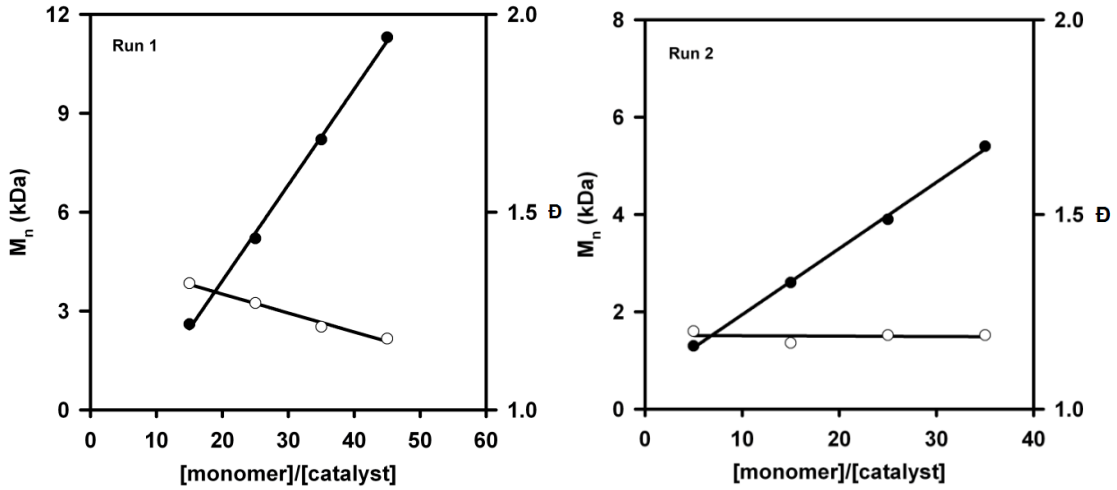

Figure S2.13 Plots of M_n (●) and Đ (○) versus [monomer]/[catalyst] for the polymerization of monomer **3** using precatalyst **1**. ([**1**] = 1.5 mM, [**3**] = 23 mM, 38 mM, 53 mM, 68 mM (run 1), 8 mM, 23 mM, 38 mM, 53 mM (run 2), 25 °C, THF).

Table S2.8 Data for the plot in **Figure S2.13**, run 1.

[monomer]/[catalyst]	M_n (kDa)	Đ
15	2.6	1.37
25	5.2	1.27
35	8.2	1.21
45	11.3	1.18

Table S2.9 Data for the plot in **Figure S2.13**, run 2.

[monomer]/[catalyst]	M_n (kDa)	Đ
5	1.3	1.20
15	2.6	1.17
25	3.9	1.19
35	5.4	1.19

VII. Thiophene Regioregularity

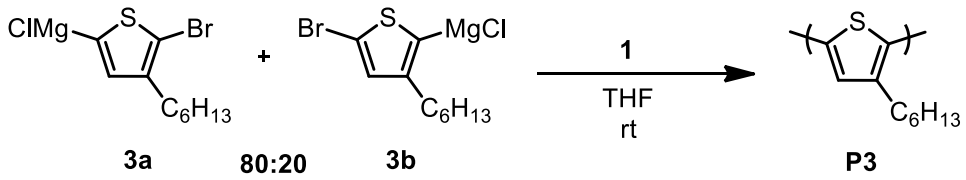

P3. A 25 mL Schlenk flask was equipped with a stir bar, precatalyst **1** (10.2 mg, 0.0150 mmol, 1 equiv), and THF (8.07 mL) in a glovebox under an N_2 atmosphere. The flask was then equipped with a septum (secured with copper wire), removed from the glovebox, and put under an N_2 atmosphere. Monomer **3** (1.93 mL, 0.466 M, 0.900 mmol, 60 equiv), with nonadecane added (as an internal standard), was then added via syringe and stirred for 90 min at rt. Aliquots (~0.5 mL) were withdrawn via syringe and immediately quenched with aq. HCl (12 M, 1 mL). Each aliquot was then extracted with $CHCl_3$ (3 x 1 mL) with mild heating and the combined aliquots were dried over $MgSO_4$. To monitor conversion, GC samples were prepared by taking aliquots (~0.25 mL) of this organic phase and diluting with CH_2Cl_3 (~0.75 mL). Conversion was determined by sum of areas (**3a** + **3b**) relative to a nonadecane internal standard.

Table S2.10 Data for the consumption of thiophene regioisomers, run 1.

% Conversion (**3a**)	% Conversion (**3b**)	Total Conversion
20	0*	14
46	3	36
58	0	44
71	5	56
85	13	68
94	20	76
98	48	87
99	95	98

* Within range of intrinsic GC error

Table S2.11 Data for the consumption of thiophene regioisomers, run 2.

% Conversion (**3a**)	% Conversion (**3b**)	Total Conversion
22	0	17
39	2	31
46	1	36
63	9	51
79	18	65
90	28	76
98	42	86

VIII. Competition Experiment

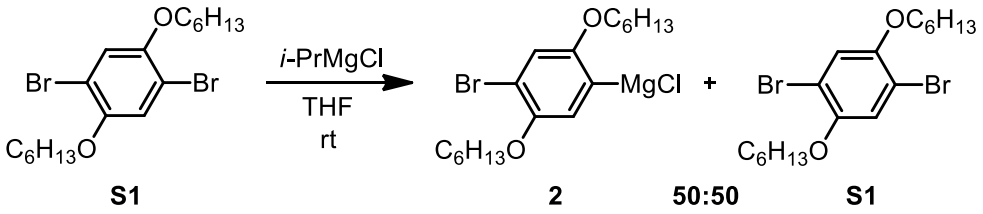

2:S1 Mixture. In the glovebox, **S1** (3.00 g, 6.88 mmol, 1.0 equiv) was dissolved in THF (7.5 mL) in a 20 mL vial equipped with a stir bar. Then, *i*-PrMgCl (1.72 mL, 3.44 mmol, 0.5 equiv) was added via syringe, the vial was capped, and the reaction was stirred overnight at rt. Approximate ratio was confirmed via GC analysis.

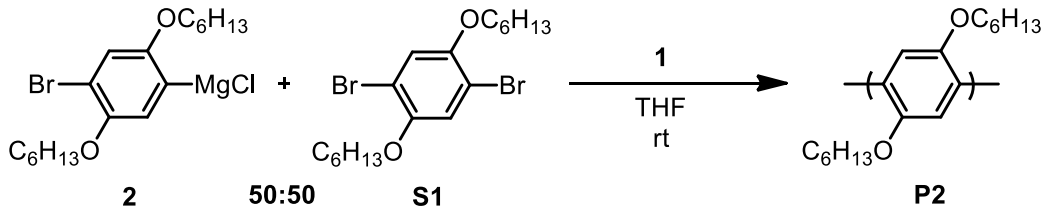

P2. A 25 mL Schlenk flask was equipped with a stir bar, precatalyst **1** (10.2 mg, 0.0150 mmol, 1 equiv), and THF (6.25 mL) in a glovebox under an N_2 atmosphere. The flask was then equipped with a septum (secured with copper wire), removed from the glovebox, and put under an N_2 atmosphere. A mixture of **2:S1** (~50:50) (3.75 mL, [**2**] = 0.268 M, 1.005 mmol, 67 equiv), with docosane added (as an internal standard), was then added via syringe and stirred for 90 min at rt. Aliquots (~0.5 mL) were withdrawn via syringe and immediately quenched with aq. HCl (12 M, 1 mL). Each aliquot was then extracted with CH_2Cl_2 (3 x 1 mL) with mild heating and the combined aliquots were dried over $MgSO_4$. To monitor conversion, GC samples were prepared by taking aliquots (~0.25 mL) of this organic phase and diluting with CH_2Cl_2 (~0.75 mL). Conversion was determined relative to docosane internal standard. To measure molecular weight and molecular weight distribution, the remaining organic phase was concentrated in vacuo, redissolved in THF (~1.5 mL) with mild heating and passed through a 0.2 μm PTFE filter for GPC analysis.

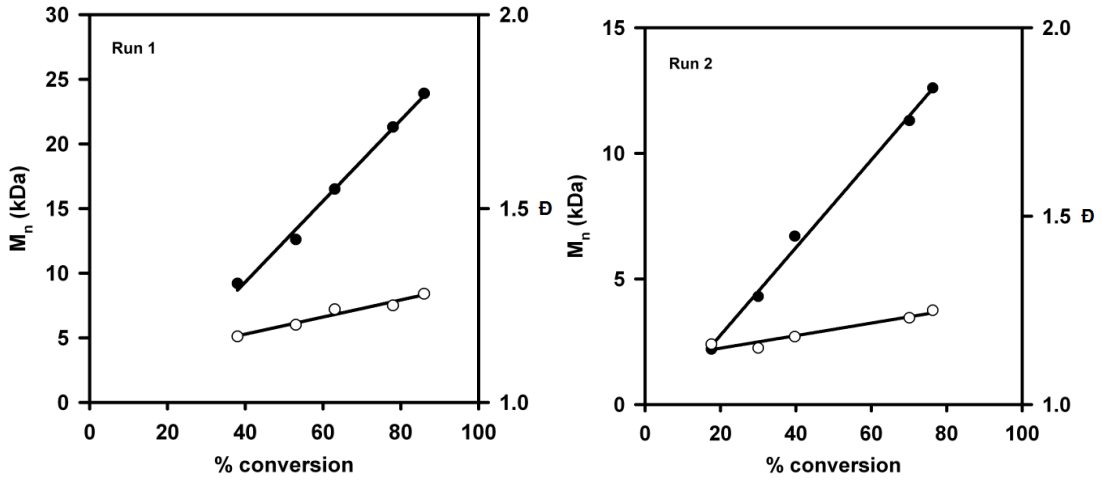

Figure S2.14 Plots of M_n (●) and Đ (○) versus conversion for the polymerization of monomer **2** with 50% **S1** using precatalyst **1**. ([**1**] = 1.5 mM, [**2**] = 101 mM (run 1), 85 mM (run 2), 25 °C, THF).

Table S2.12 Data for the plot in **Figure S2.14**, run 1.

% Conversion (**2**)	% **S1**	M_n (kDa)	Đ
38	6	9.2	1.17
53	6	12.6	1.20
63	0*	16.5	1.24
78	1	21.3	1.25
86	7	23.9	1.28

* Within range of intrinsic GC error

Table S2.13 Data for the plot in **Figure S2.14**, run 2.

% Conversion (**2**)	% **S1**	M_n (kDa)	Đ
18	4	2.2	1.16
30	5	4.3	1.15
40	0*	6.7	1.18
70	1	11.3	1.23
76	0	12.6	1.25

* Within range of intrinsic GC error

IX. MALDI-TOF MS Data

Representative Procedure for Preparation of Oligomers for MALDI-TOF MS Studies:

All actions were performed in a glovebox under N_2 atmosphere. A 20 mL vial was equipped with a stir bar. Sequentially, precatalyst **1** (10.2 mg, 0.0150 mmol, 1.0 equiv), THF (4.75 mL), and **2** (0.25 mL, 0.45 M, 0.11 mmol, 7.0 equiv) were added to the flask. After 1 h, the reaction was removed from the glovebox, and poured into aq. HCl (5 M, 5 mL). This mixture was then extracted with CH_2Cl_2 (3 x 5 mL). The combined organic layers were dried over $MgSO_4$, filtered, and concentrated in vacuo. The resulting solid was washed with MeOH (50 mL) to give **P2** as an off-white solid: M_n: 2.04 kDa, Đ: 1.21 (GPC). For the MS sample, the polymer was dissolved in minimal $CHCl_3$ (~2 mL) and filtered through a pipet column of basic, acidic, and neutral alumina to remove Pd. The solution was then concentrated in vacuo. The general procedure was followed for MALDI-TOF MS sample preparation (see General Experimental pS2).

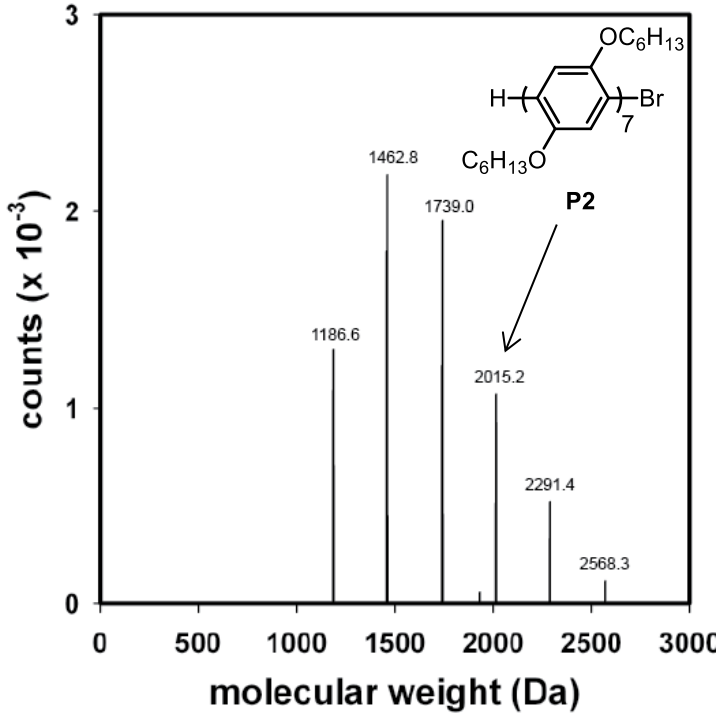

Figure S2.15 MALDI-TOF MS spectrum of **P2** initiated with precatalyst **1**.

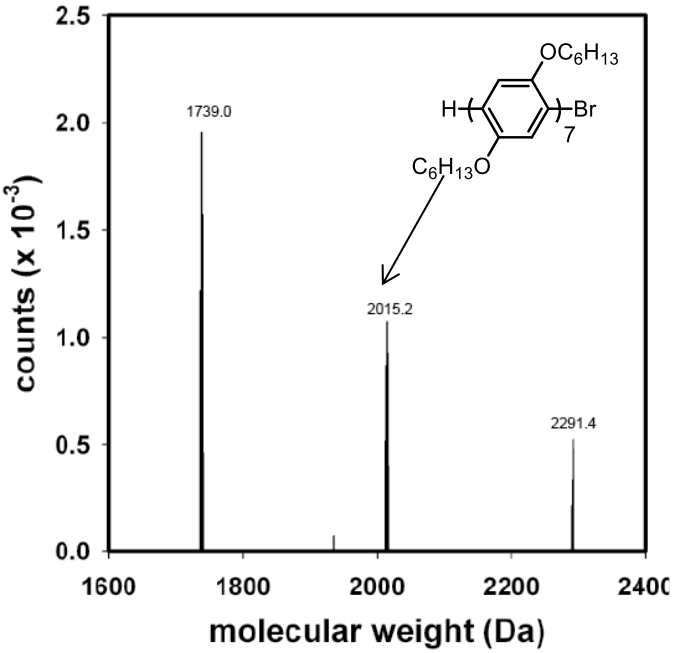

Figure S2.16 Expanded view of **Figure S2.15**.

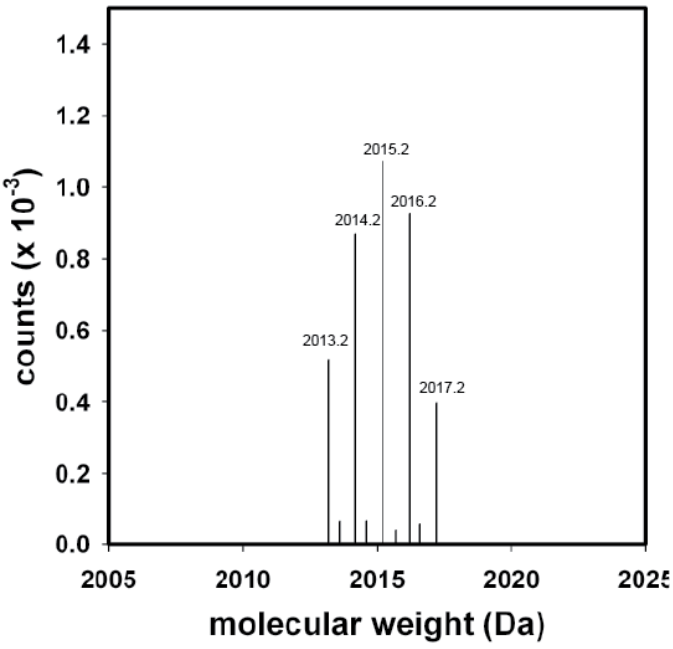

Figure S2.17 Expanded view of **Figure S2.16**.

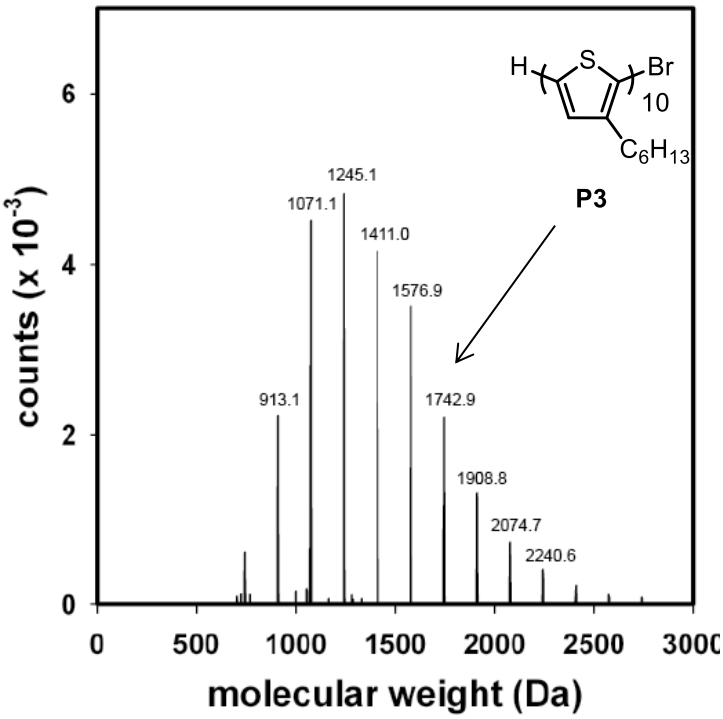

Figure S2.18 MALDI-TOF MS spectrum of **P3** initiated with precatalyst **1**.

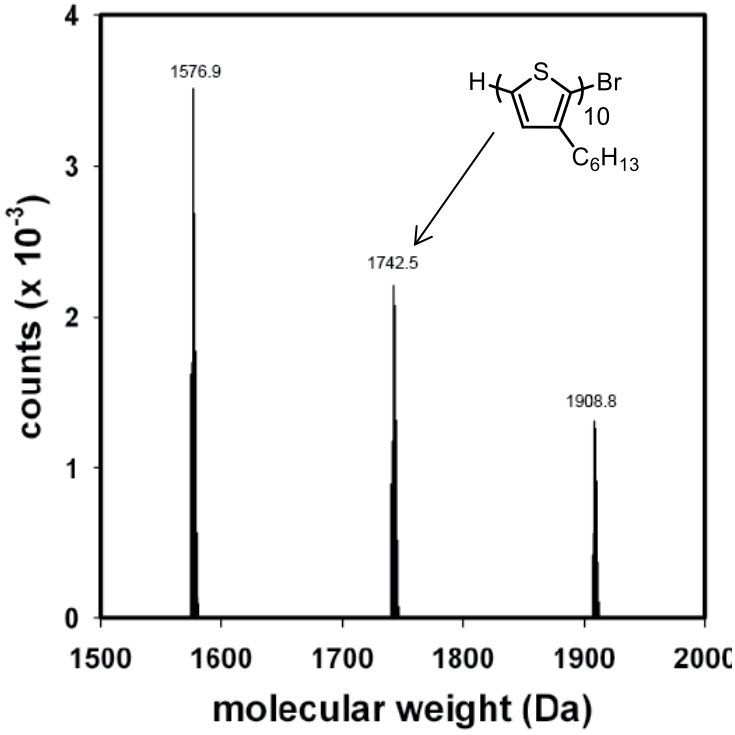

Figure S2.19 Expanded view of **Figure S2.18**.

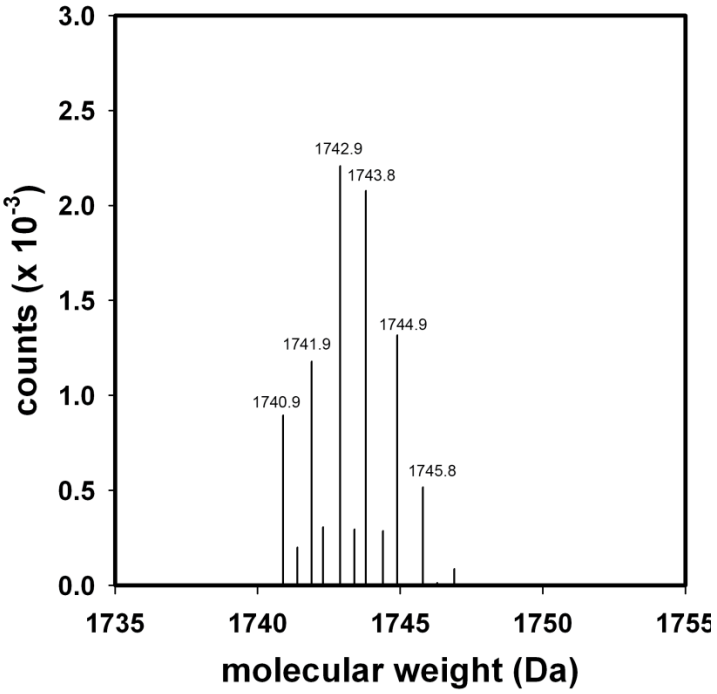

Figure S2.20 Expanded view of **Figure S2.19**.

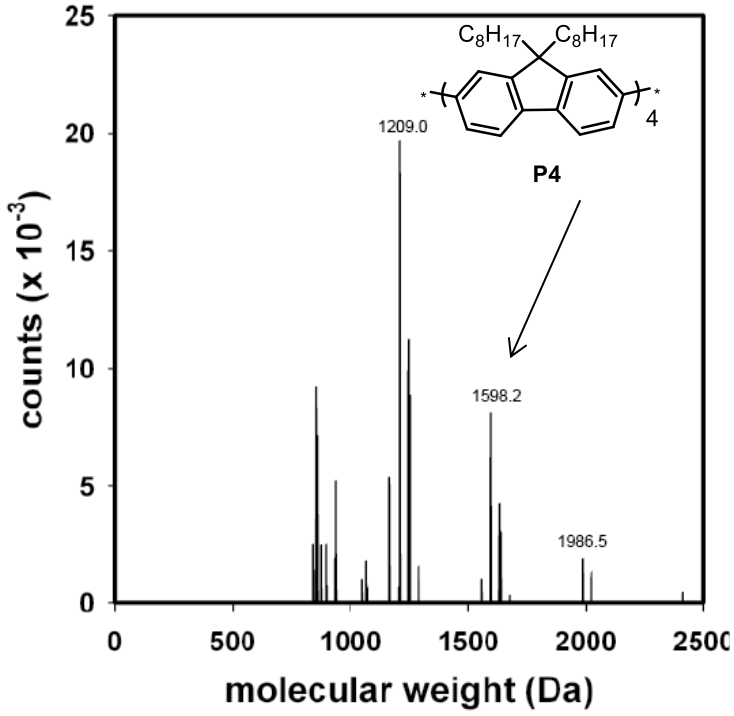

Figure S2.21 MALDI-TOF MS spectrum of **P4** initiated with precatalyst **1**.

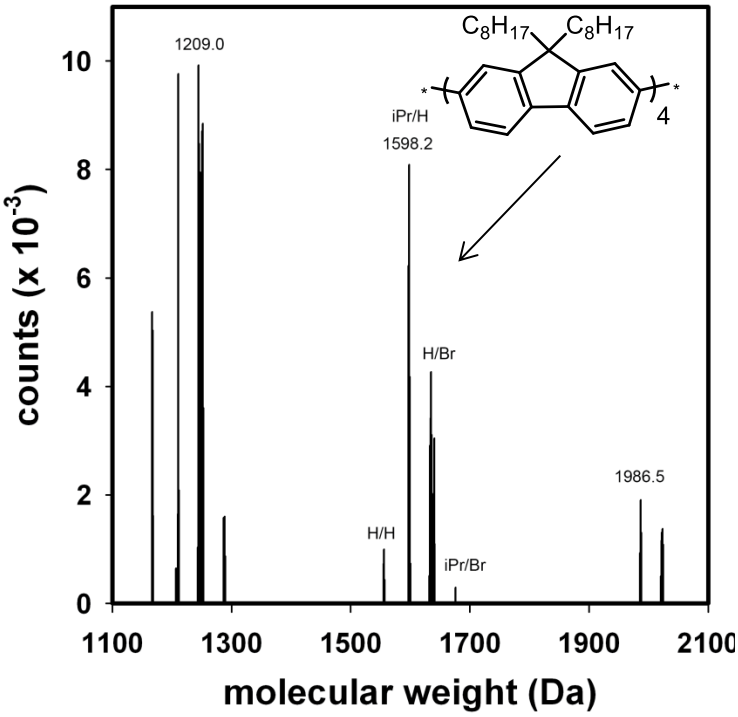

Figure S2.22 Expanded view of **Figure S2.21**.

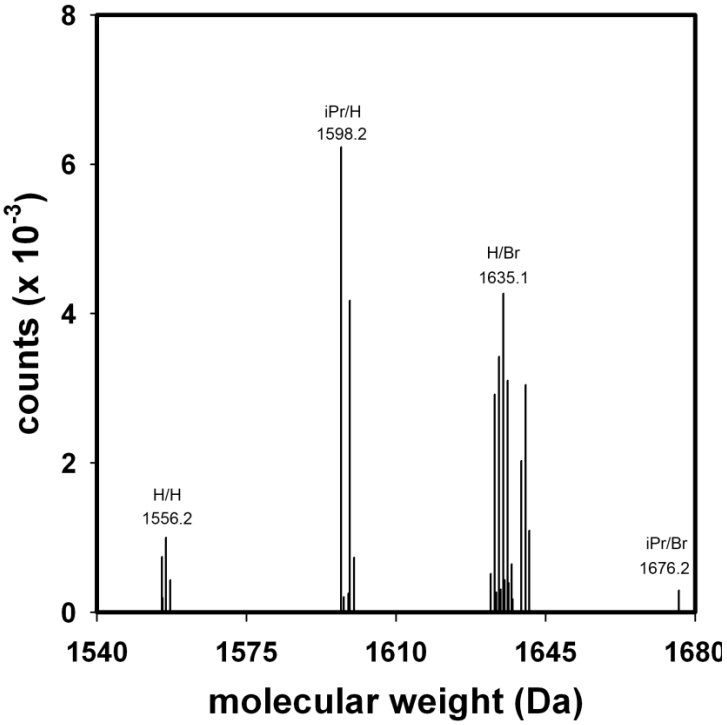

Figure S2.23 Expanded view of **Figure S2.22**.

X. Plot of $\ln([M]_0/[M])$ versus Time

Representative Procedure for studies utilizing react IR:
The IR probe was inserted through an O-ring sealed 14/20 ground glass adapter (custom-made) into an oven-dried 50 mL 2-neck flask equipped with a stir bar. The other neck was fitted with a two-way adapter fitted with a septum for injections/aliquot sampling and an N_2 line. The oven-dried flask was cooled under vacuum. The flask was then filled with N_2 and evacuated again for a total of three cycles. The flask was charged with THF (6.75 mL). After recording a background spectrum, monomer **2** (2.25 mL, 0.466 M, 1.01 mmol, 67 equiv) was added by syringe. Precatalyst **1** (10.2 mg, 0.0150 mmol, 1 equiv), dissolved in THF (1 mL), was then injected and spectra were recorded every 30 s over the entire reaction. To account for mixing, spectra recorded in the first 60 s of the reaction were discarded. Aliquots (~0.5 mL) were withdrawn via syringe and immediately quenched with aq. HCl (12 M, 1 mL). Each aliquot was then extracted with CH_2Cl_2 (3 x 1 mL) with mild heating and the combined aliquots were dried over $MgSO_4$. Conversion was determined by absorbance readings relative to starting concentration. To measure molecular weight and molecular weight distribution, the organic phase was concentrated in vacuo, redissolved in THF (~1.5 mL) with mild heating and passed through a 0.2 μm PTFE filter for GPC analysis.

Although linear plots of $\ln([M]_0/[M])$ have been used to provide evidence of a "living" polymerization,[4] this analysis assumes that the polymerization is first-order in monomer throughout the polymerization. If, on the other hand, the rate-determining step changes with conversion, then a non-linear plot can be observed, even under "living" conditions. Because the mechanism has not been established in this case, it is not possible to determine whether the observed non-linearity stems from chain termination pathways or a change in rate-determining step.

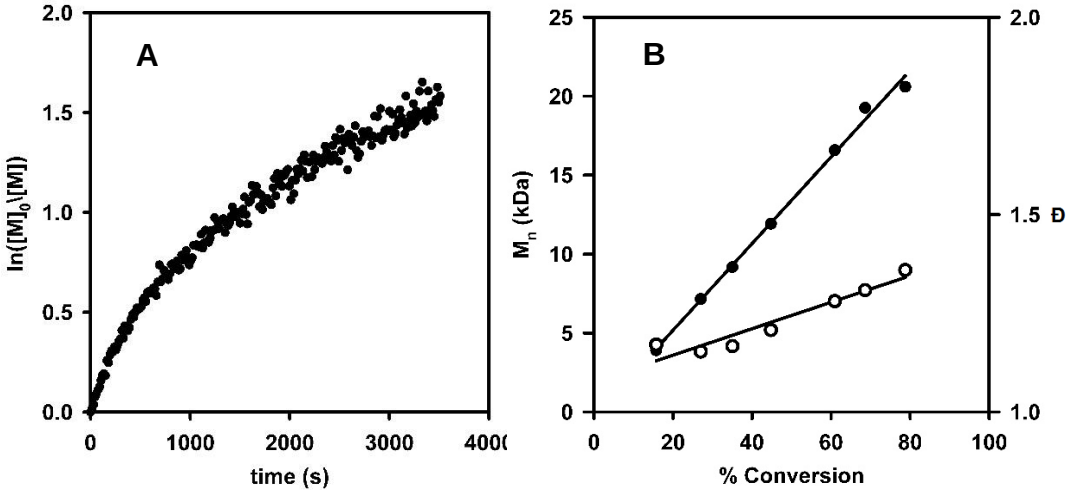

Figure S2.24 (A) Plot of $\ln([M]_0/[M])$ versus time for polymerization of **2**. ([**1**] = 1.5 mM, [**2**] = 101 mM, 25 °C, THF). (B) Corresponding plot of M_n (●) and Đ (○) versus conversion for the polymerization of **2**.

XI. Summary of Homopolymerizations

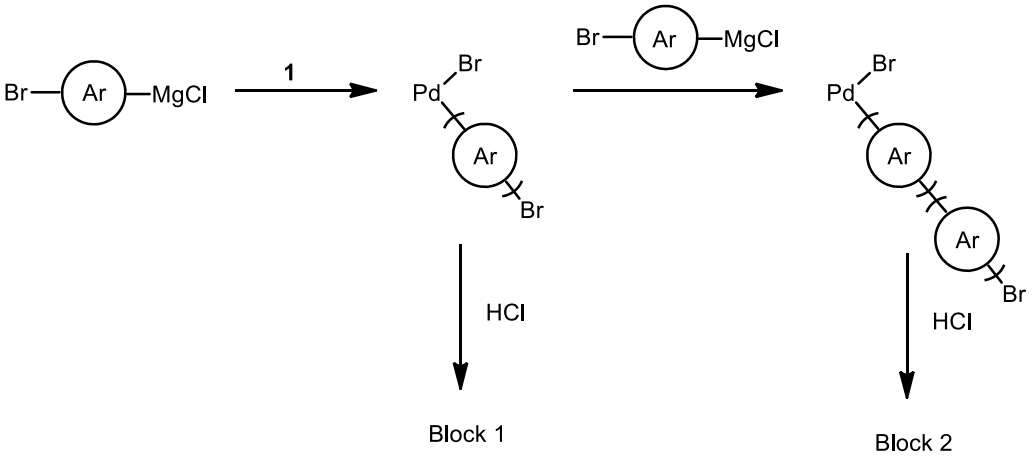

Table S2.14 Summary of GPC Data for Homopolymerizations (pgs S6 and S7).

Homopolymerization	M_n (kDa)	Đ
P2-b-P2 (Block 1)	13.8	1.13
P2-b-P2 (Block 2)	21.8	1.18
P3-b-P3 (Block 1)	11.2	1.22
P3-b-P3 (Block 2)	17.8	1.35
P4-b-P4 (Block 1)	7.0	1.97
P4-b-P4 (Block 2)	7.3	2.04

XII. Fluorene Side Reactions

(A) No consumption of *i*-PrBr was observed relative to internal standard (mesitylene), while complete consumption of *i*-PrMgCl was observed during polymerization of **4**.*

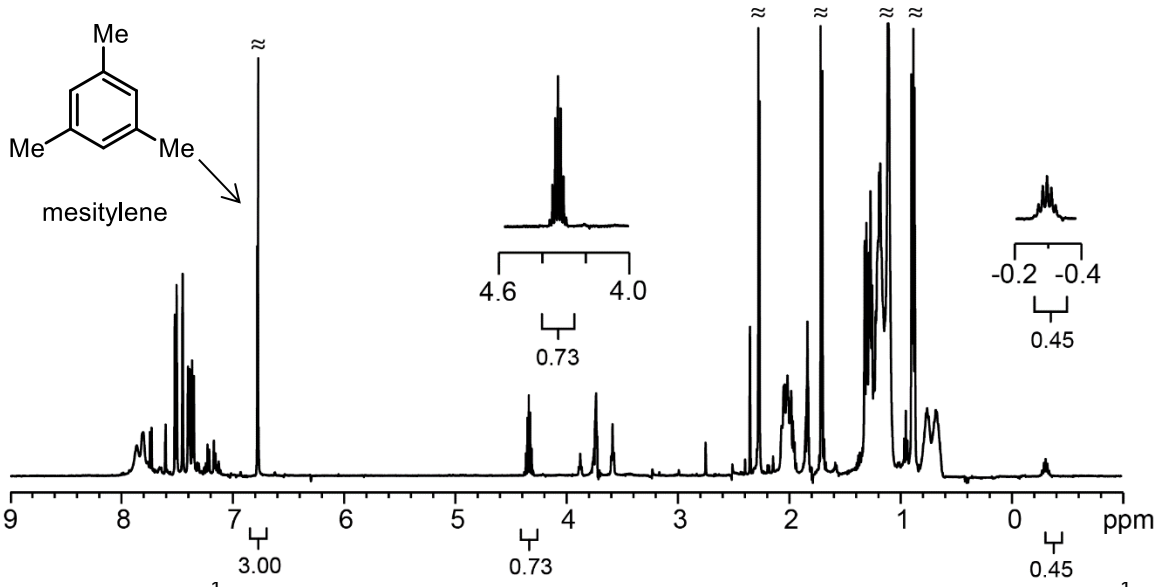

Figure S2.25 ^{1}H NMR spectrum for **4** (note: solvent suppresion was used). ^{1}H NMR (500 MHz, THF) δ 6.78 (s, 3H, Ar H), 4.36 (m, 1H, BrC*H*$(CH_3)_2$), -0.31 (m, 1H, ClMgC*H*$(CH_3)_2$).

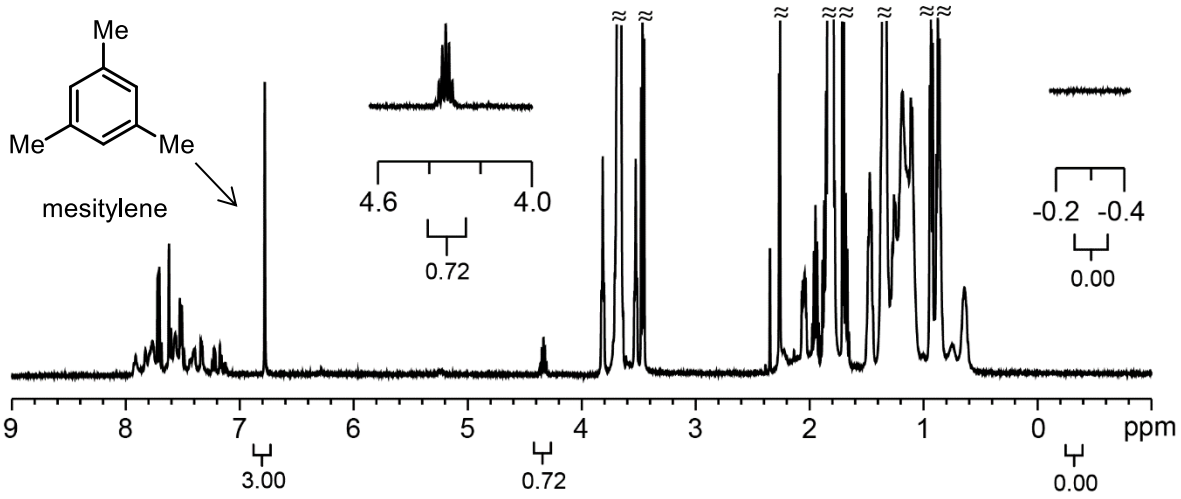

Figure S2.26 ^{1}H NMR spectrum for **P4** before quenching. ^{1}H NMR (500 MHz, THF) δ 6.78 (s, 3H, Ar H), 4.36 (m, 1H, BrC*H*$(CH_3)_2$), -0.31 (m, 1H, ClMgC*H*$(CH_3)_2$).

* These results are consistent with a control experiment wherein 1-bromodecane (20 equiv) was not consumed during the polymerization of **4** as evidenced by GC relative to internal standard.

(B) Consumption of the 2,7-dibromo-9,9-dioctylfluorene (**S3**) following Grignard metathesis was determined during the polymerization of **4**. Conversion was determined by GC relative to added internal standard (mesitylene).

Table S2.15 Conversion of 2,7-dibromo-9,9-dioctylfluorene (**S3**) during the polymerization of **4**.

Trial	% Conversion **S3**
Run 1	5
Run 2	10
Run 3	10
Run 4	11
Run 5	29

* All reactions showed > 85% monomer (**4**) conversion.

XII. References

_____

(1) (a) Lanni, E. L.; McNeil, A. J. *J. Am. Chem. Soc.* **2009**, *131*, 16573-16579. (b) Lanni, E. L.; McNeil, A. J. *Macromolecules* **2010**, *43*, 8039-8044.
(2) Locke, J. R.; McNeil, A. J. *Macromolecules* **2010**, *43*, 8709-8710.
(3) Love, B. D.; Jones, E. G. *J. Org. Chem.* **1999**, *64*, 3755-3756.
(4) Penczek, S.; Kubisa, P.; Szymanski, R. *Makromol. Chem., Rapid Commun.* **1991**, *12*, 77-80.

Appendix 3

Supporting Information for Chapter 4:
Using small molecules to identify new catalysts for catalyst-transfer polycondensation (CTP)

Contents **Page**

I. Materials

Flash chromatography was performed on SiliCycle silica gel (40-63 μm) and thin layer chromatography was performed on Merck TLC plates pre-coated with silica gel 60 F254. 2-methoxyphenylmagnesium bromide (1 M in THF) (**6**), Ni(dppe)Cl_2, Pd-PEPPSI-IPr, Buchwald precatalysts were purchased from Aldrich. All other reagent grade materials and solvents were purchased from Aldrich, Acros, EMD, or Fisher and used without further purification unless otherwise noted. THF was dried and deoxygenated using an Innovative Technology (IT) solvent purification system composed of activated alumina, copper catalyst, and molecular sieves. All glassware was oven-dried at 120 °C for at least 1 h before use. Compound **S3**[1] was prepared according to modified literature procedures.

II. General Experimental

NMR Spectroscopy: Unless otherwise noted, ^{1}H, ^{13}C, and ^{31}P NMR spectra for all compounds were acquired at rt in $CDCl_3$ or CD_2Cl_2 on a Varian vnmrs 500 operating at 500, 126, and 202 MHz or a Varian MR 400 operating at 400, 100 and 162 MHz, respectively. For ^{1}H, and ^{13}C NMR spectra in deuterated solvents, the chemical shift data are reported in units of δ (ppm) relative to tetramethylsilane (TMS) and referenced with residual solvent. Multiplicities are reported as follows: singlet (s), doublet (d), doublet of doublets (dd), triplet (t), quartet (q), multiplet (m), and broad resonance (br).

Gel-Permeation Chromatography: Polymer molecular weights were determined by comparison with polystyrene standards (Varian, EasiCal PS-2 MW 580-377,400) on a Waters 1515 HPLC instrument equipped with Waters Styragel® (7.8 x 300 mm) THF HR 0.5, THF HR 1, and THF HR 4 type columns in sequence and analyzed with Waters 2487 dual absorbance detector (254 nm). Samples were dissolved in THF (with mild heating) and passed through a 0.2 µm PTFE filter prior to analysis.

Titrations of the Grignard Reagents: An accurately weighed sample of salicylaldehyde phenylhydrazone (typically between 290-310 mg) was dissolved in 5.00 mL of THF. A 0.50 mL aliquot of this solution was stirred at rt while ArMgBr was added dropwise using a 500 µL syringe. The initial solution is yellow and turns bright orange at the end-point.[2]

Gas Chromatography: Gas chromatography was carried out using a Shimadzu GC 2010 containing a Shimadzu SHRX5 (crossbound 5% diphenyl – 95% dimethyl polysiloxane; 15 m 0.25 mm ID, 0.25 µm df) column.

III. Synthetic Procedures

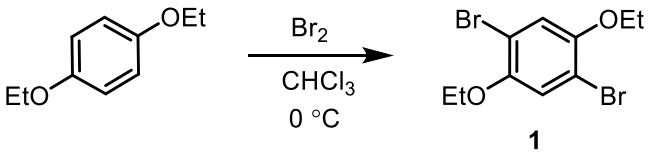

1

1.[1] A 500 mL round-bottom flask was equipped with a stir bar. Sequentially, 1,4-diethoxybenzene (13 g, 0.078 mol, 1.0 equiv), and $CHCl_3$ (90 mL) were added to the flask. The reaction flask was cooled to 0 °C in an ice/water bath and fitted with an addition funnel. Bromine (10 mL, 0.19 mol, 2.5 equiv) was added dropwise under N_2 and the pressure was vented through a solution of aq saturated Na_2SO_3 and $NaHCO_3$ (50:50). After 3 h, the reaction was quenched with an aq saturated solution of Na_2CO_3 (100 mL) and stirred vigorously until colorless. The aqueous mixture was extracted with DCM (3 x 100 mL). The organic layers were combined and washed with water (2 x 200 mL) and brine (1 x 200 mL), dried over $MgSO_4$, filtered, and concentrated in vacuo. The residue was recrystallized from DCM/methanol to produce 21 g of **1** as a white solid (83% yield).

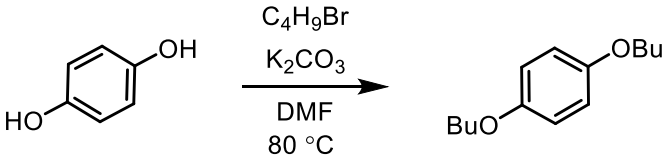

S1

S1.[2] A 500 mL round-bottom flask was equipped with a stir bar. Sequentially, hydroquinone (20. g, 0.20 mol, 1.0 equiv), anhydrous DMF (120 mL), and 1-bromobutane (49 mL, 0.45 mol, 2.5 equiv) were added to the flask. The flask was put under N_2 atmosphere and stirred vigorously while heated to 80 °C. Once at 80 °C, potassium carbonate (63 g, 0.45 mmol, 2.5 equiv) was slowly added and subsequently put under N_2 atmosphere again for 5 d. After cooling to rt, the reaction mixture was poured into water (400 mL). The reaction mixture was extracted with hexanes (3 x 200 mL). The organic layers were combined and washed with water (2 x 200 mL) and brine (1 x 200 mL), dried over $MgSO_4$, filtered, and concentrated in vacuo. The resulting oil was passed though silica gel with neat DCM as the eluent. Recrystallization from hot methanol produced 35 g of **S1** as a white crystalline solid (86% yield). HRMS (EI): Calcd. For $C_{14}H_{22}O_2$, 222.1620 [M+]; found, 222.1626.

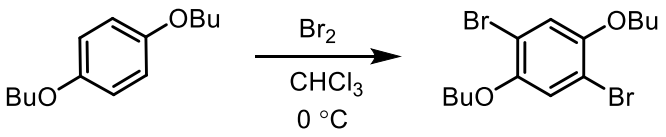

S1 **5**

5.[2] A 500 mL round-bottom flask was equipped with a stir bar. Sequentially, **S1** (17 g, 0.078 mol, 1.0 equiv), and $CHCl_3$ (90 mL) were added to the flask. The reaction flask was cooled to 0 °C in an ice/water bath and fitted with an addition funnel. Bromine (10 mL, 0.19 mol, 2.5 equiv) was added dropwise under N_2 and the pressure was vented through a solution of aq saturated Na_2SO_3 and $NaHCO_3$ (50:50). After 3 h, the reaction was quenched with an aq saturated solution of Na_2CO_3 (100 mL) and stirred vigorously until colorless. The aqueous mixture was extracted with DCM (3 x 100 mL). The organic layers were combined and washed with water (2 x 200 mL) and brine (1 x 200 mL), dried over $MgSO_4$, filtered, and concentrated in vacuo. The residue was recrystallized from DCM/methanol to produce 23 g of **5** as a white solid (79% yield). HRMS (EI): Calcd. For $C_{14}H_{20}Br_2O_2$, 377.9830 [M+]; found, 377.9824.

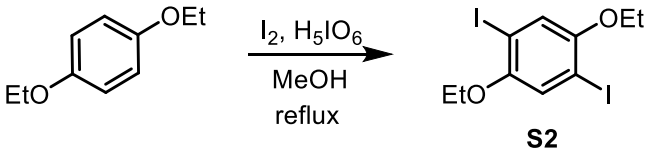

S2

S2. A 100 mL round-bottom flask was equipped with a stir bar. Sequentially, 1,4-diethoxybenzene (5.0 g, 0.030 mol, 1.0 equiv), and MeOH (50 mL) were added to the flask. Iodine (3.8 g, 0.030 mol, 1.0 equiv) and periodic acid (6.9 g, 0.030 mol, 1.0 equiv) were added with stirring. This was then heated to reflux and put under N_2 atmosphere. After 4 h, the reaction was quenched with an aq saturated solution of Na_2SO_3 (50 mL) and stirred vigorously until colorless. The aqueous mixture was extracted with DCM (3 x 50 mL). The organic layers were combined and washed with water (2 x 50 mL) and brine (1 x 50 mL), dried over $MgSO_4$, filtered, and concentrated in vacuo. The residue was recrystallized from DCM/methanol to produce 7.8 g of **S2** as a white solid (62% yield).

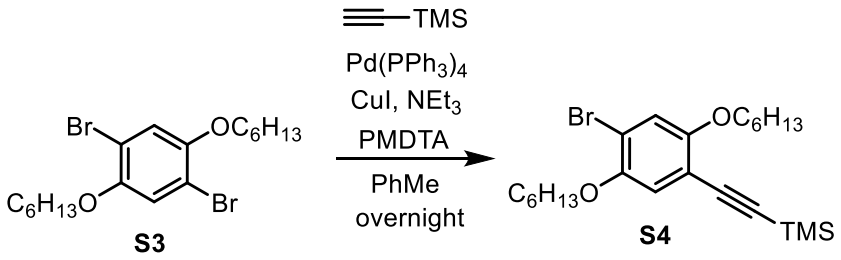

S4. A 200 mL Schlenk flask was equipped with a stir bar and charged with nitrogen three times. This flask was then charged with **S3** (0.50 g, 1.2 mmol, 1.5 equiv), trimethylsilylacetylene (0.11 mL, 0.76 mmol, 1.0 equiv), $Pd(PPh_3)_4$ (27mg, 0.038 mmol, 5 mol%), CuI (14 mg, 0.076 mmol, 10 mol %), PMDTA (0.020 mL, 0.076 mmol, 10 mol%), and PhMe (50 mL). The reaction was left to stir overnight at rt. The solution quenched with satd. NH_4Cl (50mL). The aqueous mixture was extracted with DCM (3 x 50 mL). The organic layers were combined and washed with water (2 x 50 mL) and brine (1 x 50 mL), dried over $MgSO_4$, filtered, and concentrated in vacuo. This was purified by column chromatography (20% DCM/80% hexanes) to produce 0.29 g of **S4** (84% yield). HRMS (EI): Calcd. For $C_{23}H_{370}BrO_2Si$, 453.1819 [M+]; found, 453.1821.

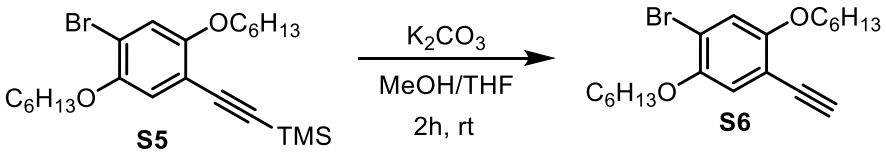

S5. A 250 mL flask was equipped with a stir bar and charged with **S4** (2.0 g, 4.4 mmol, 1 equiv), potassium carbonate (10. g, 72 mmol, 10 mol%), THF (50 mL), and MeOH (50 mL). The reaction was left to stir for 2h at rt. The potassium carbonate was filtered off and washed with THF, and concentrated in vacuo. This was purified by column chromatography (20% DCM/80% hexanes) to produce 1.1 g of **S5** (65% yield). HRMS (EI): Calcd. For $C_{20}H_{29}BrO_2$, 381.1424 [M+]; found, 381.1423.

IV. NMR Spectra

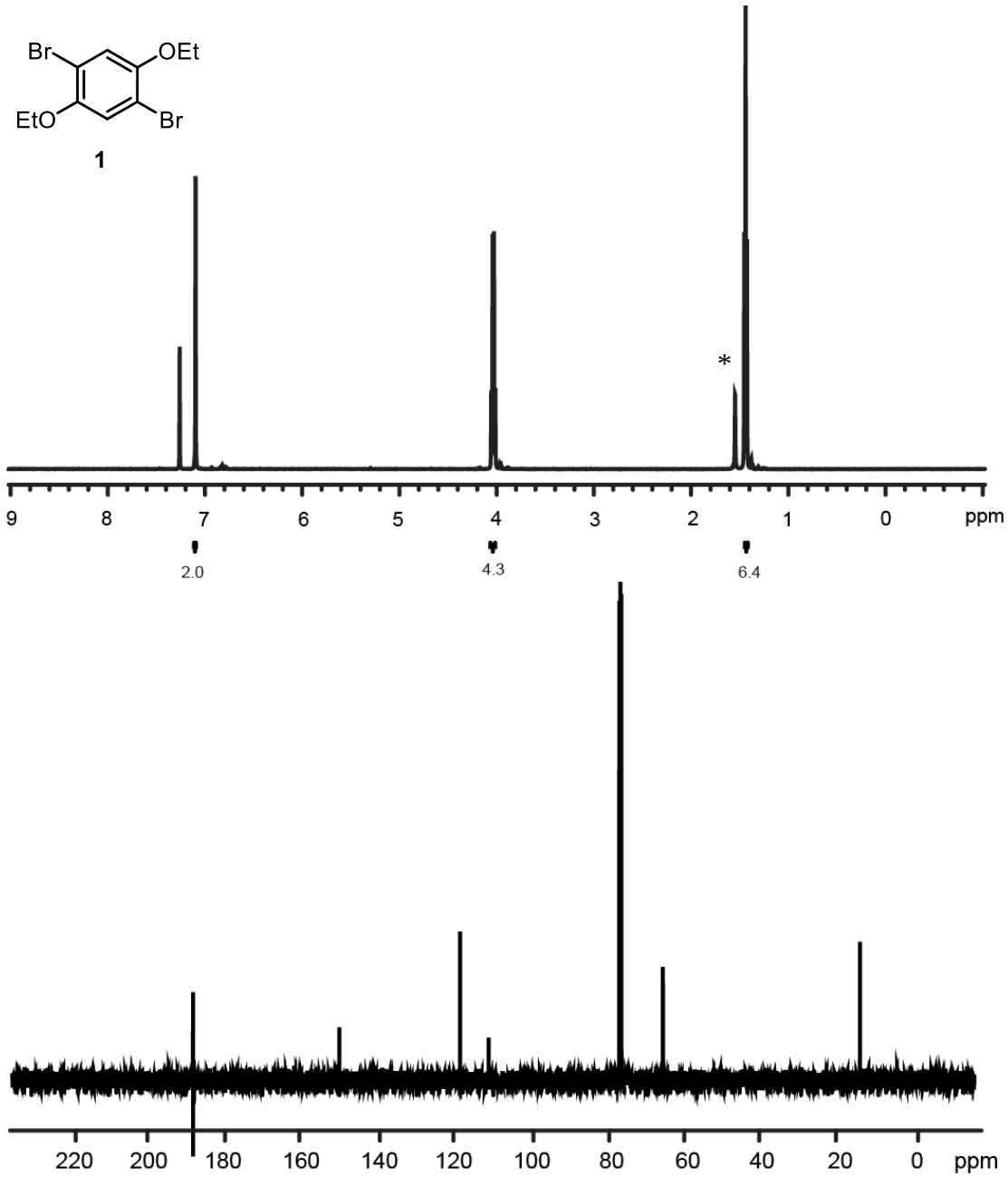

Figure S3.1 ^{1}H and ^{13}C NMR spectra for **1**. ^{1}H NMR (500 MHz, $CDCl_3$) δ 7.10 (s, 2H), 4.04 (q, *J* = 7.1 Hz, 4H), 1.47 (t, *J* = 7.1 Hz, 6H). * indicates residual H_2O. ^{13}C NMR (126 MHz, $CDCl_3$) δ 150.01, 118.67, 111.20, 65.95, 14.75.

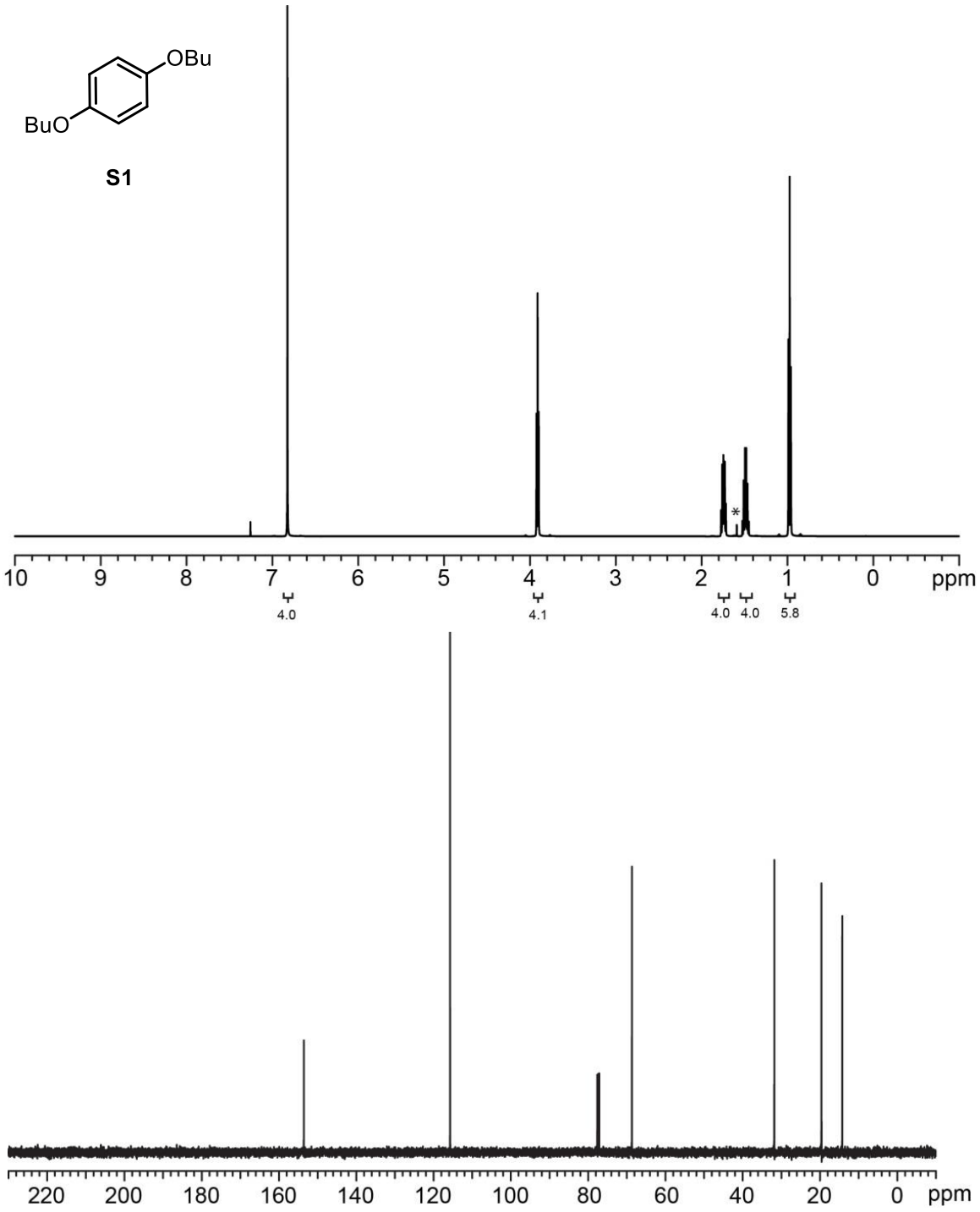

Figure S3.2 ^{1}H and ^{13}C NMR spectra for **S1**. ^{1}H NMR (500 MHz, $CDCl_3$) δ 6.83 (s, 4H), 3.92 (t, *J* = 7.0 Hz, 4H), 1.75 (m, 4H), 1.49 (m, 4H), 0.98 (t, *J* = 7.3 Hz, 6H). * indicates residual H_2O. ^{13}C NMR (126 MHz, $CDCl_3$) δ 153.19, 115.36, 68.30, 31.45, 19.24, 13.84.

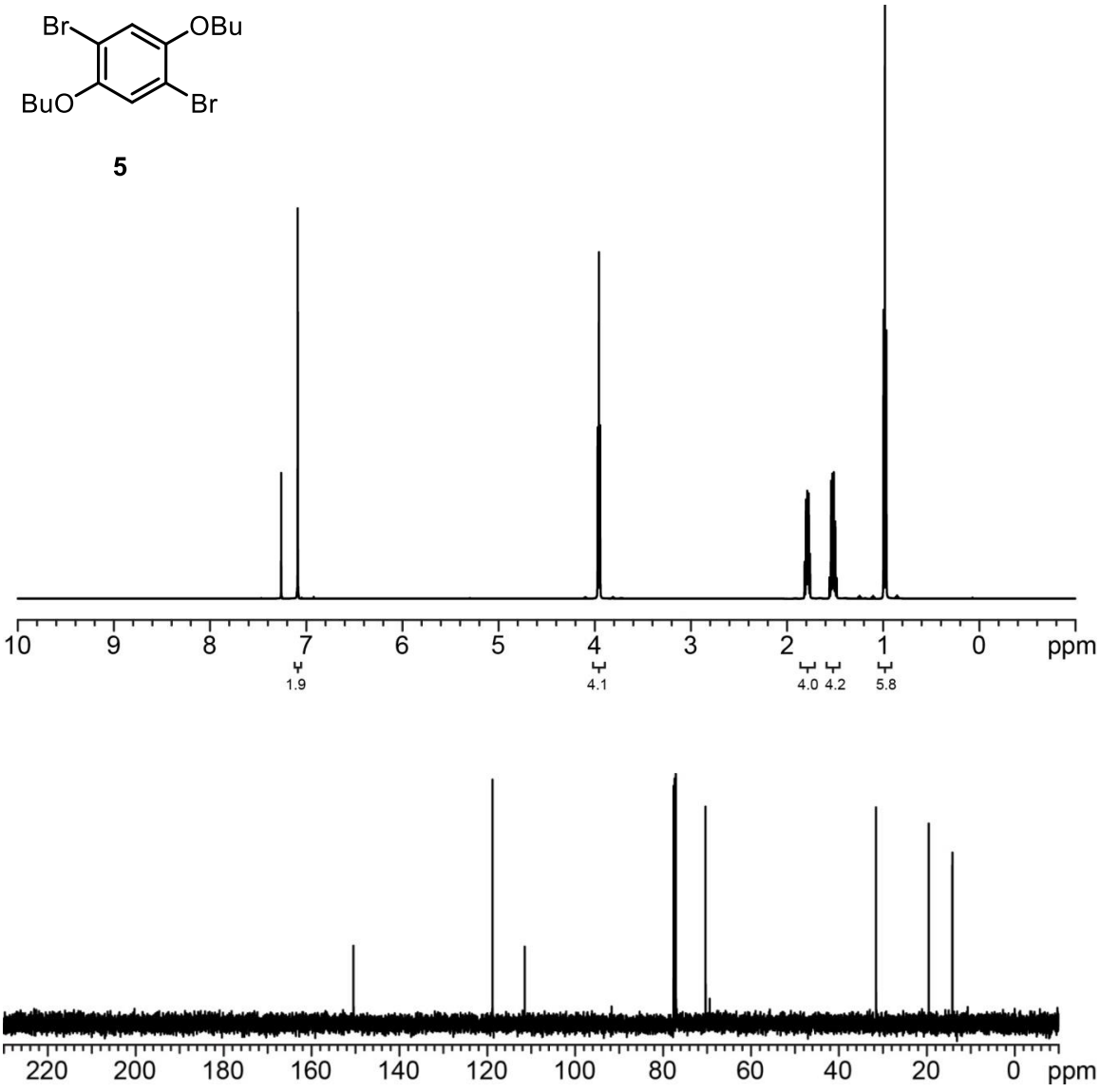

Figure S3.3 ^{1}H and ^{13}C NMR spectra for **5**. ^{1}H NMR (500 MHz, $CDCl_3$) δ 7.09 (s, 2H), 3.96 (t, *J* = 6.7 Hz, 4H), 1.79 (m, 4H), 1.53 (m, 4H), 0.98 (t, *J* = 7.2 Hz, 6H). ^{13}C NMR (126 MHz, $CDCl_3$) δ 150.08, 118.46, 111.13, 69.99, 31.19, 19.19, 13.81.

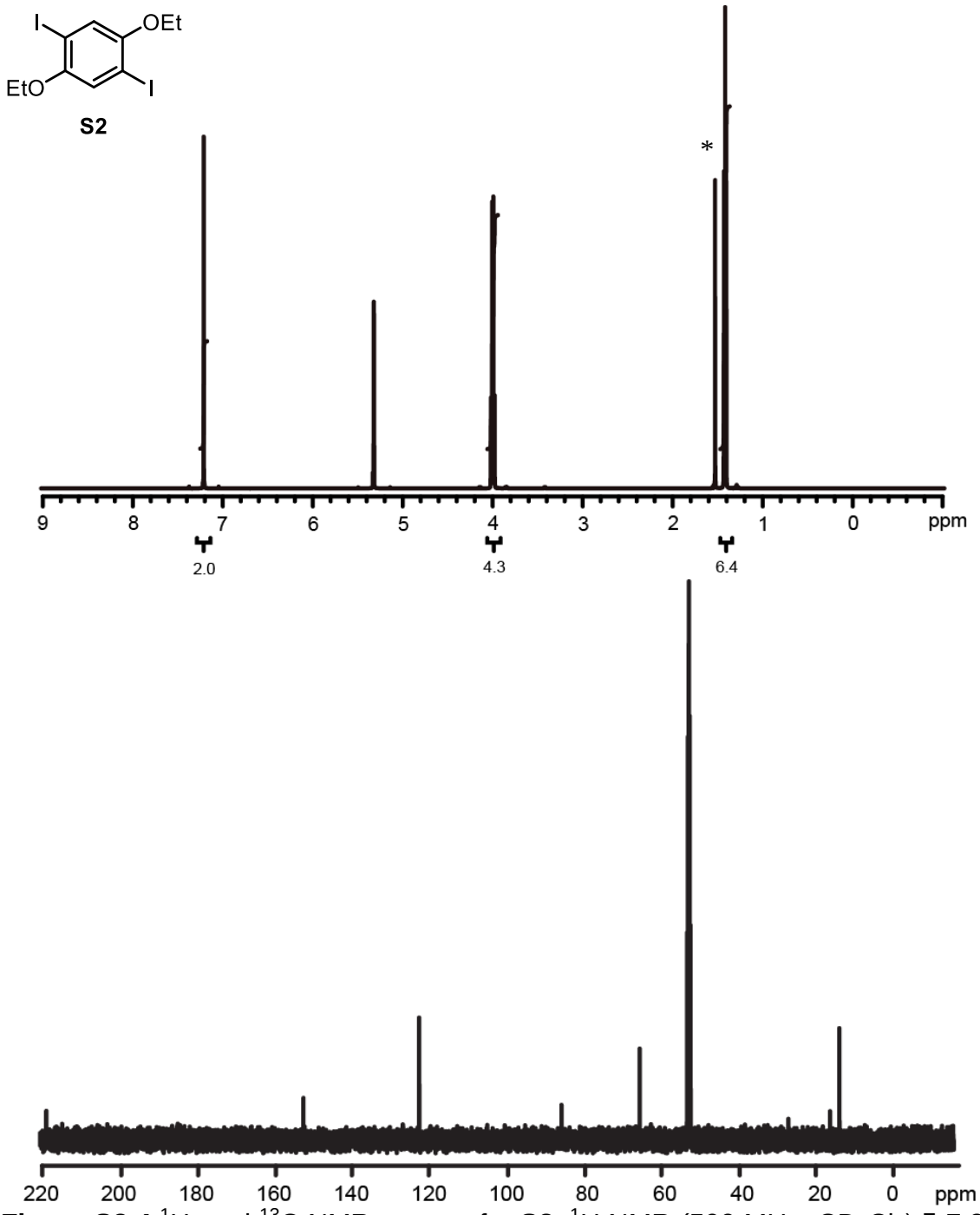

Figure S3.4 ^{1}H and ^{13}C NMR spectra for **S2**. ^{1}H NMR (500 MHz, CD_2Cl_2) δ 7.21 (s, 2H), 4.01 (q, *J* = 7.0 Hz, 4H), 1.42 (t, *J* = 7.0 Hz, 6H), * indicates residual H_2O. ^{13}C NMR (126 MHz, CD_2Cl_2) δ 152.85, 123.00, 86.29, 66.11, 14.59.

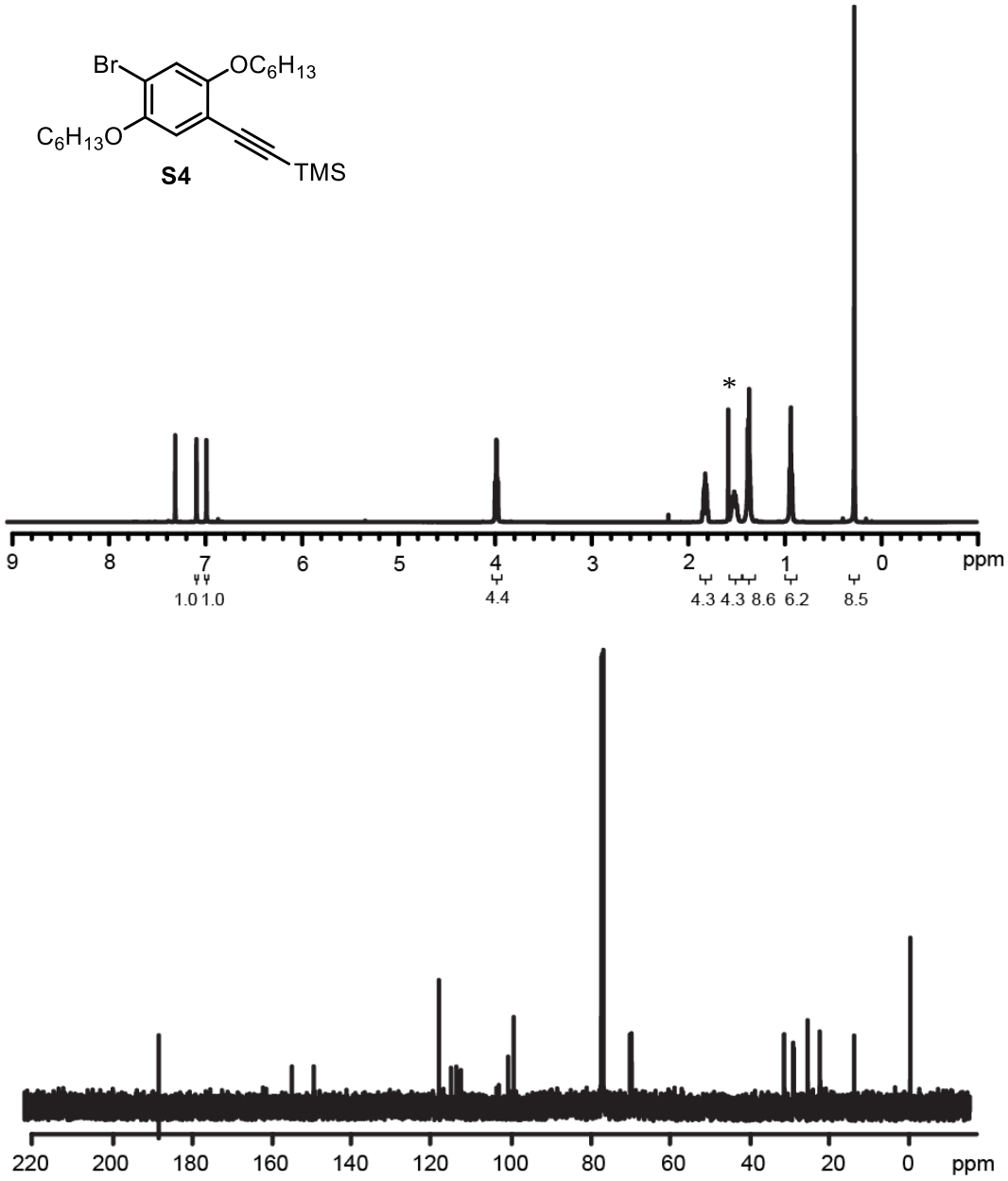

Figure S3.5 ^{1}H and ^{13}C NMR spectra for **S4**. ^{1}H NMR (500 MHz, $CDCl_3$) δ 7.04 (s, 1H), 6.94 (s, 1H), 3.97-3.91 (m, 4H), 1.83-1.75 (m, 4H), 1.54-1.43 (m, 4H), 1.39-1.30 (m, 8H), 0.95-0.87 (m, 6H), 0.26 (s, 9H). * indicates residual H_2O. ^{13}C NMR (126 MHz, $CDCl_3$) δ 154.71, 149.29, 117.93, 114.89, 113.56, 112.40, 100.61, 99.22, 70.08, 69.72, 31.60, 31.58, 29.25, 29.24, 25.67, 25.65, 22.58, 22.57, 14.05, 14.02, -0.06.

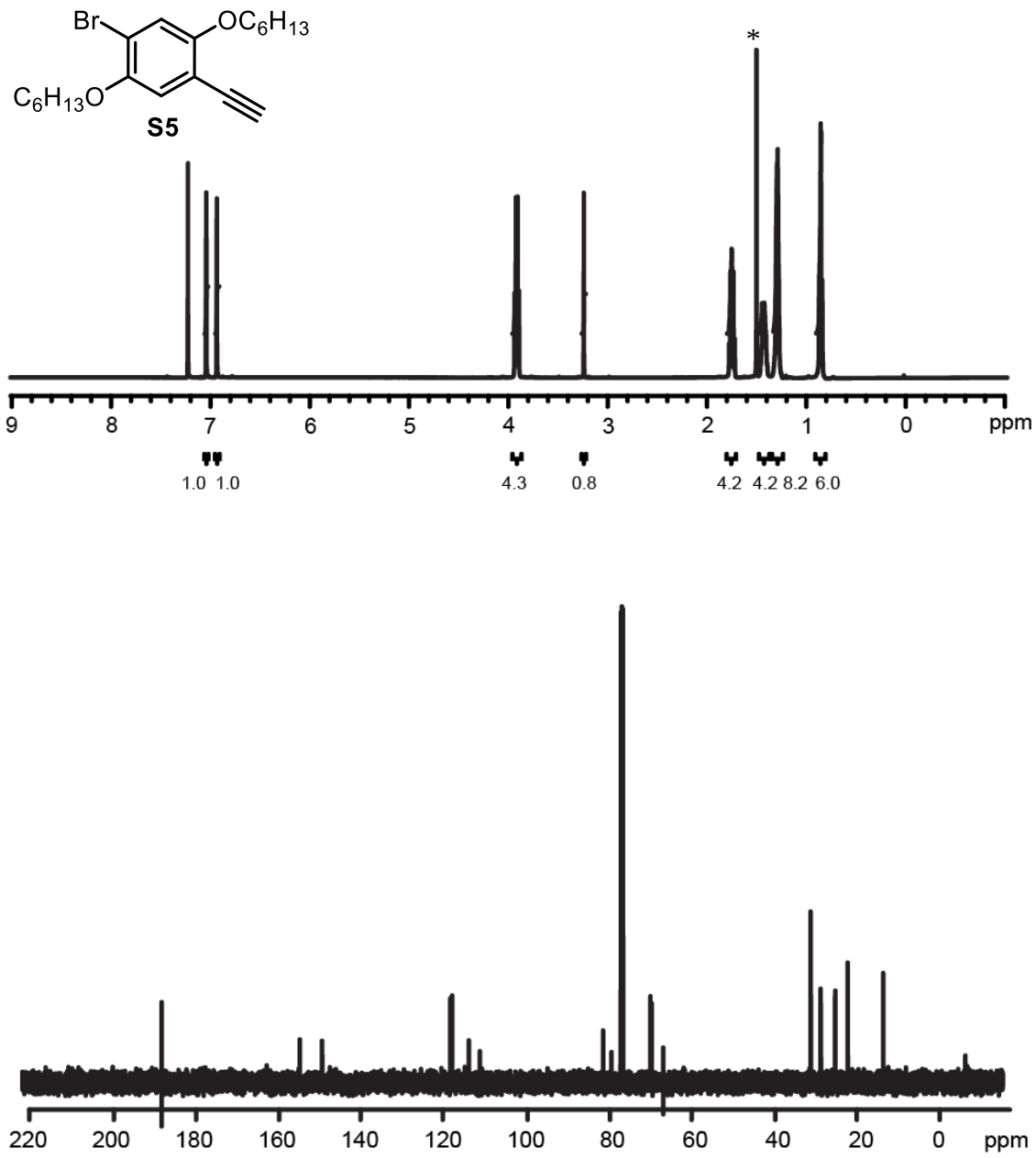

Figure S3.6 ^{1}H and ^{13}C NMR spectra for **S5**. ^{1}H NMR (500 MHz, $CDCl_3$) δ 7.08 (s, 1H), 6.97 (s, 1H), 3.99-3.93 (m, 4H), 3.29 (s, 1H), 1.84-1.76 (m, 4H), 1.52-1.43 (m, 4H), 1.39-1.31 (m, 8H), 0.94-0.88 (m, 6H). * indicates residual H_2O. ^{13}C NMR (126 MHz, CD_2Cl_2) δ 154.72, 149.34, 118.38, 117.96, 113.96, 111.28, 81.58, 79.52, 70.13, 69.89, 67.07, 67.06, 31.50, 29.94, 29.11, 29.05, 25.63, 25.55, 22.57, 14.01.

V. Selected Small Molecule Screens

The small molecule screens were initially performed with **S3**. However, we observed some decomposition of products over several hours, so we replaced **S3** with **S1** to increase stability.

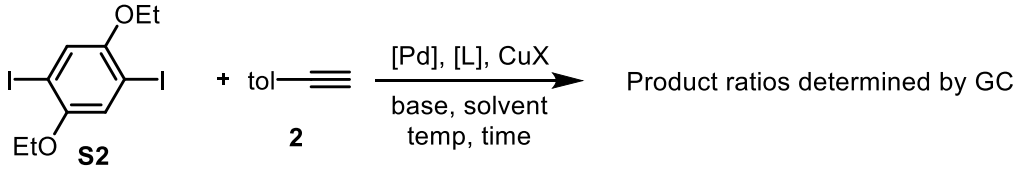

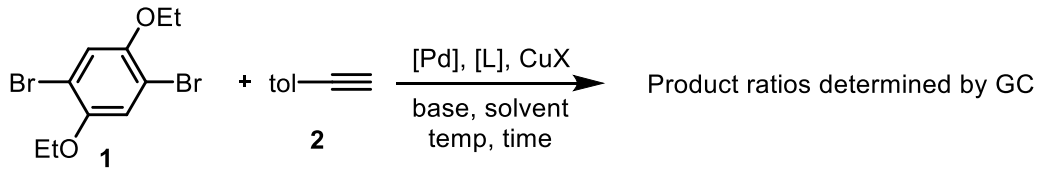

Representative Procedure for Small Molecule Screens:

In the glovebox, a 4 mL vial was equipped with a stir bar. Pd catalyst (0.0025 mmol, 1 equiv) was then carefully measured out in the vial, and the mass recorded. Relative to the amount added, sequentially phosphine ligand* (0.005 mmol, 2 equiv), CuI (2.4 mg, 0.0125 mmol, 5 equiv), **S2** (84 mg, 0.20 mmol, 80 equiv), PMDTA (2.6 µL, 0.0125 mmol, 5 equiv),$C_{19}H_{40}$ internal standard (0.33 mg, 0.0013 mmol, 0.5 equiv) were added using stock solutions in PhMe. Additional PhMe was then added to reach a total volume of 2 mL with stirring. Next, base (1 mL, 33%/vol) and **2** (13 µL, 0.10 mmol, 40 equiv) were added and the vial was the cap was secured tightly and left overnight. The following day, the vial was removed from the glovebox and quenched with hydrochloric acid (12.1 M, 3 mL) and subsequently diluted with water (8 mL). The reaction was then extracted with DCM (3 x 3 mL). The combined organic layers were dried over $MgSO_4$, filtered through a 0.2 µm PTFE filter, and subjected to GC analysis.

*Catalysts with pendant ligands did not have additional ligand added

Table S3.1 Data for small molecule screens with NEt_3 (10 equiv).

Catalyst	Ligand	% Conv. **2**	% Mono-functionalized (**3**)	% Di-functionalized (**4**)
PEPPSI-IPr	N/A	100	100	0
$Pd(OAc)_2$	$P(tolyl)_3$	100	87	13
$Pd(OAc)_2$	DavePhos	100	90	10
$Pd(OAc)_2$	CyJohn Phos	100	90	10
Gen 1 XPhos	N/A	100	50	50
Gen 2 XPhos	N/A	100	50	50
Gen 1 SPhos	N/A	100	100	0
Gen 2 SPhos	N/A	100	100	0

Table S3.2 Data for small molecule screens with NEt_3 (33% by volume).

Catalyst	Ligand	% Conv. **2**	% Mono-functionalized (**3**)	% Di-functionalized (**4**)
PEPPSI-IPr	N/A	90	100	0
$Pd(OAc)_2$	PPh_3	100	86	14
$Pd(OAc)_2$	$P(tolyl)_3$	100	100	0
$Pd(OAc)_2$	DavePhos	93	80	20
$Pd(OAc)_2$	CyJohn Phos	100	87	13
Gen 1 XPhos	N/A	100	33	67
Gen 2 XPhos	N/A	100	39	61
Gen 1 SPhos	N/A	100	64	36
Gen 2 SPhos	N/A	100	54	46

Table S3.3 Data for small molecule screens with $HNiPr_2$ (33% by volume).

Catalyst	Ligand	% Conv. **2**	% Mono-functionalized (**3**)	% Di-functionalized (**4**)
PEPPSI-IPr	N/A	63	99	1
$Pd(OAc)_2$	PPh_3	100	98	2
$Pd(OAc)_2$	$P(tolyl)_3$	100	86	14
$Pd(OAc)_2$	DavePhos	100	47	53
$Pd(OAc)_2$	CyJohn Phos	100	99	1
Gen 1 XPhos	N/A	100	60	40
Gen 2 XPhos	N/A	100	29	71
Gen 1 SPhos	N/A	100	54	46
Gen 2 SPhos	N/A	100	43	57

Table S3.4 Data for small molecule screens with PPh_3 (10 equiv).

Catalyst	Ligand	% Conv. **2**	% Mono-functionalized (**3**)	% Di-functionalized (**4**)
PEPPSI-IPr	N/A	24	100	0
$Pd(OAc)_2$	PPh_3	100	100	0
$Pd(OAc)_2$	$P(tolyl)_3$	84	100	0
$Pd(OAc)_2$	DavePhos	100	100	0
$Pd(OAc)_2$	CyJohn Phos	100	100	0
Gen 1 XPhos	N/A	27	100	0
Gen 2 XPhos	N/A	26	97	3
Gen 1 SPhos	N/A	28	100	0
Gen 2 SPhos	N/A	32	97	3

Table S3.5 Data for small molecule screens with PPh_3 (10 equiv) and THF solvent.

Catalyst	Ligand	% Conv. **2**	% Mono-functionalized (**3**)	% Di-functionalized (**4**)
PEPPSI-IPr	N/A	90	100	0
$Pd(OAc)_2$	PPh_3	45	100	0
$Pd(OAc)_2$	$P(tolyl)_3$	100	100	0
$Pd(OAc)_2$	$P(Cy)_3$	100	100	0
$Pd(OAc)_2$	DavePhos	85	91	9
$Pd(OAc)_2$	CyJohn Phos	29	98	2
Gen 1 XPhos	N/A	75	100	0
Gen 2 XPhos	N/A	93	90	10
Gen 1 SPhos	N/A	100	100	0
Gen 2 SPhos	N/A	100	81	19

Table S3.6 Data for small molecule screens with NEt_3 (10 equiv).

Catalyst	Ligand	% Conv. **2**	% Mono-functionalized (**3**)	% Di-functionalized (**4**)
Gen 1 SPhos	N/A	35	100	0
Gen 2 SPhos	N/A	23	100	0
$PdCl_2$	SPhos	77	100	0
$Pd(OAc)_2$	SPhos	84	67	33
$Pd(PhCN)Cl_2$	SPhos	44	25	75
Pd(allyl)Cl	SPhos	51	100	0

Table S3.7 Data for small molecule screens with NEt_3 (10 equiv).

Catalyst	Ligand	% Conv. **2**	% Mono-functionalized (**3**)	% Di-functionalized (**4**)
Gen 1 XPhos	N/A	29	67	33
Gen 2 XPhos	N/A	29	100	0
$PdCl_2$	XPhos	100	100	0
$Pd(OAc)_2$	XPhos	84	100	0
$Pd(PhCN)Cl_2$	XPhos	49	67	33
Pd(allyl)Cl	XPhos	59	100	0

Table S3.8 Data for small molecule screens with NEt_3 (33% by volume).

Catalyst	Ligand	% Conv. **2**	% Mono-functionalized (**3**)	% Di-functionalized (**4**)
Gen 1 XPhos	N/A	50	67	33
Gen 2 XPhos	N/A	56	67	33
$PdCl_2$	XPhos	100	100	0
$Pd(OAc)_2$	XPhos	84	33	66
$Pd(PhCN)Cl_2$	XPhos	81	40	60
Pd(allyl)Cl	XPhos	100	100	0

Table S3.9 Data for small molecule screens with $HNiPr_2$ (33% by volume) at 70 °C.

Catalyst	Ligand	% Conv. **2**	% Mono-functionalized (**3**)	% Di-functionalized (**4**)
Gen 1 XPhos	N/A	100	50	50
Gen 2 XPhos	N/A	100	50	50
$PdCl_2$	XPhos	100	100	0
$Pd(OAc)_2$	XPhos	84	75	25
$Pd(PhCN)Cl_2$	XPhos	88	60	40
Pd(allyl)Cl	XPhos	100	100	0

Table S3.10 Data for small molecule screens with NEt_3 (33% by volume) with added PMDTA.

Catalyst	Ligand	% Conv. **2**	% Mono-functionalized (**3**)	% Di-functionalized (**4**)
Gen 1 SPhos	N/A	80	25	75
Gen 2 SPhos	N/A	100	17	83
Gen 1 XPhos	N/A	100	25	75
Gen 2 XPhos	N/A	100	25	75
$Pd(PhCN)Cl_2$	XPhos	70	25	75
$Pd(OAc)_2$	XPhos	100	33	67

Table S3.11 Data for small molecule screens with NEt_3 (33% by volume) with added PMDTA, Gen 2 SPhos catalyst.

PMDTA (equiv)	% Conv. **2**	% Mono-functionalized (**3**)	% Di-functionalized (**4**)
1	100	17	83
2	100	20	80
3	93	21	79
4	94	21	79

Table S3.12 Data for small molecule screens with various bases (33% by volume) with added PMDTA, Gen 2 SPhos catalyst.

PMDTA (equiv)	pKa (conjugate acid)	% Conv. **2**	% Mono-functionalized (**3**)	% Di-functionalized (**4**)
$HNPh_2$	1	42	100	0
NBn_3	4	71	88	12
NEt_3	9	100	31	69
KOtBu	18	83	71	29

Table S3.13 Data for small molecule screens with NEt_3 (variable volume) with added PMDTA, Gen 2 SPhos catalyst.

NEt_3 (% vol)	% Conv. **2**	% Mono-functionalized (**3**)	% Di-functionalized (**4**)
15	12	59	41
25	45	36	64
33	67	27	73
50	94	15	85
75	100	10	90
100 (neat)	100	5	95

VI. Summary of Polymerizations Results

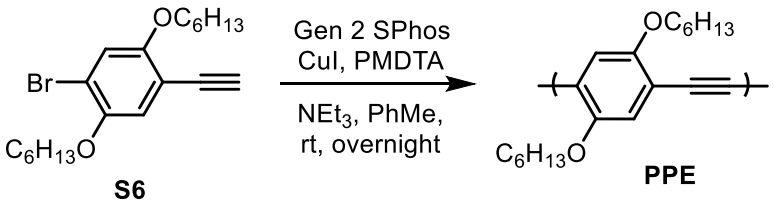

Representative Procedure for PPE Polymerizations:

All reactions were performed in a glovebox. A stock solution of **S5** (0.088 mmol, 34mg, 67 equiv) with internal standard ($C_{22}H_{46}$, ~3 mg) and a stock solution of CuI (0.0065 mmol, 1.2 mg, 5.0 equiv) with PMDTA (0.0065 mmol, 1.1 mg, 5.0 equiv) were prepared. A 4 mL vial equipped with a stir bar had Gen 2 SPhos (0.0013 mmol, 0.90 mg, 1.0 equiv) added, followed by the CuI/PMDTA solution. To this, PhMe and NEt_3 were added to make a final volume of 3 mL. Finally, monomer was added, the reaction was capped, and left for 2 days at rt. The vial was removed from the glovebox and quenched with hydrochloric acid (12.1 M, 1 mL) and subsequently diluted with water (4 mL). The reaction was then extracted with DCM (3 x 3 mL). The combined organic layers were dried over $MgSO_4$. Conversion was determined relative to the initial concentration, using the internal standard as a reference via GC. To measure molecular weight and molecular weight distribution, the organic phase was concentrated in vacuo, redissolved in THF (~1.5 mL) with mild heating and passed through a 0.2 μm PTFE filter for GPC analysis.

Table S3.14 Data for polymerization screens with NEt_3 (variable volume) with added PMDTA, Gen 2 SPhos catalyst.

NEt_3 (% vol)	% Conv. **S6**	M_n (predicted)	M_n (measured)	Đ
33	100	20.2	7.2	1.57
50	100	20.2	7.8	1.61

Table S3.15 Data for polymerization screens with NEt_3 (50% by volume) with added PMDTA.

Catalyst	% Conv. **S6**	M_n (predicted)	M_n (measured)	Đ
Gen 1 SPhos	100	15.1	4.6	4.29
Gen 2 SPhos	100	24.8	10.1	4.76
Gen 3 SPhos	100	23.3	10.3	6.08
Gen 1 XPhos	100	22.0	8.2	1.99
Gen 2 XPhos	100	23.6	12.5	2.79
Gen 3 XPhos	100	25.4	11.9	3.00

VII. M_n and Đ versus Conversion

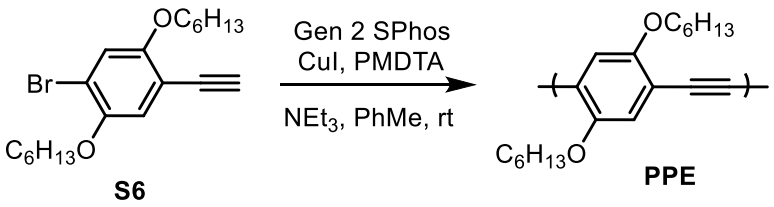

S6 **PPE**

Representative Procedure for M_n and Đ versus Conversion Studies utilizing GC analysis:

In a glovebox, **S6** (0.850 mmol, 324 mg, 67 equiv) with internal standard ($C_{22}H_{46}$, ~3 mg) and a stock solution of CuI (0.063 mmol, 12.1 mg, 5 equiv) with PMDTA (0.063 mmol, 11.0 mg, 5 equiv) were prepared. A 20 mL vial equipped with a stir bar had Gen 2 SPhos (0.013 mmol, 9.14 mg, 1 equiv) added, followed by the CuI/PMDTA solution. To this, PhMe and NEt_3 (2.5 mL, 25% by volume) were added to make a final volume of 10 mL. Finally, monomer was added, the reaction was capped, and left overnight at rt.

Samples were taken at chosen points and removed from the glovebox, quenched with HCl (1 mL), diluted with water (3 mL), extracted with DCM (2 x 3mL), a sample was taken for GC conversion. The sample was concentrated, dissolved in THF, and filtered through a 0.2 μm PTFE filter for GPC characterization.

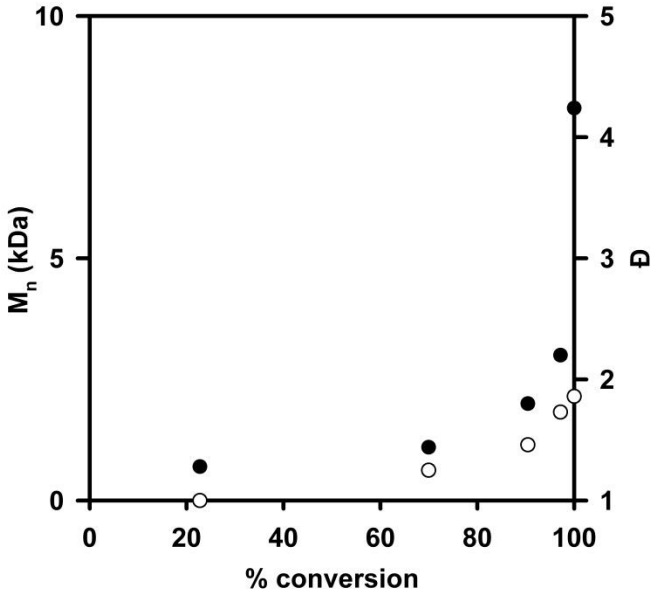

Figure S3.7 Plot of M_n (•) and Đ (○) versus conversion utilizing the most favorable small molecule conditions.

Table S3.16 Data for the plot in **Figure S3.7**.

Time (min)	% Conv. **S6**	M_n	Đ
50	23	0.7	1.00
125	70	1.1	1.25
190	90	2.0	1.46
240	97	3.0	1.73
1770	100	8.1	1.86

VIII. Summary of Small Molecule Reaction Profile

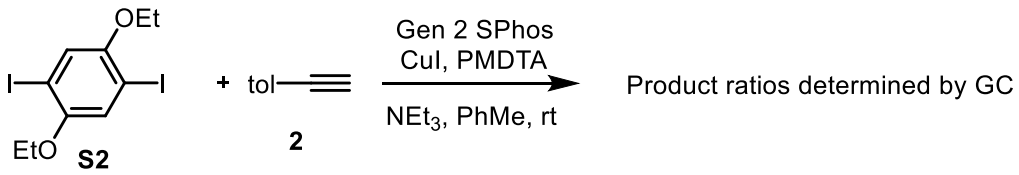

Representative Procedure for Small Molecule Reaction Profile utilizing GC analysis:

In the glovebox, a 20 mL vial was equipped with a stir bar. Gen 2 SPhos (5.8mg, 0.008 mmol, 1 equiv) was then carefully measured out into the vial. Next CuI (7.2 mg, 0.038 mmol, 5 equiv), **S2** (252 mg, 0.60 mmol, 80 equiv), PMDTA (7.8 µL, 0.038 mmol, 5 equiv),$C_{19}H_{40}$ internal standard (0.99 mg, 0.038 mmol, 0.5 equiv) were added using stock solutions in PhMe. Additional PhMe was then added to reach a total volume of 6 mL with stirring. Next, base (6 mL, 50%/vol) and **2** (39 µL, 0.30 mmol, 40 equiv) were added and reaction was capped.

Samples were taken at chosen points and removed from the glovebox, quenched with HCl (1 mL), diluted with water (3 mL), extracted with DCM (2 x 3mL), a sample was taken for GC analysis.

Table S3.17 Data for small molecule reaction profile.

Time (min)	% Conv. **2**	% Mono-functionalized (**3**)	% Di-functionalized (**4**)
30	33	91	9
60	55	65	35
90	89	34	66
120	100	24	76
150	100	18	82
180	100	13	87
300	100	13	87

IX. Summary of Competition Experiments

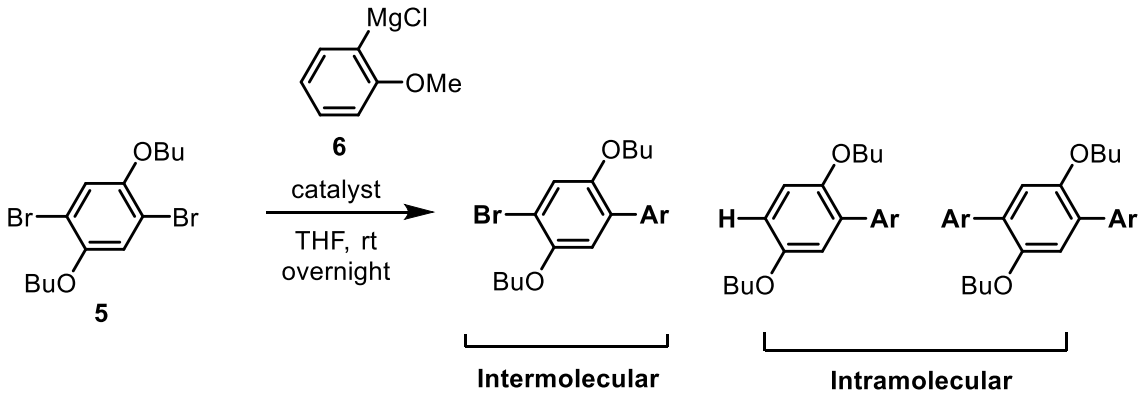

Representative Procedure for Kumada Competition Experiments:
In the glovebox, a 4 mL vial was equipped with a stir bar. Ni(dppe)Cl_2 (1.3 mg, 0.0025 mmol, 1 equiv) was then carefully measured out in the vial, and the mass recorded. Relative to the catalyst, **5** (76 mg, 0.20 mmol, 80 equiv) and $C_{19}H_{40}$ internal standard (0.99 mg, 0.038 mmol, 0.5 equiv) are measured and dissolved in 3 mL of THF. These are then added to the catalyst with stirring. Next, **6** (0.10 mL, 0.10 mmol, 1M, 40 equiv) was added and the vial was the cap was secured tightly and left overnight. The following day, the vial was removed from the glovebox and quenched with hydrochloric acid (12.1 M, 3 mL) and subsequently diluted with water (8 mL). The reaction was then extracted with DCM (3 x 3 mL). The combined organic layers were dried over $MgSO_4$, filtered through a 0.2 μm PTFE filter, and subjected to GC analysis.

Table S3.18 Data for the Kumada competition experiments with Ni(dppe)Cl_2.

6 (equiv)	**5** (equiv)	% Intra	% Inter
40	2000	1	99
40	80	1	99
20	80	1	99
10	80	2	98
5	80	2	98

Table S3.19 Data for the Kumada competition experiments with Pd-PEPPSI-IPr.

6 (equiv)	**5** (equiv)	% Intra	% Inter
40	2000	0	100
40	80	0	100
20	80	0	100
10	80	0	100
5	80	0	100

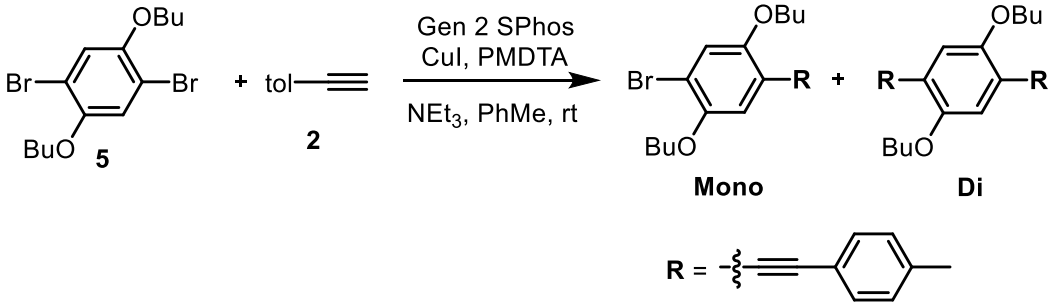

Representative Procedure for Sonogashira Competition Experiments:
In the glovebox, a 4 mL vial was equipped with a stir bar. Gen 2 SPhos (1.9 mg, 0.0025 mmol, 1 equiv) was then carefully measured out in the vial, and the mass recorded. Relative to the amount added, sequentially CuI (2.4 mg, 0.0125 mmol, 5 equiv), **5** (76 mg, 0.20 mmol, 80 equiv), PMDTA (2.6 µL, 0.0125 mmol, 5 equiv),$C_{19}H_{40}$ internal standard (0.33 mg, 0.0013 mmol, 0.5 equiv) were added using stock solutions in PhMe. Additional PhMe was then added to reach a total volume of 2 mL with stirring. Next, base (1 mL, 33%/vol) and **2** (13 µL, 0.10 mmol, 40 equiv) were added and the vial was the cap was secured tightly and left overnight. The following day, the vial was removed from the glovebox and quenched with hydrochloric acid (12.1 M, 3 mL) and subsequently diluted with water (8 mL). The reaction was then extracted with DCM (3 x 3 mL). The combined organic layers were dried over $MgSO_4$, filtered through a 0.2 µm PTFE filter, and subjected to GC analysis.

Table S3.20 Data for the Sonogashira competition experiments with Gen 2 SPhos.

2 (equiv)	**5** (equiv)	% **Mono**	% **Di**
40	2000	46	54
40	80	13	87
20	80	26	74
10	80	58	42
5	80	68	32

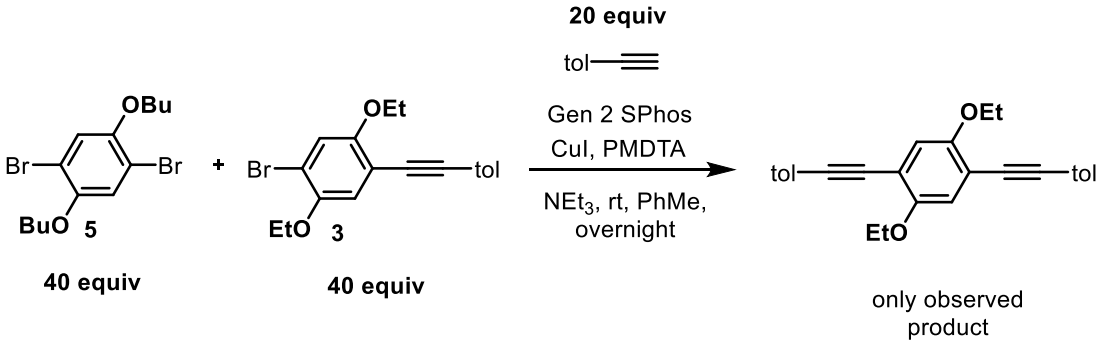

Representative Procedure for Sonogashira Reactivity Competition Experiments:
In the glovebox, a 4 mL vial was equipped with a stir bar. Gen 2 SPhos (1.9 mg, 0.0025 mmol, 1 equiv) was then carefully measured out in the vial, and the mass recorded. Relative to the amount added, sequentially CuI (2.4 mg, 0.0125 mmol, 5 equiv), **5** (38 mg, 0.10 mmol, 40 equiv), **3** (27 mg, 0.10 mmol, 40 equiv), PMDTA (2.6 µL, 0.0125 mmol, 5 equiv),$C_{19}H_{40}$ internal standard (0.33 mg, 0.0013 mmol, 0.5 equiv) were added using stock solutions in PhMe. Additional PhMe was then added to reach a total volume of 2 mL with stirring. Next, base (1 mL, 33%/vol) and **2** (13 µL, 0.10 mmol, 40 equiv) were added and the vial was the cap was secured tightly and left overnight. The following day, the vial was removed from the glovebox and quenched with hydrochloric acid (12.1 M, 3 mL) and subsequently diluted with water (8 mL). The reaction was then extracted with DCM (3 x 3 mL). The combined organic layers were dried over $MgSO_4$, filtered through a 0.2 µm PTFE filter, and subjected to GC analysis.

GC analysis showed exclusively conversion of the mono-functionalized starting material (**3**), and also showed only formation of the di-functionalized product labeled with ethoxy side-chains, indicating it originated from **3**.

X. References

(1) Lanni, E. L.; McNeil, A. J. *J. Am. Chem. Soc.* **2009**, *131*, 16573-16579.
(2) Bryan, Z. J.; McNeil, A. J. *Chem. Sci.* **2013**, *4*, 1620-1624.